

## **For Reference**

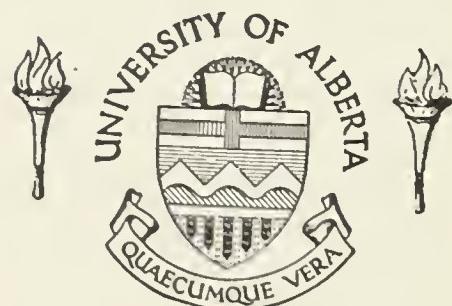
---

**NOT TO BE TAKEN FROM THIS ROOM**

## For Reference

NOT TO BE TAKEN FROM THIS ROOM

Ex LIBRIS  
UNIVERSITATIS  
ALBERTAENSIS







THE UNIVERSITY OF ALBERTA

A THEORY OF THIXOTROPIC BEHAVIOR  
AND ITS APPLICATION TO  
PEMBINA CRUDE OIL

A DISSERTATION

SUBMITTED TO THE FACULTY OF GRADUATE STUDIES  
IN PARTIAL FULFILMENT OF THE REQUIREMENTS FOR THE DEGREE  
OF DOCTOR OF PHILOSOPHY  
IN CHEMICAL ENGINEERING

FACULTY OF ENGINEERING  
DEPARTMENT OF CHEMICAL AND PETROLEUM ENGINEERING

by

R.A. RITTER, M.Sc.

EDMONTON, ALBERTA

September, 1961



Dedicated

to

my wife



#### ACKNOWLEDGEMENTS

The author wishes to express his sincere appreciation to Dr. G.W. Govier whose supervision, criticism and assistance throughout this investigation has been invaluable.

A debt of gratitude is also due to Interprovincial Pipe Line Company and Pembina Pipe Line Company for their kind financial aid, to Mr. R. Poulin and Mr. C. Middleton who assisted in gathering and processing the data, to Mr. R. Kirby and Mr. F. Butz for their many helpful suggestions during the construction of the equipment, to Mrs. I. Slator and Miss G. Thomas who typed the manuscript and to all those not mentioned here who contributed so freely of their time.

A very faint, large watermark-like image of a classical building with four prominent columns is visible in the background of the page.

Digitized by the Internet Archive  
in 2018 with funding from  
University of Alberta Libraries

<https://archive.org/details/theoryofthixotro00ritt>

## TABLE OF CONTENTS

	Page
TABLE OF CONTENTS	i
LIST OF TABLES	iii
LIST OF FIGURES	iv
I INTRODUCTION	1
II GENERAL ASPECTS OF RHEOLOGY	5
Mechanistic Theories	10
Theories Based on Mechanical Analogs	10
Microrheological Theories	12
Non-Mechanistic Theories	16
III THEORIES OF THIXOTROPY	27
IV MODIFIED THEORY OF THIXOTROPY	40
Comparison of Theories	51
V EXPERIMENTAL PROGRAM	54
Characterization of the Crude Oil Sample	55
The Viscometer and Associated Equipment	56
Calibration of Torsion Wires	67
End Effect Correction	70
Flow Stability in the Viscometer Annulus	71
Water Seal Device	74
Calibration of Thermocouples and Stopwatch	75
Sample Storage	76
Experimental Procedure	80
VI EXPERIMENTAL RESULTS	83
VII INTERPRETATION OF RESULTS	110
Calculation of Shear Stress and Shear Rate	110
Initial and Limiting Shear Stress	113
Stress Contribution of the Newtonian Solvent	124
Evaluation of Experimental Results	128
Evaluation of Rate Constants	129
Discussion	136
Design of Flow Systems	146
VIII CONCLUSION	154
NOMENCLATURE	156



## BIBLIOGRAPHY

160

## APPENDIX

1. Derivation of Equation (70)
2. Characterization of Pembina Crude Oil
3. Calibration of Viscometer Torsion Wires
4. End Effect Correction
5. Calibration of Stopwatch and Thermocouples
6. Change in Composition of Crude Oil in Storage
7. Rheological Data
8. Estimation of Initial Shear Stress
9. Stability of Flow Pattern in the Viscometer



## LIST OF TABLES

<u>Table No.</u>	<u>Title</u>	<u>Page</u>
1.	Schedule of experiments	82
2.	Rate constant, $k_A$	131
3.	Rate constant, $k_B$	133
1-2	Crude oil characterization	1-2
2-2	Analysis of gas phase in equilibrium with crude oil	5-2
3-2	Gas fraction analysis	6-2
4-2	True boiling point distillation data	10-2
5-2	Physical properties of liquid distillate	11-2
1-3	Values of constant "a" in equation (72)	7-3
2-3	Wire constant determined by viscometer calibration	19-3
1-5	Calibration data for stopwatch	1-5
1-6	Computed values of K and KP for each volatile component	4-6
2-6	Changes in composition of crude oil in storage	6-6
1-7	Shear stress decay data	3-7
2-7	Shear stress growth data	48-7
3-7	Computed rheological data	57-7
1-8	Evaluation of initial shear stress	4-8
2-8	Initial shear stress at various temperatures and rotational speeds	6-5
1-9	Values of M for each of the stability criterion	1-9
2-9	Comparison of stability criterion	2-9



## LIST OF FIGURES

	Page
1. Types of rheological behavior	6
2. Types of rheological behavior	7
3. True boiling point distillation curve	57
4. True boiling point distillation curve	58
5. Alberta rotational viscometer	61
6. Viscometer accessories	62
7. Alberta rotational viscometer	63
8. Alberta rotational viscometer	64
9. Alberta rotational viscometer	65
10. Crude oil storage vessel	77
11. Shear stress vs time (Decay curve)	84
12. Shear stress vs time (Decay curve)	85
13. Shear stress vs time (Decay curve)	86
14. Shear stress vs time (Decay curve)	87
15. Shear stress vs time (Decay curve)	88
16. Shear stress vs time (Decay curve)	89
17. Shear stress vs time (Decay curve)	90
18. Shear stress vs time (Decay curve)	91
19. Shear stress vs time (Decay curve)	92
20. Shear stress vs time (Decay curve)	93
21. Shear stress vs time (Decay curve)	94
22. Shear stress vs time (Decay curve)	95



	Page
23. Shear stress vs time (Decay curve)	96
24. Shear stress vs time (Decay curve)	97
25. Shear stress vs time (Decay curve)	98
26. Shear stress vs time (Growth curve)	99
27. Shear stress vs time (Growth curve)	100
28. Shear stress vs time (Growth curve)	101
29. Shear stress vs time (Growth curve)	102
30. Shear stress vs time (Growth curve)	103
31. Shear stress vs time (Growth curve)	104
32. Shear stress vs cup speed	113
33. Shear stress vs cup speed	114
34. Shear stress vs cup speed	115
35. Shear stress vs cup speed	116
36. Shear stress vs cup speed	117
37. Shear stress vs shear rate	118
38. Shear stress vs shear rate	119
39. Shear stress vs shear rate	120
40. Shear stress vs shear rate	121
41. Shear stress vs shear rate	122
42. Initial and final shear stress vs temperature	125
43. Initial and final shear stress vs temperature	126
44. Initial and final shear stress vs temperature	127
45. Correlation based on equation (70)	130
46. Rate constant, $k_A$ vs $1/\theta$	132



47. Rate constant, $k_B$ vs shear rate	134
48. Shear stress vs time	138
49. Newtonian solvent viscosity vs temperature	140
50. Shear stress vs time (Decay curve)	142
51. Shear stress vs time (Decay curve)	143
52. Shear stress vs time (Decay curve)	144
53. Shear stress vs shear rate	148
54. Pipe line flow system	149
1-3 Deflection vs cup speed	9-3
2-3 Deflection vs cup speed	10-3
3-3 Deflection vs cup speed	11-3
4-3 Deflection vs cup speed	12-3
5-3 Deflection vs cup speed	13-3
6-3 Deflection vs cup speed	14-3
7-3 Deflection vs cup speed	15-3
8-3 Wire diameter vs wire constant	18-3
1-1 End effect correction	2-4
1-5 Thermocouple calibration	2-5
1-8 Shear stress vs time	2-8
2-8 Change in shear stress vs time interval number	3-8
3-8 Shear stress vs time plus 10 seconds	5-3



## ABSTRACT

Consideration has been given to the quantitative definition of the complex behavior of a thixotropic fluid. The fluid selected for examination was Pembina crude oil which at low temperatures displays a consistency behavior highly dependent on time of shearing.

A review of the relevant recent literature revealed certain deficiencies in all of the present theories of the mechanism of thixotropic behavior. A modified theory was developed in which the factors, believed to be significant in the study of the behavior of Pembina crude oil, were incorporated. This theory is based on a thixotropic model consisting of a loosely bonded network structure of long chain molecules dispersed in a Newtonian solvent. The mechanism of network destruction is assumed to be somewhat analogous to that of a chemical reaction. Mathematical expressions describing the assumed mechanism were developed and their application to Pembina crude oil was tested through an extensive experimental program.

All experimental work was performed with the aid of the Alberta Rotational Viscometer, a specially designed instrument which provided accurate temperature control and precise shear stress and shear rate measurement. The routine of analysis consisted of measurement of shear stress as a function of time of shearing at each of several shear rates and test temperatures. The shear rates employed ranged approximately from  $30 \text{ sec}^{-1}$  to  $300 \text{ sec}^{-1}$  while the testing temperature ranged from  $90^{\circ}\text{F}$  to  $30^{\circ}\text{F}$ . A number of additional experiments were also



performed at shear rates of  $1000 \text{ sec}^{-1}$  to  $1500 \text{ sec}^{-1}$  in order to determine the consistency of the Newtonian solvent. The thermal history of the majority of the crude oil samples tested, consisted of storage at  $75^{\circ}\text{F}$  for a period of ten days. However, for purposes of comparison, the effect of storage at  $15^{\circ}\text{F}$  on the consistency behavior was also investigated and certain selected results are presented.

Correlation of the experimental data in terms of the theoretically predicted logarithmic relationship was quite satisfactory in that the entire consistency decay curve could be described within the limits of accuracy of the data provided that the initial and final values of shear stress were known. Furthermore the nature of the experimentally determined rate constants was found to be consistent with that predicted by the theory.

In view of these results it was concluded that the behavior of at least one thixotropic fluid, Pembina crude oil, could be adequately defined in terms of the kinetic behavior of a relatively simple network model.



## I INTRODUCTION

The concept of viscosity is probably older than recorded history for it originated at the time primitive man first became aware of the difference in, "thickness," or, "heaviness," between fluids. Yet, in spite of its long history, the intrinsic nature of this fundamental property has only been clearly explained in comparatively recent times. Even after the brilliant hypothesis propounded by Newton <sup>(31)</sup> in his Principia,

"Resistentiam quae oritur ex defectu lubricitatis partium Fluidi, caeteris paribus, proportionalem esse velocitati qua partes Fluidi separantur ab invicem,"

very little advance took place in this subject until the turn of the nineteenth century. At that time Navier <sup>(34)</sup> and Stokes <sup>(48)</sup> suggested that real fluids differed from the ideal (inviscid) fluids by virtue of an internal resistance, now known as viscosity. The manifestations of this property were later demonstrated by the French physiologist, Jean Poiseuille <sup>(39)</sup> in his classical experiments designed to explain the flow of blood through the blood capillaries. It is interesting to note that, had he in fact used blood rather than water in these experiments, his results, which ultimately led to the renowned Poiseuille law, would have been discouraging indeed. For, shortly thereafter, Watson <sup>(54)</sup> showed that the flow behavior of blood was very complex and did not conform to the provisions of Newton's hypothesis. Other fluids, whose flow behavior, or rheological properties, were inexplicable in terms of the "ideal" model, were then discovered in rapid succession. Many attempts were made to classify and explain these deviations and thus



began the study of non-Newtonian rheology.

Among these fluids, which for lack of a better expression, may be called anomalous, are found a large number of Alberta crude oils. Whereas the consistency of the Newtonian fluid at any specified temperature and pressure may be expressed in terms of a constant viscosity, the consistency of these crude oils, especially at low temperature, must be defined with respect to shear rate, time of shearing and previous thermal and shear history.

Clearly, from an engineering point of view, the relationships existing between these variables must be known in order that such calculations as are involved in pipeline design may be executed with reasonable accuracy. To this end, a program of research on this problem was initiated in 1951 in the Department of Chemical and Petroleum Engineering at the University of Alberta under sponsorship of the Interprovincial Pipe Line Company Limited.

Certain aspects of this work, which consisted of rheological and pilot pipe line studies of several crude oils, will be mentioned later. Suffice it to say here, that the early studies of Redwater, Fosterton, Success, Cantaur and Pembina crude oils were undertaken with the essentially practical objective of evaluating the effect of shear rate on apparent viscosity for purposes of pipe line design and throughput calculations. Information obtained was very useful for these applications however, especially in the case of Pembina crude oil, it was soon realized that the highly complex relationships between the numerous variables governing consistency behavior could



not be resolved by this simple, direct approach. As a result, the data obtained were very difficult to evaluate or reproduce. It appeared then, that a more profitable procedure might be to investigate the independent effects of each variable under carefully controlled conditions. The instrument considered most suitable for this fundamental study was the rotational viscometer since, in addition to its relative simplicity of operation, it offered several distinct advantages over other types. Most significant among these was the ease of accurate control of testing conditions and standardization of sample handling techniques.

The particular viscometer chosen for the investigation was the Alberta Rotational Viscometer. Originally designed and constructed by J.V. Fisher<sup>(16)</sup>, this instrument was modified to provide adequate means of precise temperature control and measurement and to minimize the evaporation loss of low molecular weight hydrocarbons from the oil samples during analysis.

Although the various crude oils encountered in Alberta display a variety of rheological properties, ranging from Newtonian to time dependent or thixotropic, only one fluid, Pembina crude oil, was selected for analysis. The reasons for this choice were twofold. First, Pembina crude oil appeared to possess all of the anomalies likely to be found in other crude oils. Second, by so restricting the scope of the investigation, a reasonably thorough scrutiny of the behavior of this fluid was possible.



It was originally intended that a quantitative evaluation of the individual effects of time of shearing, shear rate, temperature, shear history and thermal history on consistency behavior would be included in the investigation. However, for reasons which will be explained later, the last two of these were given only qualitative study while the first three were studied in some considerable detail.

The particular characteristic which distinguishes a thixotropic fluid from all others is the isothermal reduction in consistency with time at constant shear rate. The exact nature of the physical changes responsible for this behavior are not known at present. However, one possible and the generally accepted explanation is that a portion of the viscous resistance is due to the occurrence of loosely bonded network structures which dissociate under the action of shear. If, in fact, this is true, it is reasonable to assume that the mechanism of network destruction is somewhat analogous to a chemical reaction and might be described in a similar kinetic fashion.

In this study, a theory, based on these assumptions, was developed and tested by means of experimental observation. The resulting correlation was rather gratifying since at least some measure of confirmation of the proposed theory was achieved. In addition several interesting conclusions concerning the effects of shear rate, temperature and shear history were drawn and shown to be consistent with the anticipated behavior of a network structure.



## II GENERAL ASPECTS OF RHEOLOGY

The fundamental concept of viscosity is derived from Newton's hypothesis that the resistance offered to the motion of two parallel plates separated by a fluid is proportional to the relative velocities of the plates. In mathematical terms viscosity is simply the proportionality constant in the equation.

$$\tau = -\frac{\mu}{g_c} \left( \frac{dv}{dx} \right) \quad (1)$$

where  $\tau$  is the unit frictional retarding force or unit

shear stress,  $lb_f/ft^2$

$dv/dx$  is the velocity gradient,  $sec^{-1}$

$\mu$  is the viscosity,  $lb_m/sec.ft.$

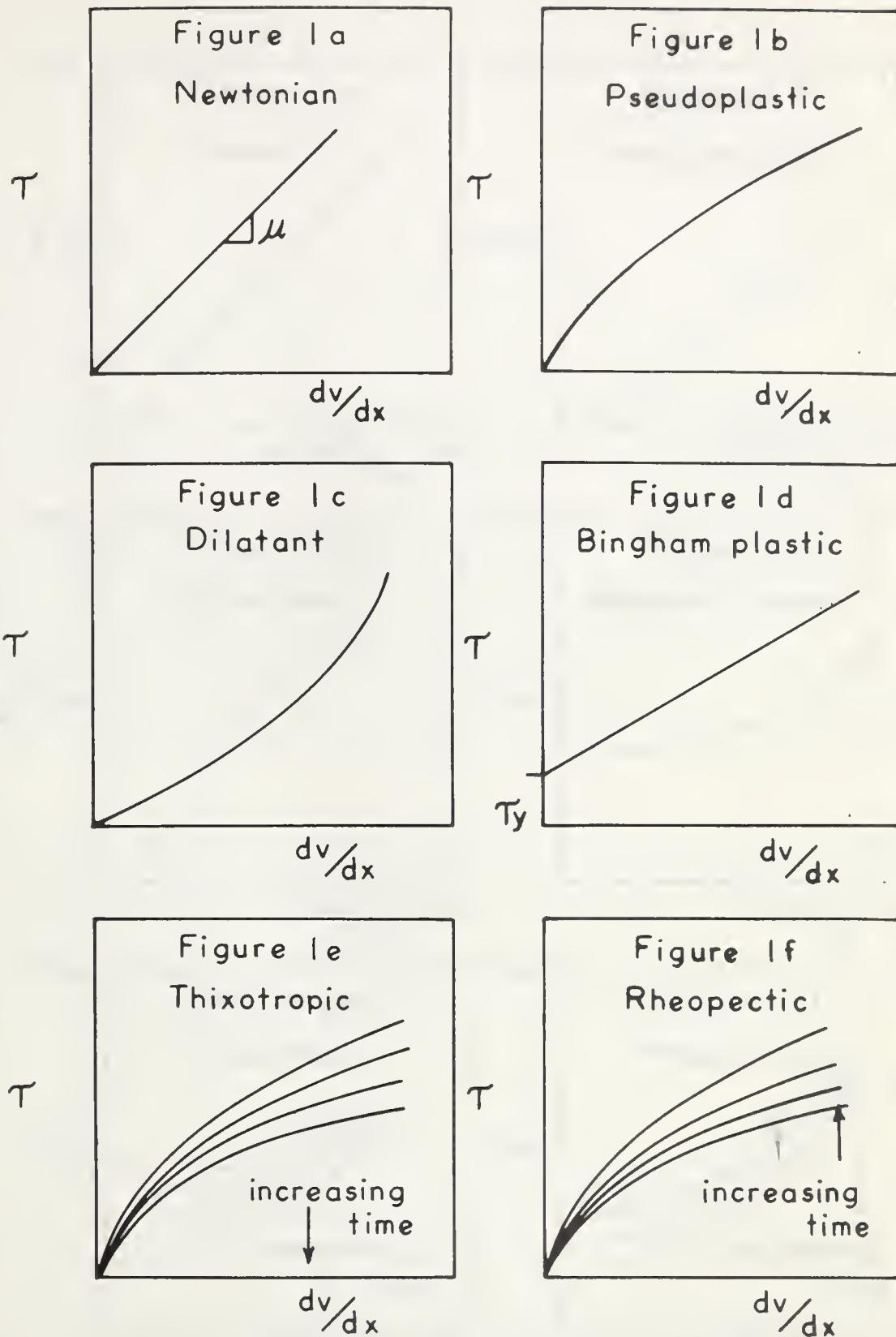
and  $g_c$  is the dimensional conversion factor,

$lb_m ft/lb_f sec^2$

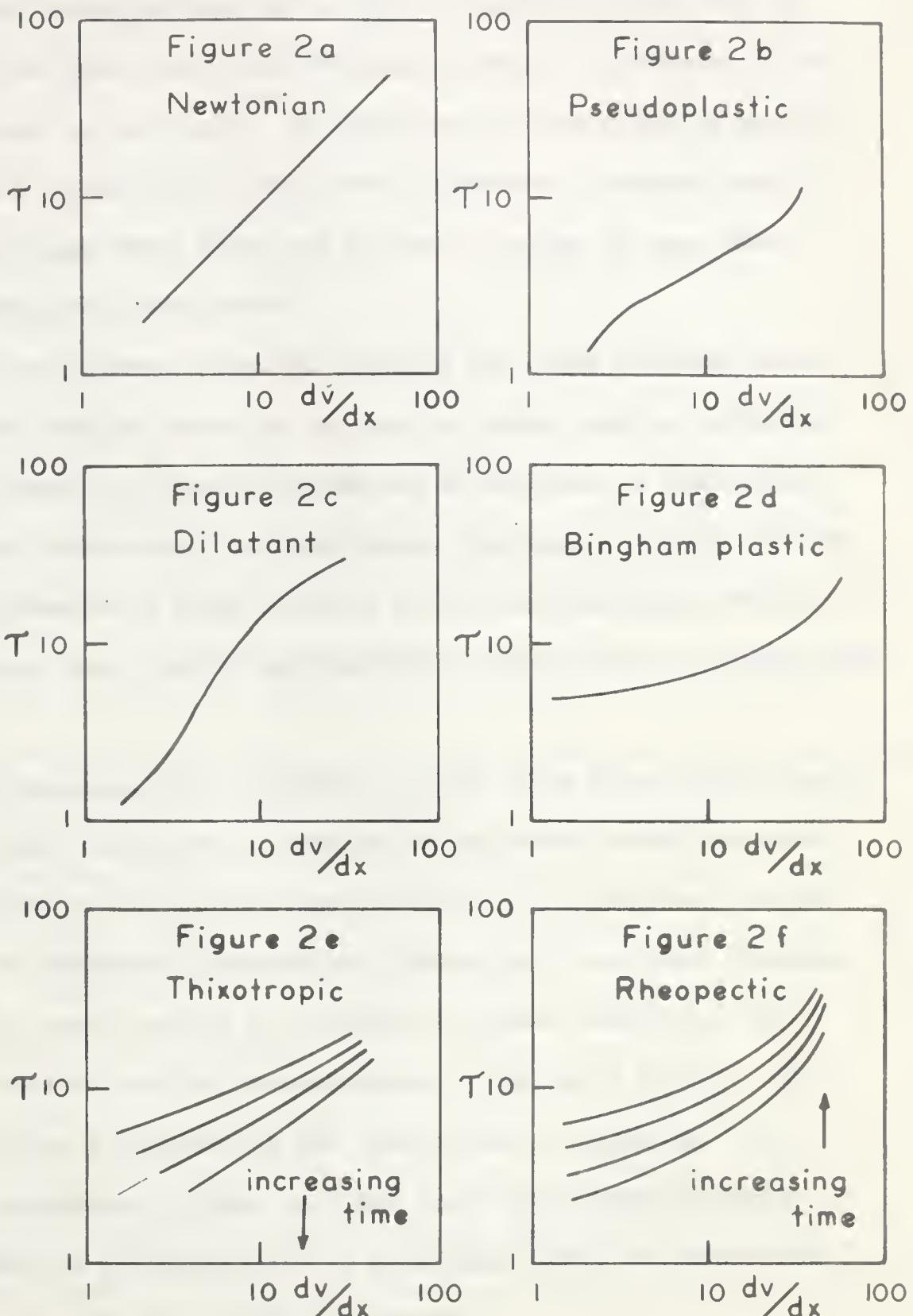
If, as has been assumed in the hypothesis, the viscosity coefficient is in fact constant, a plot of  $\tau$  vs  $dv/dx$  describes a straight line passing through the origin on arithmetic coordinates and a line of slope equal to one on logarithmic coordinates. This is illustrated on Figures (1a) and (2a).

In a manner somewhat analogous to the ideal gas law, which relates the pressure, volume and temperature of a gas, this relationship provides a reasonable approximation to the flow equation for many fluids over a limited range of temperature, pressure and rate of shear. However, most liquids at some conditions and some liquids at all conditions demonstrate marked deviations from this "ideal" behavior. For certain liquids, those classified as pseudoplastics, the consistency is found











to decrease with increasing shear rate or shear stress. Thus, on arithmetic coordinates (Figure 1b), the curve relating shear stress with shear rate passes through the origin, is concave to the rate of shear axis at low shear rates and eventually attains a constant slope as the shear rate is increased. On logarithmic coordinates (Figure 2b) the shear stress versus shear rate curve approaches a slope of unity at both low and high shear rates and displays a slope of less than unity at intermediate shear rates.

For the dilatant class of liquids, the curve relating shear stress to shear rate is convex to the rate of shear axis on arithmetic coordinates (Figure 1c) thereby indicating an increase in consistency with increasing shear rate. On logarithmic coordinates (Figure 2c) the curve again approaches a slope of unity at low and high shear rates but, in this instance, the slope at intermediates shear rates is greater than unity.

The Bingham plastic exhibits a yield value below which elastic deformation rather than flow is encountered and above which the shear stress, in excess of the yield value, is directly proportional to the shear rate. On arithmetic coordinates (Figure 1d), the curve relating shear stress to shear rate is a straight line which intersects the shear stress axis at a value corresponding to the yield stress. The slope of this line is defined as the coefficient of rigidity. On logarithmic coordinates (Figure 2d), the curve for Bingham plastics is similar to that for pseudoplastics at high shear rates but approaches a slope of zero as the shear rate is reduced.



The thixotropic and rheopectic classes of liquids exhibit a time dependent consistency behavior. At a sustained, constant shear rate, the consistency of a thixotropic liquid is observed to decrease with time to some lower limiting value while, for any specified time of shearing, the relationship between shear stress and shear rate is similar to that which characterizes the pseudoplastic liquid. Thus on arithmetic coordinates (Figure 1e), the relationship between shear stress and shear rate for such a liquid may be represented by a family of curves which are concave to the rate of shear axis and for which the parameter is duration of shear. On logarithmic coordinates (Figure 2e) each curve, corresponding to a constant time of shearing, is again similar in form to that of the pseudoplastic liquid discussed previously.

The rheopectic liquid may be regarded as the antithesis of the thixotropic liquid since, at constant shear rate, the consistency tends to increase with duration of shear. However, since very few of these systems have been studied, the exact form of the curve relating shear stress with shear rate at any time of shearing is not known. The arithmetic (Figure 1f) and logarithmic (Figure 2f) plots presented here merely illustrate one possible type of rheopectic behavior.

While these deviations may be viewed as anomalies, it is probably more correct to consider equation (1) to be the limiting case of a more general flow theory, even though no such universal rheological equation of state has ever been discovered.



### Mechanistic Theories

The behavior of certain fluids may be described in terms of both viscous and non viscous or elastic forces. That is, the stresses arising within a liquid subjected to an external force depend on both the rate of deformation and the extent of deformation. The former leads to an irreversible process in which energy is dissipated as heat while the latter leads to a reversible process from which the energy may theoretically be recovered upon removal of the applied force. The Newtonian or ideal fluid, then, is one in which the elastic component of stress is zero whereas the opposite situation describes the ideal or Hookeian solid. Real materials, which may in accordance with this concept be called viscoelastic, exhibit a whole spectrum of behavior from the totally viscous to the totally elastic.

### Theories Based on Mechanical Analogs

Many approaches have been used to describe the behavior of such materials in terms of simple models. Perhaps the earliest of these, based on the Maxwell and Kelvin or Voigt bodies<sup>(41)</sup>, compare the material to a system of Hookeian springs and viscous dashpots arranged in series and in parallel respectively.

The mathematical expression for the Maxwell body, which considers the total rate of elongation under an applied stress as the sum of the individual contributions from the spring and dashpot, may be written

$$\frac{dv}{dx} = \frac{1}{G} \left( \frac{dT}{dt} \right) + \frac{g_c T}{\mu} \quad (2)$$



The corresponding expression pertaining to the Voigt body, for which the total stress is the sum of the stresses acting on each component, takes the form

$$\tau = G \left( \frac{\Delta l}{l} \right) + \frac{\mu}{g_c} \left( \frac{dv}{dx} \right) \quad (3)$$

In each case  $\tau$  is the shear stress,  $lb_f/ft^2$

$G$  is the shear modulus of the spring,  $lb_f/ft^2$

$\mu$  is the viscosity,  $lb_m/ft \text{ sec}$

$dv/dx$  is the shear rate,  $\text{sec}^{-1}$

and  $\Delta l/l$  is the unit strain in the spring.

Inspection of the models indicates that the Maxwell body, under the action of an applied stress, will initially undergo elastic deformation followed by unrestricted viscous flow. Under the same conditions the Voigt body will undergo deformation at a decreasing rate until the elongation of the spring is proportional to the applied force whereupon deformation will cease. Furthermore the Maxwell body at constant strain will experience stress relief due to the action of the spring on the dashpot. This stress relief effect is conveniently expressed in terms of the ratio between the viscosity coefficient and the spring modulus. The resulting parameter is called the relaxation time and is the time required for the stress to relax to  $1/e$  of the initial stress. In an analogous manner, removal of the stress from the Voigt body results in strain recovery which may be characterized by a retardation time representing the time required for the strain to recover to  $1/e$  of its initial value.<sup>(1)</sup> These parameters have been



used extensively in describing the behavior of viscoelastic materials.

Although it has been demonstrated<sup>(24)</sup> that either model may be used to explain viscoelastic behavior, the Maxwell body is generally applied to those substances normally classified as liquids while the Voigt body is used in connection with solids.

The behavior of certain viscoelastic liquids may adequately be defined by theories based on these models or various modifications and combinations of them. Included among these liquids are many dilute and concentrated high polymer solutions subjected to small deformation<sup>(62)(63)(27)</sup> and Bingham plastics, all of which may be considered as "linear" since elastic effects follow Hooke's law and viscous effects are Newtonian. On the other hand the non linear behavior demonstrated by pseudoplastics under conditions of varying shear rate and thixotropic liquids in general cannot readily be explained in terms of these models alone.

#### Microrheological Theories

A second approach, based on the theory of absolute reaction rates, has been proposed by Eyring<sup>(15)(8)</sup>. The system is here represented by a cell model in which the motion of one molecule of the liquid past its neighbors involves passage over a potential barrier. The presumed mechanism may be described briefly as follows.

Density fluctuations within a liquid free of stress provide sufficiently large openings to permit neighboring molecules to associate, undergo rotation as a couplet in any direction, and then again to dissociate. Under the influence of an applied stress, rotation in the



direction of the stress will be favored and the material will be observed to flow. Although several steps are involved in the process, it may be shown that the "activation energy of hole formation" or potential energy required to establish the free space is likely the rate determining factor. The similarity between this mechanism and the activation energy theory pertaining to chemical reaction kinetics is apparent.

Here again, as with the theories based on the previously described Maxwell and Voigt models, the relationships resulting from mathematical analysis of the cell model describe simple systems reasonably well. Complex rheological behavior cannot be readily explained without the introduction of many qualifying assumptions.

The second microrheological approach toward formulation of a generalized equation of state is the molecular theory. In this instance an attempt is made at defining rheological behavior in terms of the radial distribution of molecules and molecular velocities around a reference molecule. Hence a thorough understanding of intermolecular forces<sup>(22)</sup> is required. In reality, due to the very limited knowledge of complex molecular interaction, precise mathematical relationships between viscosity and intermolecular potential cannot be established. At best the viscosity of the simplest systems can only be predicted as to order of magnitude<sup>(9)</sup>. In spite of these apparent deficiencies, it is reasonable to expect that the most significant future advancement toward the formulation of a general theory will come about through extension and refinement of the molecular theory since



consideration is here given to the fundamental cause of energy dissipation.

Many of the difficulties inherent in the application of the molecular theory have been avoided by again resorting to models. These models take the form of simplified molecular structures whose properties may be defined in relatively simple mathematical terms and are consistent with the observed behavior of the material.

The model most commonly chosen, the so called Rouse model,<sup>(46)</sup> consists of freely coiling chains comprising Hookean springs connected by universal joints. The state of the model is then defined in terms of the vector distance between ends, assumed to follow a Gaussian distribution,<sup>(66)</sup> and the force exerted on the springs.

As might be expected, the mathematical relationships describing viscoelastic materials subjected to small strains in terms of this model are equivalent to those obtained through analysis of the Maxwell model<sup>(64)</sup>. The movement of chains past each other or the destruction and instantaneous reformation of weak bonds between chains corresponds identically with the behavior of the spring and dashpot in the earlier model.<sup>(2)(24)</sup>

The concept of a molecular chain model may, with some modification, be applied at least qualitatively to many materials exhibiting pseudoplastic and thixotropic behavior under the influence of sustained shear of variable magnitude and is therefore of particular interest to the present study. Prior to shearing, the condition of a pseudoplastic liquid may be visualized as consisting of randomly



oriented coiled chains suspended in a solvent and more or less isolated from each other. This latter condition implies that extensive chain entanglement does not occur. Viscous drag arising from shear in the system will tend to uncoil the chains and orient them in the direction of flow<sup>(38)</sup>. Brownian motion, on the other hand, opposes the orientation and thereby causes the chain to assume a final position which is somewhat inclined to the direction of flow.<sup>(45)(67)(18)</sup> Now, since the chain extends through regions of differing velocity, viscous forces are generated which occasion a certain amount of energy dissipation. If the shear stress in the fluid is increased by an increase in the shear rate, the influence of the orienting viscous force is also increased while Brownian motion remains unchanged. The net result is a greater degree of chain alignment in the direction of flow, less energy dissipation at the surface of the chains and consequently a reduction in observed structural viscosity. Furthermore, since the process is reversible, the flow curve for the material will be reproducible with both increasing and decreasing shear rate.

The mechanism responsible for thixotropic behavior, encountered in undiluted liquid polymers and numerous other fluids, is exceedingly more complex since close proximity permits extensive entanglement of the coiled chains. The resistance to flow offered by such agglomerates will undoubtedly be much greater than that produced by the same concentration of individual particles. Moreover the application of shear, in addition to aligning the chains, causes dissociation or disentanglement of the loosely bonded network segments<sup>(17)</sup>. Since the



latter process is not instantaneous, but may in fact require a significant length of time, the shear stress at constant shear rate is observed to decrease with time to some low constant value. A further complication is added by the reentanglement of chains due to Brownian movement and subsequent dissociation of the new links. Thus the limiting value of shear stress, obtained after a sufficient duration of shearing, does not represent a network-free condition but rather a state of equilibrium between dissociation and recombination of chains. Considerable evidence supporting this mechanism has been obtained in the present study and will be discussed later.

#### Non-Mechanistic Techniques

Many elegant theories have been developed in connection with the various models mentioned in the foregoing paragraphs. Yet, except for those which pertain to extremely simple systems, such as the dilute suspension of spheres analyzed by Einstein,<sup>(14)(19)</sup> the theories are of rather limited utility. When the chosen model is sufficiently simple to permit thorough mathematical analysis, the mathematical relationships do not, in general, describe the observed behavior. On the other hand, a model which adequately describes the properties of the system is so complex that the resulting mathematical expressions are often difficult or impossible to apply.

From an engineering point of view, the need for suitable generalizations is so urgent that empirical or semi-empirical correlations have been found more immediately useful. This empirical approach has,



in some instances, provided techniques which may be confidently applied to a wide variety of design problems. A striking example may be cited with respect to Bingham plastic liquids whose rheological properties are arbitrarily defined by the equation

$$\tau - \tau_y = - \frac{\eta}{g_c} \left( \frac{dv}{dx} \right) \quad (4)$$

where  $\tau_y$  is the yield stress below which the material behaves essentially as a solid undergoing only elastic deformation,  $lb_f/ft^2$ .

and  $\eta$  is the coefficient of rigidity,  $lb_m/\text{sec.ft.}$

For any fluid flowing in a circular pipe it may readily be shown that

$$\tau = \frac{(\Delta P) r}{2 L} \quad (5)$$

where  $\Delta P$  is the pressure drop along the pipe  $lb_f/ft^2$

$r$  is the distance from the center of the pipe to any point in the fluid, ft.

and  $L$  is the length of the pipe, ft.

By substituting this relationship into equation (4) and assuming negligible kinetic and end effects, Buckingham<sup>(10)</sup> was able to solve the differential equation. The resulting expression

$$v = \frac{g_c}{\eta} \left( \frac{\Delta P}{4L} (R^2 - r^2) - \tau_y (R - r) \right) \quad (6)$$



described the velocity profile in a pipe under laminar flow conditions in terms of coefficient of rigidity, pressure drop, radius and yield stress. Then, recognizing that the total volume of fluid flowing is defined by

$$Q = \int_0^R 2\pi r dr (v) \quad (7)$$

where  $Q$  is the flow rate,  $\text{ft}^3/\text{sec.}$

and  $v$  is the velocity,  $\text{ft/sec.}$

he was able to derive the following relationship between flow rate, pressure drop and the properties of the system.

$$Q = \frac{\pi D^4 g_c}{128 \eta L} \left( \Delta P - \frac{4}{3} \left( \frac{4L T_y}{D} \right) + \frac{(32 L T_y)^4}{3 (\Delta P)^3 D^4} \right) \quad (8)$$

where  $D$  is the pipe diameter,  $\text{ft.}$

Equation (8), which applies to laminar flow, provides a method for design computation which is theoretically as accurate as the flow equation used to describe the rheological properties.

The validity of equation (8) has been experimentally verified through correlation of data in a manner which was found successful for Newtonian fluids. Relatively simple manipulation of equation (8) and comparison of the results with the well known Fanning equation

$$\frac{\Delta P}{\rho} = - \frac{2 f L v^2}{g_c D} \quad (9)$$

where  $f$  is the friction factor,

and  $\rho$  is the density  $\text{lbm/ft}^3$



yields an equation for Bingham plastics

$$f = \frac{16 \eta}{D v \rho} \left[ \frac{1}{1 - \frac{4}{3 \Delta P} \left( \frac{4 L T_y}{D} \right) + \frac{1}{3 (\Delta P)^4} \left( \frac{4 L T_y}{D} \right)^4} \right] \quad (10)$$

which has essentially the same form as the corresponding equation for laminar flow of Newtonian fluids

$$f = \frac{16 \mu}{D v \rho} \quad (11)$$

and reduces to it when  $T_y$  is equal to zero.

Experimental data obtained by Govier and Winning<sup>(61)</sup> and correlated in terms of equation (10) produced satisfactory results.

Other approaches involving dimensional analysis have also been studied by Govier and Winning<sup>(61)</sup> and Hedstrom<sup>(25)</sup>. Govier and Winning found that for laminar flow the experimentally determined friction factor could be related to Reynolds' number (based on the coefficient of rigidity) if a dimensionless group, the yield value, was used as a parameter. The mathematical expression of this statement is simply

$$f = \phi \left( \frac{D v \rho}{\eta}, \frac{D T_y g_c}{v \eta} \right) \quad (12)$$

where the second term in parenthesis is the yield value.

The method employed by Hedstrom was basically similar except that the yield value was replaced by another dimensionless group,



since called the Hedstrom number, which has the form

$$\frac{D^2 \rho T_y g_c}{n^2}$$

and represents the product of the Reynolds' number and the yield value.

It might also be pointed out that both authors demonstrated adequate correlation between friction factor and Reynolds' number regardless of the yield value or Hedstrom number in the fully developed turbulent flow region.

In a technological sense it may be said that the behavior of Bingham plastics is reasonably well understood. Unfortunately this same statement cannot be applied to pseudoplastic liquids. It is evident from the foregoing discussion that the primary problem confronting the formulation of a theory which adequately describes the flow of non-Newtonian fluids is one of accurately defining the flow curve in simple mathematical terms. This task has never been fully accomplished in the case of pseudoplastic fluids although several notable attempts have been made.

The most primitive expression used to define the consistency of these materials is similar in form to the statement of Newton's hypothesis and may be written

$$T = - \frac{\mu'}{g_c} \left( \frac{dv}{dx} \right) \quad (13)$$

where  $\mu'$ , the apparent viscosity, represents the slope of a line



drawn from the origin to any specified point on the flow curve. Then, since the flow curve is non-linear, this coefficient is not constant but varies in accordance with the shear rate. For purposes of pipe line design under turbulent flow conditions, the apparent viscosity is evaluated in a suitable viscometer either at a shear rate approximating that expected at the pipe wall or at a very high shear rate under which condition it becomes essentially constant. The selected value of the coefficient is then used in place of viscosity in evaluating a modified Reynolds' number.

Correlations based on apparent viscosity have been found quite suitable in the turbulent flow region but fail to characterize laminar flow adequately. This situation might be anticipated on two counts. First, in turbulent flow the apparent viscosity is relatively constant due to the high shear rates. Second, as the Reynolds' number increases the friction factor becomes less dependent on viscous forces, therefore reasonably large errors in the consistency parameter may be tolerated. In laminar flow, since the shear rate varies from zero at the center of the pipe to a maximum at the wall and since the friction factor is directly proportional to the viscosity, an apparent viscosity evaluated at a single shear rate cannot be expected to properly define the entire system. Briefly, the major criticism of apparent viscosity is that this parameter has no fundamental significance and does not therefore represent a real property of the fluid.



A second expression, developed by Eyring and Powell<sup>(40)(46a)</sup> to describe the flow curve of pseudoplastic materials,

$$\tau = - \frac{\mu}{g_c} \left( \frac{dv}{dx} \right) - \frac{1}{B} \sinh^{-1} \left( \frac{dv/dx}{C} \right) \quad (14)$$

has been integrated numerically and presented in the form of charts relating pressure drop to flow rate by means of dimensionless groups.<sup>(11)</sup> Agreement between predicted and experimental results has been promising in spite of the fact that equation (14) does not accurately define the behavior of all pseudoplastics.

Probably the most significant contributions to the interpretation of pseudoplastic flow behavior have been made in connection with those fluids whose flow curve may be approximated by an empirical power law equation of the type

$$\tau = - K \left( \frac{dv}{dx} \right)^n \quad (15)$$

If  $K$ , the fluid consistency index and  $n$ , the flow behavior index, may be considered as essentially constant over the shear rate range of interest, this equation may be integrated.<sup>(56)</sup> A useful form of the resulting equation expresses pressure drop along a pipe in terms of average fluid velocity and the properties of the system under laminar flow conditions.

$$\Delta P = 4K \left( \frac{6n+2}{n} \right)^n \frac{(v)^n L}{(D)^{n+1}} \quad (16)$$



Comparing equation (16) with the Fanning equation and the friction factor - Reynolds' number relationship for laminar flow of a Newtonian fluid, led Weltman<sup>(57)</sup> to the following definition of friction factor

$$f = \frac{16}{R_e} \left( \frac{3n+1}{4n} \right) \quad (17)$$

in which the Reynolds' number is defined by

$$R_e = \frac{D v \rho}{\mu''} \quad (18)$$

The consistency  $\mu''$  is evaluated at the wall shear rate and may be shown to be

$$\mu'' = K \left[ \left( \frac{3n+1}{n} \right) \left( \frac{2v}{D} \right) \right]^{n-1} \quad (19)$$

Equation (17) describes a family of curves on logarithmic coordinates which are parallel to the familiar curve corresponding to Newtonian fluids. The latter curve merely represents the limiting case in which "n" is equal to unity.

The primary difficulty encountered in the application of equations (16) and (17) to pipe line design, arises from the assumption that "n" is constant. In reality "n" is not constant over the full range of shear rates, but approaches unity as the shear rate approaches zero at the center of the pipe. Although this limitation may not be serious in some cases, it is significant that most pseudoplastics



demonstrate a variable flow behavior index to values of shear rate considerably greater than zero. Consequently the accurate solution of equation (15) may require time-consuming averaging techniques.

In order to overcome this problem a somewhat different approach, based on a theoretical analysis of non-Newtonian fluids originally performed by Mooney<sup>(33)</sup> has been proposed by Metzner and Reed<sup>(31)(32)</sup>. Assuming that the flow curve of any fluid may be described by equation (13) treating  $\mu'$  as a variable coefficient, and assuming further that slip at the wall is negligible, Mooney developed the following expression relating shear rate at the pipe wall to flow rate and pressure drop.

$$-\left(\frac{dv}{dr}\right)_w = \frac{3}{4} \left(\frac{8v}{D}\right) + \frac{1}{4} \left(\frac{D\Delta P}{4L}\right) \left[ \frac{d(8v/D)}{d(D\Delta P/4L)} \right] \quad (20)$$

Multiplying and dividing the differential term by  $8v/D$  and rearranging yields

$$-\left(\frac{dv}{dr}\right)_w = \frac{3}{4} \left(\frac{8v}{D}\right) + \frac{1}{4} \left(\frac{8\gamma}{L}\right) \left[ \frac{d(\ln 8v/D)}{d(\ln D\Delta P/4L)} \right] \quad (21)$$

Mooney further demonstrated that the quantity  $8v/D$  was independent of pipe diameter provided only that the shear stress at the wall was constant.

Considering only the last term of equation (21) Metzner defined a flow behavior index  $n'$  such that

$$n' = \frac{d(\ln D\Delta P/4L)}{d(\ln 8v/D)} \quad (22)$$



Then, assuming  $n'$  to be a constant independent of shear stress at the pipe wall, he integrated equation (22) which yielded

$$\frac{D\Delta P}{4L} = K' \left( \frac{8v}{D} \right)^{n'} \quad (23)$$

Again, since  $8v/D$  is not a function of pipe diameter at constant wall shear stress, equation (23) should also be independent of pipe diameter at any particular value of  $D\Delta P/4L$ . Hence, evaluation of  $n'$  and  $K'$  by means of a capillary viscometer provides the information necessary for calculation of pressure drop at any desired flow rate in a pipe of specified diameter.

If on the other hand  $n'$  is not constant but varies with shear stress, equation (23) describes the tangent to a curve relating  $D\Delta P/4L$  to  $8v/D$  at the particular wall shear stress in question. Pipe line pressure drop may then be estimated by selecting the appropriate value of  $n'$  corresponding to the obtaining shear stress at the wall.

For the sake of convenience in application, equation (23) has also been restated in terms of friction factor and Reynolds' number

$$f = \frac{16}{Re} \quad (24)$$

where  $Re = \frac{D^{n'} v^{2-n'} \rho}{\gamma_1}$

and  $\gamma_1 = g_c K' S^{n'-1}$



Here again the Reynolds' number reduces to the conventional form for Newtonian fluids in which case  $n'$  is unity.

It must be pointed out that equation (24) does not provide a test for any set of experimental data for which  $n'$  and  $K'$  have been determined through application of equation (23) since such results must, by definition, conform to the relationship in equation (24). The utility of this equation is realized in the prediction of pipe line pressure drop when  $K'$  and  $n'$  have been independently determined by means of some suitable viscometer, preferably of the capillary type.

Dodge and Metzner<sup>(13)</sup> have extended the application of the generalized Reynolds' number to the turbulent flow region and have proposed an empirical correlation between friction factor and Reynolds' number with  $n'$  as parameter. Later a mathematical expression relating friction factor and Reynolds' number was also developed by these authors<sup>(13)</sup> and presumed to be the general case for which the familiar von Karman equation is a specific solution peculiar to Newtonian fluids. This equation may be written in the form

$$\sqrt{\frac{1}{f}} = \frac{4 \cdot C}{(n')^{0.75}} \log \left( Re f^{\{ -n'/2 } \right) - \frac{C \cdot 4}{(n')^{1.2}} \quad (25)$$

and provides reasonably good agreement between predicted and experimentally measured friction factors for a number of pseudoplastic liquids.



### III THEORIES OF THIXOTROPY

It may be concluded from the preceding discussion that, while the selection of a simple expression which accurately describes the rheological properties of pseudoplastic fluids has been difficult, a number of empirically derived approximations are available and provide a suitable basis for most engineering calculations. This same situation does not exist with respect to thixotropic fluids. Variations in apparent viscosity with time at constant temperature and shear rate and the complex interactions between these variables have perpetually confounded the formulation of an equation which adequately defines the behavior of these materials. For example, the apparent viscosity at any shear rate and, in fact, at any time of shearing is not constant but rather is dependent upon the cumulative effects of previous shearing at other shear rates. Clearly then, such relationships as the power law equation are inapplicable, since the parameters K and n, which are reasonably constant for many pseudoplastics, become variables which may change drastically with time of shearing.

In recent years many attempts have been made to describe, both qualitatively and quantitatively, the consistency decay of thixotropic fluids. A number of the more significant approaches are reviewed in the following pages with particular emphasis placed on those which are relevant to the present study.

Weltman and coworkers<sup>(58)(59)(21)</sup> have demonstrated the combined effects of shear rate and duration of shear on the behavior



of thixotropic fluids such as greases and polymers. For this purpose they employed a rotational viscometer, so equipped that the shear rate could be varied continuously, at a predetermined rate, from zero to a maximum and back to zero again. The shear stress generated within the fluid, when plotted as a function of the instantaneous shear rate, exhibited a hysteresis loop. The exact form of the curve was found to depend on rate of change of shear rate, maximum shear rate encountered and the number of cycles completed. Furthermore the area enclosed by the curves decreased with increases in any of the above variables and eventually became zero after a sufficient number of cycles. The final curve was therefore similar in form to the conventional pseudoplastic flow curve. It was also observed that the original thixotropic condition could be regained only through subsequent thermal treatment of the samples.

These results indicate that thixotropic fluids are irreversibly altered by shear action and that the structural changes are accompanied by a decrease in consistency to some lower limiting value. To provide a quantitative measure of thixotropic behavior these authors suggested two coefficients which are defined by

$$M_n = \frac{n_1 - n_2}{g_c \ln(\omega_2 / \omega_1)} \quad (26)$$

$$B_n = -\frac{t}{g_c} \left( \frac{dn}{dt} \right) \quad (27)$$



where  $M\eta$  is the loss in shear stress per unit increase in shear rate and denotes the structural change with increasing shear.

$B\eta$  is the change in plastic viscosity with time multiplied by the time of shearing and represents the structural change arising from prolonged shear at a constant shear rate.

$\eta$  is the slope of the shear stress vs shear rate curve at any specified shear rate, lb<sub>m</sub>/ft.sec.

and  $\omega$  is the angular velocity of the viscometer cup, radians/sec.

Although this interpretation provides a relatively simple technique for comparing one thixotropic fluid with another, it suffers from several serious limitations. First, experiments involving a time variable shear rate do not permit separation of the individual effects of time, shear rate or shear history on the consistency. Since at any time the observed behavior of the fluid is the net result of several complex phenomena, a suitable mathematical definition must incorporate all pertinent variables. Second, the coefficients  $M\eta$  and  $B\eta$  do not represent any real property of the system and, like apparent viscosity, are of limited utility in engineering design.

A somewhat more fundamental approach has been taken by other investigators. The decay in shear stress with time at constant shear rate is attributed to the destruction of a loose network structure.



Umstatter<sup>(52)(53)(26)</sup> originally drew attention to the similarity between the mechanism involved in structural change and the characteristics of the Maxwell model. This model has been defined mathematically by the expression

$$\frac{dT}{dt} = G \frac{dv}{dx} - \frac{T}{\lambda} \quad (28)$$

where  $G$  is the shear modulus of the spring,  $\text{lb}_f/\text{ft}^2$

$\lambda$  is the relaxation time  $\mu/G$ , seconds

and  $t$  is the time of shearing, seconds

Integrating this expression at constant rate of shear he obtained

$$\ln \left[ G \lambda \left( \frac{dv}{dx} \right) - T \right] + C_1 = - \frac{t}{\lambda} \quad (29)$$

or its equivalent form

$$T - G \lambda \left( \frac{dv}{dx} \right) = C_1 e^{-\frac{t}{\lambda}} \quad (30)$$

Substituting the boundary conditions into equation (30) at  $t = 0$

and  $t = \infty$  gives

$$T_0 = G \lambda \left( \frac{dv}{dx} \right) + C_1 \quad (31)$$

$$T_\infty = G \lambda \left( \frac{dv}{dx} \right) \quad (32)$$

which may then be subtracted

$$T_0 - T_\infty = C_1 \quad (33)$$



Now, substituting equations (32) and (33) into equation (30) gives the expression

$$\tau = \tau_\infty + (\tau_0 - \tau_\infty) e^{-t/\lambda} \quad (34)$$

Dividing each term of equation (34) by  $dv/dx$ , the constant shear rate, yields the final exponential relationship

$$\mu = \mu_\infty^l + (\mu_0^l - \mu_\infty^l) e^{-t/\lambda} \quad (35)$$

Experimental verification of equation (35) has never been demonstrated. This is not surprising in view of the grossly oversimplified treatment of such a complex system. No consideration is given to the actual nature of the structural changes which occur. Yet, it is inherently assumed in the derivation that, in terms of a network model, the excess or structural stress (over and above that obtaining at  $t = \infty$ ) is proportional only to the number of networks present, all networks are identical in behavior, a network which has undergone a single cleavage no longer contributes to the structural stress and finally, degenerated network particles do not recombine to form new structure. The presence of these assumptions may be recognized by the nature of the derived expressions. Equation (32) which is clearly the definition of a Newtonian fluid, presupposes a final state devoid of structure rather than one of dynamic equilibrium between network decay and reformation. Furthermore, equation (34) is exactly analogous to the kinetic relationships for a first order irreversible chemical reaction in which the concentration of networks is expressed as a function of structural stress.



All of the assumptions outlined above are highly unlikely, since, in the actual case, networks of many sizes will occur and each will contribute to the structural stress in accordance with its size. It is therefore reasonable to conclude that, as the deformation progresses, the average size of networks will be diminished and the reduction in stress resulting from the destruction of these smaller units will be comparatively lower. The dependence of stress on network size may be simply explained in terms of the chosen model. Structural stress arises from the resistance to flow offered by the network. Then, since a network which extends over many shear planes will encounter a larger variation in fluid velocity than a smaller, partially oriented structure, viscous drag on the large network will be proportionately greater.

A further discrepancy in this assumption is also evident. The fact that thixotropic fluids demonstrate partial recovery of structure when shear is interrupted, suggests that recombination of network units will occur at all shear rates.

In order to account for the possible regeneration of internal structures, Goodeve<sup>(23)</sup> proposed a mechanism of destruction and reformation of structure which could be interpreted kinetically. This theory will be reviewed in some detail since it forms the basis of more recent approaches including the present one.

Considering two particles of a scaffolding structure connected by a single link as his elementary model, he postulated that,



under the influence of shear, distortion would proceed in accordance with Hooke's law

$$F = G' \Delta l \quad (36)$$

until the link ruptured.

$F$  in equation (36) is the force on the structure,  $\text{lb}_f/\text{ft}^2$   
 $G'$  is the modulus,  $\text{lb}_f/\text{ft}^2$ . per unit of extension  
 $\Delta l$  is the extension of the structure, ft.

Goodeve further assumed that, in a uniform velocity gradient,  $dv/dx$ , the extension at any time,  $t$ , is approximately

$$\times \left( \frac{dv}{dx} \right) t$$

where  $x$  is the distance, in feet, between shear planes drawn through each particle in the direction of flow. The force acting on the link at this time will then be

$$F = G' \times \left( \frac{dv}{dx} \right) t \quad (37)$$

Eventually the force will reach a critical value  $F_c$  and the link will be destroyed. Equation (37) accordingly becomes

$$t_c = \frac{F_c}{G' \times \left( \frac{dv}{dx} \right)} \quad (38)$$

where  $t_c$  represents the life of the link.

If it is then assumed that the overall rate of link destruction may be expressed as

$$\frac{dN}{dt} = - \frac{N}{t_c} \quad (39)$$



where  $N$  is the number of links, substitution of equation into equation (39) yields

$$\frac{dN}{dt} = - \frac{NG^1x}{F_c} \left( \frac{dv}{dx} \right) \quad (40)$$

Concurrent with the destruction of links, new links are formed due to collision of small particles. Since the rate of collision is assumed by Goodeve to be proportional to the velocity gradient and the square of the concentration of potential partners in the link, the rate of link production is

$$\frac{dN}{dt} = k(2N_0 - 2N)^2 \left( \frac{dv}{dx} \right) \quad (41)$$

Combining equations (40) and (41) gives an expression for the net rate of destruction of the links

$$\frac{dN}{dt} = k(2N_0 - 2N)^2 \left( \frac{dv}{dx} \right) - \frac{NG^1x}{F_c} \left( \frac{dv}{dx} \right) \quad (42)$$

Goodeve terminated his analysis at this point without attempting to express equation (42) in terms of measurable quantities such as shear stress.

Although Goodeve's theory is more plausible than that proposed by Umstatter, several unsubstantiated assumptions are made and will be discussed in connection with the derivation of the present theory.

One serious criticism of equation (42) is that it does not



permit quantitative experimental verification since neither  $N$  nor  $F_C$  are readily determined. This objection has been overcome by Storey and Merrill<sup>(49)</sup> during recent investigations of the rheological behavior of amylose and amylopectin, the two principal constituents of starch.

The mechanism of network destruction and reformation assumed by Storey and Merrill is essentially similar to that suggested by Goodeve. However, the resulting mathematical relationships are somewhat more general and are expressed in terms of quantities which are attainable through conventional viscometric techniques. These authors assumed, as did Goodeve, that the total stress generated within a thixotropic fluid experiencing shear, is the sum of a Newtonian component arising from the solvent and unassociated network particles and a second component provided by the network structure. The mathematical relationship between these components and the shear stress was assumed to be

$$\frac{\tau}{\left(\frac{dv}{dx}\right)} = \alpha N + \mu \quad (43)$$

or alternately

$$\tau_s = \tau - \tau_\mu = \alpha N \left( \frac{dv}{dx} \right) \quad (44)$$



The structural stress,  $T_s$  is the stress contributed by the network only and represents the difference between the total observed stress,  $T$  and the stress resulting from shear of the Newtonian solvent,  $T_\mu$ .

Furthermore, the rate of destruction of links was assumed to be completely defined by

$$\frac{dN}{dt} = -k_1 N \left( \frac{dv}{dx} \right) \quad (45)$$

In spite of the obvious similarity between equation (45) and equation (40) one distinct difference does exist. Goodeve assumed that the probability of link destruction, or more specifically the rate constant, was equivalent to the product  $G(x)$  divided by  $F_c$ . This situation is rather unlikely since orientation of the network, which must be some function of shear rate, is undoubtedly a factor of considerable importance. Although the problem could be resolved by assigning a shear rate dependent quality to "x", Goodeve makes no direct reference to this and, in fact, considers "x" to be constant. Equation (45) does not define the nature of the rate constant at this point and is, therefore, somewhat more general.

The relationship proposed by Storey and Merrill for the recombination process

$$\frac{dN}{dt} = k_2 (N_0 - N) \quad (46)$$



in which  $N_0$  is the number of links prior to shearing, again differs in two important respects from that stated by Goodeve in equation (41). It is here assumed that bond cleavage releases one molecule each time. Hence, the concentration of single molecules is given by  $(N_0 - N)$ . Furthermore, if the reformation reaction arises from collisions between these particles and the remaining network and if the Brownian movement may be considered as the principal cause of collision, the reaction is first order and independent of shear rate. This is equivalent to assuming that the number of networks present at any time is large compared with the number of fragments colliding with them.

The complete rate equation describing the net decay of network structure has the form

$$\frac{dN}{dt} = k_1 N \left( \frac{dv}{dx} \right) + k_2 (N_0 - N) \quad (47)$$

and may be integrated to give the general solution

$$N = N_0 e^{-\left[ k_2 + k_1 \left( \frac{dv}{dx} \right) \right] t} + \frac{\alpha N_0}{1 + \frac{k_1}{k_2} \left( \frac{dv}{dx} \right)} + \frac{\alpha N_0}{1 + \frac{k_1}{k_2} \left( \frac{dv}{dx} \right)} e^{-\left[ k_2 + k_1 \left( \frac{dv}{dx} \right) \right] t} \quad (48)$$



Substituting this expression for  $N$  into equation (43) gives

$$\frac{\tau}{\left(\frac{dv}{dx}\right)} = \alpha N_0 e^{-\left[k_2 + k_1\left(\frac{dv}{dx}\right)\right]t} + \frac{\alpha N_0}{1 + \frac{k_1}{k_2}\left(\frac{dv}{dx}\right)}$$

$$+ \frac{\alpha N_0}{1 + \frac{k_1}{k_2}\left(\frac{dv}{dx}\right)} e^{-\left[k_2 + k_1\left(\frac{dv}{dx}\right)\right]t} + \mu \quad (49)$$

The validity of equation (49) was tested by the authors with data obtained from a rheological study of amylose. To accomplish this, two special cases were chosen. After prolonged shear at constant shear rate, the first and third term on the right hand side of equation (49) become negligible and the expression reduces to

$$\frac{\tau_\infty}{\left(\frac{dv}{dx}\right)} = \frac{\alpha N_0}{1 + \frac{k_1}{k_2}\left(\frac{dv}{dx}\right)} + \mu \quad (50)$$

where  $\tau_\infty$  is the shear stress after prolonged shear,  $\text{lb}_f/\text{ft}^2$   
Assuming that  $k_1/k_2$  ( $dv/dx$ ) is large compared with unity  
(i.e. at high shear rates), equation (50) may be further simplified to

$$\frac{\tau_\infty}{\left(\frac{dv}{dx}\right)} = \frac{\alpha N_0}{\frac{k_1}{k_2}\left(\frac{dv}{dx}\right)} + \mu \quad (51)$$



which describes a linear relationship between

$$\frac{\tau_\infty}{\left(\frac{dv}{dx}\right)} \quad \text{and} \quad \frac{1}{\left(\frac{dv}{dx}\right)}$$

The correlation presented by the authors does in fact confirm the suitability of equation (51).

In the second case, the rate of shear is chosen sufficiently high to make the third term in equation (49) negligible (since  $dv/dx$  appears in both the denominator and the negative exponent). The remaining terms may then be rearranged to give

$$\ln \left[ \frac{\tau}{\left(\frac{dv}{dx}\right)} - \frac{\alpha N_o}{\frac{k_1}{k_2} \left(\frac{dv}{dx}\right)} - \mu \right] = k_1 \left(\frac{dv}{dx}\right)^t + \ln \alpha N_o \quad (52)$$

which is again a linear relationship between

$$\left[ \frac{\tau}{\left(\frac{dv}{dx}\right)} - \frac{\alpha N_o}{\frac{k_1}{k_2} \left(\frac{dv}{dx}\right)} - \mu \right] \quad \text{and} \quad \left(\frac{dv}{dx}\right)^t$$

on semilogarithmic coordinates.

Storey and Merrill's correlation of their experimental data in terms of equation (52) cannot be considered as entirely satisfactory since, for dilute solutions, deviation from the predicted curve range as high as 200 percent. This has been attributed partly to the inaccuracy of measurement coupled with the sensitivity of the correlation.



#### IV A MODIFIED THEORY OF THIXOTROPY

It is the considered opinion of this author that certain aspects of the theory advanced by Storey and Merrill are not consistent with the anticipated behavior of a network type model. Therefore a new theory is presented here, in which an attempt is made to incorporate several important features omitted from the previous theories.

Both the model chosen for study and the method of interpretation are basically similar to those of Goodeve and Storey and Merrill. The primary differences between the theories are apparent in the nature of certain underlying assumptions and will be pointed out during the development of the new theory.

In defining the contribution of network links to the observed shear stress, equation (44) states that the structural component of stress is directly proportional to the rate of shear for any specified concentration of links. This is tantamount to assuming that, either the orientation of the networks is stable and their resistance to flow is simply proportional to the rate at which the fluid passes the network segments, or changes in network orientation, caused by changes in shear rate, are small in terms of their effect on the structural stress. However, it is more likely that the improved network alignment, accompanying an increase in shear rate, will limit the increase in velocity gradient acting along the network segments, and thereby partially compensate for the higher shear rate. Furthermore, due to inertial effects associated with the uncoiling of chains,



the force required to disrupt the structure will vary in some unknown fashion with the shear rate. Thus the interaction between the fluid and the coiled chains cannot be described by the simple proportionality of equation (44).

It is interesting to note that Billington<sup>(6)(7)</sup> in a similar treatment of network models, assumed the structural stress, which he called an instantaneous yield stress, to be entirely independent of shear rate. That is, the strength of the network is considered to be unrelated to the rate of application of the disruptive forces. He also states that an increase in the instantaneous value of the observed stress, accompanying an increase in shear rate, is entirely due to intensified shear of the residual Newtonian liquid and does not involve an increase in yield stress. Although no qualifying statement is offered, this implies that alignment of the network in the direction of flow proceeds to such an extent that the viscous drag on the chains is not significantly altered by a change in shear rate.

Both Storey and Merrill's and Billington's concepts, concerning the influence of shear rate on the structural stress, were tested with data obtained during the course of the present investigation. According to equation (44) the value of  $T_s/(dv/dx)$  measured at the instant the sample is subjected to shear action, should be independent of shear rate, since  $N_0$  is a constant representing the number of links in the original, unsheared sample. On the other hand, Billington suggests that  $T_s$ , measured at the same instant, should be independent of shear rate. In fact, neither  $T_s/dv/dx$  nor  $T_s$  were found to be invariant over the shear



rate range studied. The appropriate relationship appeared to be intermediate between the two.

To avoid the difficulty of defining precisely the nature of the relationship between  $T_s$  and  $dv/dx$ , the following general expression has been chosen

$$T_s = \alpha' N \phi\left(\frac{dv}{dx}\right) \quad (53)$$

where the symbol  $\phi\left(\frac{dv}{dx}\right)$  designates some function of shear rate.

The second stage in the development of the theory concerns the rate of decay of network structure. Both Goodeve and Storey and Merrill presumed this to be directly proportional to the shear rate since the component of stress along the chain increases directly as the viscous drag. This condition would exist provided the chains remained inclined at some constant angle to the direction of flow. But here again no account is taken of the increasing stress component which tends to align the chains in the direction of flow. As a result, the probability of finding a network which is favorably oriented for dissociation, is diminished. Furthermore the inertial properties of the chain segments, which oppose rapid disentanglement of the networks, will also counteract the influence of increased shear rate.

Although the combined influence of these two mechanisms may not entirely compensate for the effects of the increased shear rate on the chains, they are likely of the same order of magnitude and are assumed compensating as a first approximation. If this argument is



acceptable, the rate constant  $k$ , in equation (45) is an inverse function of shear rate and the kinetic expression may be modified to read,

$$\frac{dN}{dt} = -k'_1 N \quad (54)$$

where  $k'_1$  is independent of shear rate.

Equation (54) may be generalized, to remove the limitations of the above assumptions, by including some function of the shear rate on the right hand side. However, this was found to be unnecessary in the correlation of the data.

The method of defining the nature of the network structure presents one final problem. The term  $N$  (number of links between chains) used as the characteristic parameter by Storey and Merrill does not distinguish between concentration and size of the individual network structures. Yet each of these might be expected to have an independent influence on the behavior of the fluid. For the present purpose the reaction representing network destruction is presumed to be of the type



for which the concentration of original network,  $A$ , is designated by the symbol  $(A)$ , while  $(B)$  denotes the concentration of network fragments,  $B$ , which do not contribute to structural stress. The effect of network size must then be treated separately as will be demonstrated later.



In accordance with the new terminology, equations (53) and (54) may be revised to read

$$\tau_s = \alpha^i(A) \phi\left(\frac{dv}{dx}\right) \quad (55)$$

and

$$\frac{d(A)}{dt} = -k_A^i(A) \quad (56)$$

If now equation (55) is differentiated with respect to time, the following expression results

$$\frac{d\tau_s}{dt} = \alpha^i \left[ \phi\left(\frac{dv}{dx}\right) \frac{d(A)}{dt} + (A) \frac{d[\phi(\frac{dv}{dx})]}{dt} \right] \quad (57)$$

If it is now assumed, as seems reasonable, that  $\frac{d[\phi(dv/dx)]}{dt}$

at constant shear rate is zero, the last term is also zero and equation (57) reduces to

$$\frac{d\tau_s'}{dt} = \alpha^i \phi\left(\frac{dv}{dx}\right) \frac{d(A)}{dt} \quad (58)$$



Rearranging equation (55) to

$$(A) = \frac{\tau_s}{\alpha' \phi(\frac{dv}{dx})} \quad (59)$$

and equation (58) to

$$\frac{d(A)}{dt} = \frac{\frac{d\tau_s}{dt}}{\alpha' \phi(\frac{dv}{dx})} \quad (60)$$

and substituting the resulting equations (59) and (60) into equation (56) yields

$$\frac{d\tau_s}{dt} = - k_A' \tau_s \quad (61)$$

To this point the structural degradation process has been assumed to involve only the breakdown of "A" networks to the ineffective "B" fragments. In reality, the large structures must undergo successive stages of size reduction before ultimately achieving a stable configuration. This implies a reaction of the type symbolized by



Now, since large networks, which encounter the highest velocity gradients, undoubtedly furnish the greatest resistance to flow and therefore the greatest changes in resistance through degradation, the time rate of change in stress should be dependent upon average network size. At present it is impossible to derive an exact mathematical expression to adequately describe the consecutive



reaction illustrated above in terms of measurable shear stress components. It is certain, however, that the average particle size will decrease with increased duration of shear. As a first approximation it is assumed that the average network size is inversely proportional to time of shearing. Accordingly equation (61) may be rewritten

$$\frac{d \bar{\tau}_s}{d t} = - \frac{k_A \bar{\tau}_s}{t} \quad (62)$$

The rate constant  $k_A$  should now be independent of shear rate and time of shearing. Moreover, in view of the fact that viscosity, and consequently drag on the chains, increases with a reduction in temperature, one would anticipate that the rate constant would increase with decreasing temperature.

The reformation of network structure is here assumed to result from the entanglement of imperfectly aligned ends and branches of passing fragments and the rate of such bond formation is considered to be equally dependent on both potential partners involved in the reaction. This is equivalent to assuming a second order reverse reaction similar to that proposed by Goodeve. The second order reaction may be written in terms of concentration, then, in a manner similar to that described above, expressed in terms of the structural stresses involved. Thus

$$\frac{d \bar{\tau}_s}{d t} = k_B^1 (\bar{\tau}_{s0} - \bar{\tau}_s)^2 \quad (63)$$



where  $\tau_{so}$  denotes structural stress at zero time.

One notable difference between equations (41) and (63) is apparent. Goodeve suggested that the rate of recombination was directly proportional to the shear rate due to an increase in collision frequency. However the probability of link formation must depend upon misalignment of chains and, since high shear rates tend to oppose this condition, the rate constant must be reduced as the shear rate increases. The relative magnitudes of these conflicting influences cannot be predicted a priori. The nature of the function relating  $k'_B$  and shear rate must, therefore, be determined experimentally.

In order to complete this mechanistic interpretation of network restoration, consideration must again be given to the effect of time of shearing. The gradual reduction in average particle size resulting from sustained shear and the associated reduction in rate of change of structural stress have been described in connection with network decay. Through an analogous argument, it is now postulated that recombination of large fragments will tend to increase the stress more markedly than recombination of the small fragments produced by prolonged shearing. The net result will be a systematic decrease in rate of stress recovery and, as in the previous case, is accounted for by modifying equation (63) to

$$\frac{d\tau_s}{dt} = \frac{k_B(\tau_{so} - \tau_s)^2}{t} \quad (64)$$



The rate constant,  $k_B$ , in equation (64) is recognized to be a function of shear rate and temperature but should be independent of time of shearing. More specifically,  $k_B$ , at constant shear rate, would be expected to increase with increasing temperature due to the more pronounced misalignment of chains brought about by greater Brownian motion. Following this same argument, greater misalignment at high temperatures should provide  $k_B$  with a greater sensitivity to shear rate. That is, the reduction in  $k_B$ , associated with an increase in shear rate, should be larger at elevated temperatures.

The net rate of decay of structural stress at constant shear rate may now be described by combining equations (62) and (64)

$$\frac{d \tau_s}{d t} = \frac{k_B (\tau_{so} - \tau_s)^2}{t} - \frac{k_A \tau_s}{t} \quad (65)$$

Prolonged shear of a thixotropic fluid eventually produces a condition of equilibrium between network structure and dissociated fragments at which time

$$\frac{d \tau_s}{d t} = 0 \quad (66)$$

and equation (65) becomes

$$\frac{k_B (\tau_{so} - \tau_{s\infty})^2}{t} = \frac{k_A \tau_{s\infty}}{t} \quad (67)$$

$$k_B = \frac{k_A \tau_{s\infty}}{(\tau_{so} - \tau_{s\infty})^2} \quad (68)$$



Substitution of equation (68) into equation (65) gives

$$\frac{d\tau_s}{dt} = \frac{k_A}{t} \left[ \frac{\tau_{s\infty}(\tau_{so}-\tau_s)^2}{(\tau_{so}-\tau_{s\infty})^2} - \tau_s \right] \quad (69)$$

which upon integration may be shown to yield (Appendix 1)

$$\log \left[ \frac{\tau_s - \tau_{s\infty}}{\frac{(\tau_{so})^2}{\tau_{s\infty}} - \tau_s} \right] = -k_A \left[ \frac{\tau_{so} + \tau_{s\infty}}{\tau_{so} - \tau_{s\infty}} \right] \log t - \log C \quad (70)$$

where

$$C = \left[ \frac{\frac{(\tau_{so})^2}{\tau_{s\infty}} - \tau_{s1}}{\tau_{s1} - \tau_{s\infty}} \right]$$

$\tau_{s\infty}$  = structural stress at  $t = \infty$

$\tau_{s1}$  = structural stress at  $t = 1$  minute

Equation (70), which represents the final expression

derived on the basis of the present theory, may be seen to describe a straight line relationship between

$$\left[ \frac{\tau_s - \tau_{s\infty}}{\frac{(\tau_{so})^2}{\tau_{s\infty}} - \tau_s} \right] \quad \text{and} \quad t$$

on logarithmic coordinates with a slope of

$$-k_A \left[ \frac{\tau_{so} + \tau_{s\infty}}{\tau_{so} - \tau_{s\infty}} \right] \quad (71)$$

and an intercept  $C$  at  $t = 1$  minute.



The form of equation (70) is such, that a knowledge of the structural shear stress obtaining at any time during the interval  $t = 0$  to  $t = \infty$  permits direct evaluation of the theory. The required structural stress values may be obtained through measurement of the total shear stress and the shear stress contributed by the Newtonian solvent.

The Newtonian solvent referred to in this discussion is, in reality, composed of both solvent and degraded network fragments which do not contribute to the structural stress. It follows then, that the magnitude of this component may be determined after prolonged shearing at very high shear rates. Under these conditions the rate of network regeneration is negligible and the resulting fluid is free of structure. Assuming that a change in concentration of network fragments does not appreciably alter the behavior of the solvent, the Newtonian viscosity so obtained may be considered appropriate over the entire range of shear rates. This assumption, which is probably valid when the volume fraction of particles is small, cannot be analytically justified in the present case. However, the crude oil components responsible for network formation are presumed to occur in relatively small proportions since many other crude oils of similar composition display only Newtonian behavior at comparable temperatures.

For purposes of comparison, the assumptions involved in the derivation of the present theory, as well as those pertaining to the Storey and Merrill theory, are briefly summarized below. In



each case, these assumptions are arranged in approximately the same order as they appear in the development of the theory.

The approach outlined in the preceding paragraphs is not intended as a rigorous microrheological interpretation of thixotropic behavior. Clearly, a system of such complexity cannot be completely defined without recourse to molecular theory. Rather, a plausible explanation is offered, in which an attempt is made to consider all pertinent variables in their true perspective and to express them in terms of quantities readily determined through conventional viscometric techniques. The mathematical expression resulting from this interpretation of thixotropy has been evaluated by experiment and these matters are discussed in the succeeding sections.

Comparison of Assumptions in the Storey and Merrill

Theory and the Modified Theory

Storey and Merrill Theory

1. The total stress generated within a thixotropic fluid by shear action may be considered as the sum of a Newtonian component, arising from shear of the solvent and network fragments, and a structural stress component, which reflects the resistance to flow offered by the network structure.
2. The structural stress component is proportional to the product of the number of network links and the shear rate.



3. The rate of link destruction is proportional to the product of the number of network links and the shear rate.
4. The rate of change of structural stress, arising from the rupture or reformation of network links does not depend on the size of the network and is therefore independent of time of shearing.
5. The network recombination process is analogous to a first order chemical reaction and is independent of shear rate.

#### Modified Theory

1. As in the Storey and Merrill theory, the total stress is here also considered to be the sum of a Newtonian component and a structural stress component.
2. The structural stress component is proportional to the product of the number of network links and some function of the shear rate.
3. The rate of link destruction is proportional to the number of network links and is independent of the shear rate.
4. The rate of change of structural stress, arising from the rupture or reformation of network links is dependent on the average size of the network and is therefore assumed to be inversely proportional to time of shearing.
5. For any given concentration of networks, the nature of the function relating structural stress to shear rate is independent of time of shearing.



6. The network recombination process is analogous to a second order chemical reaction and is dependent on shear rate.
7. The Newtonian component of the total stress, evaluated at high shear rates, is appropriate at all shear rates.



V EXPERIMENTAL PROGRAM

The data necessary for the verification of equation (70) were obtained through a study of the transient rheological behavior of Pembina crude oil under the influence of shear for an extended period of time. Prepared samples of this fluid were subjected to shear in a specially designed rotational viscometer and the relationship between total shear stress and time was determined at varying conditions of shear rate and temperature. The viscosity of the Newtonian solvent, required for the calculation of the structural stress component, was also measured at each temperature by applying a suitably high shear rate to the sample.

In addition to these principal measurements, considerable effort was devoted to an evaluation of the effect of shear history on the rheological properties. Although quantitative interpretation of this phase of the investigation was not possible, the results added support to certain conclusions drawn in connection with the rate constants  $k_A$  and  $k_B$ .

The experimental aspects of this study may logically be divided into three major topics, namely, characterization of the fluid, design and operation of the equipment and the determination of rheological properties. Each of these are discussed in detail in the following text.



### Characterization of the Crude Oil Sample

As previously mentioned, Pembina crude oil, which is of Lower Cretaceous origin and located in the Cardium formation of western Alberta, was chosen for study because of the decidedly thixotropic behavior of this fluid. At any constant shear rate, the shear stress decreases appreciably with time and at a rate which is sufficiently slow to permit accurate measurement. However, the choice is not without disadvantage. Pembina crude oil, being a mixture of innumerable compounds, is very difficult to classify in terms of the constituents responsible for its observed behavior. At best, the physical properties of the fluid may be compared to those of other crude oils on the basis of standardized analysis (3)

A large sample of Pembina Crude oil was obtained at the well head and transported to the laboratory in a sealed container. Appropriately sized samples of the vapor and liquid phases were subsequently removed for analysis according to the following schedule.

#### Liquid Analysis

Specific Gravity

Basic Sediment and Water

Saybolt viscosity at 70°F and 100°F

U.S.B.M. Pour Point

Carbon Residue

U.S.B.M. Distillation.

#### Vapor Analysis

Chromatographic Analysis

The results of these analysis and all pertinent well data



are tabulated in Appendix 2.

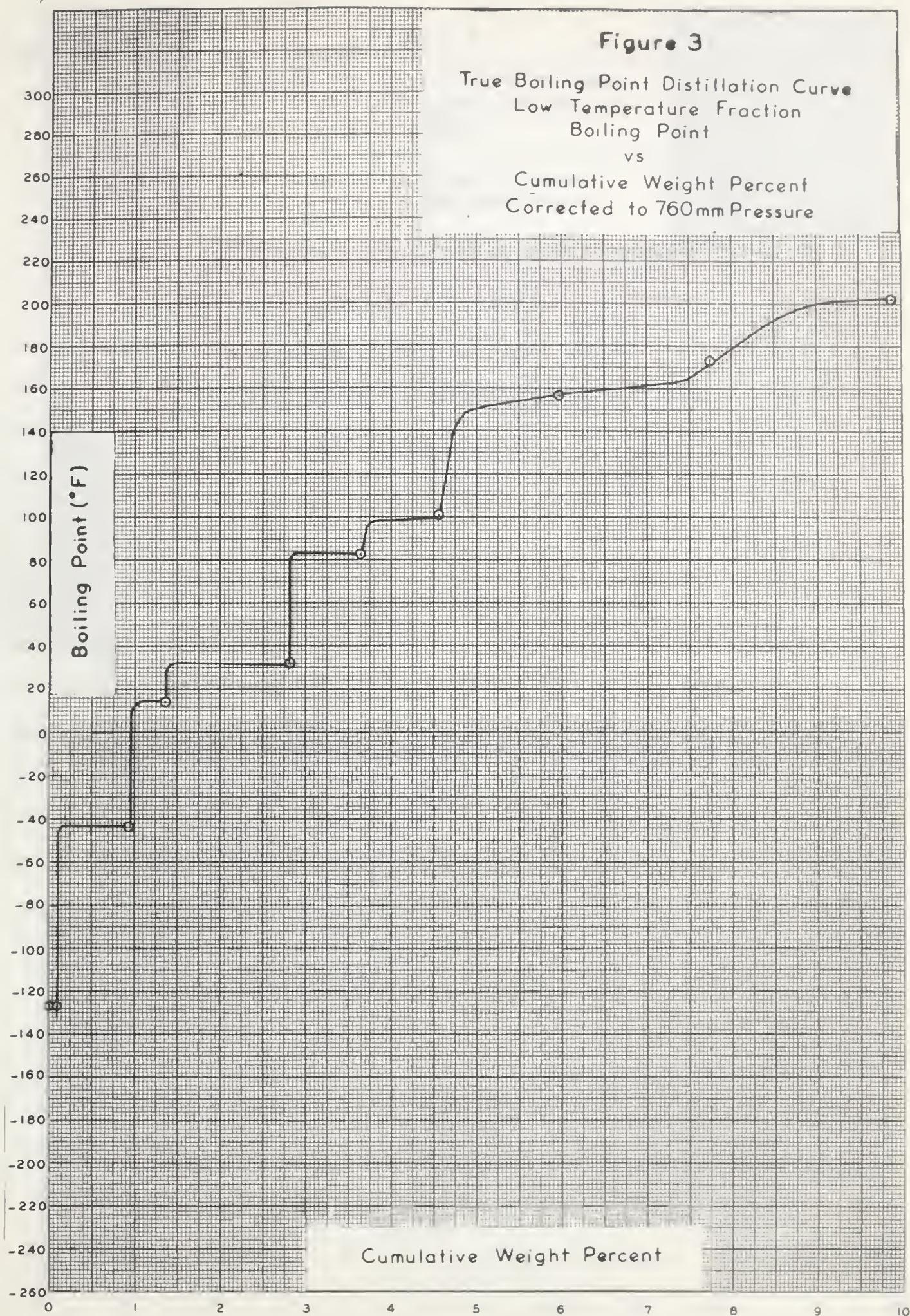
To supplement the above routine tests, the crude oil sample was further characterized by means of true boiling point distillation. A Podbielniak high temperature fractional distillation column, operated at an absolute pressure of 704, 38.7 and 4.8 mm. of mercury, was utilized for this purpose. The non-condensable vapors (methane to pentane) were collected for chromatographic analysis while the individual liquid fractions were subjected to specific gravity, refractive index and aniline point analysis. The results of these analysis are also tabulated in Appendix 2. The relationship between cumulative weight percent distilled and boiling point, corrected to 760 mm. pressure, according to an approximate method outlined in Appendix 2, is presented graphically in Figures (3) and (4).

Unfortunately, such information provides no clue to the cause of thixotropic behavior, since the components responsible for this property undoubtedly remain with the high boiling point residue which cannot be resolved by fractionation. One portion of the analytical data proved to be of considerable value in the development of a satisfactory sample handling technique and will be discussed under the appropriate heading.

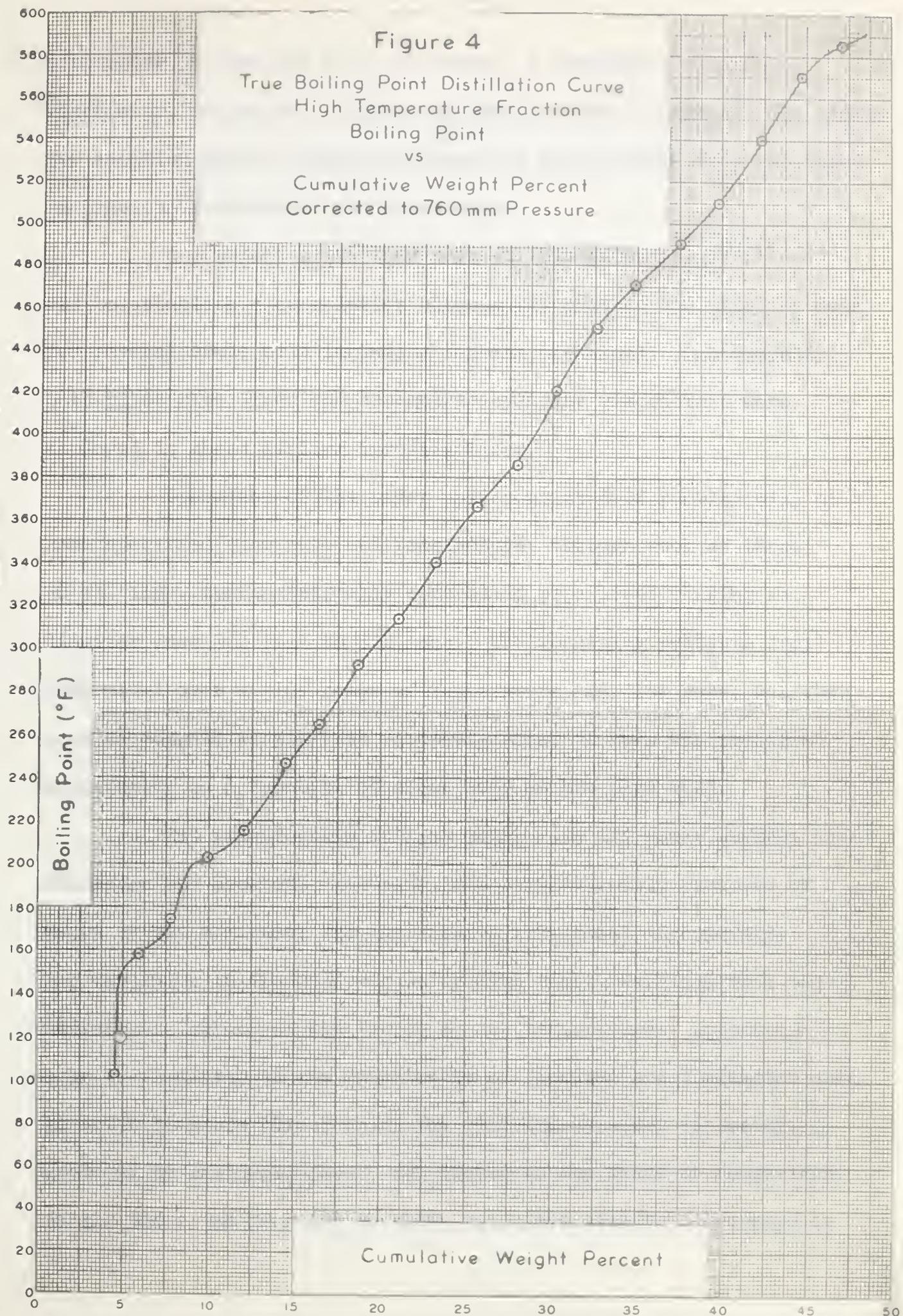
#### The Viscometer and Associated Equipment

The selection of a suitable instrument for any rheological study is based on the nature of the fluid in question and the type of information desired. It may alternatively be a capillary tube











viscometer, a cone and disc viscometer, a concentric cylinder viscometer, or any one of numerous modifications of these. The reason for adoption of the latter instrument in the present study was based on previous experience with crude oils.

One object of earlier work at this laboratory<sup>(30)(4)</sup> was to establish a correlation between viscometric and pipeline data for several crude oils including Pembina crude oil. Consequently, both pilot pipe lines and concentric cylinder viscometers were employed in these earlier investigations.

Operation of the pilot unit consisted of pumping oil, at some specified flow rate and temperature, through each of three 28 ft. long, thermostatically controlled pipe lines ranging in diameter from 3/8 inch to 5/8 inch. The resulting pressure drop, determined over a wide range of temperature and flow rate, was then used to compute an apparent viscosity which in turn was presented graphically as a function of shear rate at the pipe wall.

The relationship between shear rate and shear stress, and therefore the apparent viscosity, was simultaneously measured by means of the McMicheal and the Alberta rotational viscometers. The variation in apparent viscosity with time, resulting from the thixotropic nature of the fluids at low temperatures, presented some difficulties in the correlation of pipeline and viscometer data. In order to avoid this problem the limiting apparent viscosity, produced by prolonged shear, was chosen as the basis of comparison. In all cases, an increase in shear rate gave rise "to a decrease in



apparent viscosity. Agreement between the pipeline and viscometer data was satisfactory at temperatures above 40°F. However, at lower temperatures the results showed appreciable deviation. For this reason it was decided that the problem demanded a more fundamental study of thixotropic decay and that the Alberta rotational viscometer, after certain modification, was most suitable for this purpose. The rotational viscometer offers certain advantages over other techniques. For example, unlike the capillary or pipeline viscometers in which shear rate varies from zero at the center to a maximum at the wall, the rotational instrument provides a nearly constant shear rate throughout the entire fluid. Other advantages include precise temperature control, ease of operation and sample preparation and, of particular significance to the present study, a means by which samples may be subjected to prolonged shear action.

The Alberta Viscometer, illustrated in its present form in Figures (5) to (9) consists essentially of a hollow lucite bob (A), 1.582 inches in diameter and a rotating stainless steel cup (B), 1.761 inches inside diameter. The bob has an overall length of 4.860 inches (not including the spindle and chuck) and is provided with a conical bottom having an apex angle of 151 degrees. Two copper-constantan thermocouples (C) are located on the bob wall 1.344 inches and 3.656 inches from the bottom to permit accurate measurement of the oil temperature. This operation merely involved connecting the appropriate lead line clips (R) to the copper and constantan rings (U) situated



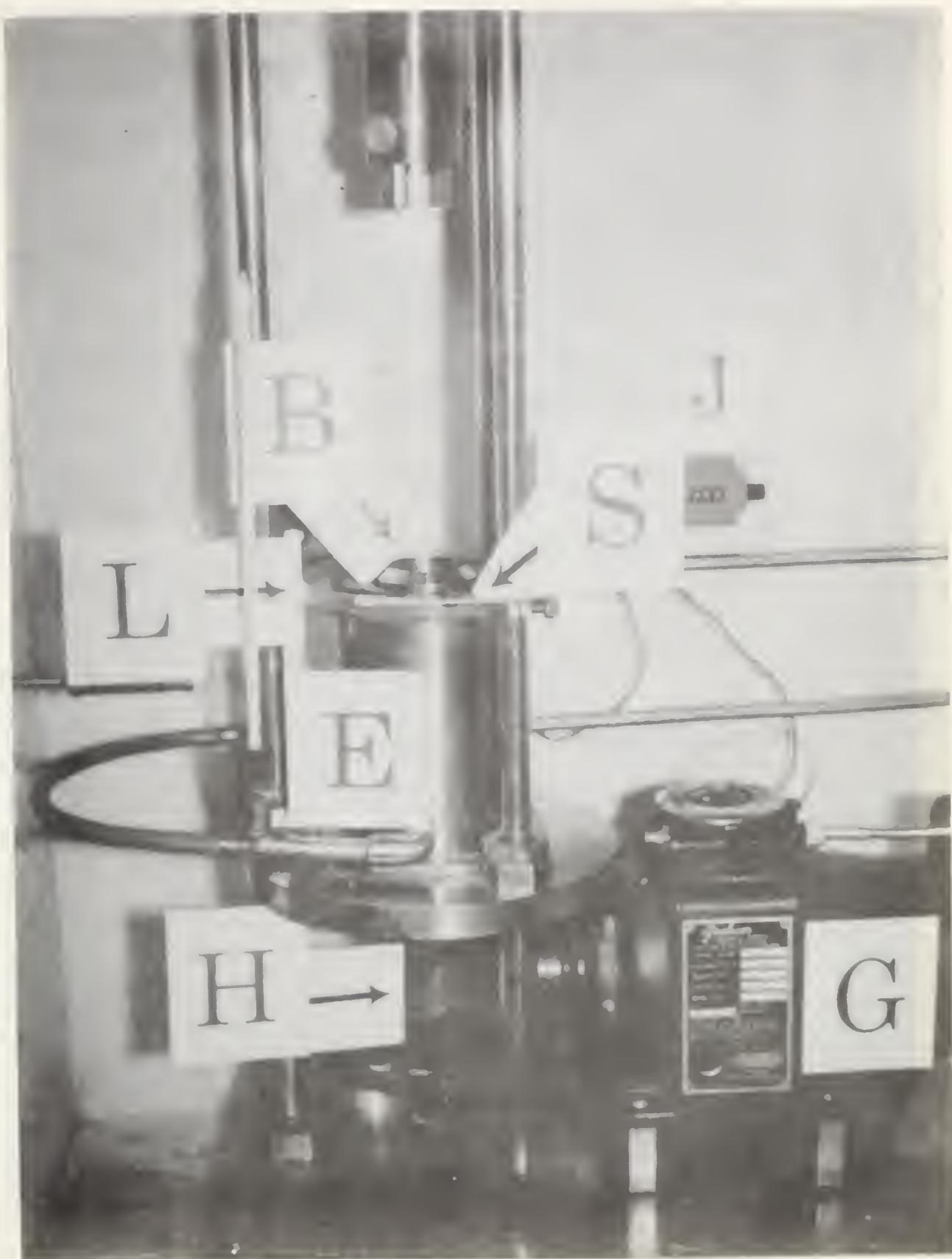


FIGURE 5

ALBERTA ROTATIONAL VISCOMETER



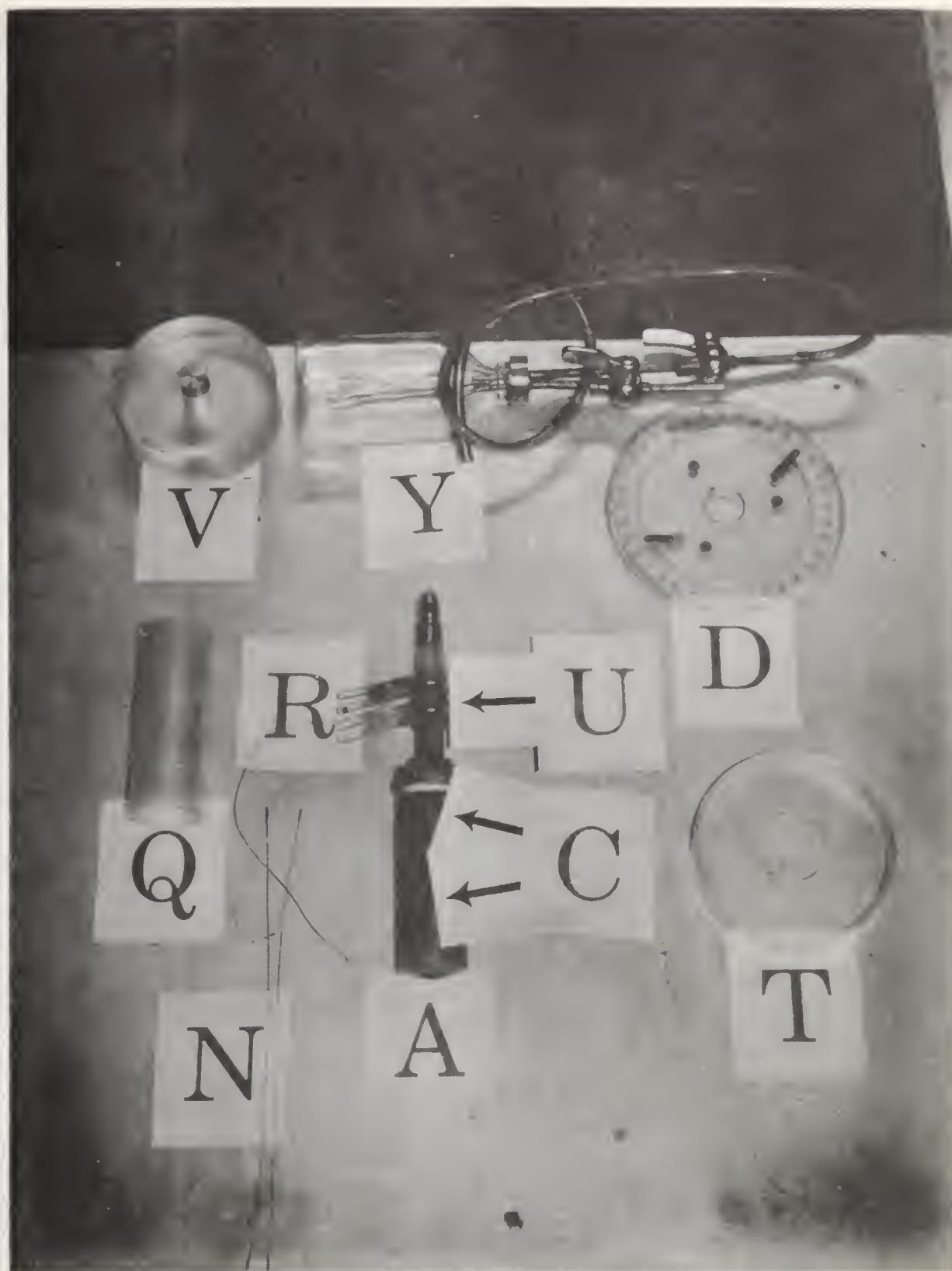


FIGURE 6

VISCOMETER ACCESSORIES



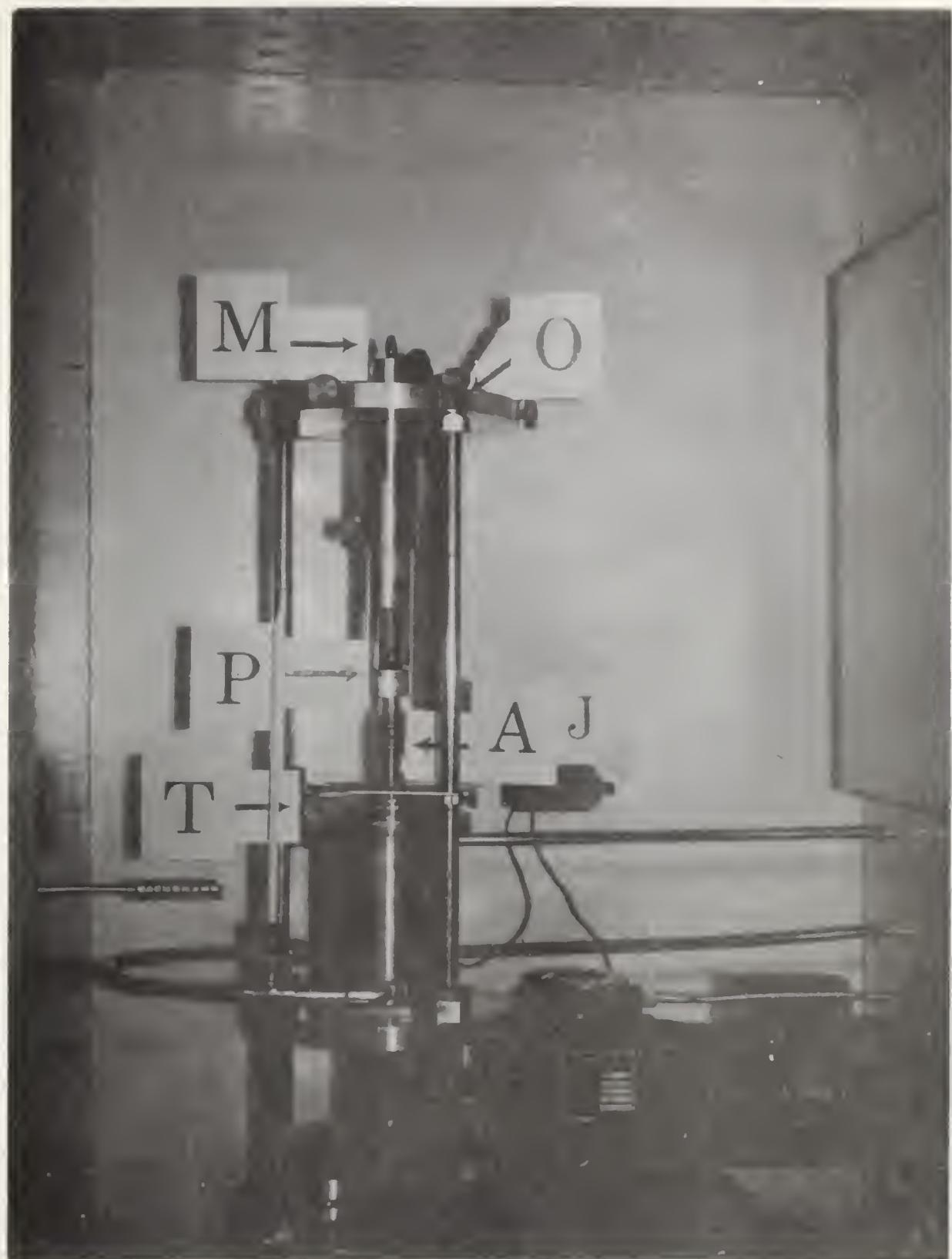


FIGURE 7

ALBERTA ROTATIONAL VISCOMETER





FIGURE 8  
ALBERTA ROTATIONAL VISCOMETER





FIGURE 9

ALBERTA ROTATIONAL VISCOMETER



on the bob spindle. The bob is further provided with a protractor (D) which, in conjunction with an indicator (S) mounted on the stationary viscometer framework, is used to ascertain the bob deflection. One component of a water sealing device (T), the purpose of which will be described later, is also situated on the bob.

The 4.671 inch deep cup is surrounded by an ethylene glycol-water bath (E) whose temperature may be controlled to within  $0.1^{\circ}\text{F}$  at any temperature above  $0^{\circ}\text{F}$  by means of an Aminco refrigerator unit (F). The second component of the water sealing device (L) is mounted at the upper edge of this bath. A synchronous motor and Graham transmission combination (G), acting through a gear train (H) furnish the motive force necessary for rotation of the cup at any desired constant speed within the range from 0 to 500 RPM. The cup is also equipped with a bottom inlet line (I) for introduction of oil samples and a counting device (J) for accurate measurement of the angular velocity.

The entire assembly is mounted in an insulated, thermostatically controlled circulating air bath (K) to reduce the temperature gradient between the ambient air and the oil sample. The temperature in this cabinet may be controlled within  $\pm 1^{\circ}\text{F}$  at temperatures above  $10^{\circ}\text{F}$ .

During operation, the bob is suspended from the upper chuck (M) by means of any one of several 10 inch long calibrated torsion wires (N) and aligned, through adjustment of the platform (O) so as to be concentric with the cup. The vertical position of the bob



with respect to the cup, may be adjusted by means of the elevator (P). However in all experiments the bob extended 4 inches into the cup (as measured from the base of the conical bottom). This represents the maximum possible immersion into the oil sample and is most desirable since the end effect of the bob is minimized.

In order to achieve the high shear rates necessary for measurement of the Newtonian solvent viscosity, a lucite cylinder (Q), 1.640 inch inside diameter, was inserted into the cup thereby reducing the width of the annulus formed between the cup and bob.

The complete viscometer assembly, with its auxilliary equipment, is illustrated in Figure (9).

#### Calibration of Torsion Wires

The action of a tangential force, such as shear stress on the bob wall of a rotational viscometer, causes the bob to rotate which, in turn, produces an opposing torque in the suspension wire. Provided the wire is not deformed beyond its elastic limit, the deflection, D, of the bob is directly proportional to the applied stress,  $\tau$ . This relationship may be represented by

$$\tau = aD \quad (72)$$

where the constant "a" is a function of the properties and diameter of the wire and the geometry of the system. Thus, calibration of the torsion wires involves the evaluation of "a" and may be accomplished by either of two relatively simple procedures.



The first method requires measurement of the shear modulus of the wire which is then related to the constant "a" through the dimensions of the wire. For this purpose it may be shown that (Appendix 3)

$$a = \frac{G \pi r^4}{(720) L d R^2} \quad (73)$$

where  $G$  = shear modulus,  $\text{lb}_f/\text{ft}^2$ .

$r$  = radius of the torsion wire, ft.

$L$  = length of the torsion wire, ft.

$d$  = depth of immersion of the bob, ft.

$R$  = radius of the bob, ft.

The shear modulus is readily obtained by means of a torsion pendulum since for such an arrangement

$$G = \frac{2 L C}{\pi r^4} \quad (74)$$

where  $C = \left(\frac{2\pi}{P}\right)^2 \frac{I}{g_c}$  (75)

$P$  is the period of vibration of the pendulum, sec.

and  $I$  is the moment of inertia of the suspended mass,  $\text{lb}_m \text{ft}^2$ ,

which in this case consisted of a lucite and brass disc (v)

A second and more common method of calibration is accomplished with the viscometer. A Newtonian fluid of known viscosity is placed in the viscometer and the deflection of the bob, produced by rotation



of the cup at several predetermined speeds, is noted. It may be seen from the definition of a Newtonian fluid

$$\tau = - \frac{\mu}{g_c} \left( \frac{dv}{dx} \right) \quad (1)$$

that knowledge of the shear rate and viscosity permits an independent calculation of shear stress. The ratio of shear stress to bob deflection then gives the desired value of the proportionality constant, "a", defined by equation (72). In order to perform these computations, the relationship between shear rate and cup speed is required. Reiner and Riwin <sup>(42)</sup> have established this relationship which is based on the geometry of the viscometer and may be written

$$- \left( \frac{dv}{dR} \right)_R = \frac{4\pi S R_1^2 R_2^2}{(R_2^2 - R_1^2) R^2} \quad (76)$$

where  $S$  = rotational speed of the cup, RPS,

$R_1$  = radius of the bob, ft,

$R_2$  = radius of the cup, ft,

and  $(dv/dR)_R$  = shear rate in the fluid at radius  $R$ , sec<sup>-1</sup>.

Various wires, ranging in size from 22 gauge to 30 gauge, were found necessary to cover the full range of shear stress encountered in the viscometer. These were calibrated, in terms of shear stress at the bob wall, by both of the techniques described above (Appendix 3). The resulting values of "a" obtained by each method were comparable, demonstrating a maximum deviation of only 3%.



End Effect Correction

Motion of the fluid in contact with the conical bottom of the viscometer bob generates a shear stress which varies from a maximum at the base to zero at the apex. The torque developed at this point contributes to the observed deflection of the bob and must therefore be considered during calibration of the torsion wires or when variable depth of bob immersion is employed. This effect is most readily accounted for in terms of an equivalent length of cylindrical bob. That is to say, when a Newtonian liquid is subjected to shear in the viscometer annulus and the resulting ratio of deflection to speed is plotted as a function of depth of bob immersion (measured from the base of the conical section), the straight line described by the data does not pass through the origin but rather intersects the horizontal axis at a negative value equal to the effective length of the cone. The measured depth of immersion may then be adjusted by simply adding the equivalent bob length to it. This method assumes that the bottom of the cup is sufficiently removed from the conical section of the bob to avoid any interaction between the two even at maximum immersion of the bob. The nature of the experimental data indicates that this complication does not arise with the present instrument.

Theoretically, end effect corrections of this type are suitable only for Newtonian fluids since, due to changes in shear rate, the consistency of a non-Newtonian fluid varies over the surface



of the cone. The magnitude of the correction would therefore be expected to depend on the rheological properties of the particular fluid in question. This situation is not as serious as it might initially appear. The largest variation in viscosity will likely occur in the region approaching the apex of the cone which also represents a region of reduced torque due to both lower shear rate and radius. Hence the net deflection of the bob will not be materially influenced by this fluid. Furthermore, at maximum immersion, relatively large errors in the end effect correction are tolerable since it is equivalent to only 5.3% of the total bob length.

In view of these qualifications, results obtained by the above method are considered to be satisfactory and have been used in the present study (Appendix 4).

#### Flow Stability in the Viscometer Annulus

Nothing has yet been said concerning the flow pattern encountered in the viscometer annulus. In all equations pertaining to concentric cylinder viscometry, it is inherently assumed that the basic flow is laminar. However, this condition is not guaranteed and some suitable test of hydrodynamic stability is necessary. Several criteria have been suggested for this purpose which are based on the properties of the fluid and the geometry of the instrument. The earliest of these, proposed by Couette<sup>(12)</sup> and quoted by Barr<sup>(5)</sup>



takes the form

$$R_r = \frac{2\pi S R_1 (R_2 - R_1) \rho}{\mu} \quad (77)$$

where, for stability, the dimensionless quantity  $R_r$  must be less than 1900. Other investigators have subscribed to the same basic form of equation but the critical values have been found to range as high as 32,000 depending on the dimensions of the apparatus.

Taylor<sup>(50)(51)</sup> carried out an extensive mathematical and experimental study of the problem and concluded that, for a viscometer in which end effects are small and negligible, stability was assured when  $R_r$  of equation (77) satisfied the inequality

$$R_r < C \quad (78)$$

where  $C$  is a constant, the value of which is dependent on the ratio

$$\frac{R_2 - R_1}{R_2}$$

For the Alberta viscometer the constant  $C$  assumed a value of 3,500.

A more recent mathematical analysis by Serrin<sup>(47)</sup> provided a stability criterion

$$\frac{2\pi (S_2 - S_1) \rho}{\mu} \leq (R_2^2 - R_1^2) \left[ \frac{\pi}{R_1 R_2 \log \left( \frac{R_2}{R_1} \right)} \right]^2 \quad (79)$$



intended for the general case in which both bob and cup are rotating in the same direction with speeds  $S_1$  and  $S_2$  respectively.

For the particular case at hand  $S_1 = 0$  and equation (79) becomes

$$\frac{2\pi S_2 \rho}{\mu} \leq (R_2^2 - R_1^2) \left[ \frac{\pi}{R_1 R_2 \log \left( \frac{R_2}{R_1} \right)} \right]^2 \quad (80)$$

which, upon substitution of the appropriate values of  $R_1$  and  $R_2$ , reduces to

$$\frac{2\pi S_2 \rho}{\mu} \leq 217 \quad (81)$$

Comparison of equation (81) with the equivalent form of Taylor's equation

$$\frac{2\pi S_2 \rho}{\mu} \leq 7,700 \quad (82)$$

demonstrates a very wide discrepancy between these two stability criteria. Somewhat more confidence must be placed in equation (82) which, unlike equation (81) is based on numerous experimental observations.

Certain selected data were tested with each of these criteria and the results are presented in Appendix 9. It was found necessary to consider only those data obtained at  $90^{\circ}\text{F}$  and  $75^{\circ}\text{F}$  both with and without the auxiliary sleeve in the viscometer cup. At lower temperatures, the viscosity was sufficiently high to dampen out any turbulent fluctuations and to maintain hydrodynamic stability.



Based on the criteria suggested by Taylor, Couette, etc. stability of the laminar flow pattern was consistently guaranteed. The magnitude of  $R_r$  was found to lie well below even the most conservative estimate of 1900. On the other hand, Serrin's criterion suggests a region of instability for both temperatures at a shear rate of  $300 \text{ sec.}^{-1}$ . Yet the accuracy, with which the uppermost point on Figure (37) conforms to the characteristic curve of the Newtonian fluid, discredits this suggestion. Without further proof to the contrary, laminar flow in the annulus must, in this instance, be considered as stable.

#### Water-Seal Device

The greatest obstacle encountered in the determination of network decay over extended periods of time arises from the loss of low molecular weight hydrocarbons from the oil sample in the viscometer. Preliminary studies indicated that, at a temperature of  $70^{\circ}\text{F}$ , the viscosity of the oil increased 5 percent in 45 minutes at a shear rate of  $25 \text{ sec}^{-1}$  and 12 percent in 45 minutes at a shear rate of  $275 \text{ sec}^{-1}$ . At lower temperatures the change in viscosity was correspondingly less but under no conditions did it appear insignificant.

In order to limit the extent of these losses, a device was constructed which isolated the oil in the viscometer from its surroundings. As previously mentioned, this device consisted of two components; a lucite cap (T in Figure 6), mounted on and forming an airtight seal with the bob and a stationary water trough (L in Figure 5) located at the upper edge of the constant temperature bath



surrounding the cup. With the bob in position, the cap extended into the trough to form a continuous water seal around the oil sample. The rapidly circulating air in the viscometer cabinet was thereby prevented from sweeping across the surface of the oil and a hydrocarbon rich atmosphere was maintained above the sample. Even though the small head of water in the seal (approximately 1/4 inch) was incapable of retaining all of the vapor, evaporation losses were minimized. The small changes in viscosity which still persisted (4 percent in 45 minutes at 70°F and 275 sec.<sup>-1</sup>) had to be tolerated since any further improvement would require drastic modification of the viscometer design.

#### Calibration of Thermocouples and Stopwatch

To avoid unnecessary errors which might be introduced into the experiments by auxilliary equipment, the static error of the thermocouples was determined by comparison with an accurately standardized thermometer and the stopwatch used for measurement of cup speed was calibrated over the range from 1 minute to 4 minutes. Since the stopwatch was situated inside the viscometer cabinet (not shown on the figures), the effect of temperature on the calibration was also ascertained and found to be negligible.

The results of these calibrations are tabulated in Appendix 5.



Sample Storage

The nature of Pembina crude oil is such, that certain difficulties arise in the selection of a suitable mode of sample storage. Conventional methods employing stationary containers were inadequate, since small particles of wax tended to settle from the oil even at room temperature. The composition of any particular sample was then dependent upon the time of removal from the container and the original location of the sample in the container. To maintain a homogeneous suspension of the solid phase, a special drum and framework were fabricated (Figure 10). Due to the diagonal mounting of the axis, a continuous mixing action was achieved by rotating the drum at 2 RPM. Samples of oil for analysis were readily obtained through the valve (W) by briefly interrupting the motion of the drum when the valve was at the lowest position in its travel.

A second problem which demanded careful consideration was the change in composition of the oil in storage. Although the loss of low molecular weight hydrocarbons from the vessel could be easily prevented by means of an airtight seal, the removal of liquid samples caused an increase in volume of the vapor phase and therefore additional vaporization of the light components. To determine the change in composition of the oil as the quantity in storage diminished, a material balance was written in differential form and,





FIGURE 10

CRUDE OIL STORAGE VESSEL



through mathematical manipulation, eventually reduced to

$$\log \left( \frac{x_0}{x} \right) = \left[ \frac{\left( \frac{K P}{R T} \right) - \left( \frac{P_{ave}}{R T} \right)}{\left( \frac{\rho}{M W} \right)} \right] \log \left( \frac{V_0}{V} \right); \quad (83)$$

where  $x_0$  is the initial mole fraction of any constituent

$x$  is the mole fraction of the same component at  
a time when the liquid volume is  $V$ ,

$K$  is the constant describing the vapor liquid  
equilibrium for that component

$P$  is the vapor pressure above the liquid,  $\text{lb}_f/\text{ft}^2$

$\rho$  is the density of the liquid,  $\text{lb}_m/\text{ft}^3$

$MW$  is the average molecular weight of the liquid,  
 $\text{lb}_m/\text{mole}$

$T$  is the average absolute temperature,  ${}^{\circ}\text{R}$

$V_0$  is the initial liquid volume,  $\text{ft}^3$

$V$  is any liquid volume for which  $X$  is to be  
calculated,  $\text{ft}^3$

and  $R$  is the gas constant,  $\text{ft lb}_f/\text{mole } {}^{\circ}\text{R}$

The complete derivation of equation (83) is presented

in Appendix 6.

The initial concentration of each volatile component in  
the liquid phase and the average molecular weight of the crude oil  
were obtained from the distillation data (Appendix 2). Hence, if  
the average pressure in the vessel were known, the composition of



the liquid phase at any time during removal of samples could be estimated. Direct solution of equation (83) was not possible, however, since the instantaneous pressure, and therefore the average pressure, are related to the unknown liquid composition. A trial and error solution was necessary and was conducted in the following manner.

The total change in pressure, caused by a decrease in liquid volume from 6.4 ft<sup>3</sup> to 1.6 ft<sup>3</sup>, was assumed and the final concentration of each component from methane to pentane computed through equation (83). The composition of the vapor phase in equilibrium with this liquid was calculated (see Appendix 6) and the sum of the mole fractions, so determined, was compared to unity. Any deviation was construed as an error in the assumed pressure. The calculation was repeated a sufficient number of times at other average pressures to reduce this deviation to an insignificant level. The results of these calculations, which are tabulated in Appendix 6, indicated that substantially all of the methane, 33.4 percent of the ethane and 8.6 percent of the propane, as well as lesser amounts of the other components initially present in the oil, would be lost during storage. The change in concentration of the propane and higher molecular weight hydrocarbons was not considered to be excessive in terms of their influence on the rheological behavior of the crude oil. On the other hand, in view of the large change in concentration of the methane and ethane, consideration was originally given to the use of an appropriate hydrocarbon gas mixture to displace the liquid from the storage



vessel. However, since the initial concentrations of methane and ethane were extremely low ( $1.4 \times 10^{-3}$  and  $7.75 \times 10^{-3}$  mole fraction respectively) and since they would not be retained by the viscometer water seal in any event, this method was abandoned. Air, under pressure, was finally chosen as suitable displacing fluid for the oil.

It is interesting to note that duplicate analyses, performed at intervals throughout the experimental investigation, did not exhibit variations which could be attributed to changes in composition of the oil in storage.

#### Experimental Procedure

The program of experiments was designed to measure quantitatively the variation in shear stress with time at constant rate of shear and to investigate the separate effects of temperature, shear history and thermal history on this behavior. To this end, small samples of crude oil (approximately 200 cc) were obtained from storage, maintained at a constant temperature,  $T_H$ , for a period of ten days, then placed in the viscometer for analysis. Selection of the ten day curing period was based on a number of preliminary experiments which indicated that no significant changes in behavior occurred after this length of time.

The routine of viscometric analysis consisted of a sequence of steps which may be outlined as follows. The temperature of the assembled viscometer and viscometer cabinet was adjusted to the desired testing condition,  $T_T$ , and the apparatus allowed to reach



thermal equilibrium. An appropriate amount of oil was then introduced into the cup by gravity flow through a flexible tube connecting the sample bottle (Y in Figure 6) with the bottom inlet of the cup. To avoid excessive shearing of the sample, this operation was carried out very slowly requiring approximately five minutes for the transfer of 100 cc of oil. The protractor, water-seal device and thermocouple leads were then mounted in position and the entire system allowed to remain undisturbed for 30 minutes. Although the choice of this particular time interval was arbitrary, it did guarantee the attainment of thermal equilibrium in the oil sample without incurring inordinate losses of the light hydrocarbons. Furthermore, the rheological behavior of the oil did not change appreciably when the residence time was increased to 60 minutes.

Following measurement of the oil temperature, the thermocouple leads were disconnected and the viscometer cup set in motion at the desired angular velocity,  $S_H$ . The resulting bob deflection was noted at 15 seconds, 30 seconds, 60 seconds and every minute thereafter for a period of 55 minutes or until the deflection did not change more than 1 percent in 10 minutes. The instantaneous shear stress,  $T$ , was computed from these measurements. The rotational speed of the cup was then altered to a second predetermined value,  $S_T$ , and the deflection of the bob, or shear stress  $T_T$ , determined as a function of time. Upon completion of these tests the oil temperature was again measured, the sample removed from the cup and discarded and the viscometer cleaned and prepared for the subsequent test.



The complete schedule of experiments is illustrated in Table (I). The procedure outlined above was repeated for all possible combinations of the four variables ( $T_H$ ,  $T_T$ ,  $S_H$  and  $S_T$ ) appearing in the table.

TABLE I

$T_H$ *	75		45		15		$^{\circ}\text{F}$
$T_T$ *	90	75	60	45	30	$^{\circ}\text{F}$	
$S_H$ *	0.5		2.5		4.5		RPS
$S_T$ *	0.5	1.5	2.5	3.5	4.5	RPS	

In addition to the above tests, the limiting value of shear stress, occasioned by prolonged shear at very high shear rates, was determined at each test temperature to permit valuation of the Newtonian solvent viscosity. These shear rates were achieved by inserting the lucite sleeve (Q in Figure 6) into the cup thereby reducing the width of the annulus from 0.0995 inches to 0.0292 inches. The maximum attainable shear rate in the viscometer was increased from approximately  $600 \text{ sec}^{-1}$  to  $1500 \text{ sec}^{-1}$  by this technique.

\*  $T_H$  - Cure temperature,  $^{\circ}\text{F}$

$T_T$  - Test temperature,  $^{\circ}\text{F}$

$S_H$  - Initial cup speed, RPS

$S_T$  - Final cup speed, RPS



## VI EXPERIMENTAL RESULTS

For reasons which will be explained later, the results presented here pertain only to those experiments in which the curing temperature,  $T_H$ , was  $75^{\circ}\text{F}$ . The basic data pertaining to these experiments are tabulated in Appendix (7) while the remaining data are available in the author's laboratory note book.

Due to the design of the viscometer and the nature of the experimental procedure, the basic data were obtained in the form of bob deflection as a function of time of shearing at constant cup speed and test temperatures. The bob deflection was then converted to the equivalent shear stress by means of equation (72) for the sake of convenience in subsequent interpretation. The relationship existing between shear stress and time at each testing condition is presented graphically in Figures (11) to (31). Figures (11) to (25) represent all of the data obtained from the  $S_H$  portions of the tests while Figures (26) to (31) represent selected data from the  $S_T$  portions of the tests.

Inspection of Table (I) reveals that at any test temperature five duplicate experiments were performed at each of the three  $S_H$  cup speeds. This was necessary to prepare the oil samples for the succeeding tests at the five  $S_T$  cup speeds. Consequently, in Figures (11) to (25) the smooth curve is defined by the average of five independent analyses whereas only one analysis was available for each of the  $S_T$  curves illustrated in Figures (26) to (31). The accuracy



Figure 11

Shear Stress Decay Curve  
Shear Stress  
vs  
Time  
Cure Temperature 75 °F  
Test Temperature 90 °F  
Cup Speed 0.522 RPS

$T \times 10^4$  (lb $\text{f}$ /in $^2$ )

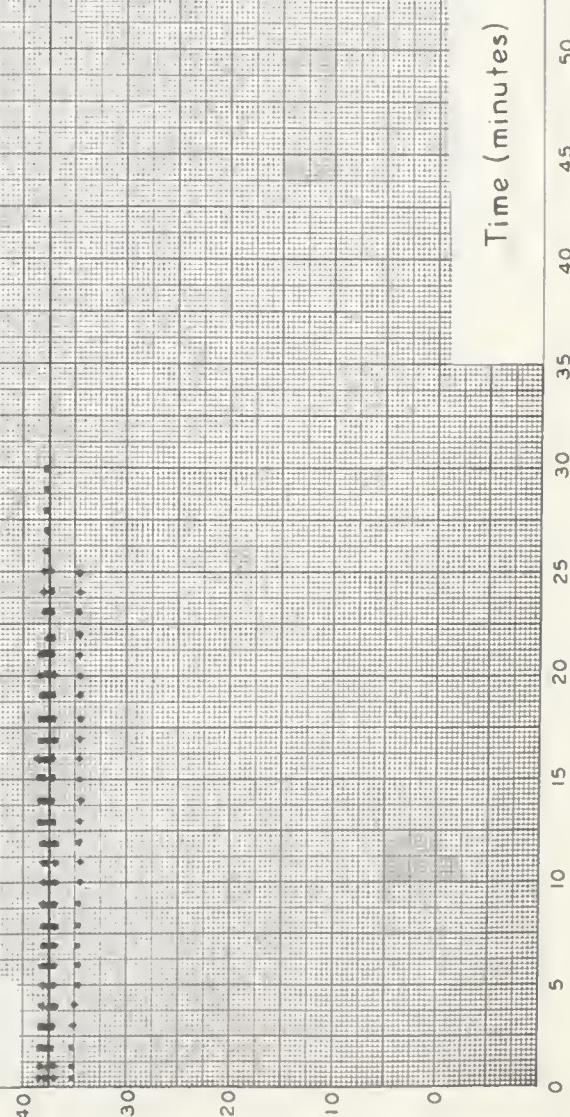




Figure 12

Shear Stress Decay Curve  
Shear Stress  
vs  
Time

Cure Temperature 75°F  
Test Temperature 90°F  
Cup Speed 2.472 RPS

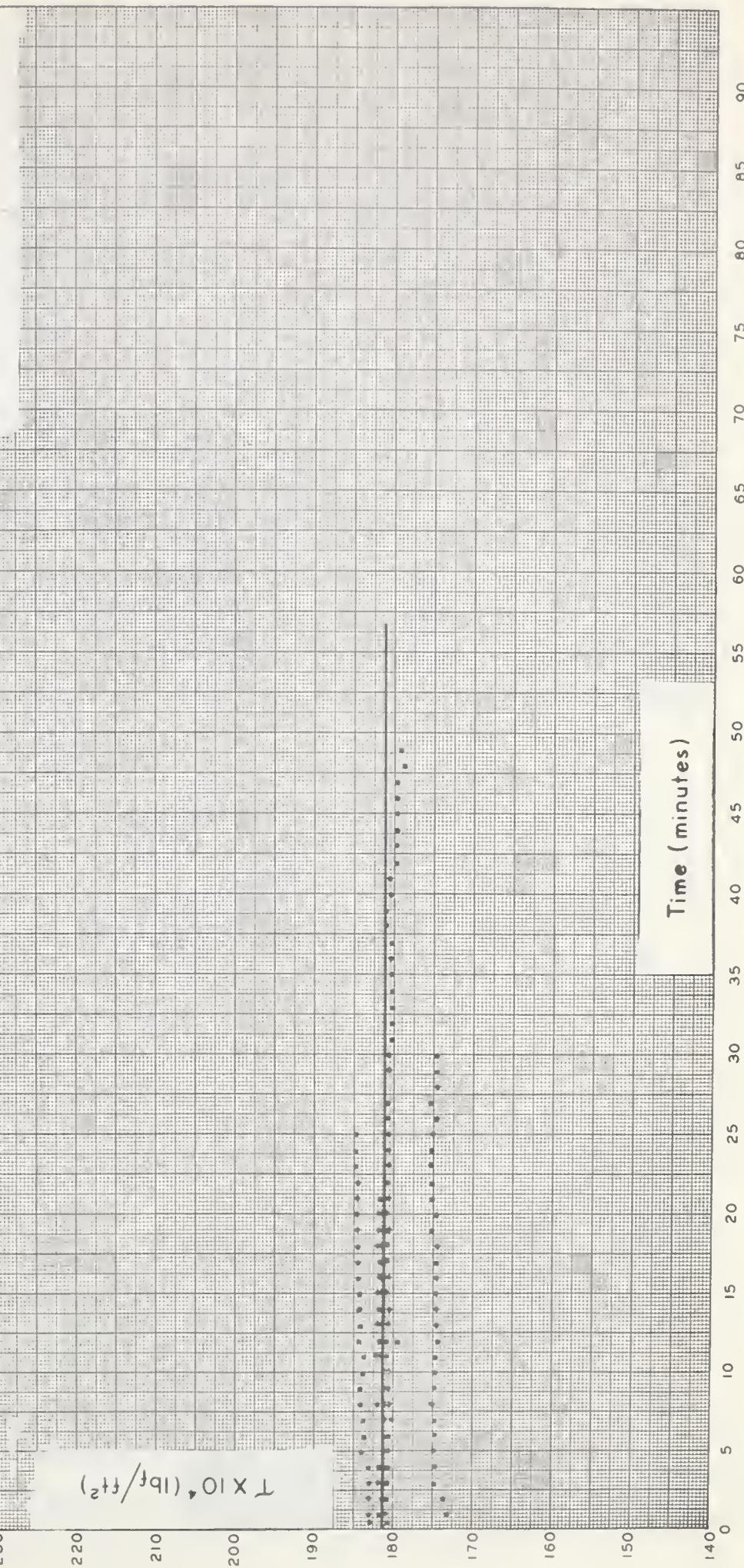




Figure 13

Shear Stress Decay Curve  
Shear Stress  
vs  
Time

Cure Temperature 75° F  
Test Temperature 90° F  
Cup Speed 4.456 RPS

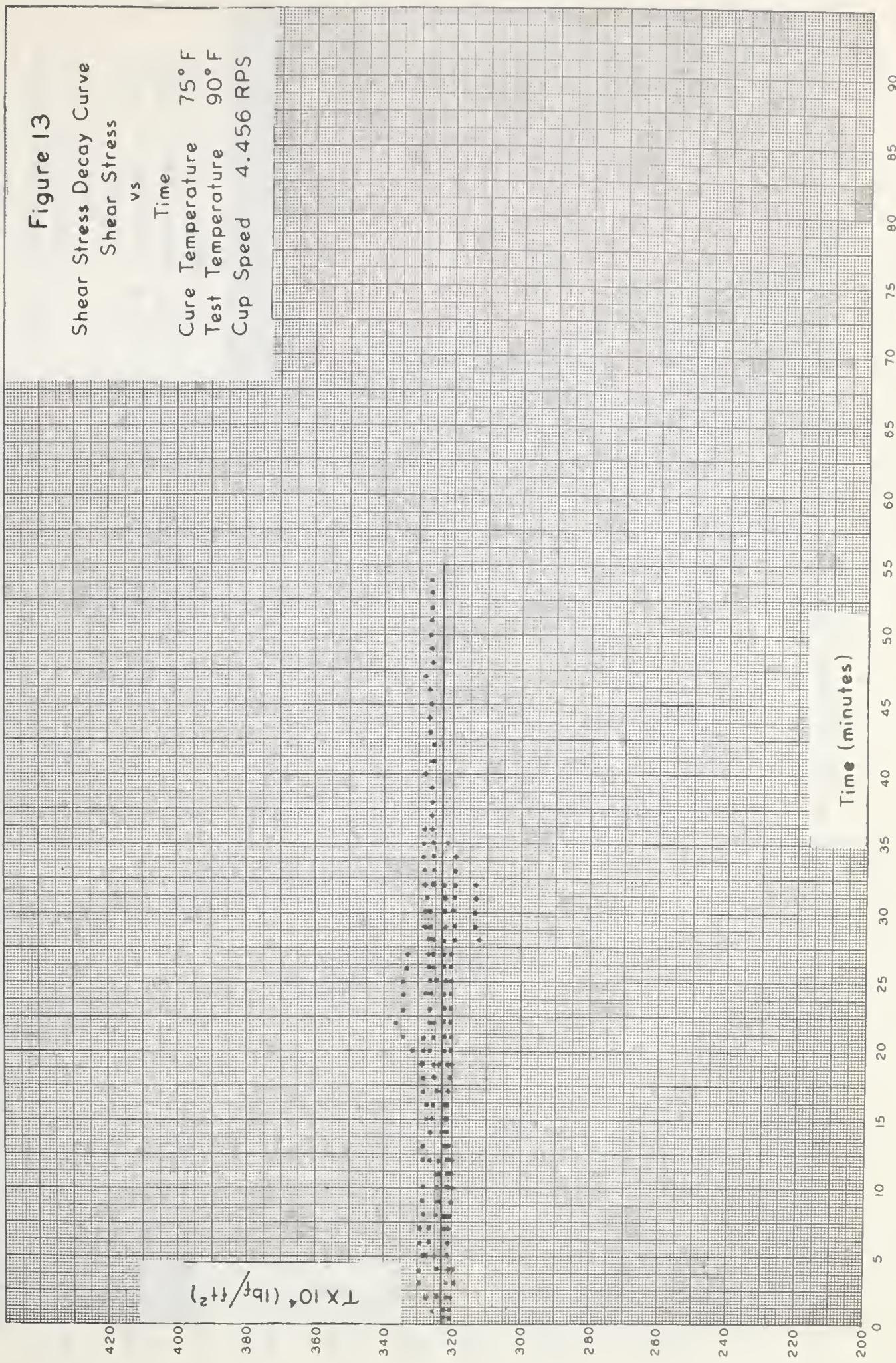




Figure 14

Shear Stress Decay Curve  
Shear Stress  
vs  
Time  
Cure Temperature 75° F  
Test Temperature 75° F  
Cup Speed 0.509 RPS

220  
200  
180  
160  
140  
120  
100  
80  
60  
 $T \times 10^4 (\text{lb}^f/\text{ft}^2)$

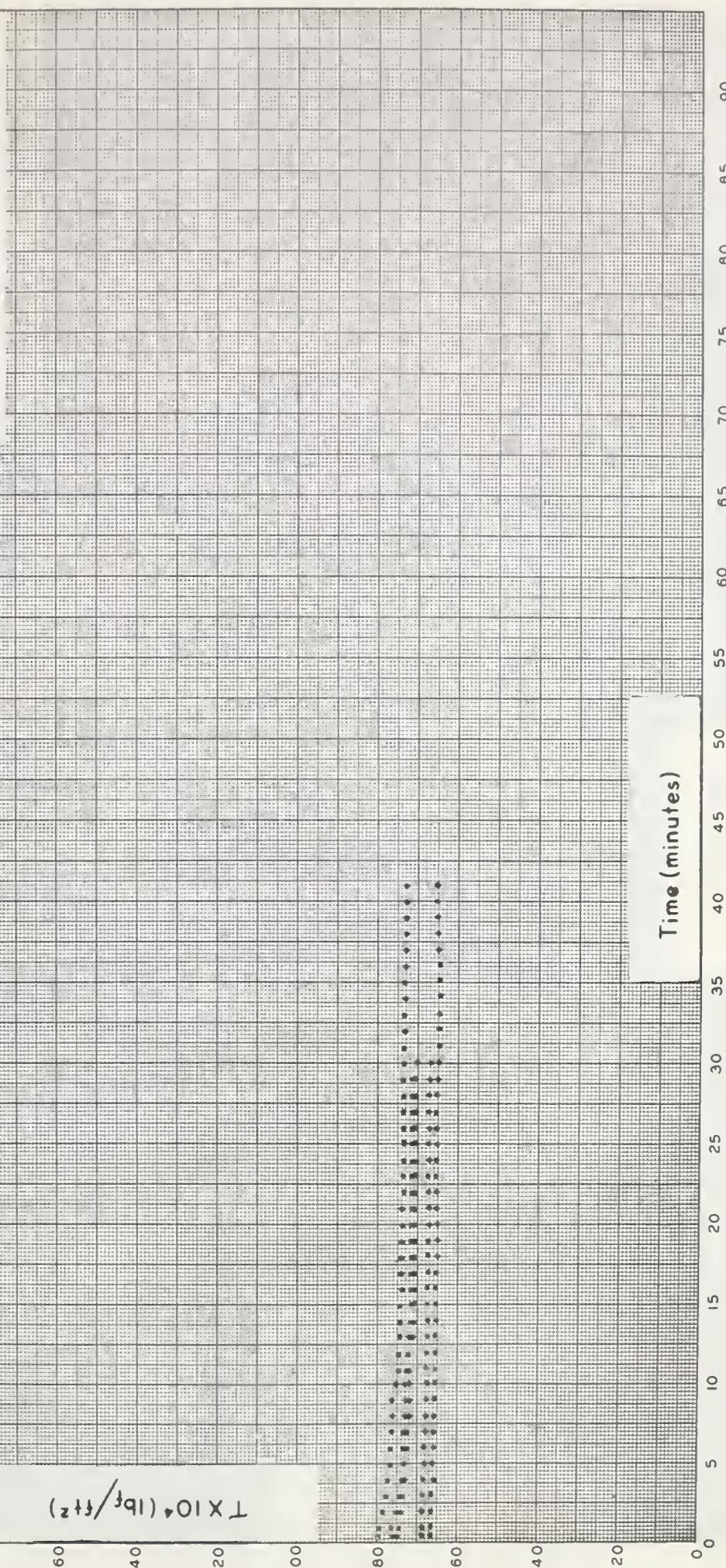




Figure 15

Shear Stress Decay Curve  
Shear Stress vs Time

Cure Temperature 75°F  
Test Temperature 75°F  
Cup Speed 2.495 RPS

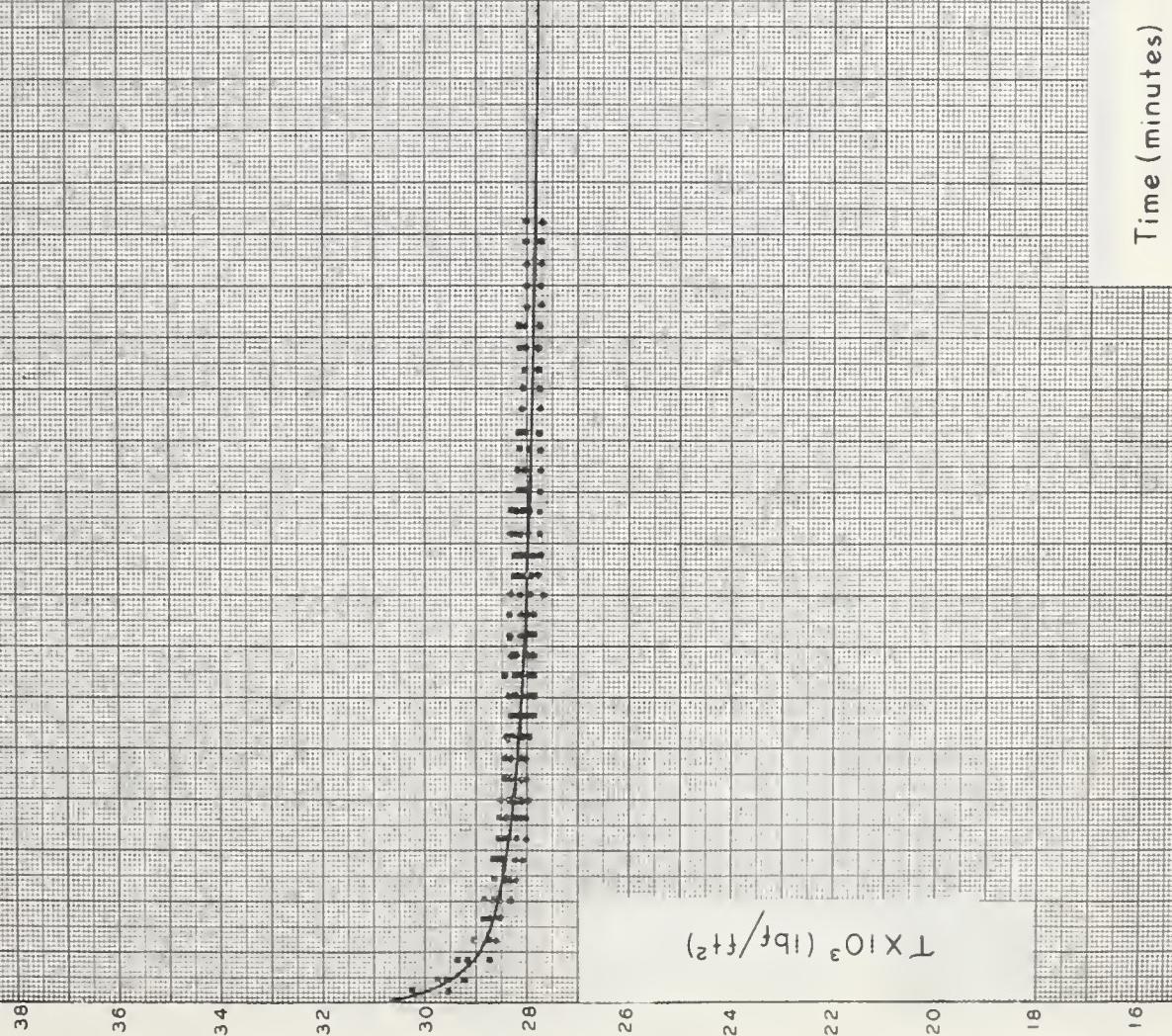




Figure 16

Shear Stress Decay Curve  
Shear Stress vs Time  
Cure Temperature 75°F  
Test Temperature 75°F  
Cup Speed 4.471 RPS

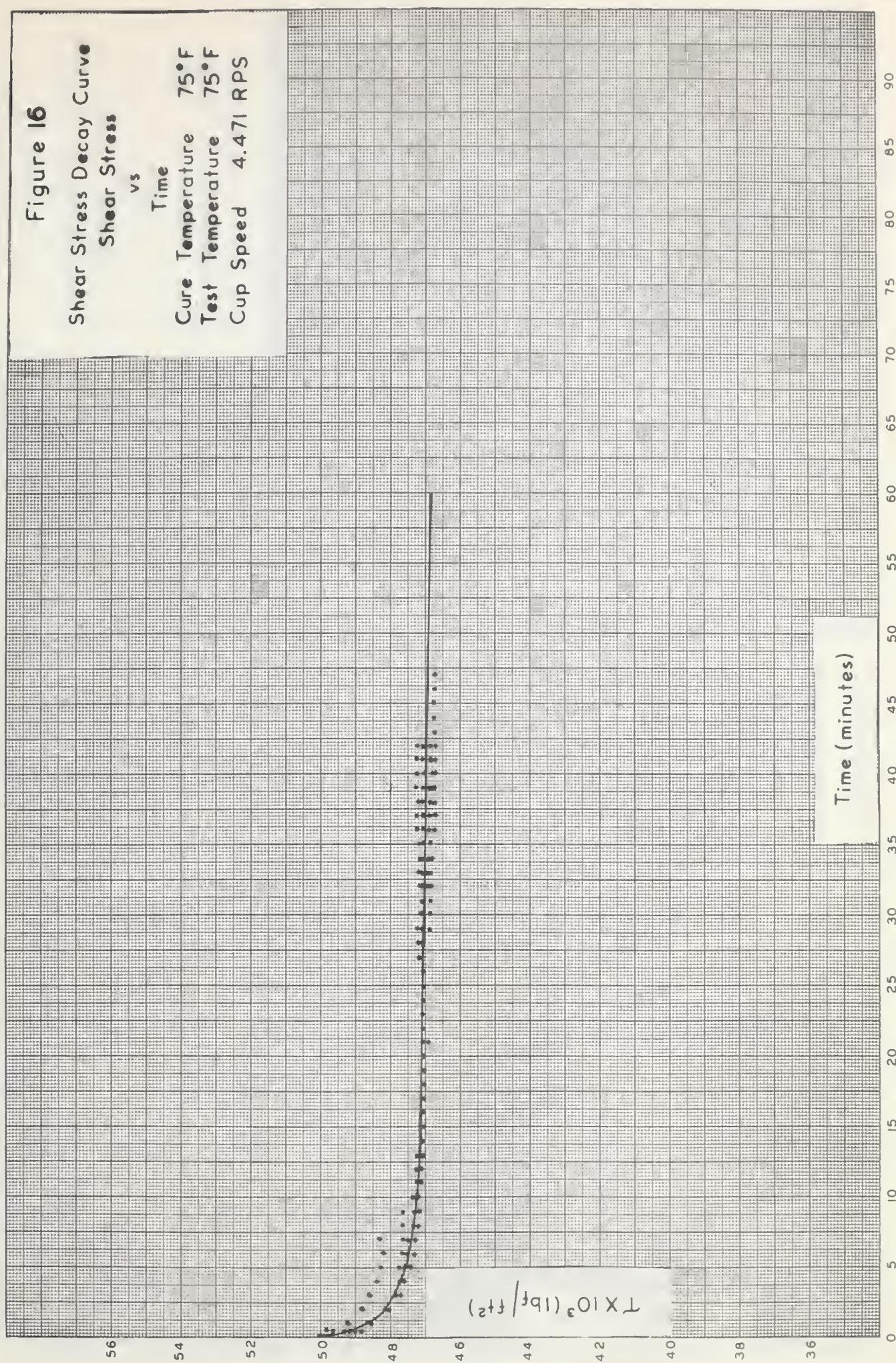




Figure 17

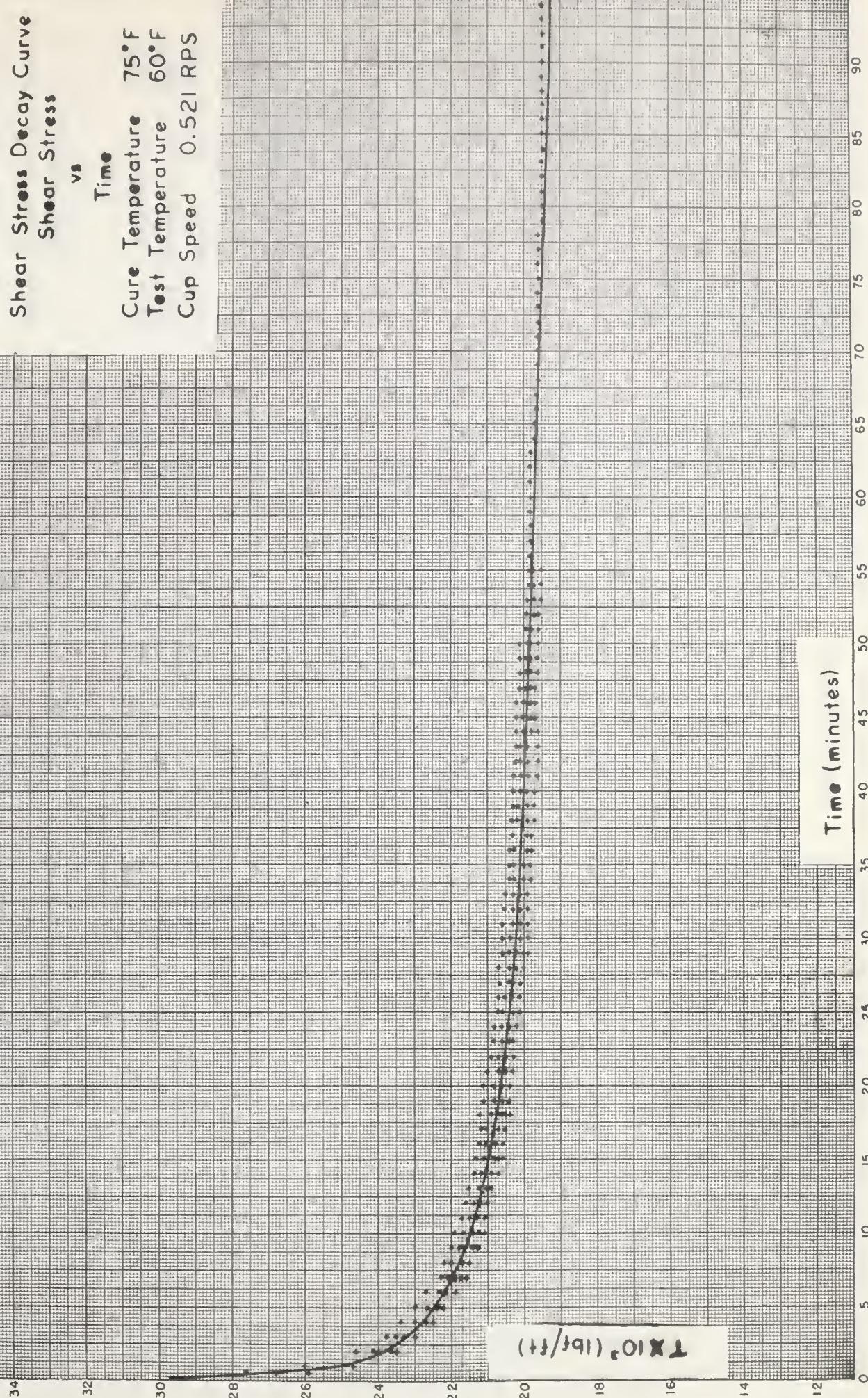




Figure 18

Shear Stress Decay Curve  
Shear Stress

vs

Time

Cure Temperature 75°F  
Test Temperature 60°F  
Cup Speed 2.498 RPS

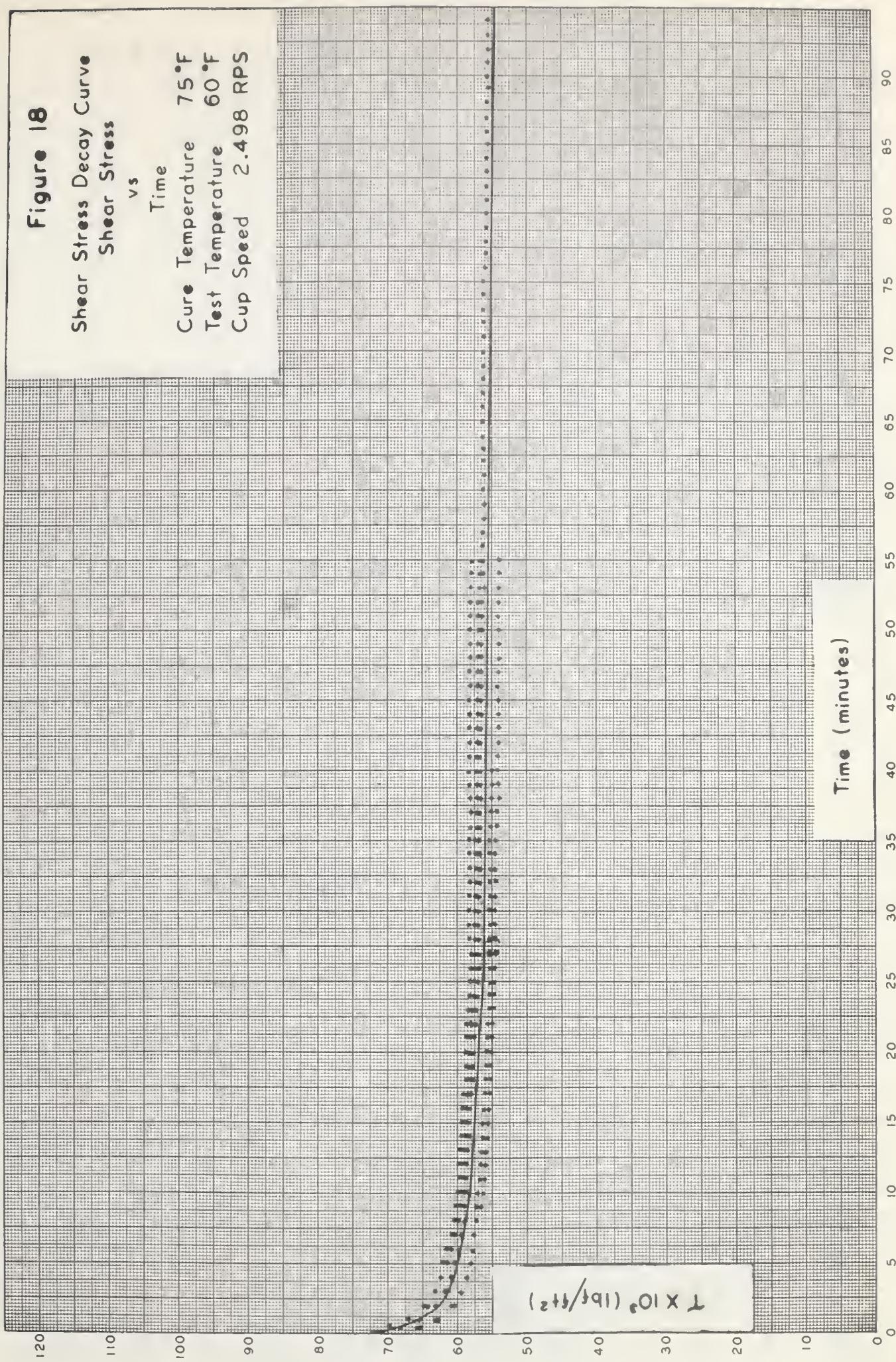




Figure 19

Shear Stress Decay Curve  
Shear Stress  
vs  
Time  
Cure Temperature 75°F  
Test Temperature 60°F  
Cup Speed 4.478 RPS

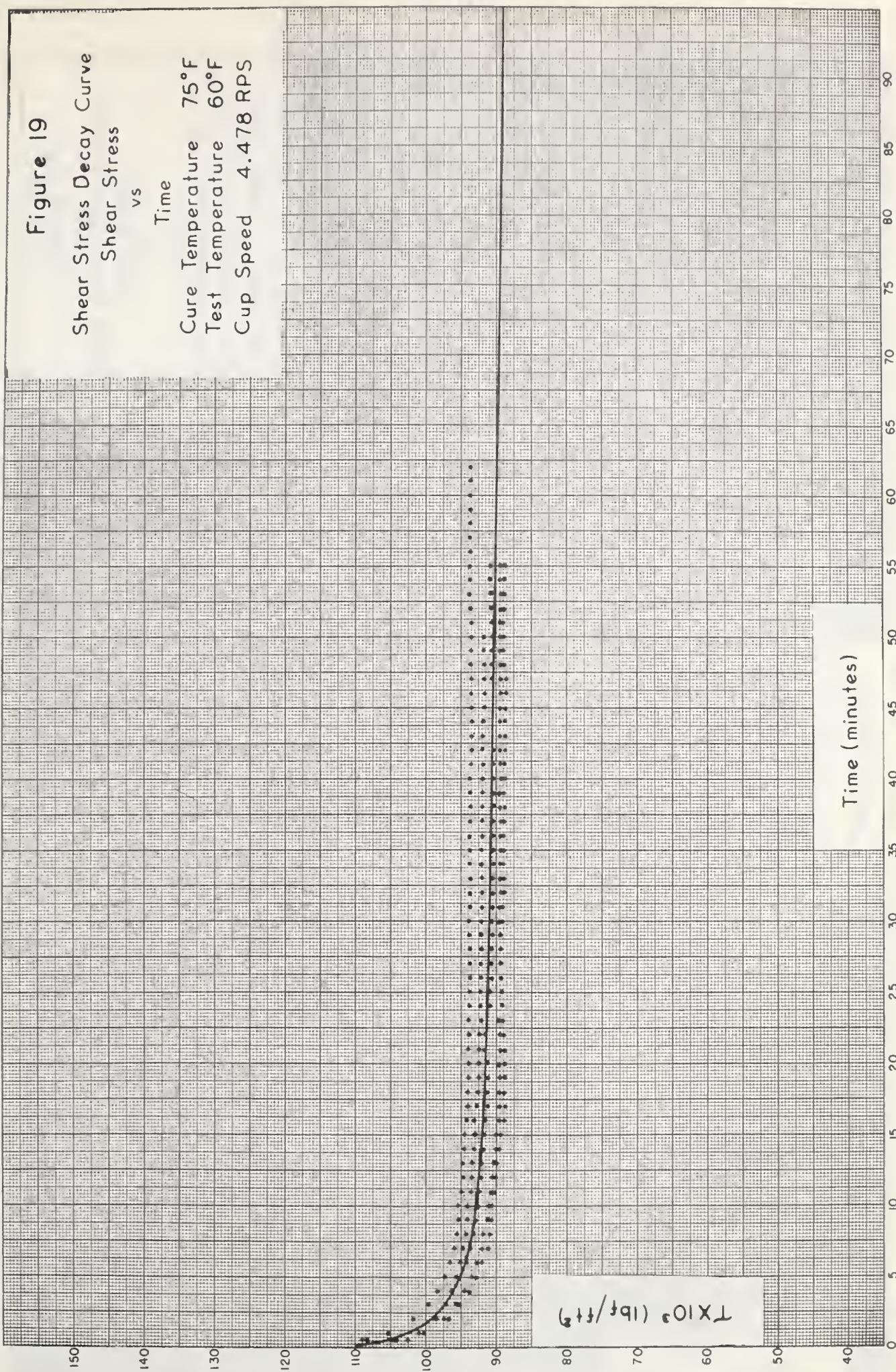




Figure 20

Shear Stress Decay Curve  
Shear Stress  
vs  
Time  
Cure Temperature 75 °F  
Test Temperature 44.5 °F  
Cup Speed 0.525 RPS

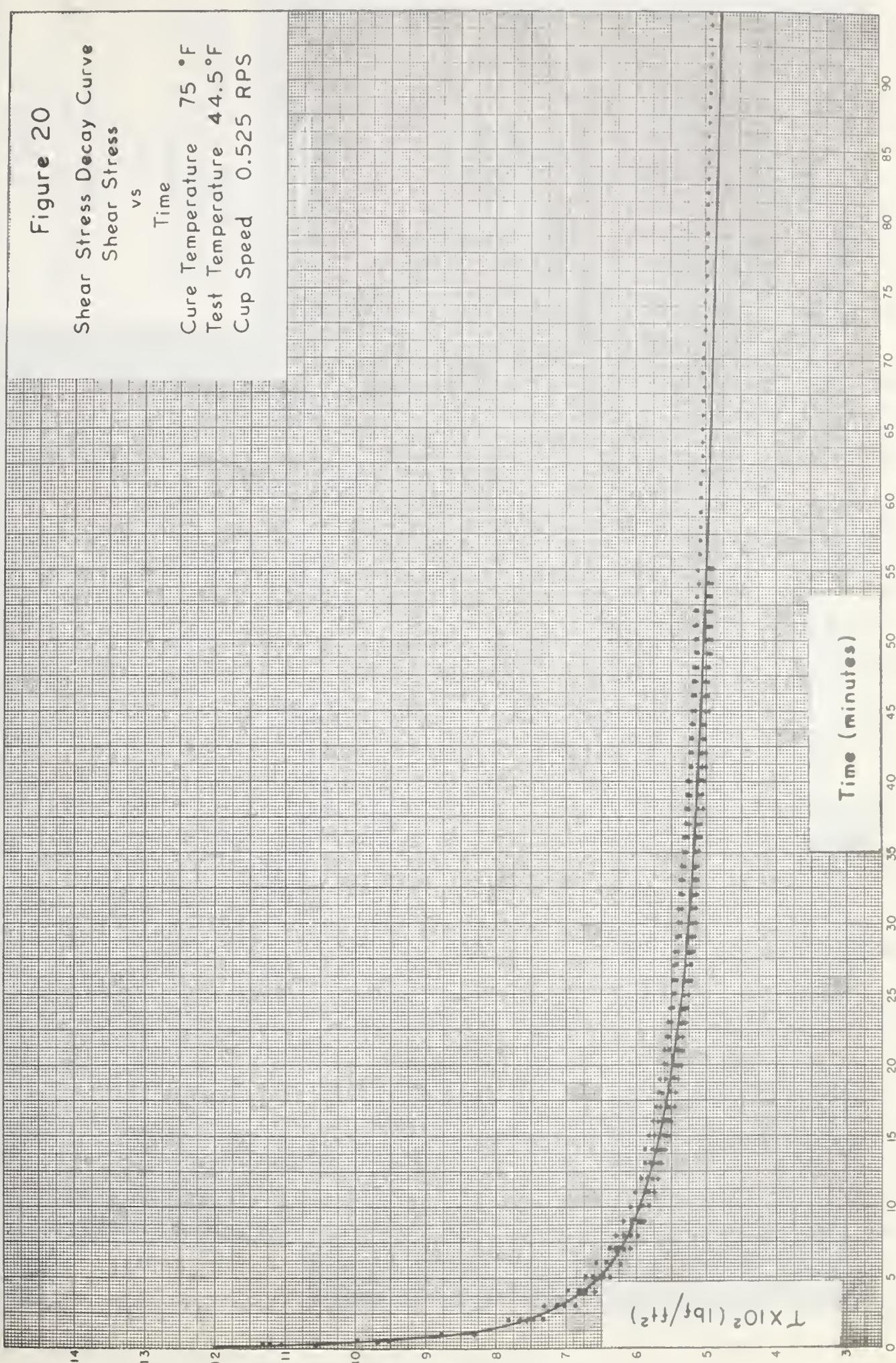




Figure 21

Shear Stress Decay Curve  
Shear Stress  
vs  
Time  
Cure Temperature 75°F  
Test Temperature 44.5°F  
Cup Speed 2.497 RPS

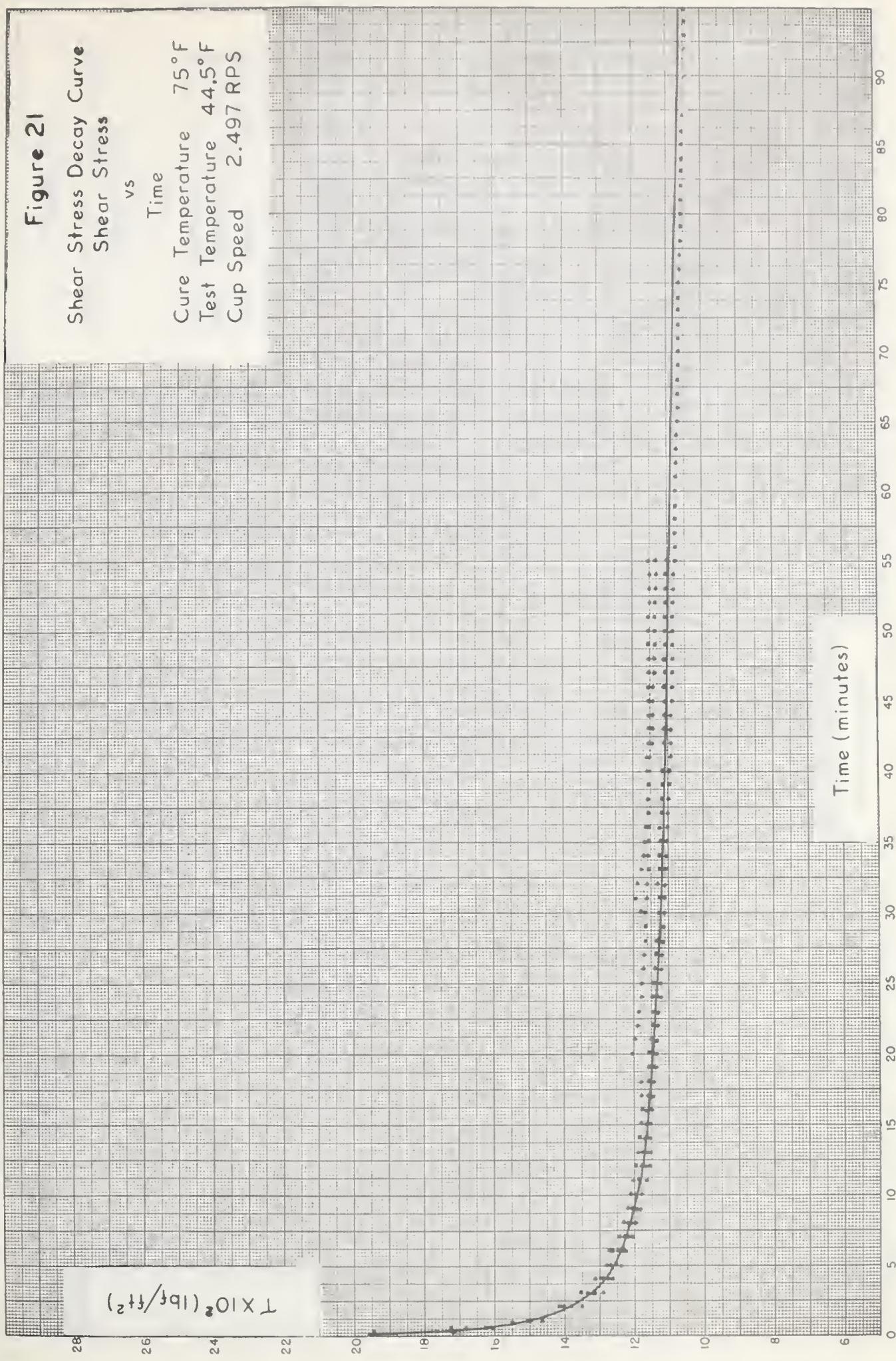




Figure 22

Shear Stress Decay Curve  
vs  
Time

Cure Temperature 75°F  
Test Temperature 44.5°F  
Cup Speed 4.483 RPS

$T \times 10^2$  ( $\text{lb}_f/\text{in}^2$ )

32 30 28 26 24 22 20 18 16 14 12 10

Time (minutes)  
90 85 80 75 70 65 60 55 50 45 40 35 30 25 20 15 10 5 0

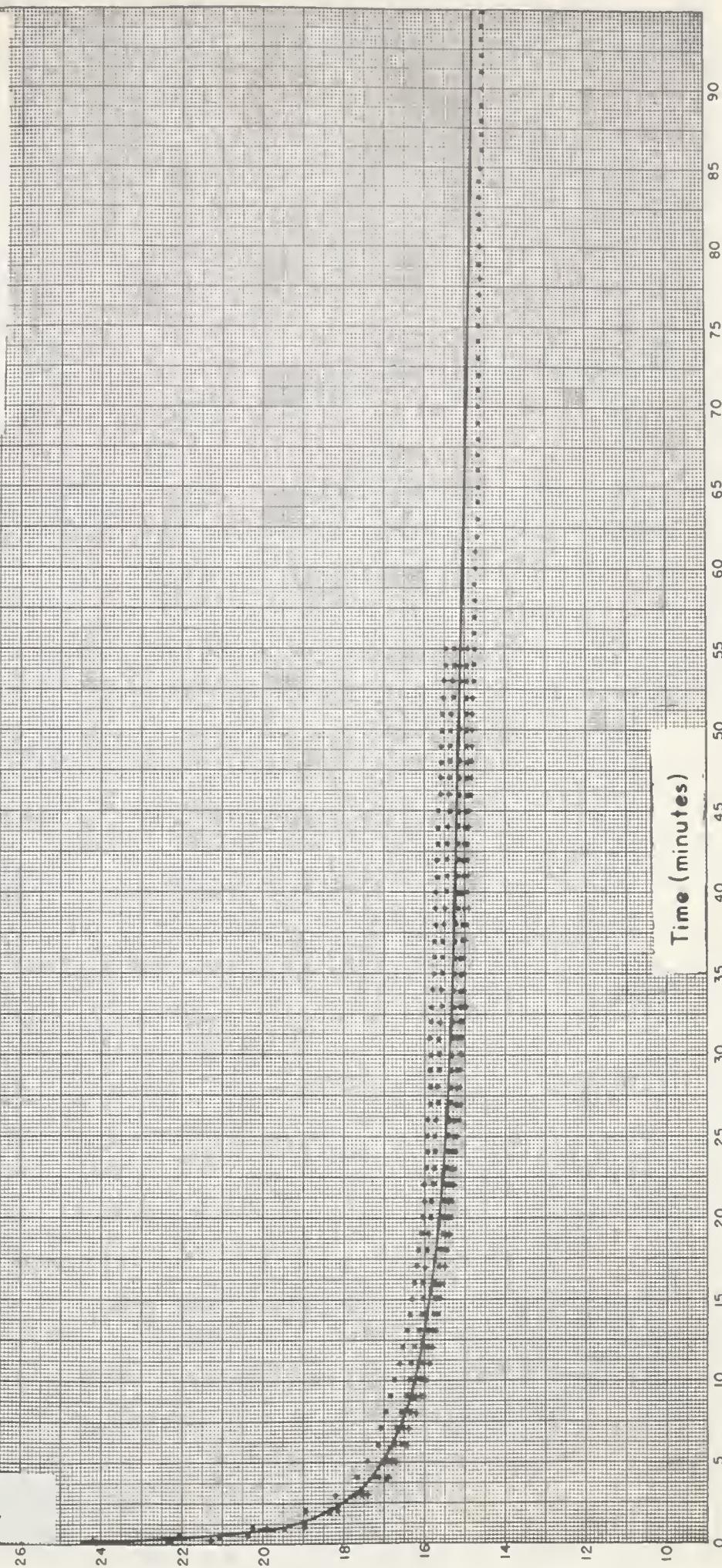




Figure 23

Shear Stress Decay Curve  
Shear Stress  
vs  
Time

Cure Temperature 75°F  
Test Temperature 30°F  
Cup Speed 0.538 RPS

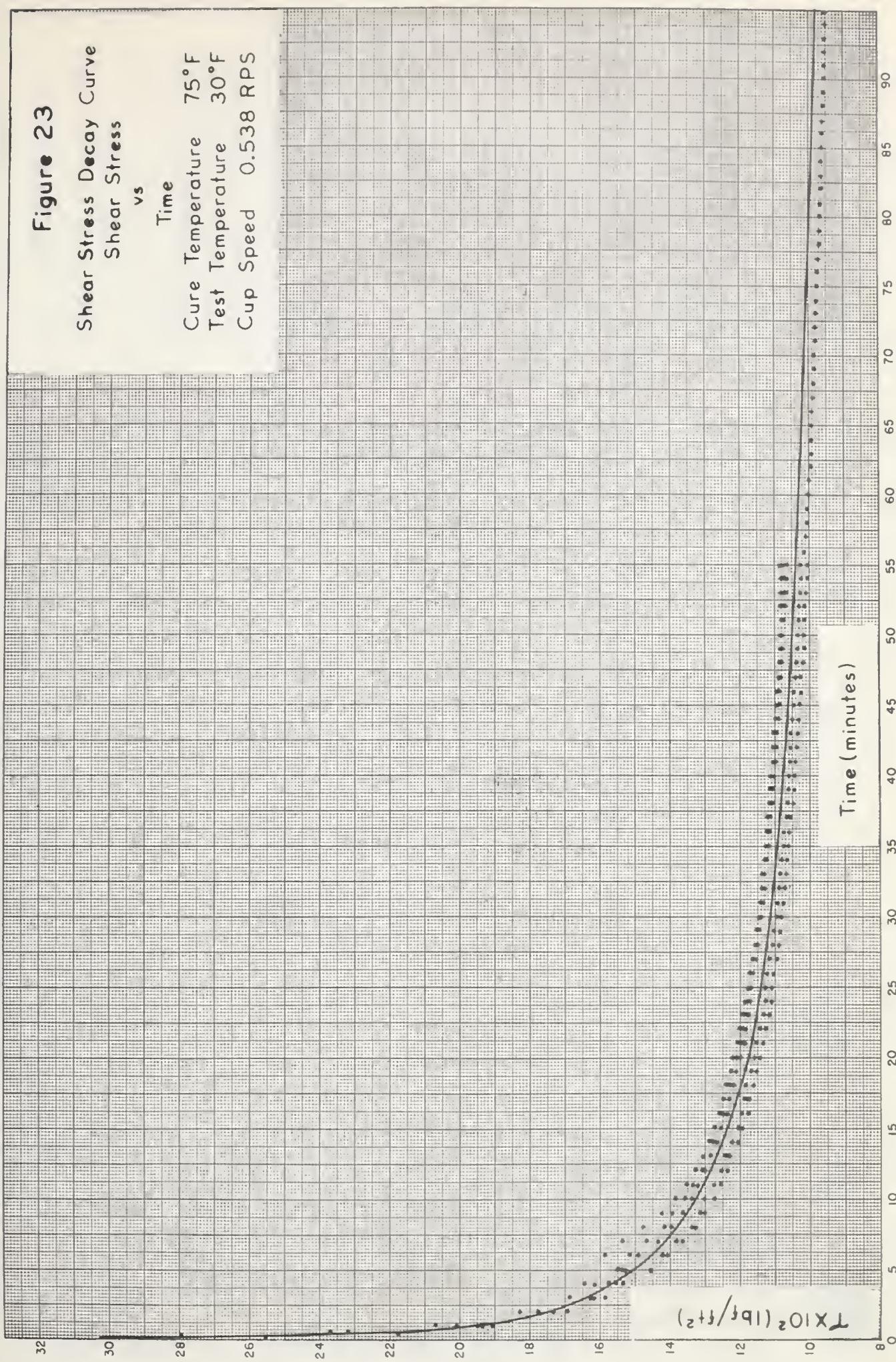




Figure 24

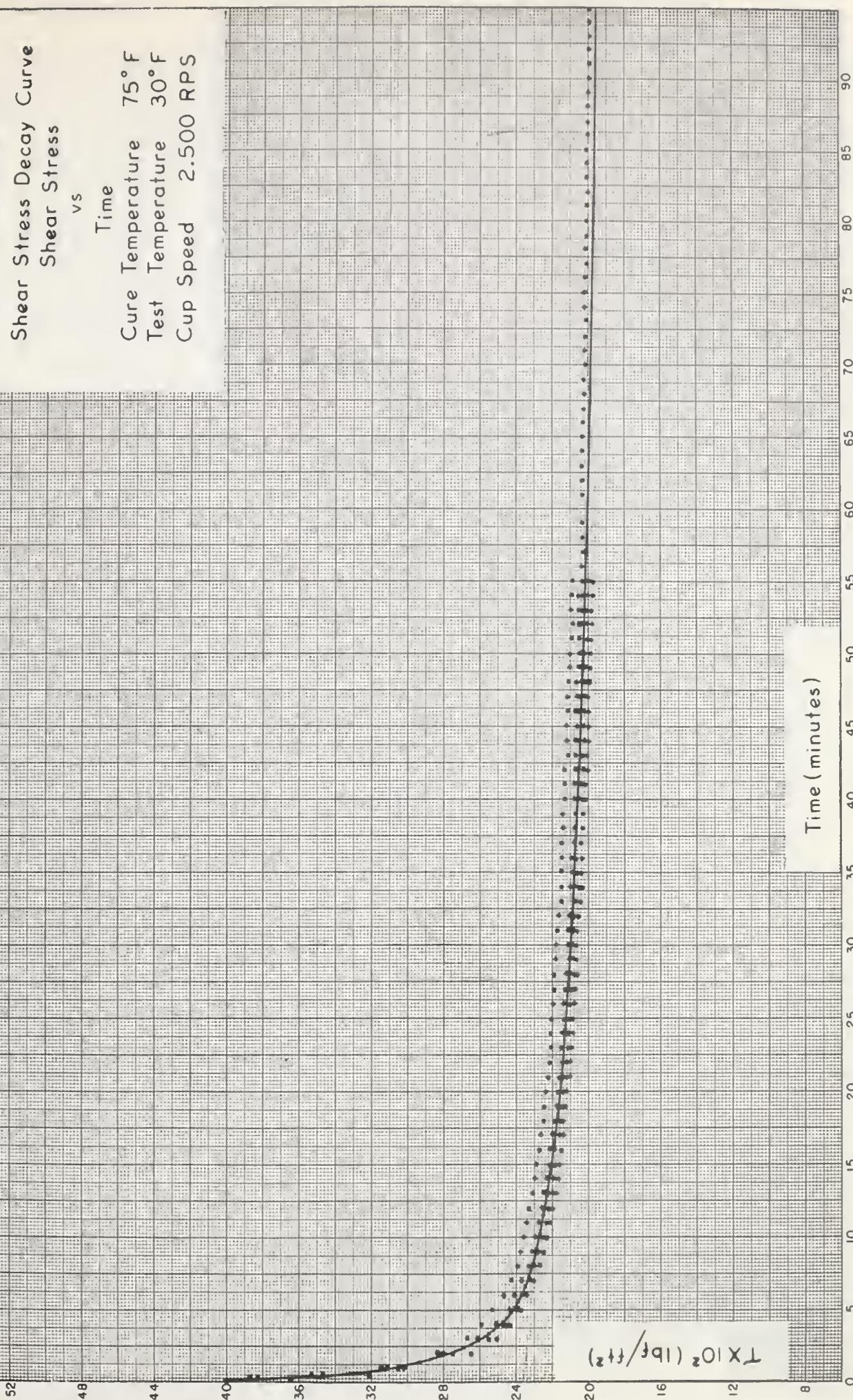




Figure 25

Shear Stress Decay Curve  
Shear Stress vs  
Time

Cure Temperature 75°F  
Test Temperature 30°F  
Cup Speed 4.510 RPS

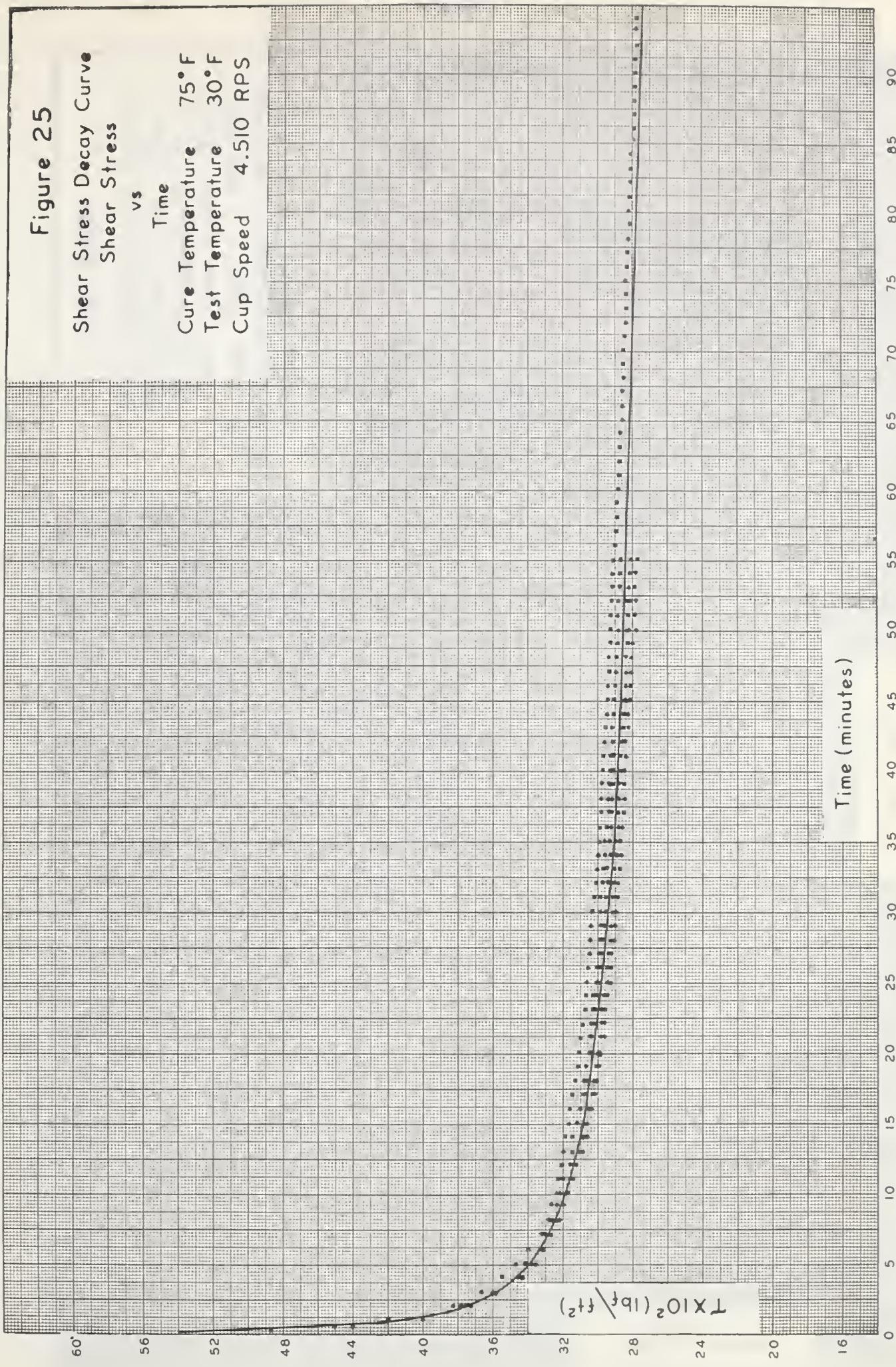




Figure 26

Shear Stress Growth Curve  
Shear Stress vs Time  
Cure Temperature 75°F  
Test Temperature 60°F  
● Cup Speed 0.506 RPS  
● Previous Cup Speed 2.494 RPS  
x Cup Speed 0.510 RPS  
Previous Cup Speed 4.470 RPS

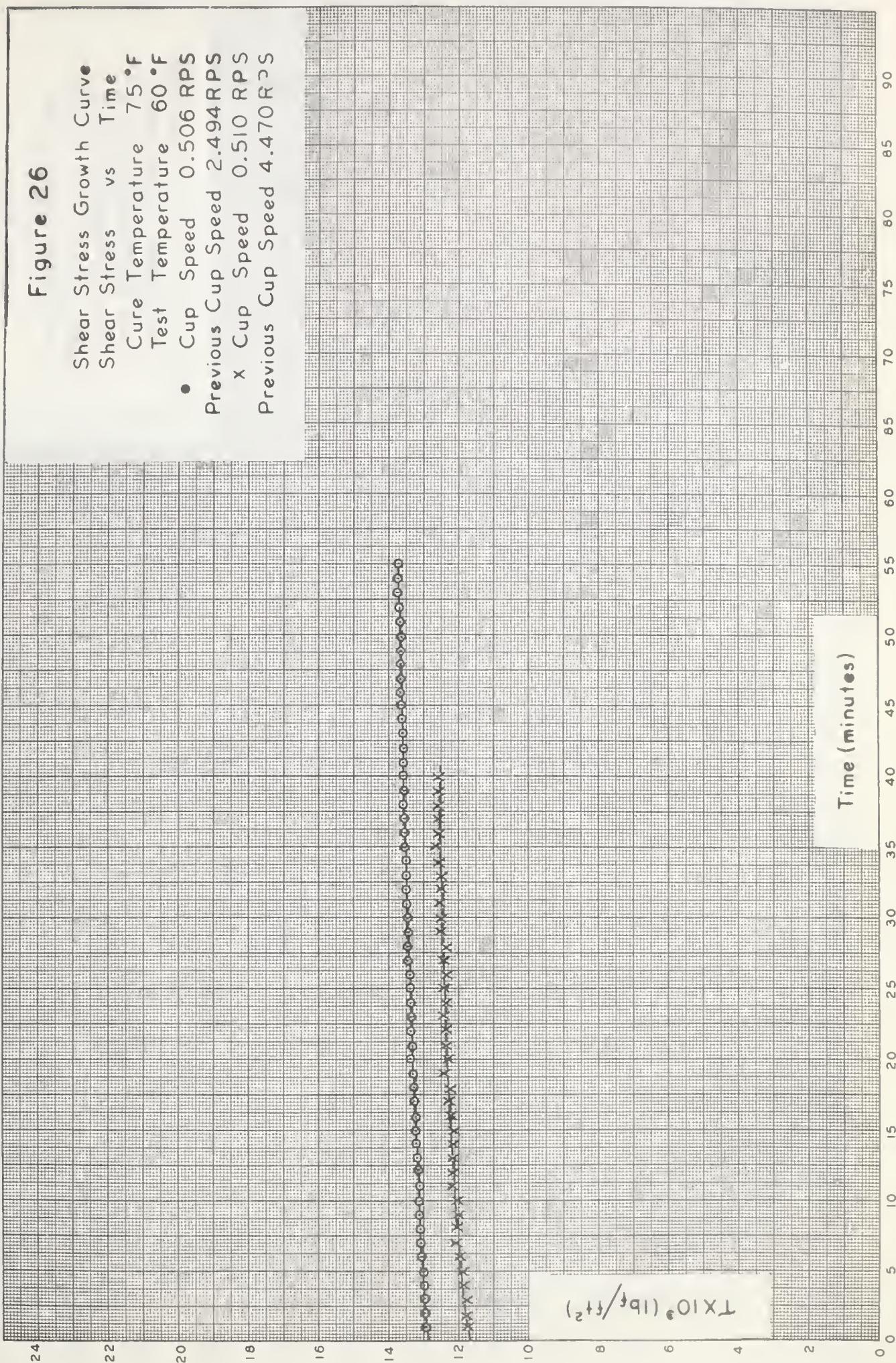




Figure 27

Shear Stress Growth Curve  
Shear Stress vs Time  
Cure Temperature 75°F  
Test Temperature 60°F  
Cup Speed 2.497 RPS  
Previous Cup Speed 4.468 RPS

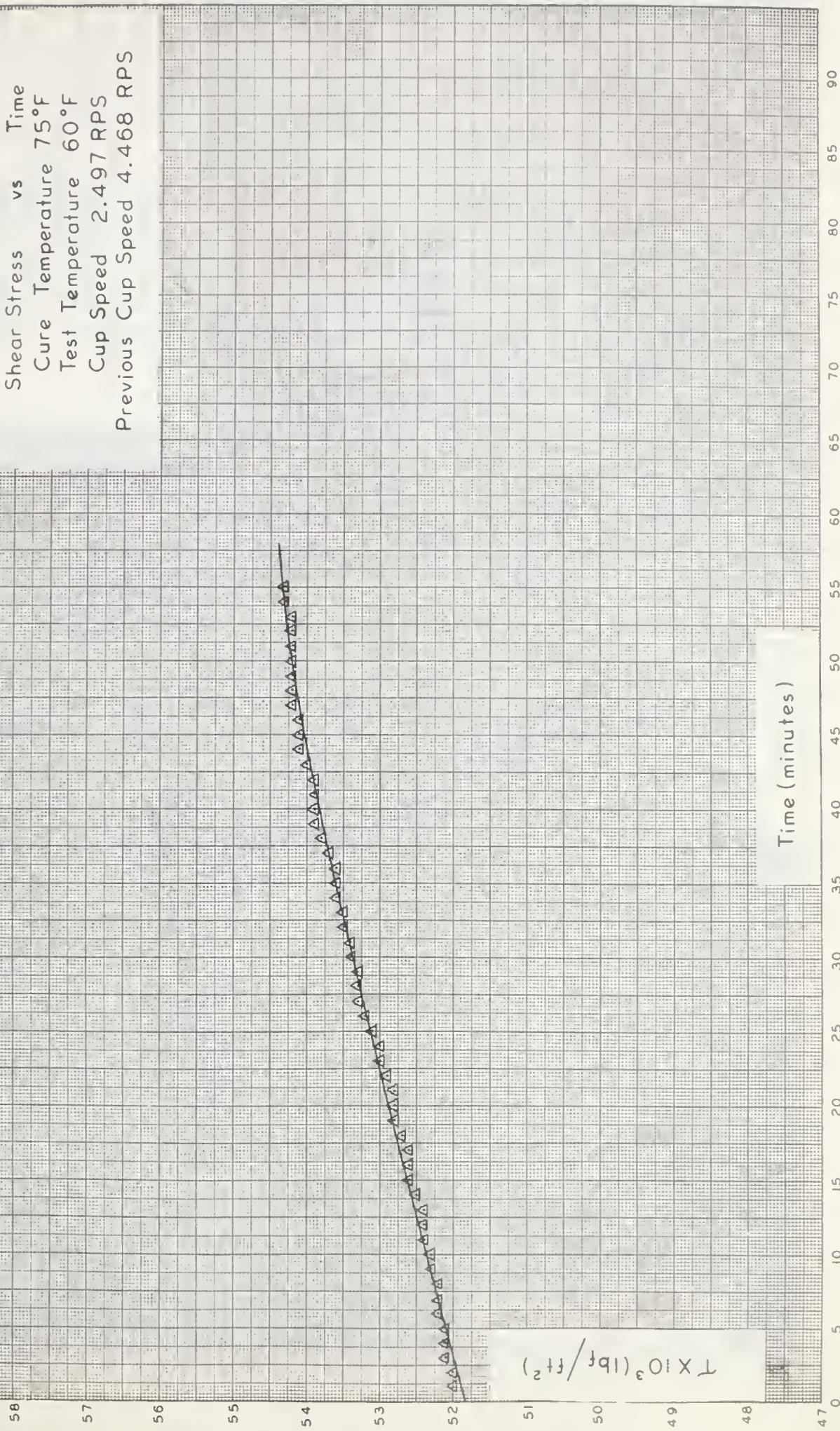




Figure 28

Shear Stress Growth Curve  
Shear Stress vs Time  
Cure Temperature 75 F°  
Test Temperature 44.5 F°  
○ Cup Speed 0.520 RPS  
Previous Cup Speed 2.492 RPS  
X Cup Speed 0.534 RPS  
Previous Cup Speed 4.490 RPS

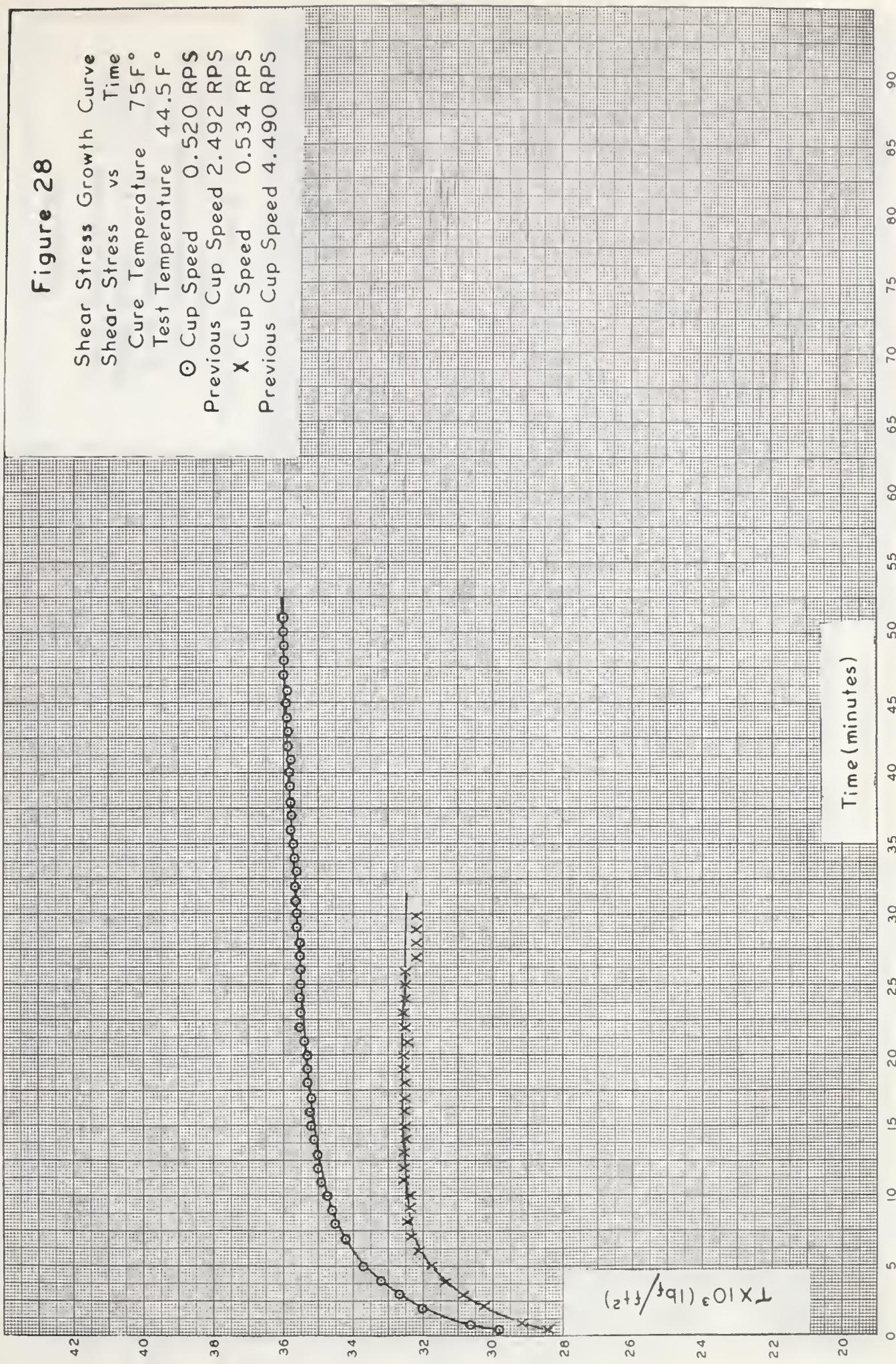




Figure 29

Shear Stress Growth Curve  
Shear Stress vs Time  
Cure Temperature 75°F  
Test Temperature 44.5°F  
Cup Speed 2.492 RPS  
Previous Cup Speed 4.483 RPS

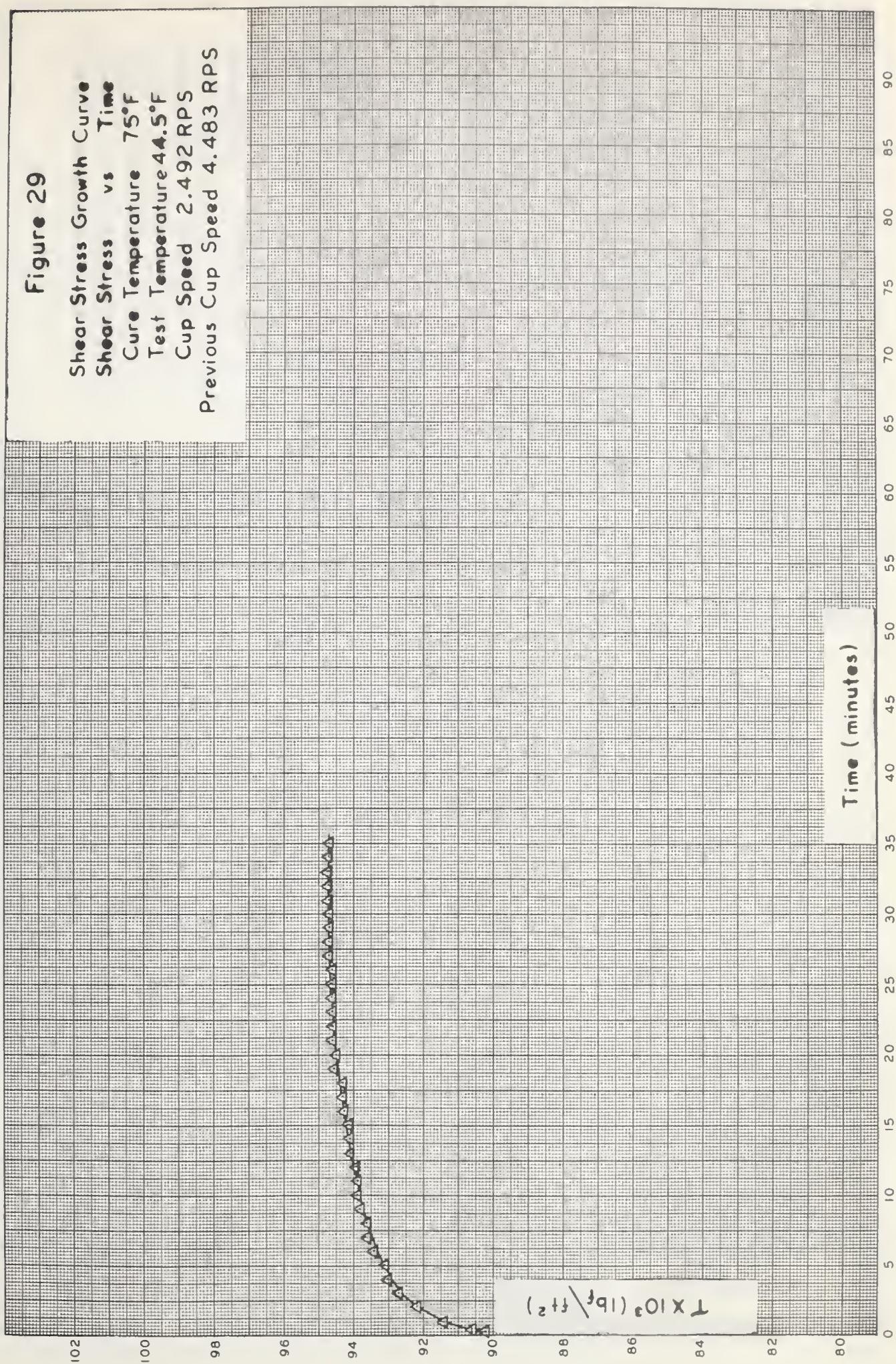




Figure 30

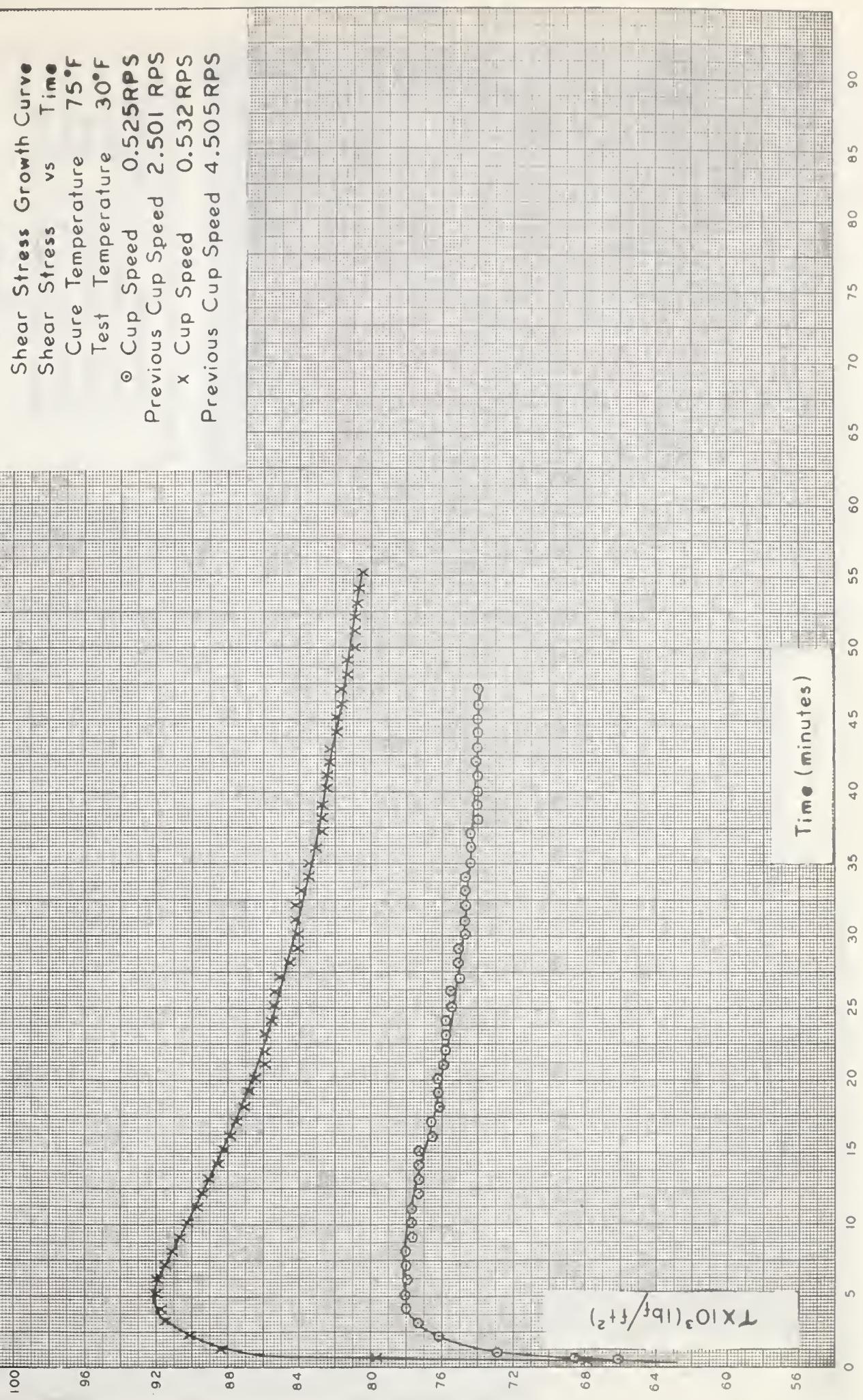
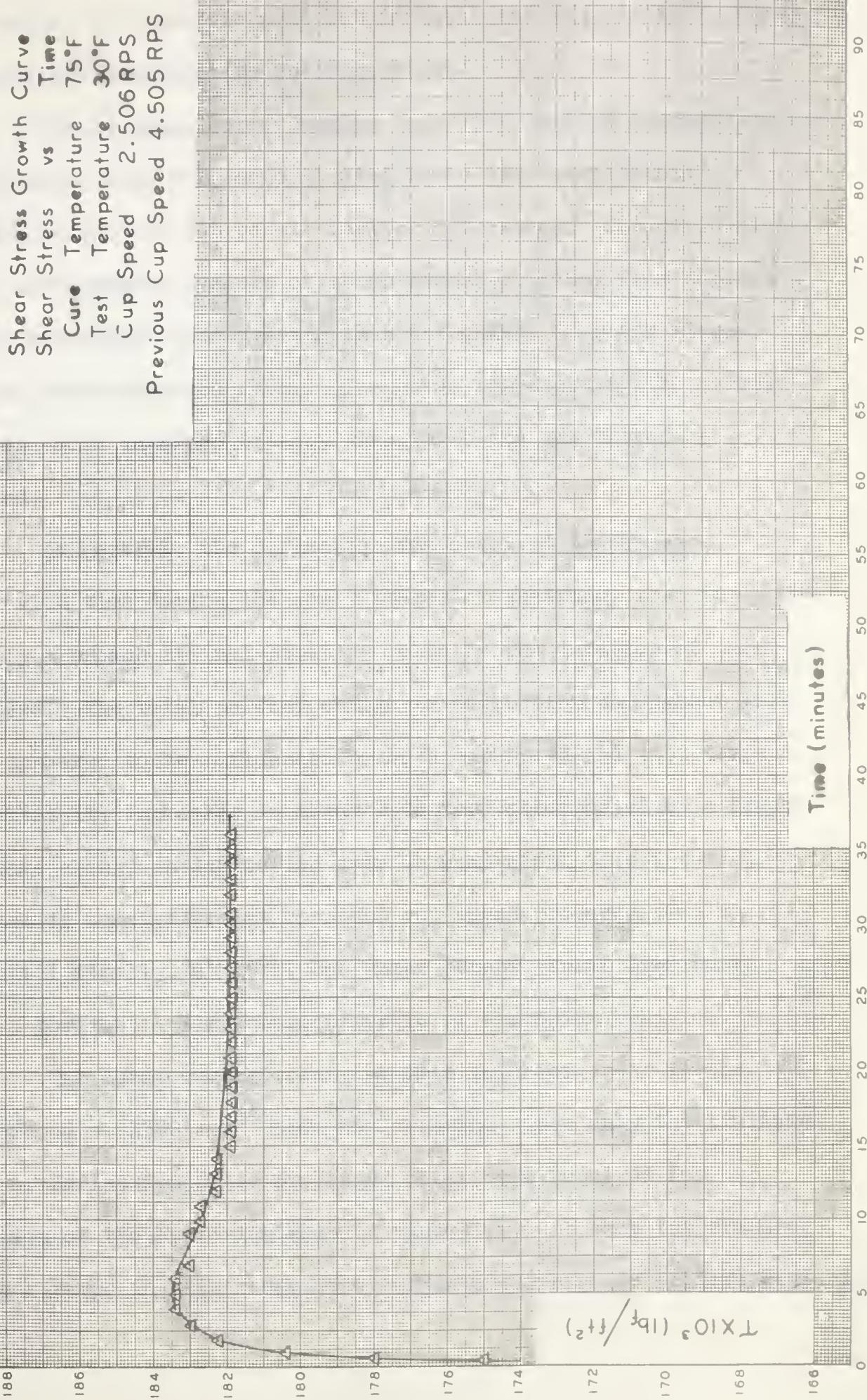




Figure 31





of the latter is therefore somewhat doubtful and was, in fact, found inadequate for quantitative interpretation.

The  $S_H$  data, corresponding to a 75°F testing temperature and a cup speed of 0.52 RPS, demonstrated large and inexplicable variations which did not permit further processing. The difference between instantaneous values of shear stress obtained from duplicate analysis was found to be greater than the change in shear stress resulting from prolonged shear. The curve representing the average values of these data was totally unreliable and was therefore discarded.

In general, the deflection was observed to decrease rapidly with time during the early stages of shearing, then to gradually approach a final limiting value as the duration of shear progressed. The total percent change in deflection throughout this period appeared to be influenced by both cup speed and test temperature. That is, increases in shear rate were accompanied by a lower percentage change in deflection over an equivalent time interval. Increases in temperature at constant cup speed produced similar results until finally, at 90°F, the shear stress versus time curve became a horizontal line characteristic of Newtonian behavior.

The decay curves resulting from rates of shear in the neighborhood of  $1500 \text{ sec}^{-1}$  were not assessed since only the limiting values of deflection after prolonged shear were required for prediction of the Newtonian solvent viscosity. At each temperature the shear rates in this range were sufficiently high to achieve Newtonian



behavior or to allow estimation of the Newtonian viscosity through moderate extrapolation. Graphical representation of the data obtained in this phase of the investigation will not be attempted here, since certain other aspects of data processing must first be considered.

Viscous resistance to shear in a fluid results in the dissipation of energy in the form of heat which, unless efficiently removed, may cause an appreciable rise in the temperature of the fluid. The extent of such temperature changes and the associated errors in viscosity measurement have been investigated by several authors<sup>(60)(65)(29)(68)</sup>, and shown to be quite significant in many cases. The problem was considered to be of particular importance to the present study since prolonged shear at high shear rates, coupled with the highly temperature sensitive rheological properties of Pembina Crude oil, could cause extremely large errors.

Temperature measurement of the oil at the bob wall before and after each test indicated that the rate of heat transfer to the cooling bath surrounding the viscometer cup was sufficiently high to avoid excessive temperature gradients. The maximum increase in temperature, even at high shear rates, was found to be approximately 0.5°F. This small change in temperature undoubtedly influenced the rheological behavior of the oil to some extent. However, no attempt was made at estimating the magnitude of the error which might be introduced, since the effects of this variable were indistinguishable from those produced by other, more important, variables.



Control of the viscometer cup speed proved to be satisfactory in all cases. The values tabulated in Appendix (7) represent the mean of four or five measurements, obtained at intervals throughout each test, which demonstrated a maximum variation of 0.5 percent.

The rather large deviations in experimental data, apparent on Figures(11) to (25) are believed due to inconsistencies in the crude oil samples. Since these curves represent alterations in the structure of a network, they will reflect changes in any variable which influences the nature of the structure. In addition to intentional shear in the viscometer annulus, such variables include shearing during introduction of the sample and the rate of sample cooling in the cup. Numerous experiments were performed to evaluate the effects of these variables, however, the results were inconclusive. At best it might be said that the properties of the network structure are dependent upon the method of sample preparation and that a standardized procedure is essential if reproducible results are desired.

Several tests involving the measurement of network decay displayed very erratic behavior in that the bob deflection initially decreased in the customary manner, then gradually increased for a brief period of time and finally fell rapidly to an inordinately low value. This behavior is clearly illustrated by some of the data on Figures (13)and(16). Careful examination revealed that, during the period of increasing deflection the oil level rose steadily and that a considerable amount of oil was discharged from the viscometer cup



by centrifugal action. Eventually the moving oil layer collapsed and the remaining fluid returned to its proper position in the cup. However, the quantity of oil was then insufficient to produce the correct bob deflection. Although this phenomenon is not clearly understood, two possible explanations may be suggested.

Many investigators<sup>(44)(20)</sup> have observed the so called Weisenberg effect<sup>(55)</sup> through which some non-Newtonian fluids under shear tend to move up the inner cylinder of a rotational viscometer in apparent defiance of centrifugal force. It must be pointed out, however, that certain peculiarities of the present system could not be reconciled with this explanation. First the fluid did not merely cling to the bob wall but appeared to move upward with a horizontal surface extending from the bob to the cup. Second this phenomenon was not encountered in every test and was most prevalent at the higher testing temperatures under which condition the oil was more nearly Newtonian in behavior.

A second and more plausible explanation of this phenomenon is that hydrocarbon vapors, released below the oil surface, were unable to escape due to interfacial forces and therefore caused the oil film to rise in the annulus. When the oil film, at the upper edge of the cup, had become sufficiently thin to rupture, the vapors escaped and released a small amount of oil which flowed back into the annulus.

Regardless of its source, this problem, once recognized, was readily overcome by momentarily interrupting the rotation of the cup,



thereby permitting the oil to assume its proper position in the annulus. This procedure did not noticeably interfere with the continuity of the experiment since, if executed at the instant the oil began to rise, the deflection of the bob immediately returned to its appropriate value upon resumption of shear.

Other problems encountered during the course of this investigation were mainly mechanical in nature and were eventually solved without undue difficulty. Since it can serve no useful purpose, a detailed discussion of these problems will not be presented here.



## VII INTERPRETATION OF RESULTS

The most interesting and valuable data concerning the rheological behavior of a thixotropic fluid, such as Pembina crude oil, was considered to be the decay of consistency with time. Consequently, attention was focused primarily upon the data pertaining to the  $S_H$  portion of the tests.

As demonstrated in the preceding section, the data obtained from the viscometric study provided the relationships between bob deflection and time at constant cup speed. For purposes of testing the validity of equation (70), this relationship had to be expressed in terms of shear stress as a function of time at constant shear rate. In addition a knowledge of the initial shear stress at zero time, the limiting shear stress after prolonged shearing and the stress contributed by the Newtonian solvent was also necessary. The method of evaluation of each of these variables will be considered separately.

### Calculation of Shear Stress and Shear rate

The calculation of shear stress at the bob wall presented no problem since the shear stress is directly related to the bob deflection through equation (72) and is independent of the nature of the fluid in the viscometer. Shear rate, on the other hand, is not independent of rheological properties and cannot therefore be computed by means of the Reiner-Riwlin equation which applies only to Newtonian fluids. Instead, it was necessary to resort to a somewhat



more time consuming procedure based on a relationship developed by Krieger and Maron<sup>(28)</sup>. Their equation, which is in the form of an infinite series, expresses shear rate at any point in the annulus in terms of cup speed and the rheological behavior of the fluid at that speed. For practical purposes, due to rapid convergence of the series when  $R_2/R_1 < 1.2$ , only the first three terms of the equation are required for a sufficiently accurate measure of shear rate at the bob wall. The final form of the equation may then be written

$$-\left(\frac{dv}{dR}\right)_w = \frac{4\pi SR_2^2}{R_2^2 - R_1^2} \left[ 1 + B_1 \left( \frac{1}{n} - 1 \right) + B_2 \left( \frac{1}{n} - 1 \right)^2 \right] \quad (84)$$

where  $S$  is the speed of rotation, RPS,

$B_1$  and  $B_2$  are constants relating to the geometry of the instrument and defined by

$$B_1 = \frac{R_2^2 - R_1^2}{2R_2^2} \left[ 1 + \frac{2}{3} \ln \frac{R_2}{R_1} \right] \quad (85)$$

$$B_2 = \frac{R_2^2 - R_1^2}{6R_2^2} \ln \frac{R_2}{R_1} \quad (86)$$

and "n" is the slope, at any desired speed, of the logarithmic curve representing shear stress as a function of cup speed.

Equation (84) has been derived specifically for time independent non-Newtonian fluids such as the pseudoplastics. Nevertheless, it has been applied to the present system since the relationship



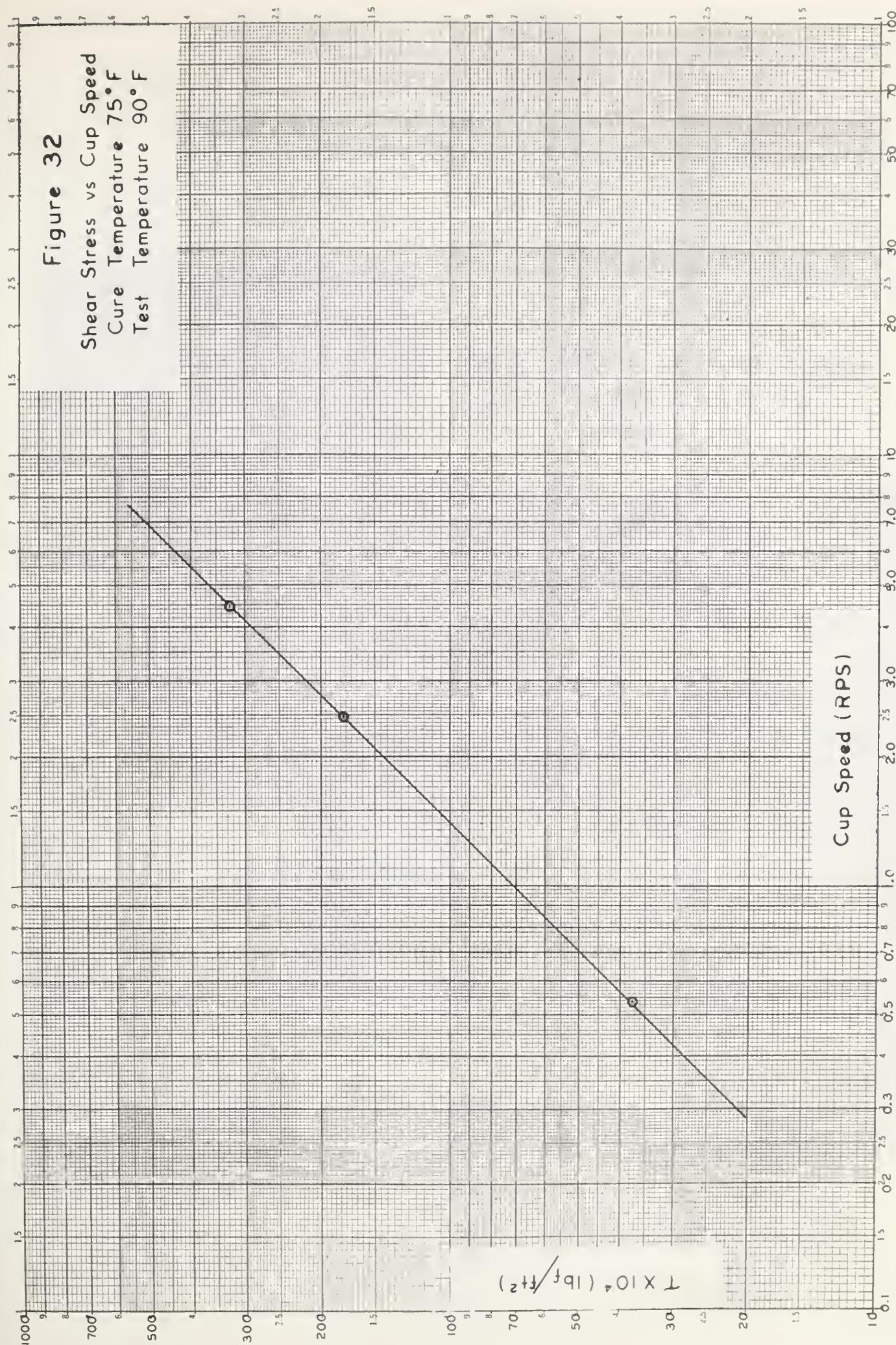
between instantaneous shear stress and speed, which may be obtained from a crossplot of the data on Figures (11) to (25) was characteristic of normal pseudoplastic liquids. That is, the behavior of the crude oil, at any instant, is not unlike that of pseudoplastic fluids. The effect of shearing time is merely to convert the oil from one type of pseudoplastic to another. Crossplots of shear stress versus cup speed at several constant values of shearing time (ie. 0.1, 0.25, 0.5, 1, 2, 5, 10, 20, 30, 60 minutes) have been prepared at each testing temperature and are presented on Figures (32) to (36). The slope of each curve was measured at three chosen cup speeds and the corresponding shear rates computed by means of equation (84). A replotting of the data from Figures (32) to (36) in terms of shear stress and shear rate was then possible and is illustrated in Figures (37) to (41). With the aid of these curves, the relationship between shear stress and time at constant shear rate was readily determined.

The final step in the above procedure is open to some criticism. The variation in true wall shear rate at constant cup speed throughout the duration of the test imposed a variable shear history upon the oil sample which probably influenced subsequent stages of network destruction. The question then arises as to whether a constant shear rate in the viscometer would produce some displacement of the lower curves on Figures (37) to (41). Unfortunately this question cannot be resolved at the present time nor can the experimental difficulty of maintaining a constant shear rate be overcome without recourse to complex cup speed programming techniques.



Figure 32

Shear Stress vs Cup Speed  
Cure Temperature 75°F  
Test Temperature 90°F





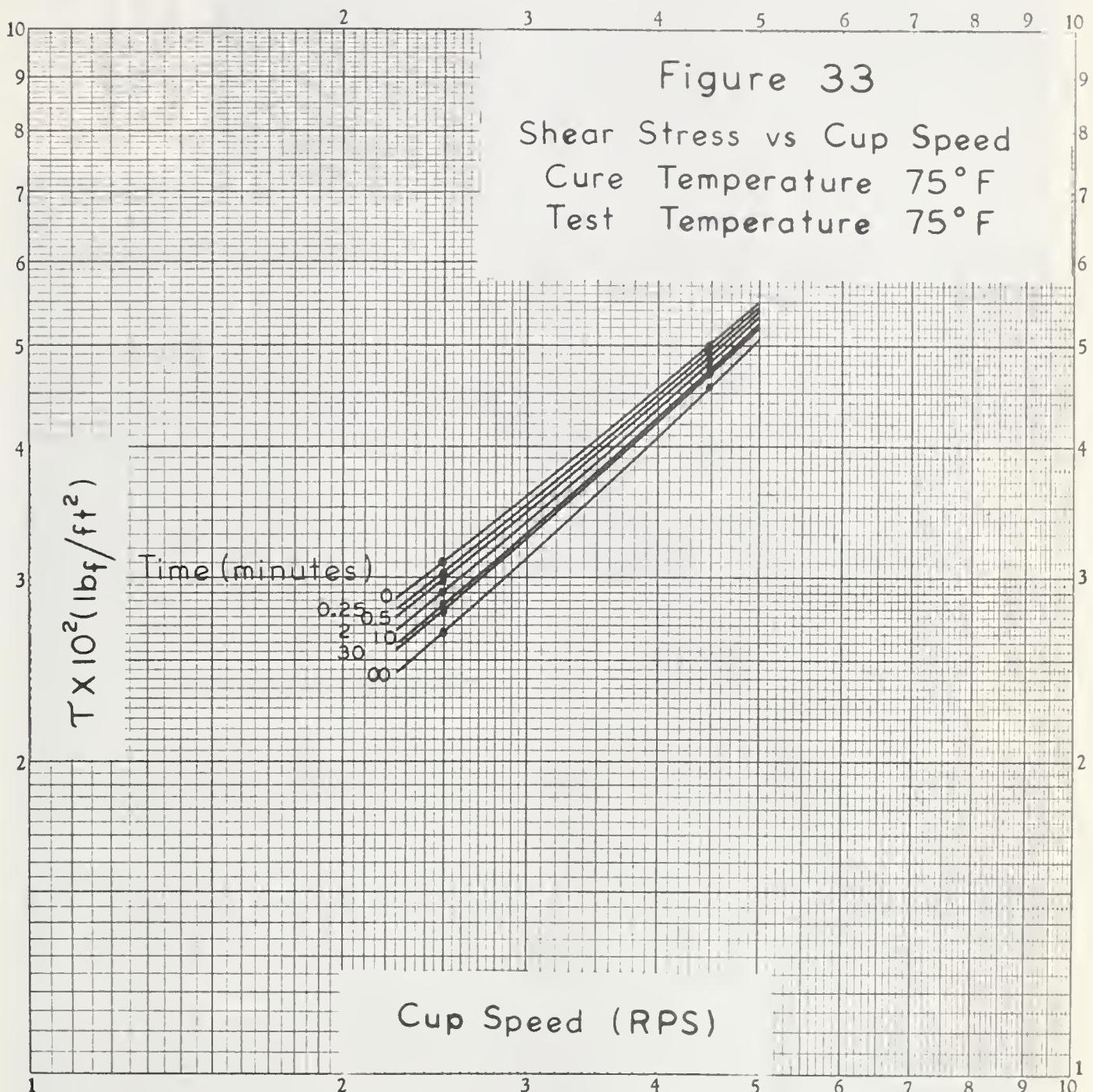




Figure 34

Shear Stress vs Cup Speed  
Cure Temperature 75°F  
Test Temperature 60°F

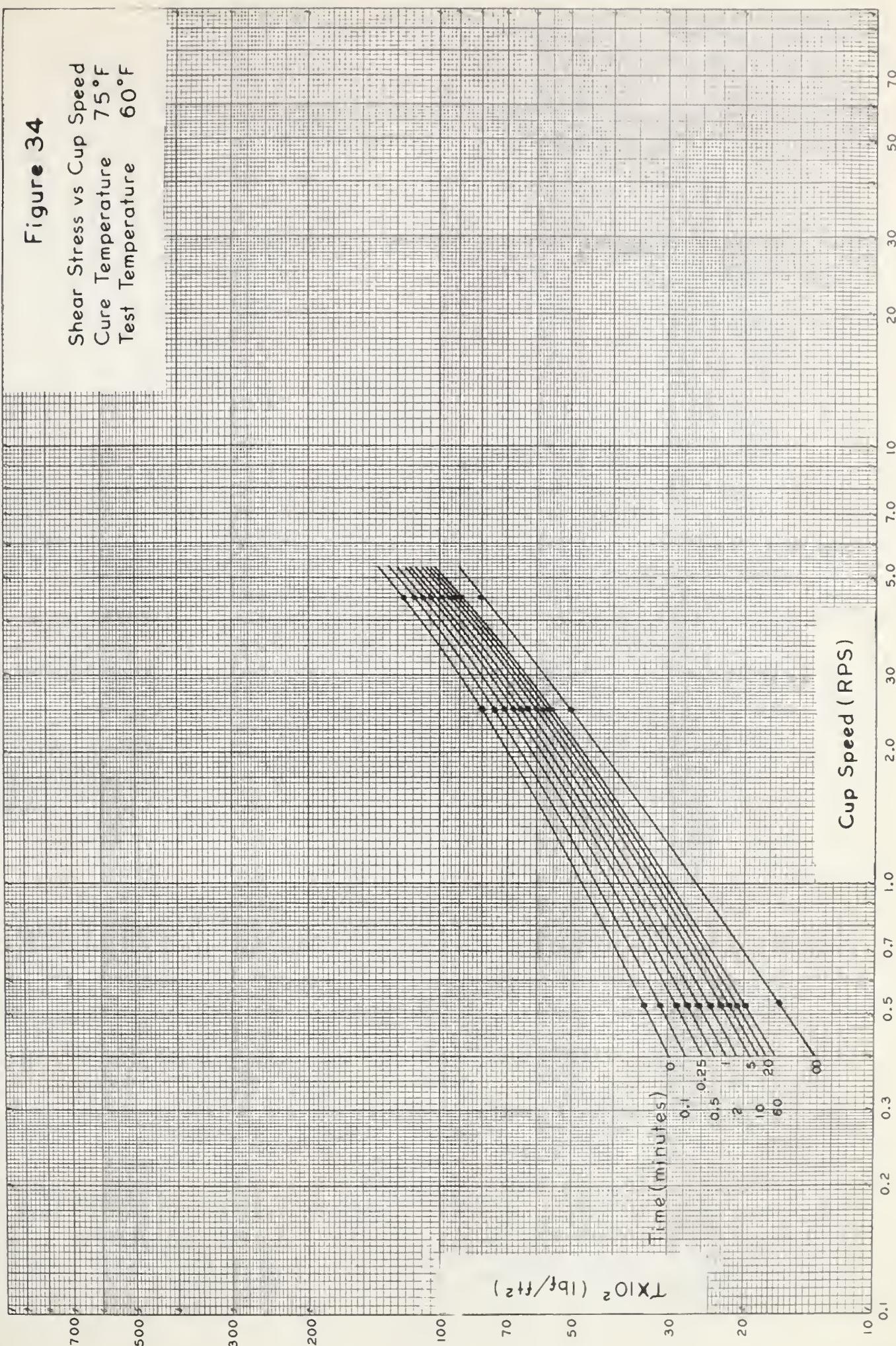




Figure 35

Shear Stress vs Cup Speed  
Cure Temperature 75°F  
Test Temperature 44.5°F

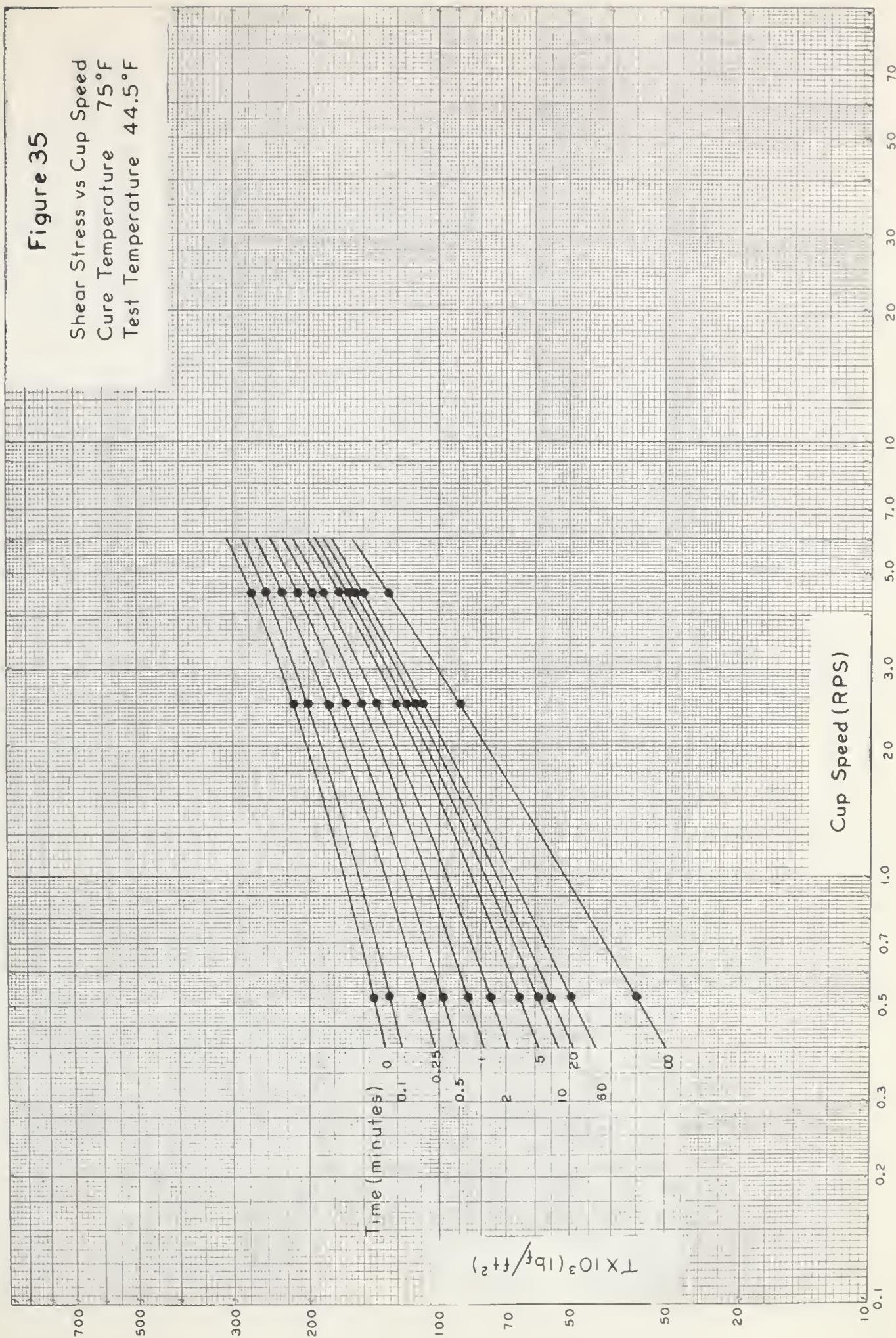




Figure 36

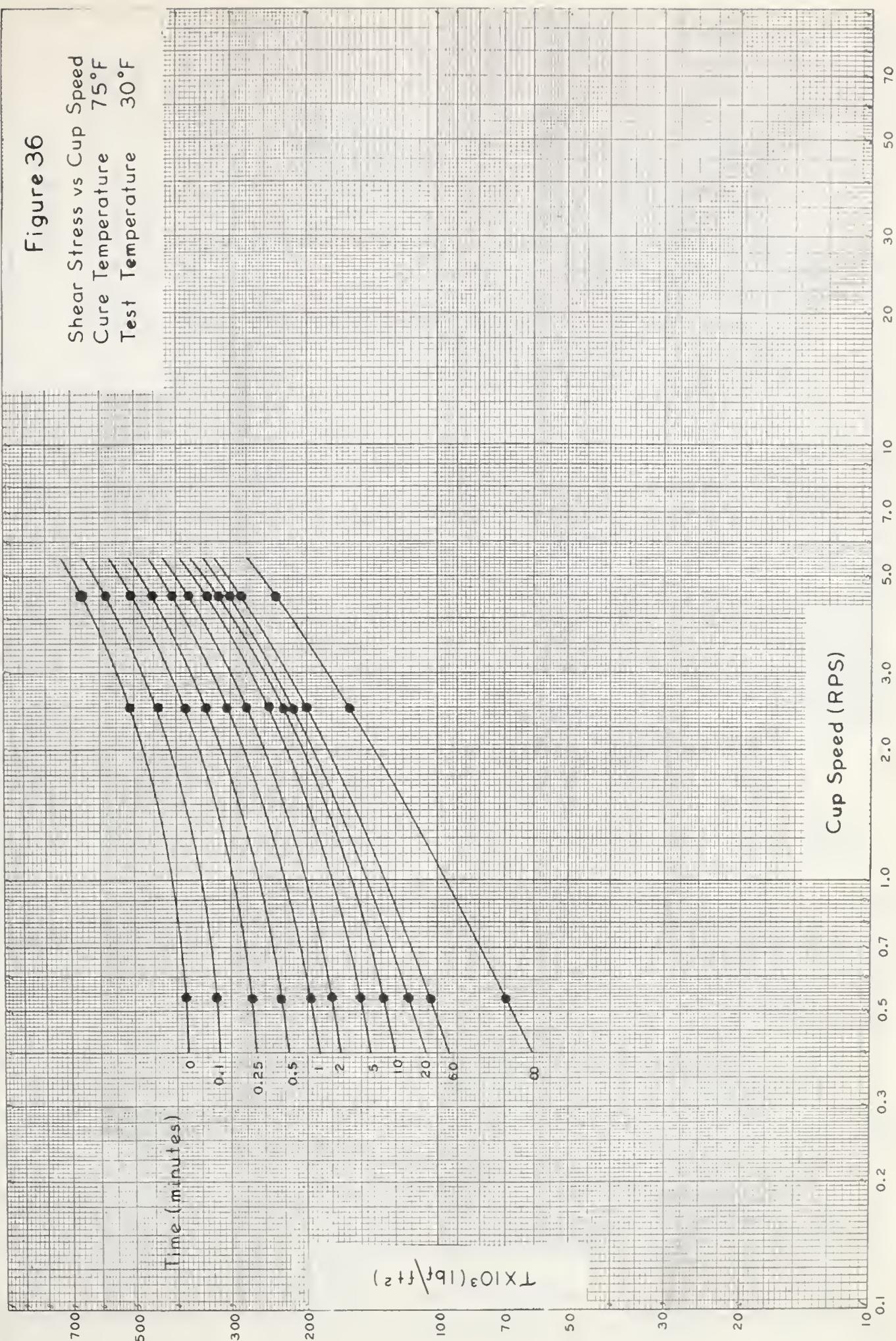




Figure 37

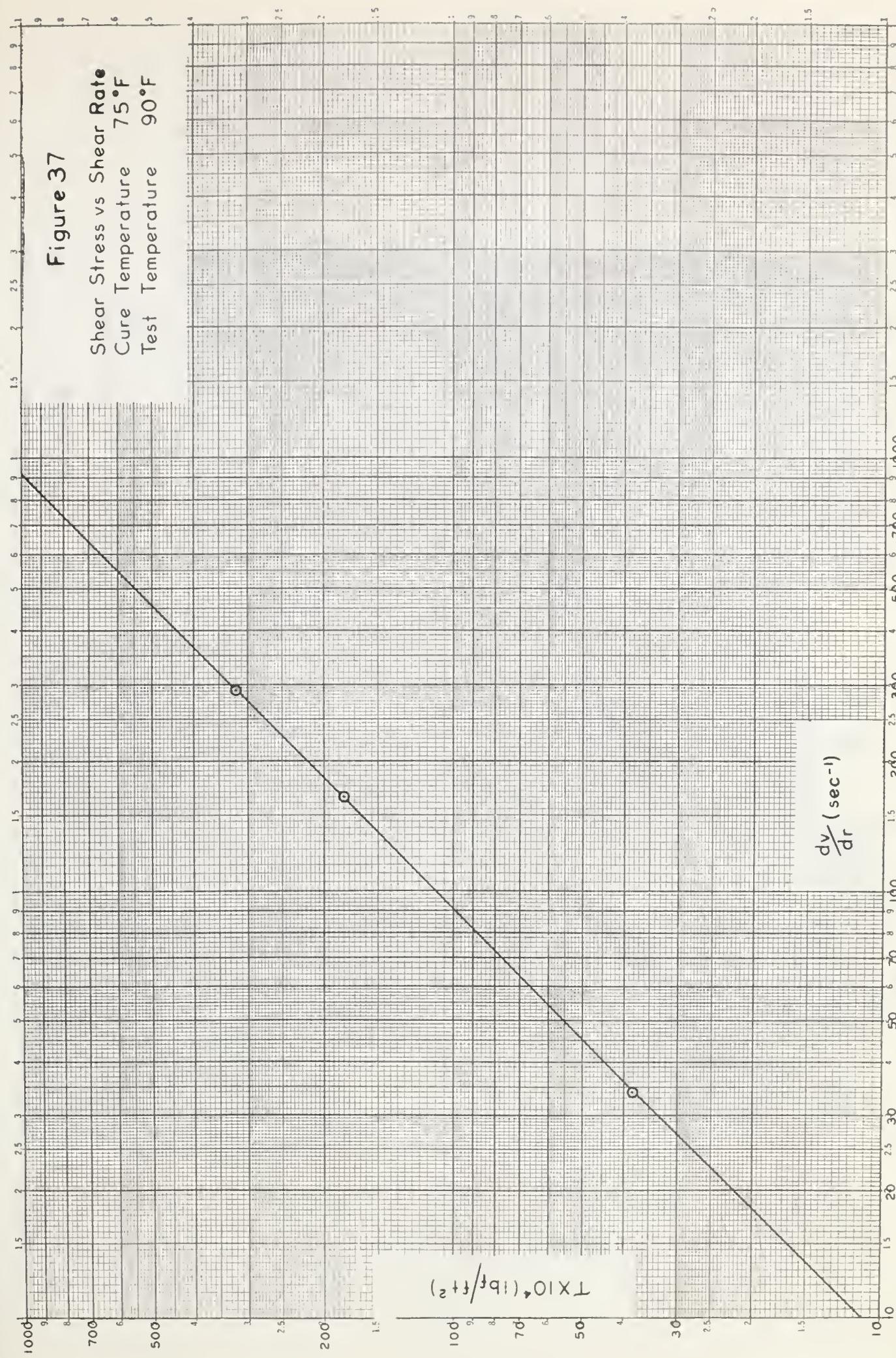




Figure 38

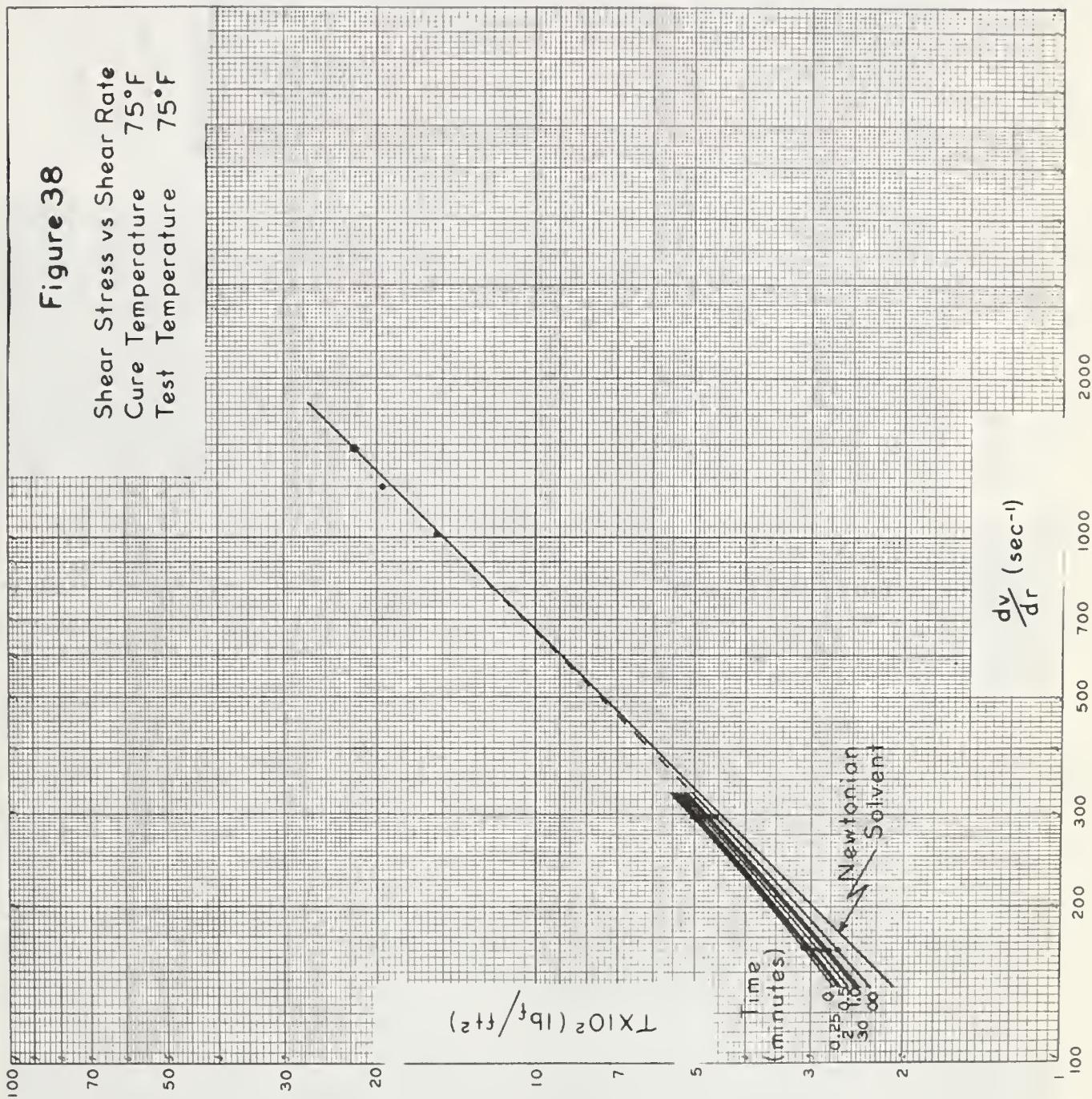
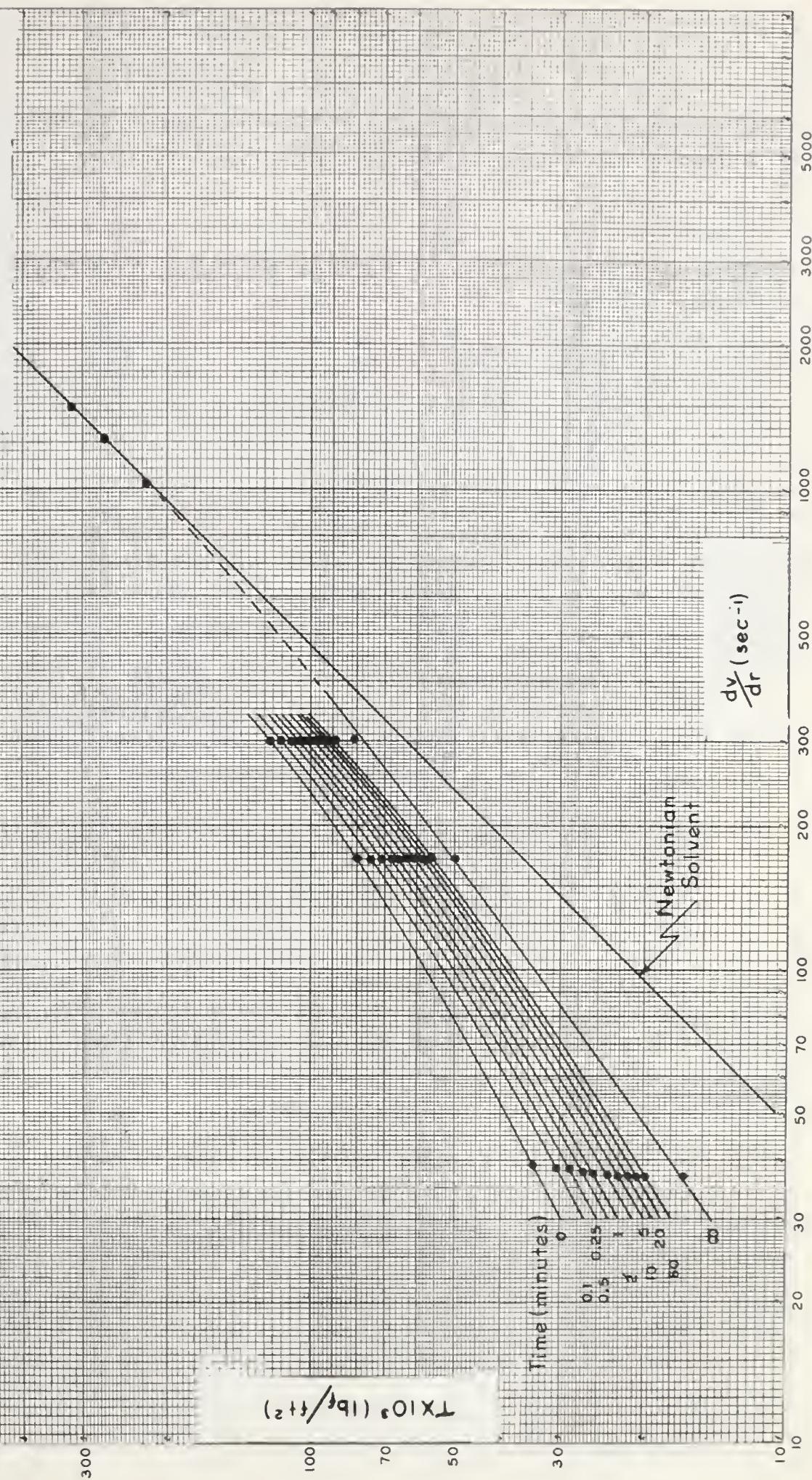




Figure 39

Shear Stress vs Shear Rate  
Cure Temperature 75°F  
Test Temperature 60°F





**Figure 40**  
Shear Stress vs Shear Rate  
Cure Temperature 75°F  
Test Temperature 44.5°F

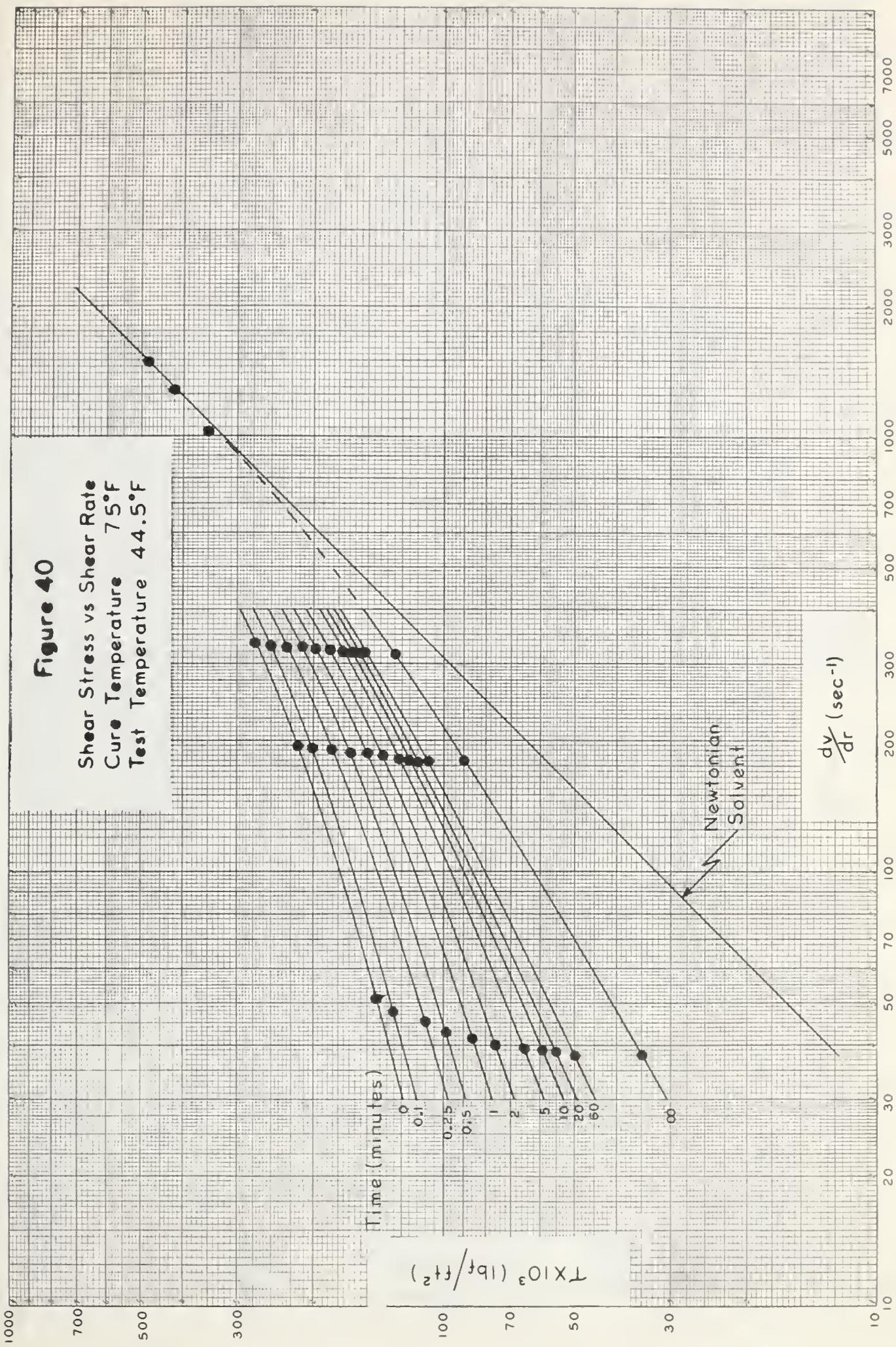
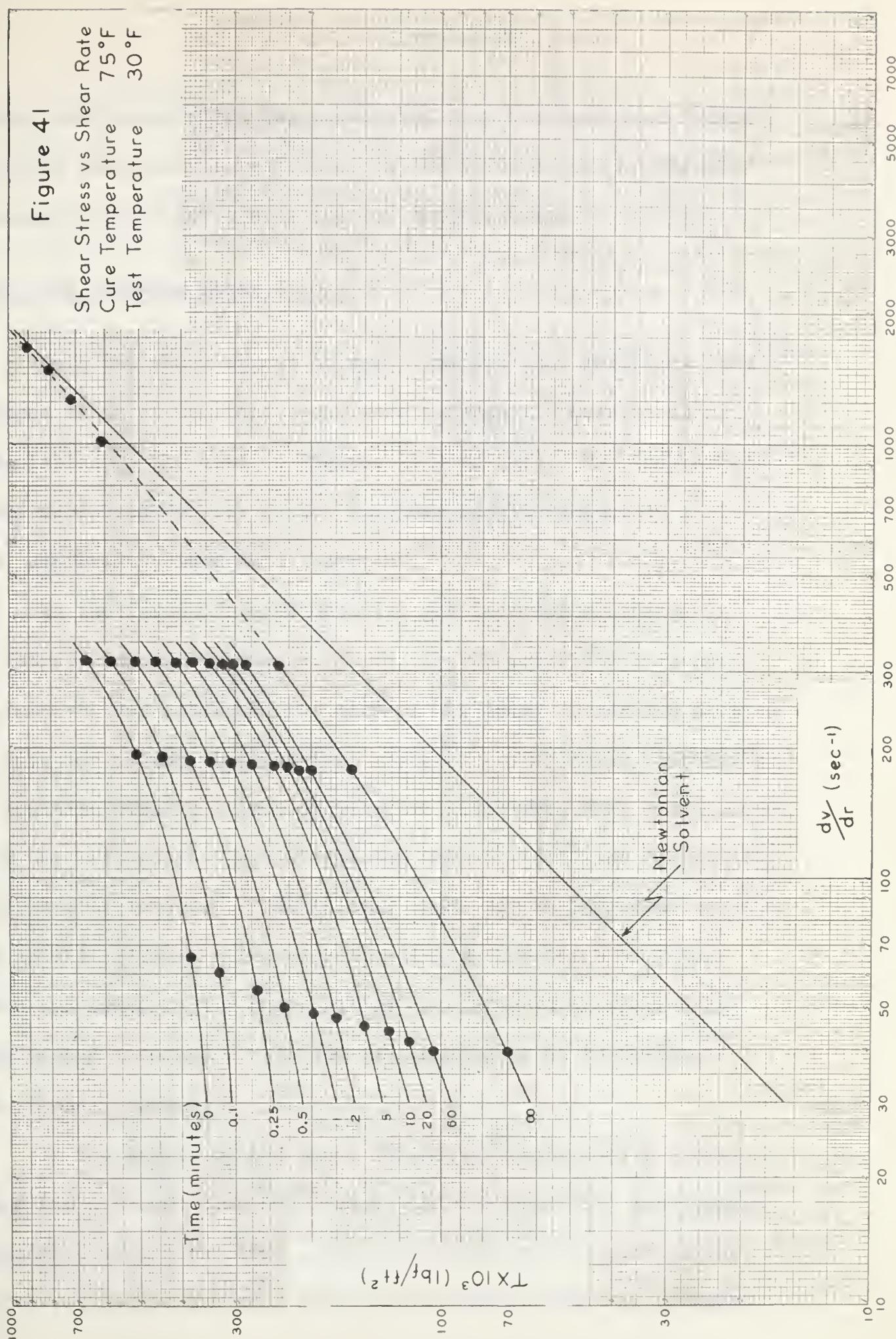




Figure 4 |





However, some consolation may be derived from the fact that drastic shear rate reduction is restricted to the first minute of shearing and occurs only at low speeds and low temperatures.

#### Initial and Limiting Shear Stress

Both the shear stress at zero time and that resulting from prolonged shear at constant speed were necessarily determined by extrapolation of the data on Figures (11) to (25). Two independent methods were used for the former and gave results which, in most cases, differed by less than 3 percent.

In the first of these methods, the incremental change in shear stress during the second, third, fourth and fifth 15 second time interval was obtained from each of the decay curves and plotted as a function of the time interval number on logarithmic coordinates. The resulting straight lines of negative slope were then extrapolated toward the left until they intersected the vertical line representing the first time interval. The initial shear stress increment was then taken as the ordinate value corresponding to the point of intersection and added to the shear stress obtaining at the beginning of the second interval. This sum was assumed to be the initial value of shear stress.

In the second method shear stress was plotted as a function of time (in seconds) plus ten seconds and the resulting curve again extrapolated toward the left. The initial stress was provided by the intersection of the near linear relationship with the vertical



line corresponding to the ten second abscissa value. Illustrative examples of these techniques are reproduced in Appendix 8.

Extrapolation of the data appearing on Figures (11) to (25) toward the right produced curves which eventually became asymptotic to a horizontal line representing the final or equilibrium shear stress. However, accurate estimation of this quantity presented a rather difficult problem for which no entirely satisfactory solution was realized. The nearly horizontal portions of the curves were poorly defined due to experimental errors and, since rather extensive extrapolation was necessary, small changes in slope drastically altered the limiting shear stress value. The errors introduced here were further magnified by the mode of correlation as will be pointed out in due course.

The initial and final values of shear stress obtained by these procedures were plotted as a function of viscometer speed on Figures (32) to (36). Then, following the Krieger and Maron approach previously outlined, these curves were replotted in terms of shear stress and shear rate on Figures (37) to (41). As a matter of record this same information is presented in a plot of shear stress versus temperature at each of three shear rates on Figures (42) to (44).

#### Stress Contribution of the Newtonian Solvent

Interpretation of the equilibrium shear stress data at high shear rates was relatively straight-forward. The shear stress was directly calculable from the bob deflection by means of equation



Figure 42

Initial and Final Shear Stress

vs

Temperature

Shear Rate  $40 \text{ sec}^{-1}$

- Initial Shear Stress,  $\tau_0$
- △ Final Shear Stress,  $\tau_\infty$

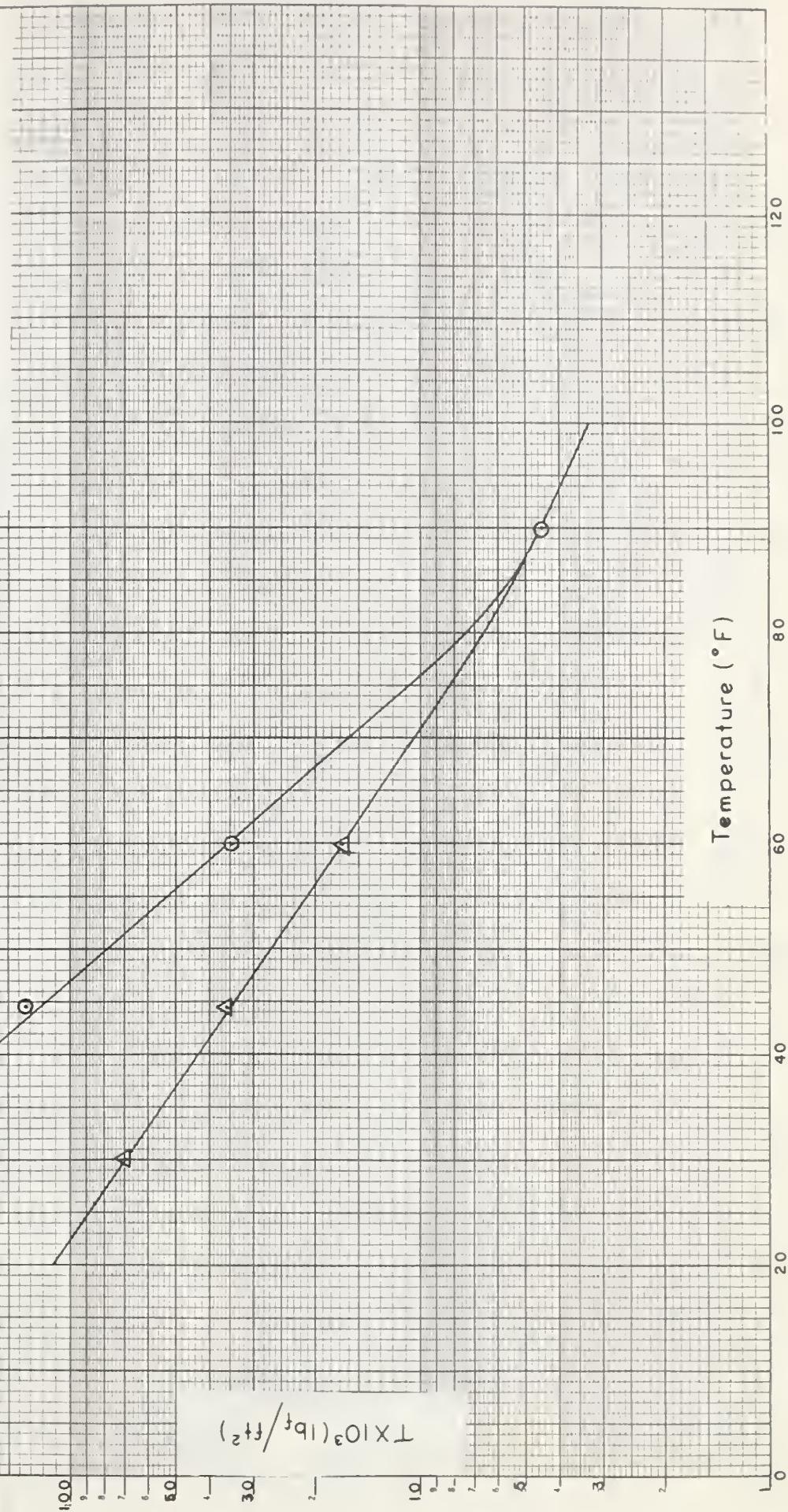




Figure 43

Initial and Final Shear Stress

vs

Temperature  
Shear Rate  $150 \text{ sec}^{-1}$   
 $\Delta$  Initial Shear Stress,  $\tau_0$   
 $\circ$  Final Shear Stress,  $\tau_\infty$

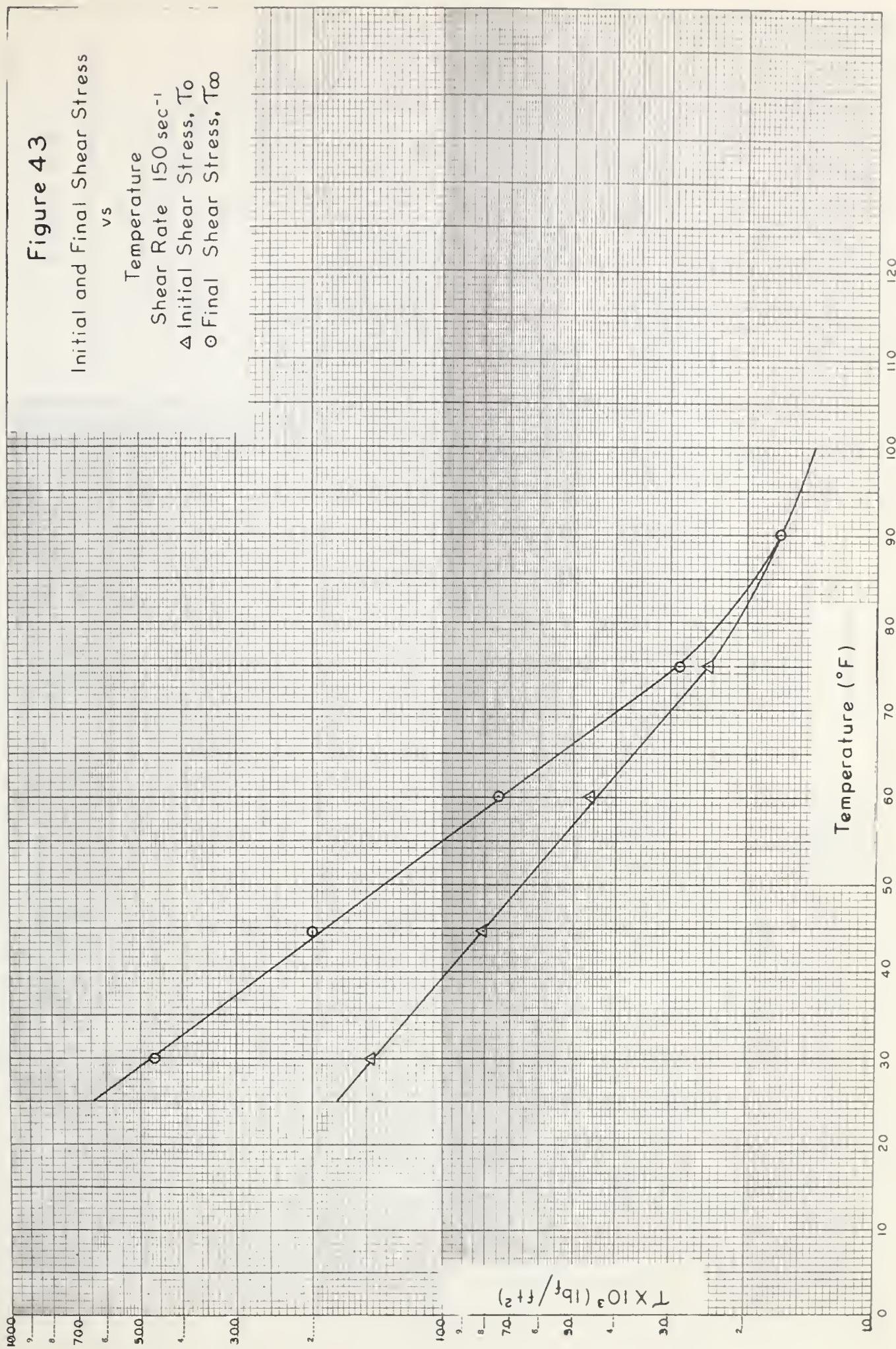
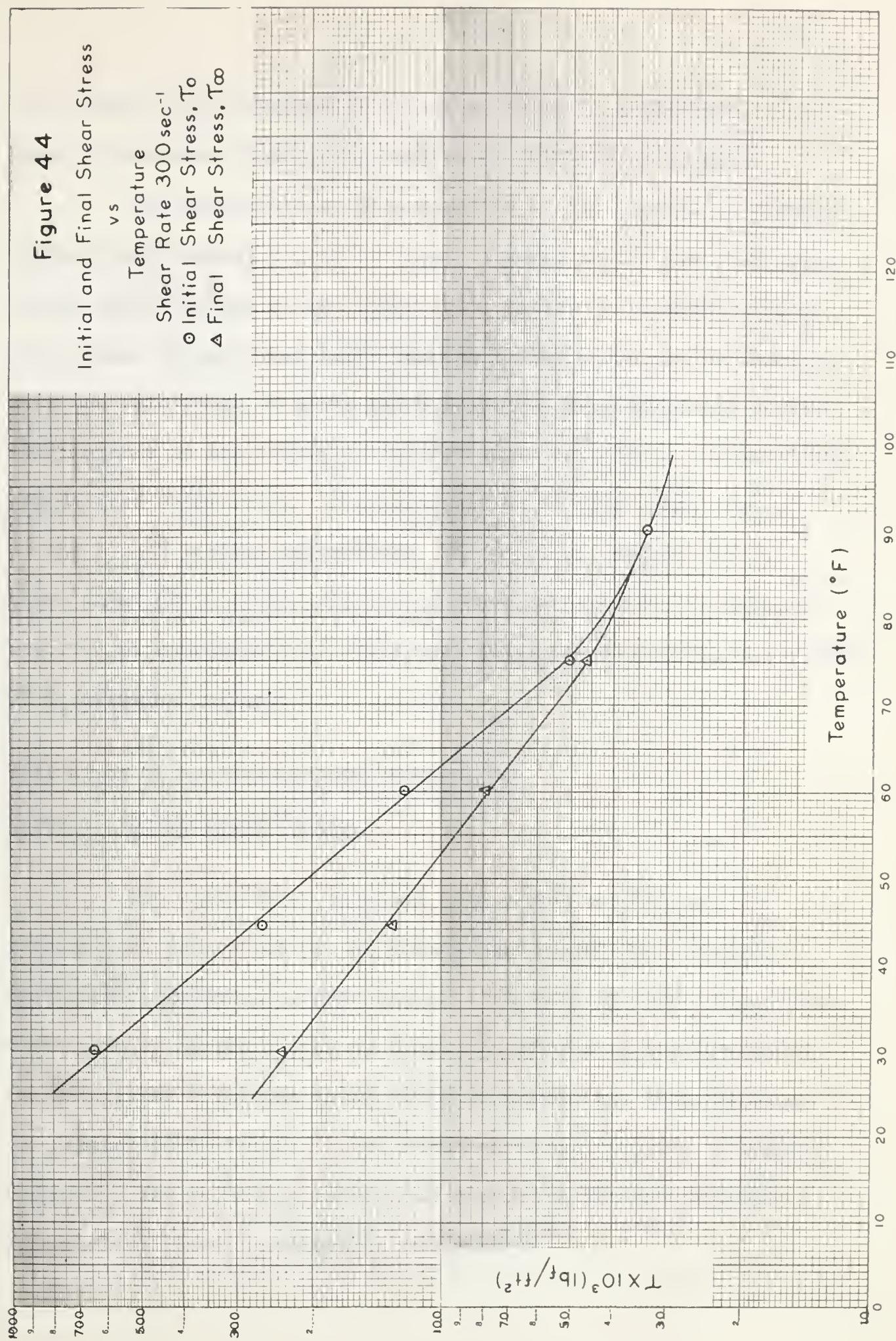




Figure 44

Initial and Final Shear Stress  
vs  
Temperature  
Shear Rate  $300 \text{ sec}^{-1}$   
○ Initial Shear Stress,  $\tau_0$   
△ Final Shear Stress,  $\tau_\infty$





(72) while the Reiner-Riwlin equation, which is applicable in the case of Newtonian fluids, was used to compute the shear rate.

The quantities so determined were also plotted on Figures (37)to(41) and joined, by way of smooth curves, to the limiting shear stress data obtained at the lower shear rates. A straight line of slope equal to unity was drawn tangent to the curve and extended over the full range of shear rates studied. Thus the shear stress attributable to the Newtonian solvent could be readily estimated at any desired shear rate. It is interesting to note that, except at the lowest testing temperature, the point of tangency to the curve invariably occurred within the range of experimental data and required no extrapolation. This fact adds some support to the concept of a Newtonian solvent.

Evaluation of the Experimental Results in

Terms of the Proposed Theory

The validity of equation (70), which constitutes the mathematical expression of the theory, was tested and seemingly confirmed by graphical representation. At each of three shear rates, corresponding approximately to those encountered in the viscometer, the associated Newtonian shear stress component was deducted from the instantaneous values of the observed stress recorded on Figures (37)to(41). The resulting structural or network stress components were then utilized in computing values of



$$\frac{\tau_s - \tau_{s\infty}}{\frac{\tau_{so}^2}{\tau_{s\infty}} - \tau_s}$$

at the various times designated on the figures. In accordance with the form of equation (70), this group was in turn plotted as a function of time on logarithmic coordinates and yielded curves which were essentially linear over three cycles. These are illustrated in Figure (45). Furthermore, the curves for the three shear rates superimposed while increases in temperature produced a marked increase in the intercept value and a slight reduction in slope.

#### Evaluation of Rate Constant $k_A$ and $k_B$

The slope of each curve on Figure (45) is defined by equation (71) as

$$\text{slope} = -k_A \left[ \frac{\tau_{so} + \tau_{s\infty}}{\tau_{so} - \tau_{s\infty}} \right]$$

which, upon rearrangement to

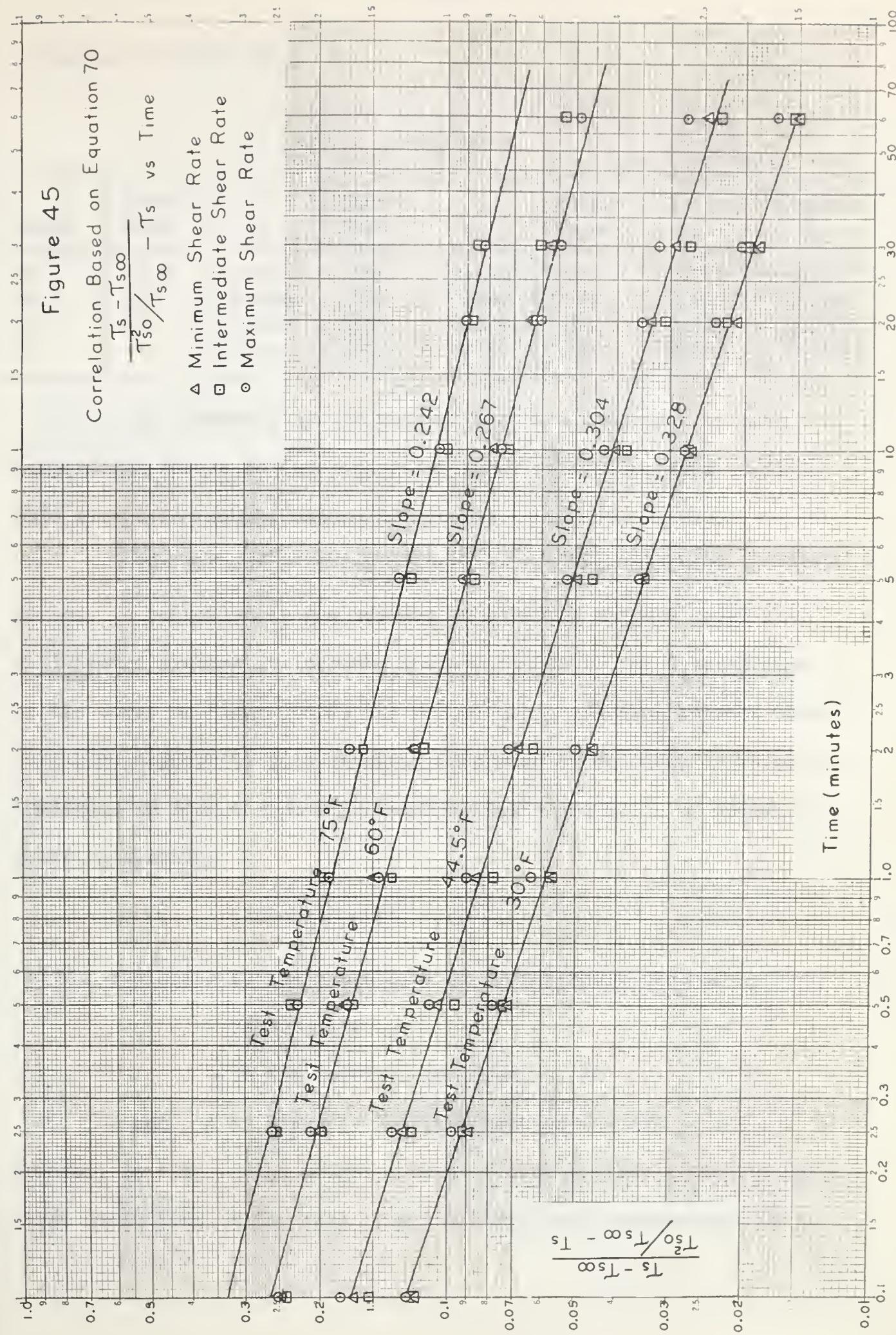
$$k_A = -\text{slope} \left[ \frac{\tau_{so} - \tau_{s\infty}}{\tau_{so} + \tau_{s\infty}} \right]$$

permits calculation of the rate constant,  $k_A$ , associated with the decay of network structure.

The values obtained at each shear rate and temperature are



Figure 45





presented in Table (2).

TABLE 2

Temp.	Shear Rate	$k_A$	Shear Rate	$k_A$	Shear Rate	$k_A$	Average $k_A$
30	39.5	0.244	178	0.236	319	0.242	0.241
44.5	38	0.207	180	0.200	318	0.212	0.206
60	37	0.128	170	0.136	300	0.142	0.135
75	--	-----	165	0.128	296	0.128	0.128

As predicted by the theory, the rate constants at each temperature should be independent of shear rate. The data confirm this except for minor, random deviations.

The influence of temperature on the rate constant is quite marked. A reduction in the testing temperature brought about the anticipated systematic increase in rate constant. As demonstrated by the curve on Figure (46), the relationship existing between these variables appears to be adequately described by an equation which is analogous in form to the well known Arrhenius equation of chemical reaction kinetics

$$k_A = A e^{\frac{b}{\theta}} \quad (87)$$

where  $b$  is the slope of a semilogarithmic plot of  $k_A$  versus  $1/\theta$

$\theta$  is the absolute temperature,  ${}^{\circ}R$

and  $A$  is given by the intercept of the curve at  $\theta = b$   ${}^{\circ}R$ .

However, in view of the meager amount of data available and the rather large deviations of the data from the curve, the significance of the

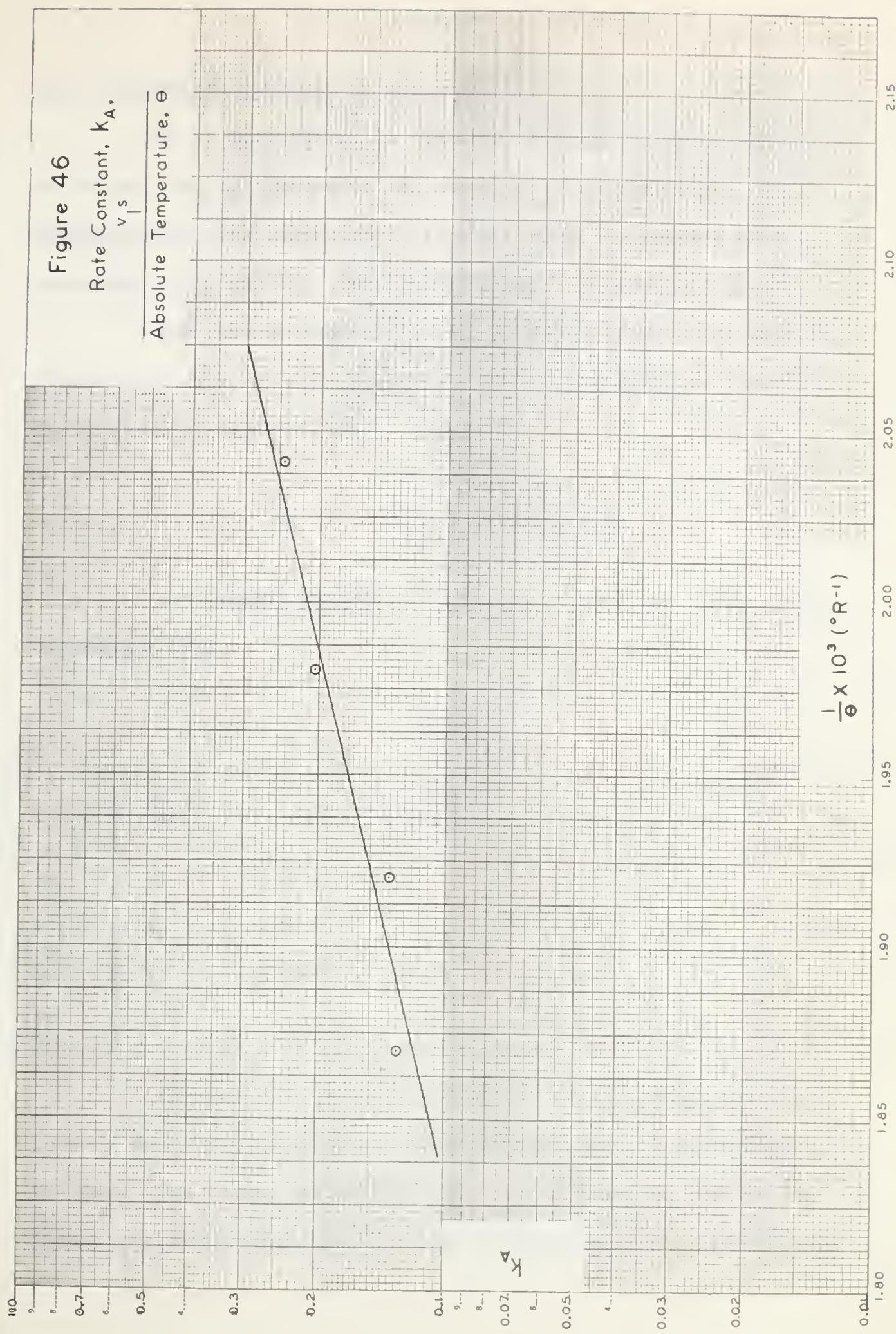


Figure 46

Rate Constant,  $K_A$ .

$v_s$

Absolute Temperature,  $\theta$





$k_A$  -  $\theta$  correlation cannot be affirmed.

It is interesting to note that extrapolation of the curve on Figure (46) is limited to temperatures below  $90^{\circ}\text{F}$  since, at approximately this temperature, Pembina crude oil behaves as a Newtonian fluid and the rate constant,  $k_A$ , becomes meaningless.

The rate constant  $k_B$  of the reverse reaction may also be evaluated at the several shear rates and test temperatures through application of equation (68). That is

$$k_B = k_A \left[ \frac{T_{s\infty}}{(T_{s0} - T_{s\infty})^2} \right]$$

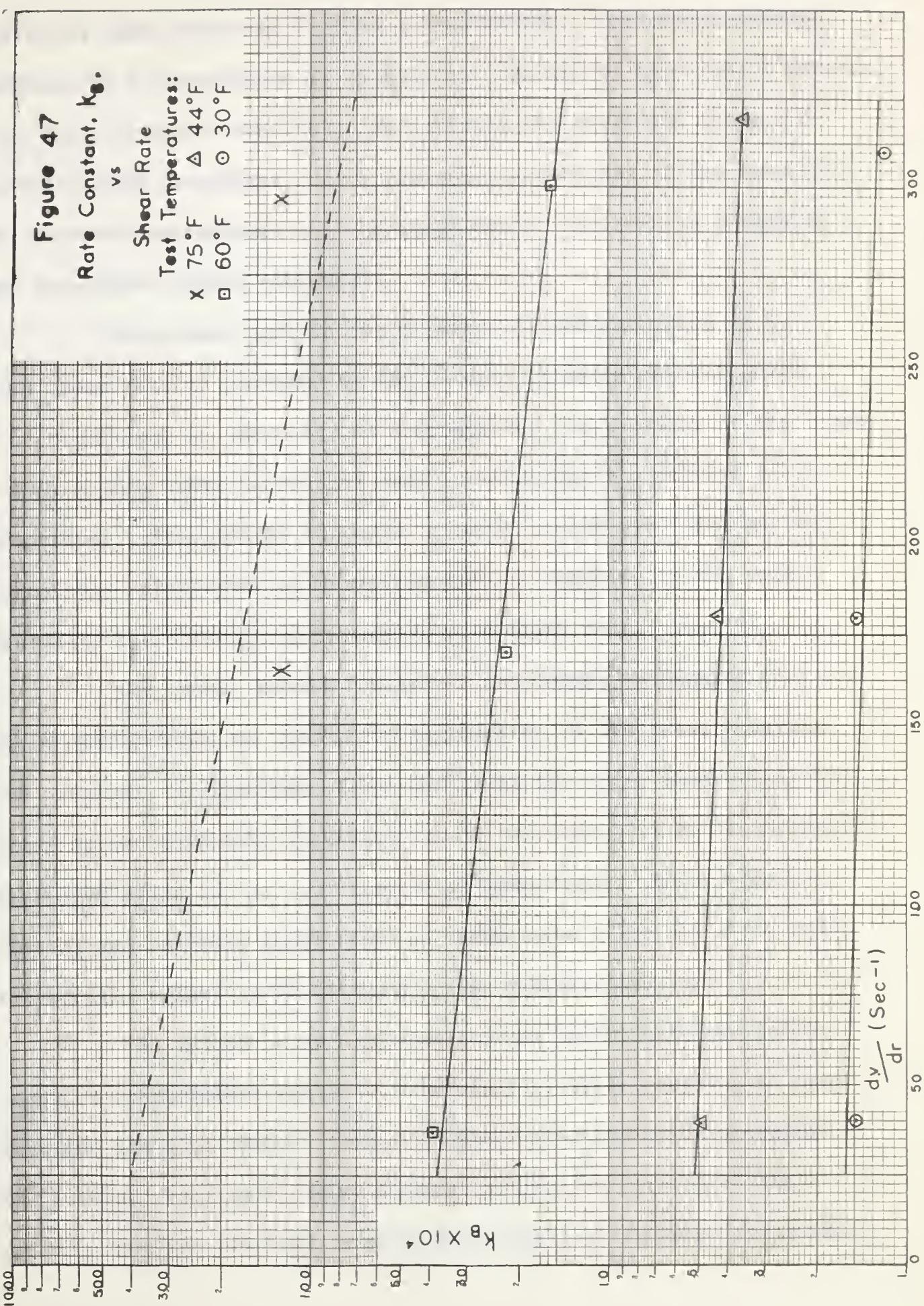
The results of these calculations are presented in Table 3 and Figure (47).

TABLE 3

Temp.	Shear Rate	$k_B$	Shear Rate	$k_B$	Shear Rate	$k_B$
30	39.5	$1.48 \times 10^{-4}$	178	$1.47 \times 10^{-4}$	310	$1.12 \times 10^{-4}$
44.5	38	$3.48 \times 10^{-4}$	180	$4.30 \times 10^{-4}$	318	$3.48 \times 10^{-4}$
60	37	$3.85 \times 10^{-3}$	170	$2.19 \times 10^{-3}$	300	$1.52 \times 10^{-3}$
75	--	---	165	$1.26 \times 10^{-2}$	296	$1.26 \times 10^{-2}$

Although the exact nature of the relationships existing between these variables cannot be determined, due to inaccuracies in the data, the trends are sufficiently well defined to confirm the theoretical prediction that the rate constant  $k_B$  will decrease with







increased shear rate and decreased temperature. The rate constants obtained at a temperature of 75°F do not conform to this rule. However, only two points are available for defining the curve and these are probably most inaccurate due to excessive weathering of the sample at the elevated temperature and the large errors involved in computing the structural stress component.

Additional qualitative evidence of the variation in  $k_B$  with shear rate is provided by the  $S_T$  data illustrated on Figures (26) to (31). Each of these curves demonstrates the behavior of the crude oil at a shear rate below that used in measuring the network decay properties. The gradual increase in shear stress with time may be reasonably interpreted as resulting from an increase in the rate constant,  $k_B$ , produced by a reduction in shear rate.

The rather peculiar shape of the curves on Figures (30) and (31) is attributable to incomplete degradation of the network during the original,  $S_H$ , portion of the test. At the lower shear rate, the shear stress initially increased due to the change in  $k_B$  then finally decreased again due to continued structural decay. This suggests that  $k_A$  may be truly independent of shear rate since all shear rates are equally effective in disrupting the network structure.

The rather large discrepancies in the  $S_T$  data precluded rigorous quantitative analysis. However, it is interesting to note that the limiting value of shear stress, after prolonged shearing at the lowered shear rate, normally fell within ten percent of that arising from the original network decay tests at the same shear rate.



This result supports the hypothesis that a genuine equilibrium state, approachable from either direction, exists at each shear rate.

Discussion

The selection of an interlocking network model and the analogy drawn between the course of its destruction and the mechanism of a first order - second order reversible chemical reaction appear, in this case, to provide a suitable explanation of the rheological behavior of Pembina crude oil. It has been theoretically predicted and experimentally verified that a logarithmic relationship exists between the defined structural stress and time of shearing, that the rate constant describing the forward reaction is dependent only on temperature and that the rate constant of the reverse reaction is a function of both temperature and shear rate.

The final correlation presented in Figure (45) may be criticized in view of the deviation of some data points from the average curve. However it must be appreciated that this correlation is a sensitive one. The method of computing structural stress, namely by deducting the Newtonian component from the total stress, tends to magnify considerably any errors arising in the measurement of the latter. This situation is most serious at high testing temperatures since the difference between the total stress and the Newtonian component is quite small. In spite of this difficulty, the average curves on Figure (45) define the original decay curves



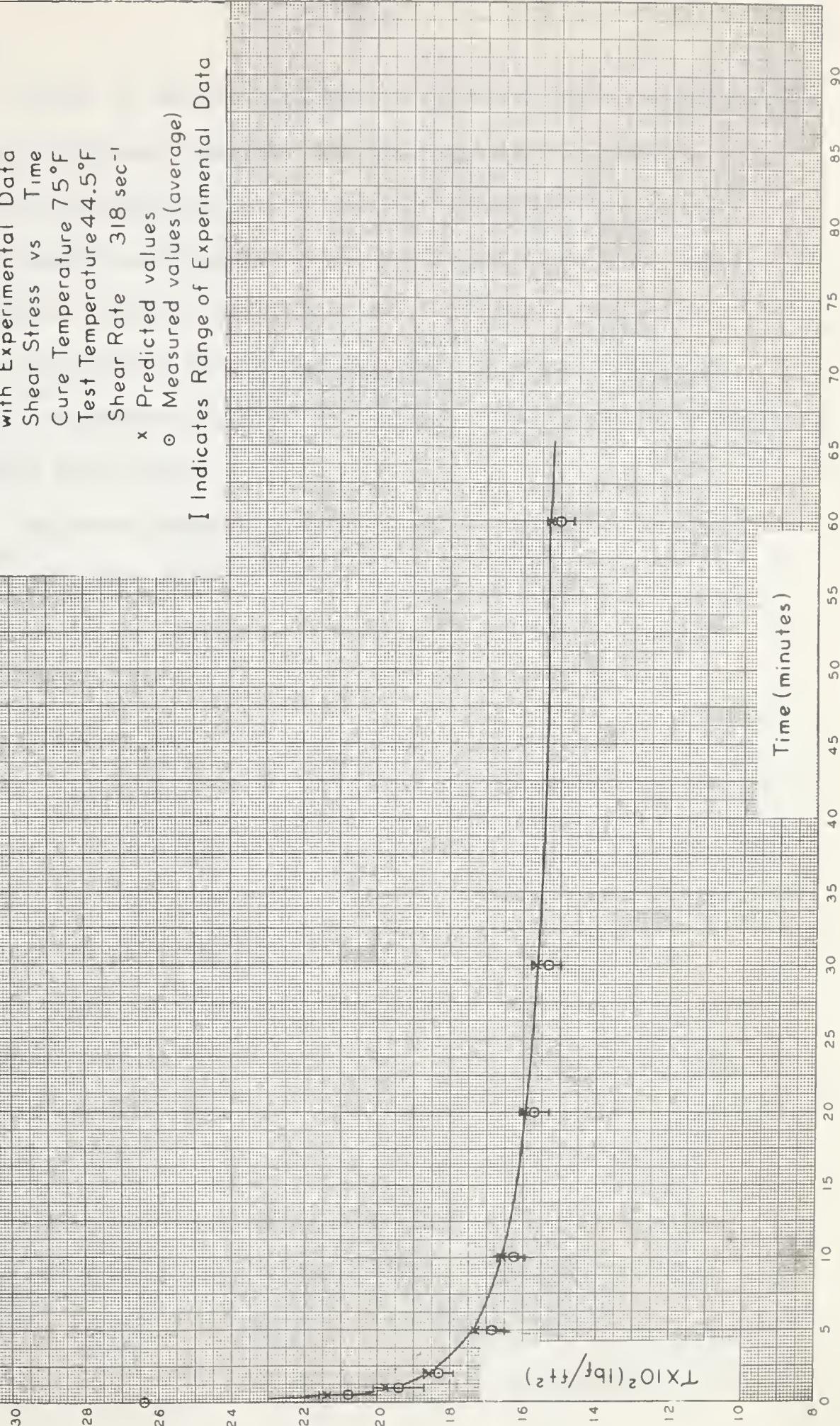
reasonably well. For example, employing ordinate values specified by the  $44.5^{\circ}\text{F}$  curve of Figure (45), which exhibits a maximum scattering of the data (up to 14 percent at 60 minutes), the decay curve corresponding to a shear rate of  $318 \text{ sec}^{-1}$  has been reconstructed in Figure (48) and may be seen to differ by less than 3 percent from the average values of the experimental data. This deviation is clearly within the range of experimental error in the measured total shear stress values.

The most important quantity involved in this analysis, and unfortunately one which could not be evaluated with the desired accuracy, is the limiting shear stress. Difficulties in extrapolation, magnification of small errors and frequent recurrence of this variable in the calculations all introduce ambiguity into the correlation. Indeed, the consequence of the entire investigation is tempered in no small degree by the uncertainty involved in the measurement of this variable. In all honesty, it may only be concluded that the data conforms to a logarithmic relationship for which the boundary conditions are specified and that these boundary conditions coincide approximately with the initial and final extrapolated values of shear stress. Nor could these problems have been overcome by extending the time of shear stress measurement beyond 60 minutes, since the influence of weathering on the consistency of the sample would cause any additional data to be totally unreliable. The only effective solution is the selection of a superior viscometer design or a non-volatile thixotropic fluid.



Figure 48

Comparison of Predicted Decay Curve  
with Experimental Data  
Shear Stress vs Time  
Cure Temperature 75°F  
Test Temperature 44.5°F  
Shear Rate 318 sec<sup>-1</sup>  
x Predicted values  
o Measured values(average)  
I Indicates Range of Experimental Data



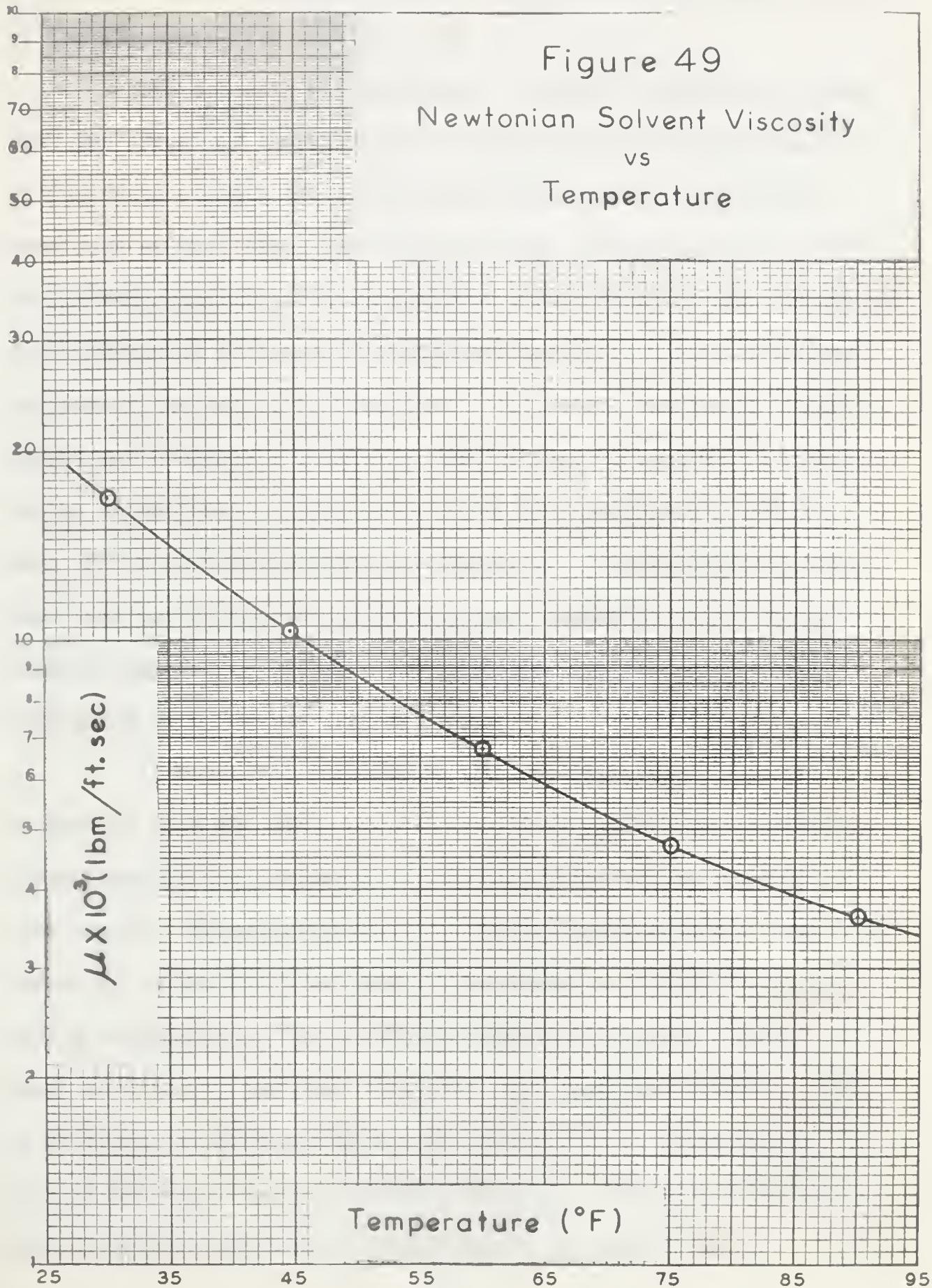


Either of the above expedients also provide a second notable advantage. If it were possible to completely destroy network structure at high shear rates without suffering the loss of low molecular weight constituents, network reformation at lower shear rates could be studied accurately. Such information would prove or disprove the existence of a stable equilibrium shear stress and furnish an independent estimate of the rate constant,  $k_B$ , not involving the original decay data.

One basic assumption involved in the proposed theory, namely the existence of a Newtonian solvent, has never been substantiated in the course of this discussion. At the present time, the information required for such confirmation is not available. However some evidence may be presented which does add credence to this notion. A plot was prepared to demonstrate the variation in observed Newtonian viscosity with testing temperature (Figure 49). The smooth curve described by the data was found to pass through the point representing the viscosity of the fluid at  $90^{\circ}\text{F}$ , under which condition Newtonian behavior is assured (Figure 37). Somewhat more positive proof could likely be attained with the aid of a different viscometer or a different fluid. Here again, the oil sample would be subjected to a very high shear rate to destroy essentially all of the network structure, whereupon the shear rate would be quickly reduced to some predetermined lower level and the growth curve measured. Extrapolation of this and other similar data, obtained at various shear rates, would provide the



Figure 49  
Newtonian Solvent Viscosity  
vs  
Temperature





initial shear stress values needed to define the rheological behavior of the structure-free solvent.

The schedule of experiments, outlined previously, stated that the effect of thermal history was studied by duplicating all of the tests at each of three curing temperatures. It was also mentioned at that time, that only the data corresponding to a  $75^{\circ}\text{F}$  curing temperature was fully analyzed. This decision was considered to be justified in view of the similar nature of the decay curves at each of the curing temperatures. In general the shape of the curves was comparable while the shear stress at equivalent locations on the curves was observed to decrease by approximately 10% for each  $30^{\circ}\text{F}$  reduction in curing temperature. Figures (50) to (52), which represent the data obtained at a curing temperature of  $15^{\circ}\text{F}$  and a testing temperature of  $60^{\circ}\text{F}$ , are included here for purposes of comparison with Figures (17) to (19).

Although the exact cause of this behavior cannot be determined from the available data, it does appear that changes in curing temperature influence the configuration of the network to some extent. This feature is most clearly demonstrated by the reduction in the limiting shear stress value occasioned by a low curing temperature. One possible explanation is that, due to reduced mobility of the chain segments, the growth of network, prior to shearing, is hindered by the low temperature. Consequently, even if the rate constants remain unchanged, the smaller average size of network fragments at any time during shear will be



Figure 50

Shear Stress Decay Curve  
Shear Stress  
vs  
Time  
Cure Temperature 15°F  
Test Temperature 60°F  
Cup Speed 0.522 RPS

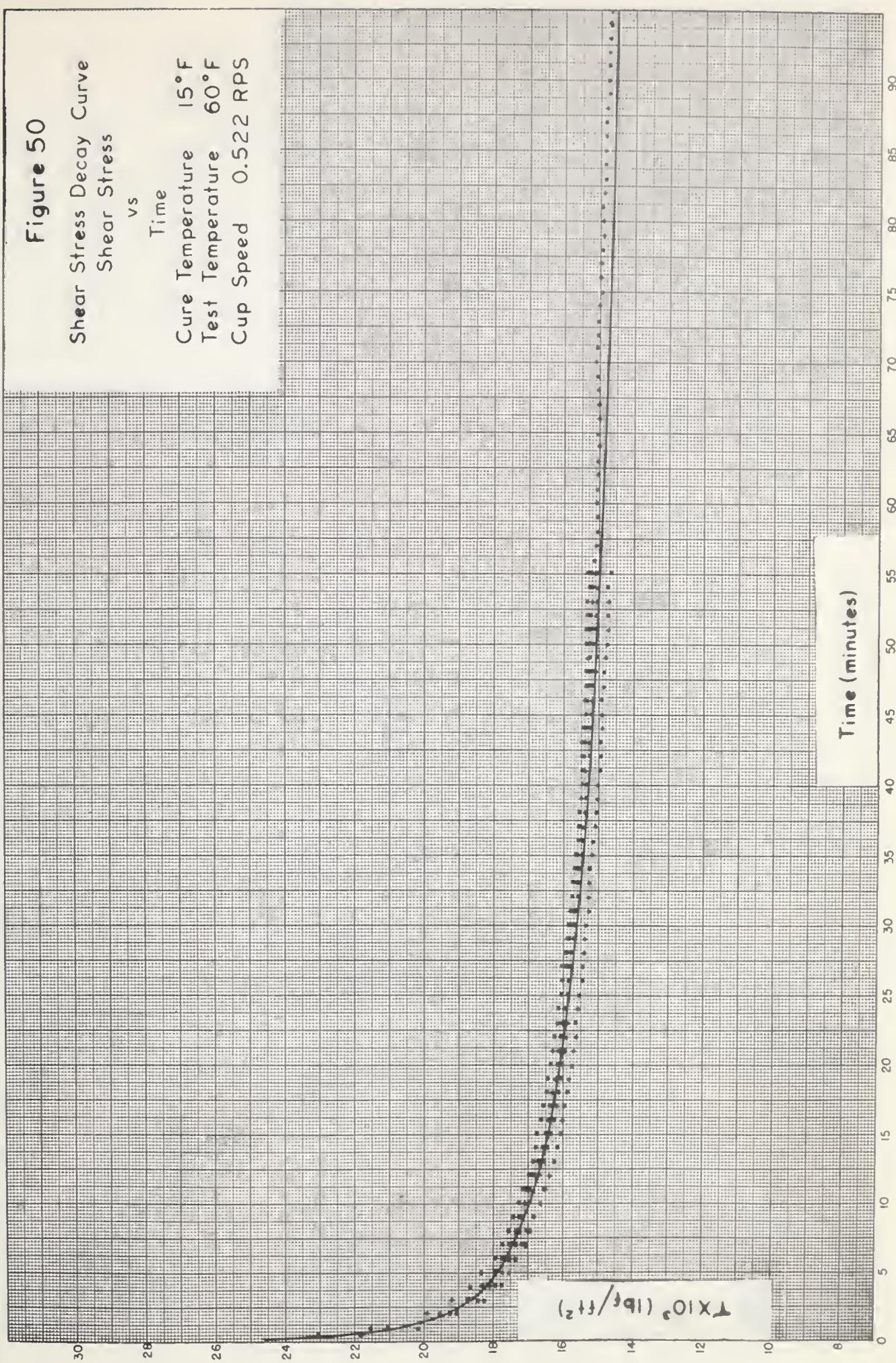




Figure 51

Shear Stress Decay Curve  
Shear Stress vs  
Time  
Cure Temperature 15° F  
Test Temperature 60° F  
Cup Speed 2.521 RPS

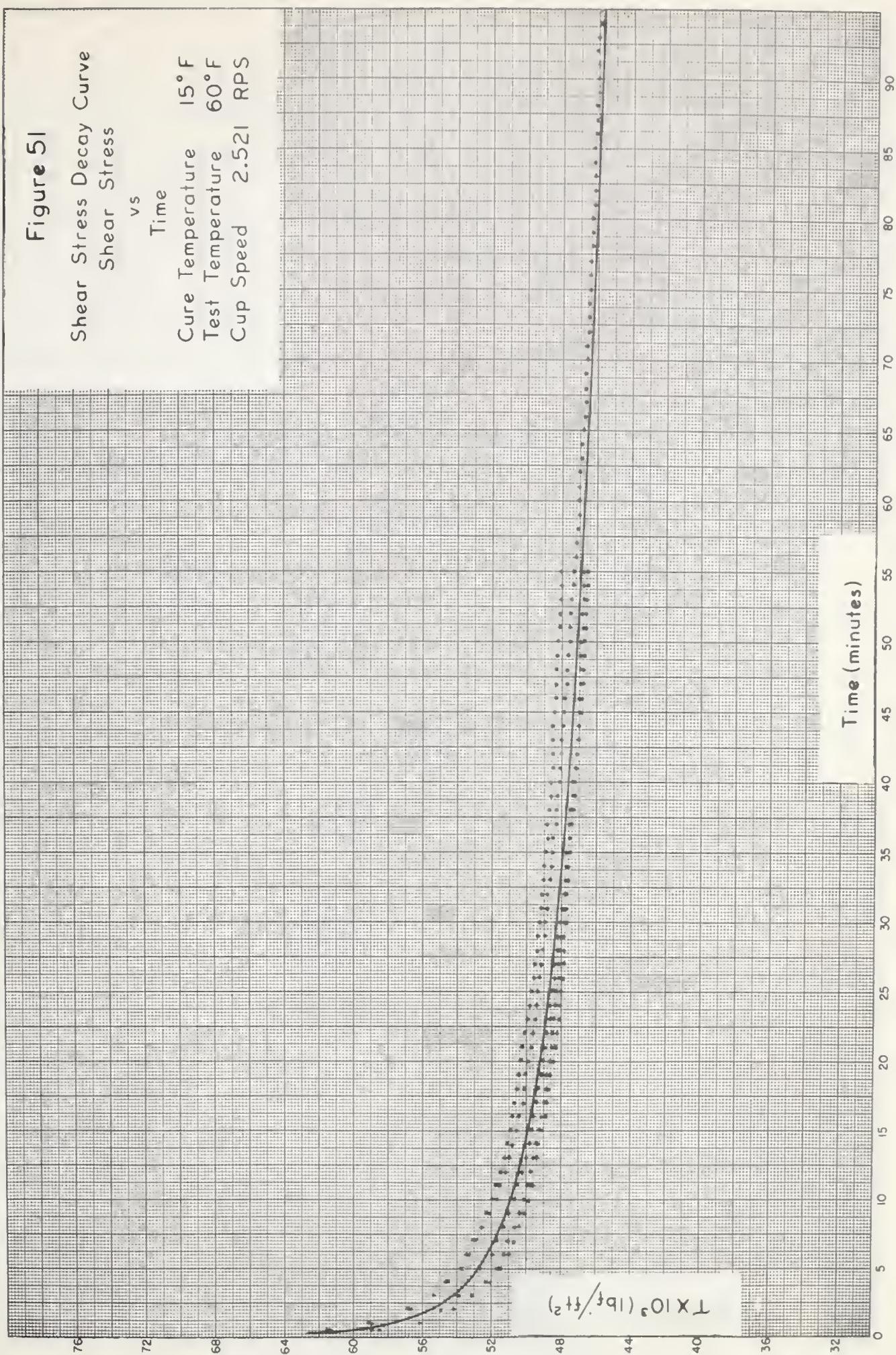
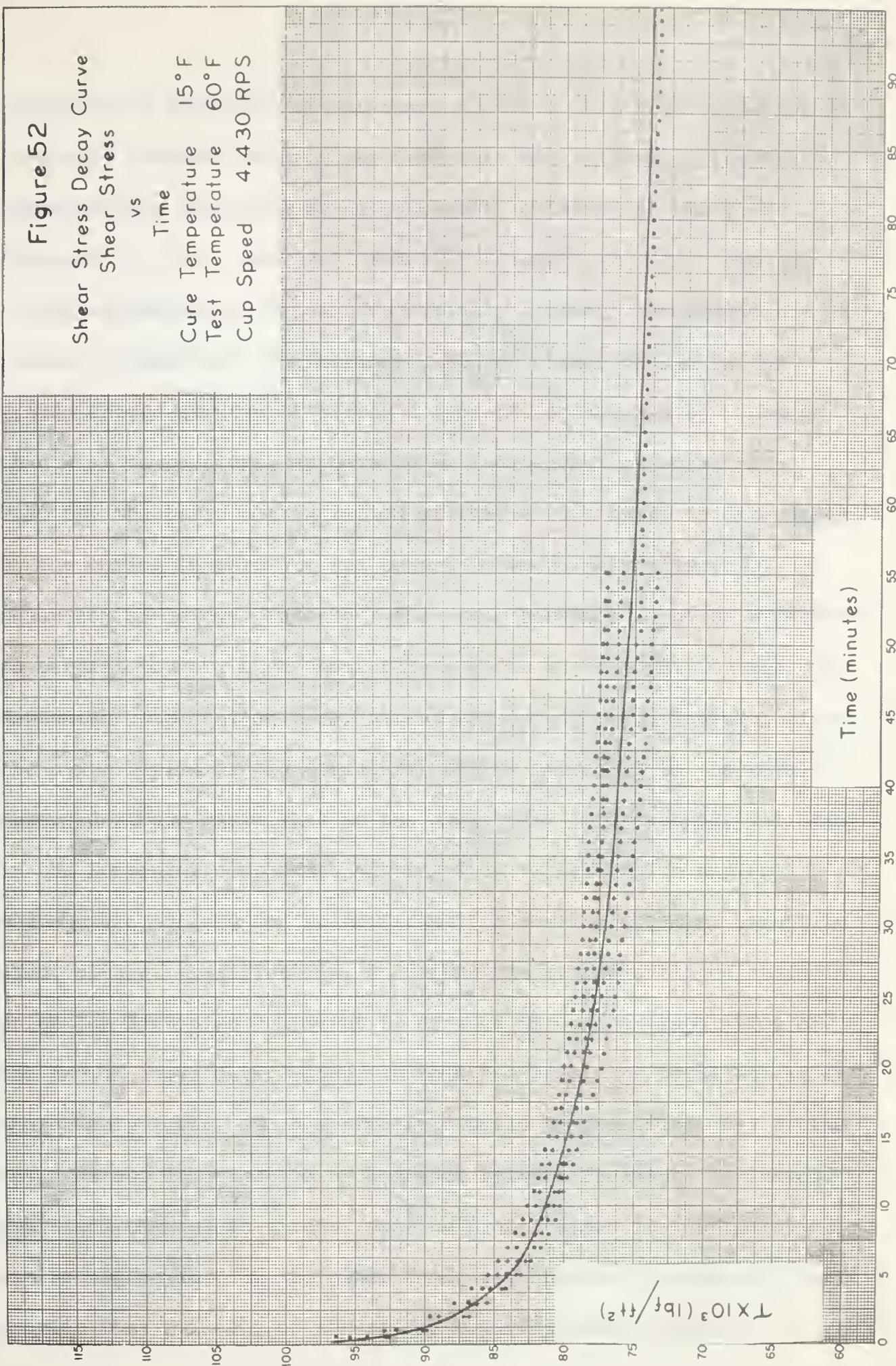




Figure 52

Shear Stress Decay Curve  
Shear Stress  
vs  
Time  
Cure Temperature 15°F  
Test Temperature 60°F  
Cup Speed 4.430 RPS





reflected in the value of the shear stress. This interpretation is partially substantiated by the fact that the difference between corresponding shear stress decay curves, obtained at the 75° F (Figures 17, 18 and 19) and 15° F (Figures 50, 51 and 52) curing temperatures, remains essentially constant throughout the period of shearing. Furthermore, the percentage change in the instantaneous structural stress component, occasioned by a change in curing temperature, appears to be independent of shear rate. That is, the basic configuration of the network units is determined by the curing temperature and cannot be measurably altered by shear action however intense. This same behavior might be expected to persist to very high shear rates, under which condition the Newtonian component of shear stress was determined. However, since the contribution of the structural stress component to the total observed stress diminishes as the shear rate is increased, variations in the Newtonian component, arising from variations in curing temperature, should be insignificant. A similar argument cannot be used, without qualification, to defend the method outlined above in which the Newtonian component is derived through extrapolation of the growth curve data, since, in this instance, the total stress is appreciably lower. Such a procedure would be justified only if the shear stress contribution of degraded network fragments is indeed small and changes in stress, arising from changes in configuration, can be neglected. On the other hand, any observed discrepancy would provide some evidence of structural modifications produced by



variations in thermal history.

The obvious influence of curing conditions on the rheological behavior of Pembina crude oil suggests that temperatures above 75° F may occasion increases in the instantaneous value of shear stress. Such behavior has, in fact, been observed by the author. However, the very limited scope of these experiments prevents statement of any firm conclusions.

#### Design of System Involving the Flow of Thixotropic Liquids

The precise design of any fluid flow system can generally be accomplished provided the rheological behavior of the fluid is completely defined. However, in view of the highly complex nature of thixotropic liquids, even relatively simple operations, are very difficult to interpret quantitatively. Consider, for example, the laminar flow of a thixotropic liquid in a circular pipe. In addition to variations in consistency resulting from variations in shear rate across the pipe at right angles to the flow (a condition which is characteristic of pseudoplastic liquids), the consistency at any specified point in the stream will also vary with time until a steady state has been achieved. Furthermore, even under steady flow conditions, the consistency of the fluid in any stream line will change for a measurable distance along the pipe due to the large time interval required for the unsheared fluid entering the pipe to achieve an equilibrium consistency level.

Employing equation (70) in some form of numerical integration, it should be possible to determine the pressure drop along any specified



section of pipe at any instant provided that the initial conditions are known and provided that the flow pattern is laminar. However, development of this rather involved method of analysis is still somewhat premature since the general utility of equation (70) has not yet been established. On the other hand, an estimate of pressure drop, which is suitable for most engineering calculations, may be obtained through an extention of the procedure described by Metzner in connection with the flow of pseudoplastic liquids. In this technique each of the curves on Figures (38) to (41) is considered as characteristic of some pseudoplastic liquid of defined rheological behavior. The effect of shearing is then merely to convert the thixotropic fluid from one type of pseudoplastic to another. If this approach is valid, the flow behavior of a pipe line system, which is initially filled with stagnant, unsheared thixotropic liquid, may be analyzed under each of the following conditions involving constant volumetric throughput. For purposes of discussion, reference will be made to the curves on Figures (53), which is a reproduction of a portion of Figure (40).

1. Consider first the transient pressure gradient condition in that downstream section of the pipe in which the fluid will eventually attain an equilibrium consistency distribution. This section is designated as "B" in the schematic illustration on Figure (54). Following initiation of flow, the liquid over any cross section of pipe will have experienced shear action for an identical period of time, albeit at a varying rate dependent on the radius. Thus the rheological behavior of the liquid is reasonably well defined by the appropriate single



Figure 53

Shear Stress vs Shear Rate  
Cure Temperature 75°F  
Test Temperature 44.5°F

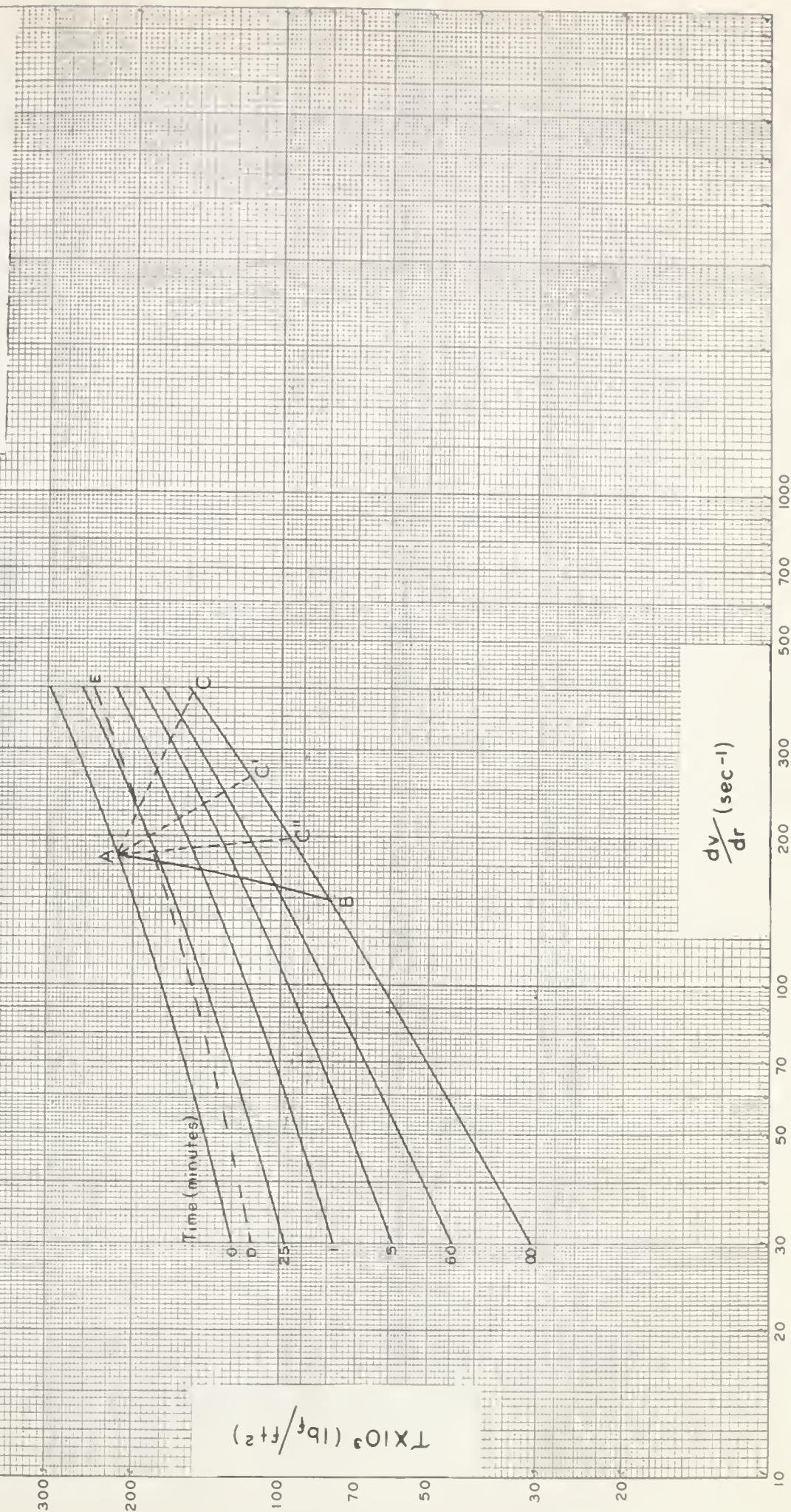




FIGURE 54  
PIPE LINE FLOW SYSTEM





curve on Figure (53). Now assuming that the value of  $n'$  in equation (15) is essentially equal to  $n$  in equation (23) over the shear rate range of interest, the instantaneous shear rate at the wall of the pipe may be calculated for any desired constant average velocity of flow by a trial and error solution of equation (21). That is, the wall shear rate at any desired flow rate and time of shearing is calculated using an assumed value of  $n'$  in equation (21). The slope of the appropriate curve on Figure (53), determined at a point corresponding to the computed wall shear rate, is then compared with the assumed value of  $n'$ . In the event that the slope differs appreciably from  $n'$ , the process must be repeated with another assumed value of  $n'$ . If the above procedure is carried out for various times of shear action, a line similar to A-B on Figure (53), may be constructed to connect points of equal flow rate. This line describes the systematic change, with respect to duration of shear, in the consistency of the liquid at the pipe wall. Then, since the wall shear stress at any time is the ordinate value corresponding to the intersection of line A-B with the appropriate curve, the instantaneous pressure gradient may be calculated from equation (5) and is approximately uniform over the entire downstream section of the pipe.

A minor discrepancy in the above argument is apparent. The shear rate at any element of liquid changes with time, hence, its rheological behavior will differ somewhat from that described by the curves on Figure (53) which have been determined at constant shear rate. However, as a first approximation it is probably reasonable to assume that this effect is negligible.



2. Stabilized pressure gradient condition in the downstream portion of the pipe may now be readily described since it merely represents the limiting case in the foregoing discussion. That is, the ordinate value corresponding to the intersection of the A-B line with the curve designated as " $\infty$ ", defines the lowest wall shear stress attained at the specified flow rate. It is interesting to note that, if a true equilibrium consistency does in fact exist at each shear rate, the limiting curve accurately represents the rheological behavior of the fluid regardless of its shear history.

3. The third case concerns the transient pressure gradient condition in the upstream pipe section ("A" on Figures (54)) extending from the inlet to the region described previously. Since unsheared liquid is continuously admitted to the pipe and since the velocity varies from a maximum at the center to zero at the pipe wall, the duration of shear is a complex function of radius and distance along the pipe. As a result, the consistency of the fluid over any pipe cross section is no longer described by a constant time curve on Figure (53) but instead conforms to a somewhat shallower curve such as D-E. That is, liquid entering in the region of lowest shear rate at the center of the pipe, moves more rapidly than fluid entering nearer the wall. Consequently, at any specified point along the upstream pipe section, the duration of shear and therefore the change in consistency of the liquid at the center of the pipe are much lower than at the wall. This feature is demonstrated by the small displacement of the point D and the large displacement of the point E from the curve designated as  $t = 0$ . Since the slope "n" of this curve is reduced, the wall shear rate, corres-



ponding to the selected flow rate, will be increased. The line corresponding to A-B in the previous case, is now displaced to some undefinable position such as A-C, A-C' or A-C", depending on the particular upstream location under examination.

4. Consider finally the stabilized pressure gradient condition in the upstream region. The wall shear stress or pressure gradient is here defined by the points C, C' and C" on Figure (53) and again varies in some fashion with distance from the pipe inlet. However, at any specified position along the pipe line, the pressure gradient is a constant independent of time.

The foregoing discussion has been directed entirely to the laminar flow of thixotropic liquids. However, turbulent flow conditions may also be described conveniently in terms of an equivalent pseudoplastic liquid. That is to say, extrapolation to a shear rate of unity of the tangent to any curve at a point corresponding to a shear rate in excess of  $500 \text{ sec}^{-1}$ , provides, as the ordinate, the value of K which, together with the slope of the tangent, n', may be used in the solution of equation (25). The value of the friction factor so determined may then be used in estimating the pressure gradient. This technique should be suitable for both unsteady state and steady state flow in the downstream pipe section but is again difficult to apply to the upstream section. Selection of  $500 \text{ sec}^{-1}$  as the minimum shear rate for evaluation of the consistency parameters is based on evidence obtained by Shaver and Merrill<sup>(47a)</sup> which indicates that effective wall shear rates in the turbulent flow region are generally of the order of  $500 \text{ sec}^{-1}$  to  $20,000 \text{ sec}^{-1}$ .



It should be noted here that, if the shear rate exceeds  $2,000 \text{ sec}^{-1}$ , the problem is considerably simplified since Pembina crude oil behaves essentially as a Newtonian fluid, at least during the period in which the pressure gradient is stable.

In spite of the problems involved in quantitatively evaluating the pressure gradient in the upstream pipe section, it must be appreciated that the major change in consistency occurs during the early stages of shear action. Consequently, the true weighted average pressure gradient will differ only slightly from that obtaining in the downstream section. In many engineering applications, such as the transportation of crude oil, the pipe lines are of such length that changes in pressure gradient near the inlet may be ignored.



## VII CONCLUSION

Pembina crude oil may, in a general sense, be classified as a thixotropic fluid. However, the molecular interactions responsible for this behaviour, the mechanism by which consistency changes occur and the influence of such variables as curing temperature, shear history, shear rate and testing temperature on the rheological properties, cannot be precisely explained due to the limitations of modern molecular theory. On the other hand, many investigators have attempted to describe the interdependence of some of these properties in terms of a simple, suitably defined model. A number of the more notable theories based on this approach have been discussed in the preceding literature review. The most popular model selected for analysis has been the combination of a Newtonian solvent and a long chain network structure which experiences successive stages of degradation under the influence of shear. In the present study, the destruction of this network, under certain specified conditions of thermal and shear history, was assumed to proceed in some manner analogous to a chemical reaction. A modified kinetic interpretation of this reaction was then performed and the validity of the resulting mathematical expressions was convincingly demonstrated by a rather extensive experimental investigation.

In spite of the apparent similarity between the chemical reaction and network decay mechanism, this approach must be viewed only as a "point d'appui" for further study. Neither this nor any



modified form of the proposed theory may be considered as generally acceptable until the qualifying assumptions present in the derivation have been justified and the behaviour of other thixotropic fluids, over a wider range of operating conditions, has been examined. If, on the other hand, this study provides some measure of guidance to future investigations of thixotropic behaviour, its primary objective will have been fulfilled.



NOMENCLATURE

A	Constant in Arrhenius equation
(A)	Concentration of original networks
a	Torsion wire constant, $\text{lb}_f/\text{ft}^2(\text{°})$
B <sub>1</sub>	Constant in Krieger and Maron equation
B <sub>2</sub>	Constant in Krieger and Maron equation
B <sub>η</sub>	Change in plastic viscosity with time multiplied by time of shearing, $\text{lb}_f \text{ sec}/\text{ft}^2$
(B)	Concentration of network fragments
b	Slope of semilogarithmic plot of $k_A$ vs $1/\theta$ , ${}^\circ R$
b	Thickness of torsion pendulum disc, ft.
C	Constant in equation (70)
c	Concentration of any crude oil component, moles
D	Diameter, ft
D	Viscometer bob deflection, (°)
d	Depth of immersion, ft
F	Force acting on network structure, $\text{lb}_f/\text{ft}^2$
F <sub>c</sub>	Critical force required to rupture network, $\text{lb}_f/\text{ft}^2$
f	Friction factor
f	Frequency, cycles/second
G	Shear modulus, $\text{lb}_f/\text{ft}^2$
G'	Shear modulus, $\text{lb}_f/\text{ft}^2$ (unit of extension)
g <sub>c</sub>	Dimensional conversion factor, $\text{lb}_m \text{ ft}/\text{lb}_f \text{ sec}^2$
I	Moment of inertia, $\text{lb}_m \text{ ft}^2$
K	Fluid consistency index, $\text{lb}_m/\text{ft}$ ( $\text{sec}$ ) <sup>2-n</sup>



K	Liquid-vapor equilibrium constant
K'	Fluid consistency index, $\text{lb}_m/\text{ft} \cdot (\text{sec})^{2-n'}$
k	Network growth rate constant
$k_1$	Network decay rate constant
$k_2$	Network growth rate constant, $\text{sec}^{-1}$
$k_A$	Network decay rate constant
$k_B$	Network growth rate constant, $\text{ft}^2/\text{lb}_f$
$k'_A$	Network decay rate constant, $\text{sec}^{-1}$
$k'_B$	Network growth rate constant, $\text{ft}^2/\text{lb}_f \text{ sec}$
L	Length, ft
$\Delta l$	Extension of network structure, ft
$\Delta l/l$	Unit strain in an elastic solid
M	Constant defined by stability criterion
$M_B$	Mass of brass cylinder of torsion pendulum, $\text{lb}_m$
$M_P$	Mass of lucite disc of torsion pendulum, $\text{lb}_m$
$M_\eta$	Loss in shear stress per unit increase in shear rate, $\text{lb}_f \text{ sec}/\text{ft}^2$
$M_W$	Molecular weight
N	Number of network links per unit volume
n	Flow behavior index
$n'$	Flow behavior index
P	Period of vibration, sec
$\Delta P$	Pressure drop, $\text{lb}_f/\text{ft}^2$
Q	Flow rate, $\text{ft}^3/\text{sec}$
q	Slope of bob deflection vs cup speed curve, ( $^\circ$ )/RPS



R	Gas constant, ft lb <sub>f</sub> /mole °R
R	Radius, ft
r	Radius, ft
Re	Reynolds' number
R <sub>r</sub>	Reynolds number defined by stability criterion
S	Rotational speed of viscometer cup, RPS
T	Absolute temperature, °R
t	Time, sec
t <sub>c</sub>	Life of network link, sec
v	Volume, ft <sup>3</sup>
v	Velocity, ft/sec
w	Weight fraction
x	Distance between shear planes, ft
x	Mole fraction in liquid phase
y	Mole fraction in gas phase
z	Total quantity of crude oil in storage, moles
dv/dx	Shear rate, sec <sup>-1</sup>
dv/dR	Shear rate, sec <sup>-1</sup>

Greek Symbols

α	Proportionality constant, lb <sub>m</sub> /ft(sec)(link)
β	Angular displacement, radians
δ,	Grouping of terms for denominator of generalized Reynolds' number, lb <sub>m</sub> /ft sec
ς	Torque, ft lb <sub>f</sub>
δ	Extension in length of longitudinal fiber, ft



$\eta$	Coefficient of rigidity, $\text{lb}_m/\text{ft sec}$
$\eta_1$	Plastic viscosity at first specified shear rate, $\text{lb}_m/\text{ft sec}$
$\eta_2$	Plastic viscosity at second specified shear rate, $\text{lb}_m/\text{ft sec}$
$\Theta$	Absolute temperature, $^{\circ}\text{R}$
$\lambda$	Relaxation time, sec
$\mu$	Viscosity, $\text{lb}_m/\text{ft sec}$
$\mu'$	Apparent viscosity, $\text{lb}_m/\text{ft sec}$
$\mu''$	Apparent viscosity evaluated at wall shear rate, $\text{lb}_m/\text{ft sec}$
$\rho$	Density, $\text{lb}_m/\text{ft}^3$
$\tau$	Unit shear stress, $\text{lb}_f/\text{ft}^2$
$\tau_y$	Yield stress, $\text{lb}_f/\text{ft}^2$
$\omega$	Angular velocity, radians/sec

#### Subscripts

$f$	Refers to final conditions
$o$	Refers to initial conditions
$R$	Parameter evaluated at any specified radius
$r$	Parameter evaluated at any specified radius
$s$	Pertaining only to the network structure
$w$	Parameter evaluated at viscometer or pipe wall
$\infty$	Refers to limiting value



BIBLIOGRAPHY

1. Alfrey, T., Rheology. Academic Press Inc., New York.  
Vol. 1, 391, 397 (1956).
2. Alfrey, T., Rheology. Academic Press Inc., New York.  
Vol. 1, 410 (1956).
3. ASTM Standards on Petroleum Products and Lubricants. (1949).
4. Bagley, H.D., M.Sc. Thesis, University of Alberta. (1955).
5. Barr, G., A Monograph of Viscometry. Oxford University Press,  
London (1931).
6. Billington, E.W., Proc. Phys. Soc. 75, 40 (1960).
7. Billington, E.W., Proc. Phys. Soc. 76, 127 (1960).
8. Bondi, A., Rheology. Academic Press Inc., New York.  
Vol. 1, 327 (1956).
9. Bondi, A., Rheology. Academic Press Inc., New York.  
Vol. 1, 324 (1956).
10. Buckingham, E., Proc. Amer. Soc. Testing Mat. 21, 1154 (1921).
11. Christianson, E.B., Ryan, N.W. and Stevens, W.E., A.I.Ch.E. Journal,  
1, 544 (1955).
12. Couette, M., Ann. Chim. Phys., 21, 433 (1890).
13. Dodge, D.W. and Metzner, A.B., A.I.Ch.E. Journal, 5 189 (1959).
14. Einstein, A., Ann. Physik 17, 549 (1905); 19, 289 (1906);  
34 591 (1911).
15. Ewell, R.E. and Eyring, H., J. Chem. Phys., 5 726 (1937).
16. Fisher, J.V., M.Sc. Thesis, University of Alberta. (1951).
17. Fox, T.G., Gratch, S. and Loshaek, S. Rheology. Academic Press  
Inc., New York. Vol. 1, 432 (1956).
18. Frisch, H.L. and Simha, R., Rheology. Academic Press Inc.,  
New York. Vol. 1, 535 (1956).



19. Frisch, H.L. and Simha, R., *Rheology*. Academic Press Inc., New York. Vol. 1 534 (1956).
20. Garner, F.H., Nissan, A.H. and Wood, G.F., *Philos. Trans. Royal Soc. London*, 243 37 (1950).
21. Green, H. and Weltman, R., *Ind. Eng. Chem., Ind. Ed.*, 18, 167 (1946).
22. Green, H., *Molec. Theory of Liquids*, Interscience Publishers, New York. (1952).
23. Goodeve, G.F. *Trans. Faraday Soc.*, 35, 352 (1939)
24. Hayashi, S., *Prog. Theor. Phys.* 82 (1959)
25. Hedstrom, B.O.A., *Ind. Eng. Chem.*, 44 651 (1952)
26. Houwink, R., *Plasticity, Elasticity and the Structure of Matter*, Harren Press (1955).
27. Kotaka, T., Kurata, M. and Onogi, S., *Prog. Theor. Phys.* 101 (1959).
28. Krieger, I.M. and Maron, S.H., *J. Appl. Phys.*, 25, 72 (1954).
29. Lower, G.W., Walker, W.C. and Zettlemoyer, A.C., *J. Colloid Science* 8, 116 (1953).
30. Masuda, A., M.Sc. Thesis. University of Alberta (1955).
31. Metzner, A.B. and Reed, J.C., *A.I.Ch.E. Journal*. 1, 434 (1955).
32. Metzner, A.B., *Adv. in Chem. Eng.* Academic Press., Vol. 1, 77 (1956).
33. Mooney, M., *Journal of Rheology*. 2, 210 (1931).
34. \*Navier, C.L., *Mem. de l'Acad. des Sciences*, 5 389 (1822)
35. Nelson, W L., *Petroleum Refinery Eng.* McGraw Hill (1941).
36. \*Newton, I. "Principia," F. Cajori, ed., Sir Isaac Newton's Mathematical Principles of Natural Philosophy and His System of the World. Univ. Cal. Pres. (1947)
37. NSGMA Engineering Data Book. 175 (1957)



38. Oldroyd, J.G., Rheology. Academic Press Inc., New York.  
Vol. 1, 654 (1956).
39. \*Poiseuille, J.L., Comptes Rendus, 15, 1167 (1842).
40. Powell, R.E. and Eyring, H., Nature. 154 427 (1944).
41. Reiner, M., Rheology. Academic Press Inc., New York.  
Vol. 1, 48 (1956).
42. Reiner, M. and Riwin, R., Kolloid Zeit. 43, 1 (1927).
43. Reiner, M., Deformation and Flow. H.K. Lewis and Co. Ltd. (1949)
44. Reiner, M., Rheology. Academic Press Inc., New York.  
Vol. 1, 52 (1956).
45. Riseman, J. and Kirkwood, J.G., Rheology. Academic Press Inc.,  
New York. Vol. 1, 511 (1956).
46. Rouse, P.E., J. Chem. and Phys. 21, 1272 (1953).
- 46a. Salt, D.L., Ryan, N.W. and Christiansen E.B. J. Colloid Science 6,  
146 (1951).
47. Serrin, J., Archive for Rational Mechanics and Analysis. 3,  
1 (1959).
- 47a. Shaver, R.G. and Merrill, E.W., A.I.Ch.E. Journal 5 181 (1959).
48. \*Stokes, G.G., Trans. Cambridge Phil. Soc. 8, 105 (1843).
49. Storey, B.T. and Merrill, E.W., J. Polymer Science. 33, 361 (1958).
50. Taylor, G.I., Phil. Trans. Royal Soc. 223A, 289 (1922).
51. Taylor, G.I., Proc. Royal Soc. of London. 157A, 546 (1936).
52. Umstatter, H., Kolloid Zeit. 70 174 (1935).
53. Umstatter, H., Einführung in Die Viskosimetrie und Rheometrie. Springer  
Verlag (1952).
54. \*Watson, Phys. Rev. 15, 20 (1902).
55. Weissenberg, K., Nature. 159, 310 (1947).
56. Weltman, R.N. Ind. Eng. Chem. 48 386 (1956).
57. Weltman, R.N., Rheology. Academic Press Inc., New York.  
Vol. 3, 238 (1960).



58. Weltman, R.N., Rheology, Academic Press Inc., New York.  
Vol. 3, 213 (1960).
59. Weltman, R.N. and Kuhns, P.W., Natl. Advisory Comm. Aeronaut.  
Tech. Note No. 3510 (1955).
60. Weltman, R.N. and Kuhns, P.W., J. Colloid Science. 7, 218 (1952).
61. Winning, M.D., M.Sc. Thesis. University of Alberta (1948).
62. Yamamoto, M., J. Phys. Soc. of Japan. 14, 313 (1959).
63. Yamamoto, M., Prog. Theor. Phys. 19 (1959).
64. Yamamoto, M., J. Phys. Soc. of Japan. 11, 413 (1956).
65. Zettlemoyer, A. and Meyers, R., Rheology. Academic Press Inc.,  
New York. Vol. 3 159 (1960).
66. Zimm, B.H., Rheology. Academic Press Inc., New York. Vol. 3,  
7 (1950).
67. Zimm, B.H., Rheology. Academic Press Inc., New York. Vol. 3,  
6 (1960).
68. Zeibig, H., Rheologic Acta. 2/3, 296 (1958).

\* References designated with an asterisk were not available to the author and are quoted in reference No. 5.



A P P E N D I C E S



APPENDIX IDERIVATION OF EQUATION (70)

The differential equation, which mathematically describes the mechanism of structural decay proposed in the present theory, has been shown to be

$$\frac{d\tau_s}{dt} = \frac{k_A}{t} \left[ \frac{\tau_{s\infty}(\tau_{so} - \tau_s)^2}{(\tau_{so} - \tau_{s\infty})^2} - \tau_s \right] \quad (1-1)$$

This expression may be rearranged to

$$\frac{d\tau_s}{dt} = \frac{k_A}{t(\tau_{so} - \tau_{s\infty})^2} \left[ \tau_{s\infty}\tau_s^2 - \tau_s(\tau_{so}^2 + \tau_{s\infty}^2) + \tau_{s\infty}\tau_{so}^2 \right] \quad (2-1)$$

or

$$\frac{d\tau_s}{\tau_{s\infty}\tau_s^2 - \tau_s(\tau_{so}^2 + \tau_{s\infty}^2) + \tau_{s\infty}\tau_{so}^2} = \left[ \frac{k_A}{(\tau_{so} - \tau_{s\infty})^2} \right] \frac{dt}{t} \quad (3-1)$$

Solution of equation (3-1) then yields

$$\begin{aligned} & \frac{1}{\sqrt{(\tau_{so}^2 + \tau_{s\infty}^2)^2 - 4\tau_{s\infty}\tau_{so}^2}} \ln \frac{2\tau_{s\infty}\tau_s - (\tau_{so}^2 + \tau_{s\infty}^2) - \sqrt{(\tau_{so}^2 + \tau_{s\infty}^2)^2 - 4\tau_{s\infty}\tau_{so}^2}}{2\tau_{s\infty}\tau_s - (\tau_{so}^2 + \tau_{s\infty}^2) + \sqrt{(\tau_{so}^2 + \tau_{s\infty}^2)^2 - 4\tau_{s\infty}\tau_{so}^2}} \\ &= \frac{k_A}{(\tau_{so} - \tau_{s\infty})^2} \ln t + C' \end{aligned} \quad (4-1)$$

Furthermore it may be shown that

$$\sqrt{(\tau_{so}^2 + \tau_{s\infty}^2)^2 - 4\tau_{s\infty}\tau_{so}^2} = \tau_{so}^2 - \tau_{s\infty}^2 \quad (5-1)$$



whereupon equation (4-1) may be written

$$\frac{1}{(\tau_{so}^2 - \tau_{s\omega}^2)} \ln \left[ \frac{2\tau_{s\omega}\tau_s - 2\tau_{so}^2}{2\tau_{s\omega}\tau_s - 2\tau_{s\omega}^2} \right] = \frac{k_A}{(\tau_{so} - \tau_{s\omega})^2} \ln t + C^1 \quad (6-1)$$

or

$$\frac{1}{(\tau_{so}^2 - \tau_{s\omega}^2)} \ln \left[ \frac{\tau_{s\omega}\tau_s - \tau_{s\omega}^2}{\tau_{s\omega}\tau_s - \tau_{so}^2} \right] - C^1 = - \frac{k_A}{(\tau_{so} - \tau_{s\omega})^2} \ln t \quad (7-1)$$

Then, at  $t = 1$  minute,  $\tau_s = \tau_{s1}$  and the R.H.S. of equation (7-1) is zero.

Therefore

$$C^1 = \frac{1}{(\tau_{so}^2 - \tau_{s\omega}^2)} \ln \left[ \frac{\tau_{s\omega}\tau_{s1} - \tau_{so}^2}{\tau_{s\omega}\tau_{s1} - \tau_{s\omega}^2} \right] \quad (8-1)$$

Substituting equation (8-1) into equation (7-1) and combining the terms on the R.H.S. gives

$$\frac{1}{(\tau_{so}^2 - \tau_{s\omega}^2)} \ln \frac{(\tau_{s\omega}\tau_s - \tau_{s\omega}^2)(\tau_{s\omega}\tau_{s1} - \tau_{so}^2)}{(\tau_{s\omega}\tau_s - \tau_{so}^2)(\tau_{s\omega}\tau_{s1} - \tau_{s\omega}^2)} = - \frac{k_A}{(\tau_{so} - \tau_{s\omega})^2} \ln t \quad (9-1)$$



or

$$\left[ \frac{(\tau_{s\infty}\tau_s - \tau_{s\infty}^2)}{(\tau_{so}^2 - \tau_{s\infty}\tau_s)} \right] - \left[ \frac{(\tau_{so}^2 - \tau_{s\infty}\tau_{s1})}{(\tau_{s\infty}\tau_{s1} - \tau_{s\infty}^2)} \right] = - \frac{k_A (\tau_{so}^2 - \tau_{s\infty}^2)}{(\tau_{so} - \tau_{s\infty})^2} \ln t \quad (10-1)$$

Then, by dividing the numerator and denominator of the logarithmic terms on the L.H.S. by  $\tau_{s\infty}$  and letting

$$C = \left[ \frac{\frac{\tau_{so}^2}{\cancel{\tau_{s\infty}}} - \tau_{s1}}{\tau_{s1} - \cancel{\tau_{s\infty}}} \right]$$

equation (10-1) becomes

$$\ln \left[ \frac{\tau_s - \tau_{s\infty}}{\frac{\tau_{so}^2}{\cancel{\tau_{s\infty}}} - \tau_s} \right] + \ln C = - \frac{k_A (\tau_{so}^2 - \tau_{s\infty}^2)}{(\tau_{so} - \tau_{s\infty})^2} \ln t \quad (11-1)$$

Equation (11-1) may finally be simplified and rearranged to the form

$$\log \left[ \frac{(\tau_s - \tau_{s\infty})}{\frac{\tau_{so}^2}{\cancel{\tau_{s\infty}}} - \tau_s} \right] = - \frac{k_A (\tau_{so} + \tau_{s\infty})}{(\tau_{so} - \tau_{s\infty})} \log t - \log C \quad (12-1)$$

which is identical in form to equation ( 70 ) on Page 49 of the text.



APPENDIX 2CHARACTERIZATION OF PEMBINA CRUDE OIL

Identification of the crude oil sample used in this investigation and the magnitude of certain of its physical properties, as determined by standard methods of analysis, are presented in Table (1-2)

TABLE 1-2

WELL NAME AND NUMBER - Mobil Oil Sbd. Drayton Valley 20 - 16

WELL LOCATION - LSD 16 Sec 20 Twp 49 Rge 7 West 5 mer

SAMPLE OBTAINED FROM TUBING

METHOD OF PRODUCTION - Pump

DEPTH OF INTERVAL - 4595 feet to 4603 feet

K.B. ELEVATION - 2752

NAME OF ZONE AND FORMATION - Cardium

SPECIFIC GRAVITY 60/60 - 0.838

API GRAVITY - 37.4°

BASIC SEDIMENT AND WATER - 0.00 percent

SULPHUR CONTENT - 0.17 weight percent

SAYBOLT UNIVERSAL VISCOSITY AT 100°F - 44 secs

USEM POUR POINT - +40°F

CARBON RESIDUE - 1.40 weight percent



(TABLE 1-2 continued)

U.S.B.M. DISTILLATION

ATMOSPHERIC PRESSURE - 698.5 mm.

FIRST DROP DISTILLED AT - 76° F

## PHYSICAL PROPERTIES OF DISTILLATE FRACTIONS

FRACTION NO.	CUT AT (°F)	PERCENT OF TOTAL	CUMULATIVE WEIGHT PERCENT	SPECIFIC GRAVITY 60/60	C- INDEX	ANTILINE POINT	SAYBOLT UNIVERSAL VISCOSITY 100°F	CLOUD TEST (°F)	REFRACTIVE INDEX 24°C
1	122	2.7	2.7	0.639	-	-			1.3619
2	167	2.9	5.6	0.687	16	58.2			1.3821
3	212	5.1	10.7	0.725	24	53.4			1.4017
4	257	5.8	16.5	0.748	26	53.0			1.4140
5	302	4.7	21.2	0.766	27	53.6			1.4252
6	347	4.5	25.7	0.784	28	56.0			1.4333
7	392	3.9	29.6	0.797	28	60.2			1.4415
8	437	4.5	34.1	0.811	29	64.4			1.4490
9	482	5.0	39.1	0.824	30	68.0			1.4573
10	527	6.9	46.0	0.837	32	73.0			1.4640

## DISTILLATION CONTINUED AT 40 min.

11	392	4.5	50.5	0.850	34	76.8	42	26	1.4708
12	437	5.3	55.8	0.857	33	81.6	50	48	1.4757
13	482	4.3	60.1	0.870	36	83.8	66	66	1.4810
14	527	5.2	65.3	0.877	36	88.6	95	80	1.4845
15	572	6.1	71.4	0.887	38	93.0	171	98	1.4898

CARBON RESIDUE OF RESIDUUM 4.60%



(TABLE 1-2 continued)

## APPROXIMATE SUMMARY

	PERCENT	SPECIFIC GRAVITY 60/60	°API	SAYBOLT UNIV. VISC. 100°F
LIGHT GASOLINE	10.7	0.693	72.7	
TOTAL GASOLINE AND NAPHTHA	29.6	0.743	58.9	
KEROSENE DISTILLATE	9.5	0.818	41.5	
GAS OIL	14.0	0.847	35.6	BELOW 50
NONVISCOSUS LUB. DISTILLATE	10.0	0.857 - 0.878	33.6 - 29.7	50 - 100
MEDIUM LUB. DIST.	8.3	0.878 - 0.892	27.7 - 27.1	100 - 200
VISCOUS LUB. DIST.	NIL	---	---	ABOVE 200
RESIDUUM	25.4	0.958	16.2	
DISTILLATION LOSS	3.2			



True Boiling Point Distillation

Characterization of the crude oil by way of true boiling point distillation was carried out in three stages which may be summarized as follows:

1 A small sample (425 gms) of crude oil was placed in the receiver or "kettle" of the Podbielniak high temp. distillation apparatus and heated sufficiently to cause vaporization of the more volatile components. All material having a boiling point below 80°F was collected, as a vapor, in a calibrated gas holder by displacement of a saturated brine solution and retained for chromatographic analysis.

2 Subsequent fractionation of the small sample provided a liquid distillate sample boiling within the range of 80°F to 95°F. At this point the temperature suddenly increased to 140°F thereby indicating that all of the pentane had been removed from the column. Two additional distillate fractions, with boiling point ranges of 140 to 155°F and 155°F to 195°F, were also collected but were later found to be unnecessary. The distillation was then discontinued and the residue in the kettle was discarded.

3 Complete fractionation of a large sample (2391 gms) of crude oil was performed at 70 $\frac{1}{4}$ , 38.7 and 4.8 mm. mercury absolute pressure to cover the boiling point range from 95°F to 585°F. Distillate fractions of approximately 70 cc volume were collected for purposes of analysis and to provide the information required to construct the true boiling point distillation curve.



To supplement the information obtained from the above procedures and to permit correlation of the data derived from each of these operations, a chromatographic analysis of the gas phase, in equilibrium with the crude oil in storage, was also performed. The exact role of this data, which is presented in Table 2-2, will become apparent later.

TABLE 2-2

ANALYSIS OF GAS PHASE IN EQUILIBRIUM WITH CRUDE OIL

Vapor Pressure above oil Sample in storage - 15.6 psia

Temperature of oil Sample in storage - 75° F

COMPONENT	N <sub>2</sub>	C <sub>1</sub>	C <sub>2</sub>	C <sub>3</sub>	iC <sub>4</sub>	nC <sub>4</sub>	iC <sub>5</sub>	nC <sub>5</sub>
VOLUME PERCENT	7.14	25.03	15.88	28.89	5.09	14.01	2.12	1.85

Analysis of Gas Fraction From Distillation

The gas fraction, obtained by the procedure outlined under item 1 above, was analyzed chromatographically and the results expressed as volume percent of each constituent. Since the total gas volume as well as the temperature and pressure in the gas holder were known, the actual weight of each component was readily calculated by means of the ideal gas law. The results of this analysis and calculation are presented in Table 3-2.



TABLE 3-2  
GAS FRACTION ANALYSIS

TOTAL GAS VOLUME - 10,400 cc

TEMPERATURE - 68° F

PRESSURE - 13.5 psia

COMPONENT	AIR	C <sub>1</sub>	C <sub>2</sub>	C <sub>3</sub>	iC <sub>4</sub>	nC <sub>4</sub>	iC <sub>5</sub>	nC <sub>5</sub>
VOLUME PERCENT	32.48	0	3.0	20.62	7.56	27.07	5.11	4.16
WEIGHT (gms)		0	0.356	3.605	1.753	6.240	1.455	1.198

TOTAL WEIGHT OF HYDROCARBONS IN GAS FRACTION - 14.610 gms.

Resolution of Gas Phase and Liquid Phase Data To Common Basis

Clearly, the quantities of isopentane and normal pentane appearing in Table 3-2 represent only a portion of these constituents actually present in the sample since considerably more occurs as the first liquid fraction boiling below 95° F. In order to determine the approximate total amounts of each isomer, several assumptions were found necessary.

- a) The first liquid fraction was assumed to contain only pentane and no butane or hexane. This appeared reasonable since the boiling point range of the fraction was 80° F to 95° F while the boiling points of butane and hexane are 31° F and 156° F respectively.
- b) The ratio of the equilibrium constants, K in equation



$$y = K x$$

given in the literature<sup>(35)(37)</sup> for iso and normal pentane, was assumed to be appropriate for this system. It should be noted that this assumption does not consider the absolute values of these constants but only the ratio between them.

Thus the total quantity of pentane in the crude oil was taken as the sum of that found in the gas phase and the entire first liquid fraction.

$$\text{Pentane in gas phase} - 1.455 + 1.198 = 2.653 \text{ gms.}$$

$$\text{Pentane in liquid phase} - \underline{4.710 \text{ gms.}}$$

$$\text{Total pentane in } 425 \text{ gm sample} - 7.363 \text{ gms.}$$

This in turn is equivalent to  $\frac{7.363}{425} = 0.01734$  weight fraction  
of the crude oil.

Now since

$$y_{iC_5} = K_{iC_5} x_{iC_5} \quad (1-2)$$

and

$$y_{nC_5} = K_{nC_5} x_{nC_5} \quad (2-2)$$

and since

$$\frac{K_{nC_5}}{K_{iC_5}} = \frac{0.6}{0.8} = 0.75$$

then

$$\frac{x_{iC_5}}{x_{nC_5}} = 0.75 \left( \frac{y_{iC_5}}{y_{nC_5}} \right)$$



From Table 2-2

$$y_{iC_5} = 0.0212$$

and

$$y_{nC_5} = 0.0185$$

therefore

$$\frac{x_{iC_5}}{x_{nC_5}} = 0.75 \left( \frac{0.0212}{0.0185} \right) = 0.86 \quad (3-2)$$

Since the molecular weights of isopentane and normal pentane are identical, the ratio of mole fractions is equal to the ratio of weight fractions. Furthermore the total weight fraction is given above as

$$w_{iC_5} + w_{nC_5} = 0.01734 \quad (4-2)$$

Equations (3.2) and (4-2) may be solved simultaneously to give

$$w_{iC_5} = 0.00800$$

and

$$w_{nC_5} = 0.00934$$

From equations (1-2) and (2-2) the actual values of the equilibrium constants are

$$K_{iC_5} = 0.69$$

$$K_{nC_5} = 0.52$$

The calculated weight fractions of the pentane isomers,



included in Table 4-2 below, complete the information required for construction of the distillation curve. (Figure(3) Page 57 of the text). In this table the weight fractions corresponding to components C<sub>1</sub> through C<sub>5</sub> were based on analysis of the 425 gm crude oil sample while those indicated for the liquid fractions, numbered 1 to 19, were based on the 2391 gm sample. Hence it was assumed that a proportionately sized fraction of each sample exhibited a boiling point below 95° F



TABLE 4-2  
TRUE BOILING POINT DISTILLATION DATA  
FOR PEMBINA CRUDE OIL

FRACTION	WEIGHT (gms)	WEIGHT PERCENT	CUMULATIVE WEIGHT PERCENT	RECORDED TEMP. FOLLOWING EACH FRACTION (°F)	TEMP. CORRECTED* TO 760 mm
C <sub>1</sub>	0	0	0		
C <sub>2</sub>	0.356	0.084	0.084		-127.5
C <sub>3</sub>	3.605	0.850	0.934		-44
iC <sub>4</sub>	1.753	0.414	1.348		+13.5
nC <sub>4</sub>	6.240	1.468	2.816		31
iC <sub>5</sub>	3.400	0.800	3.616		82
nC <sub>5</sub>	3.965	0.934	4.550		97
1	33.371	1.395	5.945	152.6	156.6
2	43.028	1.801	7.746	168.8	172.9
3	50.658	2.120	9.866	197.6	201.9
4	51.550	2.160	12.026	210.2	214.5
5	52.831	2.210	14.236	240.8	245.5
6	52.412	2.190	16.426	258.8	263.6
7	54.188	2.270	18.696	285.8	290.8
8	54.105	2.265	20.961	307.4	312.6
9	54.503	2.280	23.241	334.4	339.7
10	54.450	2.276	25.517	359.6	365.1
11	56.115	2.348	27.865	211.0	376.5
12	56.369	2.358	30.223	248.0	420
13	56.378	2.358	32.581	269.6	450
14	56.990	2.385	34.966	291.2	470
15	58.087	2.436	37.402	311.0	490
16	58.076	2.436	39.838	327.2	510
17	58.410	2.440	42.278	354.2	540
18	58.646	2.456	44.734	377.6	570
19	58.715	2.460	47.194	293.0	575
RESIDUUM	1217.5	50.9	98.1		

\* Boiling point corrections to 760 mm pressure were based on tables and nomographs available in Nelson, W.L. Petroleum Refinery Engineering, P. 131 McGraw-Hill Inc. (1941) and ASTM Standards on Petroleum Products and Lubricants, P. 815 (1949).



In order to further identify the crude oil sample, certain physical properties of the liquid fractions were determined and are presented in Table 5-2

TABLE 5-2

## PHYSICAL PROPERTIES OF LIQUID DISTILLATE FRACTIONS

FRACTION	SPECIFIC GRAVITY 60/60	REFRACTIVE INDEX	ANILINE POINT	SAYBOLT UNIV. VISCS. (secs)	CLOUD POINT
1	0.664	1.3734	-		
2	0.699	1.3888	53.6		
3	0.727	1.4010	53.8		
4	0.731	1.4041	53.8		
5	0.754	1.4173	46.0		
6	0.741	1.4104	60.2		
7	0.777	1.4315	43.0		
8	0.763	1.4226	59.2		
9	0.786	1.4362	51.2		
10	0.785	1.4345	58.3		
11	0.799	1.4420	59.5		
12	0.810	1.4467	60.1		
13	0.817	1.4524	63.2		
14	0.816	1.4517	67.8	32	
15	0.832	1.4628	67.0	34	
16	0.836	1.4622	70.8	35	
17	0.841	1.4671	70.0	37	
18	0.840	1.4651	75.2	39	
19	0.843	1.4656	79.6	41	
RESIDUUM	0.914				+14°F +22°F

It should be noted that the continuity of change in physical properties is interrupted between fractions 5 and 6 and 7 and 8. It is entirely possible that these samples were interchanged during analysis. However, the limited size of the samples precluded performance of any duplicate analysis.



APPENDIX 3CALIBRATION OF VISCOMEIER TORSION WIRES

Two independent methods of torsion wire calibration have been outlined in the preceding text.

I Consider a wire of length  $L$ , rigidly fixed at one end and subjected to a torque,  $\gamma$ , which causes the free end to rotate through an angle of  $\beta$  radians. Any longitudinal fiber, located at a distance  $r_i$  from the center, will be deformed an amount equal to the arc of a circle of radius  $r_i$  and subtended by an angle  $\beta$ . Thus the unit strain of the fiber,  $\delta/L$ , is given by

$$\frac{\delta}{L} = \frac{r_i \beta}{L} \quad (1-3)$$

and since, by Hooke's law, the shear stress is related to strain by the expression

$$\sigma = \frac{G \delta}{L} \quad (2-3)$$

the shear stress becomes

$$\sigma = \frac{G r_i \beta}{L} \quad (3-3)$$

Furthermore, the stress acting on any element of area on the wire cross section is identical with the tangential force per unit area or



$$S = \frac{dF}{dA} \quad (4-3)$$

The torque  $d\gamma$  at this point is

$$d\gamma = r_i dF \quad (5-3)$$

Therefore, from equation (4-3), it follows that

$$d\gamma = r_i(S)dA \quad (6-3)$$

Substituting equation (3-3) into equation (6-3) gives

$$d\gamma = \frac{r_i^2(G)(B)dA}{L} \quad (7-3)$$

which in turn may be written

$$d\gamma = \frac{r_i^2(G)(B)2\pi r_i dr_i}{L} \quad (8-3)$$

since  $dA = 2\pi r_i dr_i$

Integrating equation (8-3) between boundary conditions

$$\gamma = 0 \text{ at } r_i = 0$$

$$\text{and } \gamma = \gamma_r \text{ at } r_i = r$$

$$\gamma_r = \frac{\pi r^4 G B}{2 L} \quad (9-3)$$

Consider now a massive disc, suspended from the wire at its center of rotation and permitted to oscillate through an angle



of  $\pm \beta'$  radians at a frequency of  $f$  cycles/second. The angular displacement,  $\beta$ , of the disc at any time,  $t$ , is given by

$$\beta = \beta' \sin(\omega t) \quad (10-3)$$

where  $\omega$  is the angular velocity.

The deceleration of the disc due to the opposing torque developed in the wire is then

$$\frac{d^2 \beta}{dt^2} = -\beta' \omega^2 \sin(\omega t) \quad (11-3)$$

or, in view of equation (10-3)

$$\frac{d^2 \beta}{dt^2} = -\beta \omega^2 \quad (12-3)$$

The angular velocity may be defined by

$$\omega = 2\pi f \quad (13-3)$$

therefore equation (12-3) becomes

$$\frac{d^2 \beta}{dt^2} = -4\pi^2 f^2 \beta \quad (14-3)$$

Furthermore, the restoring torque in the wire causing the deceleration is

$$\gamma_r = -I \frac{d^2 \beta}{dt^2} \quad (15-3)$$

where  $I$  is the moment of inertia of the disc, therefore

$$\gamma_r = 4\pi^2 f^2 \beta I \quad (16-3)$$



Finally, since the frequency,  $f$ , is inversely proportional to the period of vibration,  $P$ , equation (16-3) may be written

$$\gamma_r = \frac{4\pi^2 B I}{P^2} \quad (17-3)$$

Comparing equations (9-3) and (17-3) it may be seen that the shear modulus,  $G$ , is given by

$$G = \frac{2LC}{\pi r^4} \quad (18-3)$$

where

$$C = \left(\frac{2\pi}{P}\right)^2 I \quad (19-3)$$

The value of  $G$  may now be determined for any wire by measuring each of the variables occurring in equation (18-3)

In order to evaluate the constant,  $a$ , of equation (72) which state

$$T = a D$$

where  $D$  is the bob deflection,

it is necessary only to recognize that the torque on the wire is related to the shear stress, acting on the viscometer bob wall, by the equation

$$T = \frac{\gamma_r}{RA} \quad (20-3)$$

where  $R$  is the radius of the bob

and  $A$  is its surface area.



From equation (9-3), since

$$\beta = \frac{2\pi D}{360}$$

$$\text{and } A = 2\pi R d$$

then

$$\tau = \frac{\pi r^4 G D}{(720) L R^2 d} \quad (21-3)$$

where  $d$  is the depth of immersion of the bob into the fluid.

Comparison of equations (72) and (21-3) indicates that

$$d = \frac{\pi r^4 G}{(720) L R^2 d} \quad (22-3)$$

Substituting equations (18-3) and (19-3) into equation (22-3) gives

$$d = \frac{\pi^2 I}{(90) P^2 R^2 d} \quad (23-3)$$

The moment of inertia of the particular pendulum used in this investigation is given by the sum of two components; thus

$$I = I_B + I_P \quad (24-3)$$

where  $I_B$  represents the moment of inertia of the central brass cylinder and  $I_P$  represents the moment of inertia of the lucite disc.

In general, the moment of inertia of a differential mass,  $d_m$ , about any axis is given by

$$I = \int r^2 dm \quad (25-3)$$

where  $r$  is the distance from the mass element to the axis.

In this instance

$$dm = \rho_b 2\pi r dr \quad (26-3)$$



where  $b$  is the thickness of the disc.

It then follows from equation (25-3) that

$$I = \int 2\pi r^3 \rho b dr \quad (27-3)$$

For the brass cylinder equation (27-3) becomes

$$I_B = \int_{r=0}^{r=r_B} 2\pi r^3 \rho_B b dr = \frac{\pi r_B^4 \rho_B b}{2} = \frac{m_B r_B^2}{2} \quad (28-3)$$

while for the lucite

$$I_P = \int_{r=r_P}^{r=r_B} 2\pi r^3 \rho_P b dr = \frac{m_P (r_P^2 - r_B^2)}{2} \quad (29-3)$$

The total moment of inertia is then

$$I = \frac{m_P}{2} (r_P^2 - r_B^2) + \frac{m_B}{2} (r_B^2) \quad (30-3)$$

The central brass cylinder of the pendulum in question had a mass of 0.2475 lb. and radius of 0.0310 ft. while the mass and radius of the lucite were 0.760 lb. and 0.173 ft. respectively.

Hence the moment of inertia of the disc is given by equation (30-3) as

$$\begin{aligned} I &= \frac{0.760}{2} (0.173)^2 - (0.0310)^2 + \frac{0.2475}{2} (0.0310)^2 \\ &= 0.01117 \end{aligned}$$

The effective depth of bob immersion in all cases was 4.225 inches (Appendix 4) and the radius of the bob was 0.790 inches



Therefore from equation (23-3)

$$a = \frac{0.800}{P^2} \text{ lb}_m/\text{ft sec}^2(\circ)$$

which, in Engineering units, becomes

$$a = \frac{0.0249}{P^2} \text{ lb}_f/\text{ft}^2(\circ) \quad (31-3)$$

The period of vibration of the 30 gauge wire was found to be 16.29 seconds. Thus the constant "a" is given by equation (31-3) as

$$a = \frac{0.0249}{(16.29)^2} = 9.40 \times 10^{-5} \text{ lb}_f/\text{ft}^2(\circ)$$

Values of this constant for other wires are presented in table 1-3.

TABLE 1-3

VALUES OF CONSTANT "a" IN EQUATION 72

Wire Gauge No.	30	28	26	24	22	20
Period (sec.)	16.29	11.58	6.42	4.26	2.63	1.55
a( $\text{lb}_f/\text{ft}^2(\circ)$ )	$9.40 \times 10^{-5}$	$18.6 \times 10^{-5}$	$6.05 \times 10^{-4}$	$13.7 \times 10^{-4}$	$3.60 \times 10^{-3}$	$10.38 \times 10^{-3}$

A plot of the wire constants as a function of wire diameter has been prepared and is presented in Figure (8-3). It is interesting to note that the slope of the line joining these points on logarithmic coordinates is theoretically defined as 0.250 by equation (22-3).



Thus

$$\log a = 4 \log r + \log \frac{G \pi}{(720) L R^2 d}$$

$$\log r = 0.250 \log a + 0.250 \log \frac{G \pi}{(720) L R^2 d}$$

Precisely this value of the slope was obtained from the experimental data.

II The second method of torsion wire calibration involved the use of the viscometer. The viscometer was assembled with the particular wire in question and a Newtonian oil of known viscosity was placed in the cup. The deflection of the bob, resulting from shear at various cup speeds, was noted. The relationship between these variables is demonstrated graphically on Figures (1-3) to (7-3).

Then since

$$\tau = - \frac{\mu}{g_c} \left( \frac{dv}{dR} \right) \quad (1)$$

and

$$\tau = a D \quad (72)$$

the constant "a" is defined as

$$a = - \frac{\mu}{g_c D} \left( \frac{dv}{dR} \right) \quad (32-3)$$

The shear rate,  $dv/dR$ , is related to cup speed,  $S$ , by the Reiner-Riwlin equation



Figure 1-3

Deflection vs Cup Speed  
for

30 gauge wire

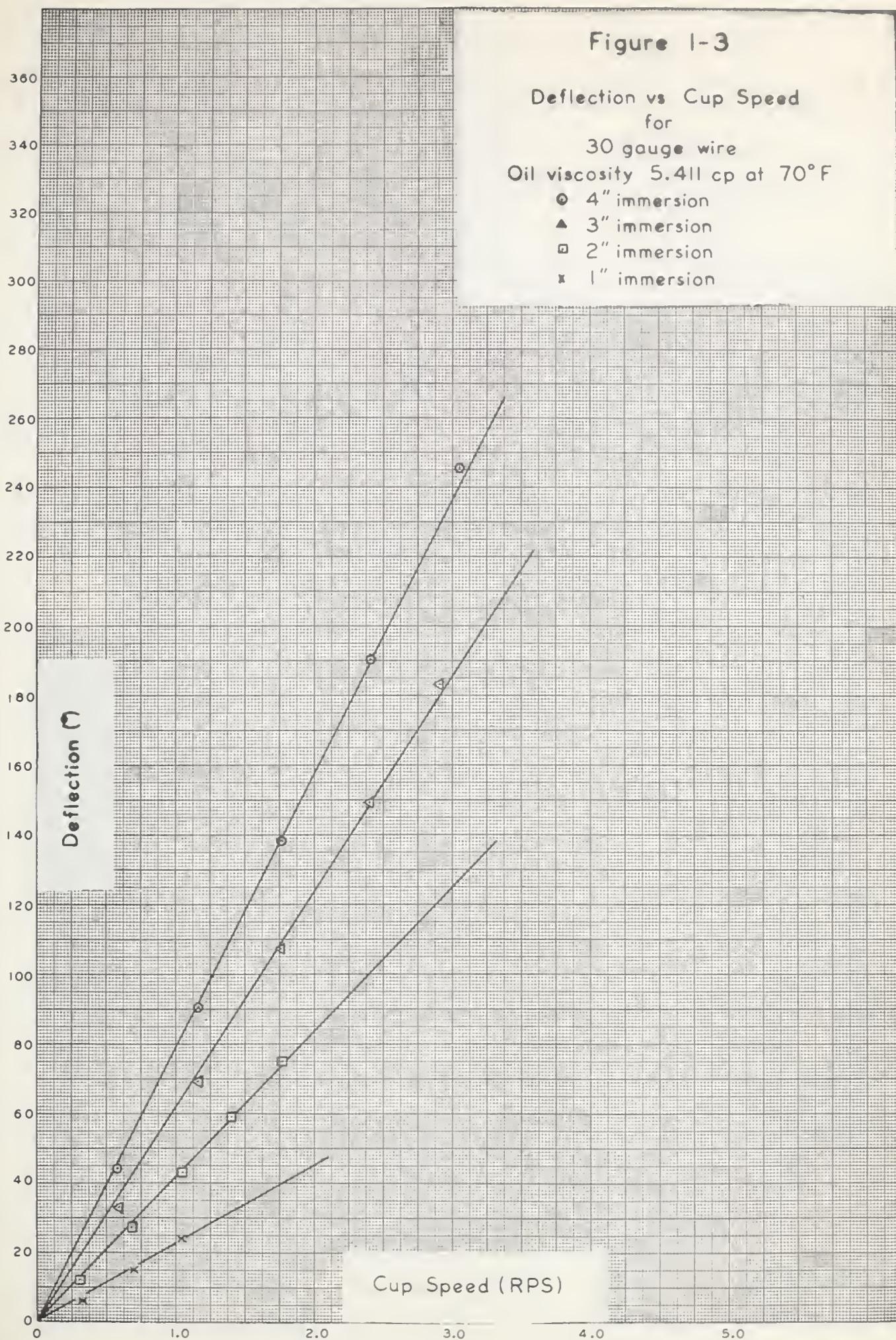
Oil viscosity 5.411 cp at 70°F

○ 4" immersion

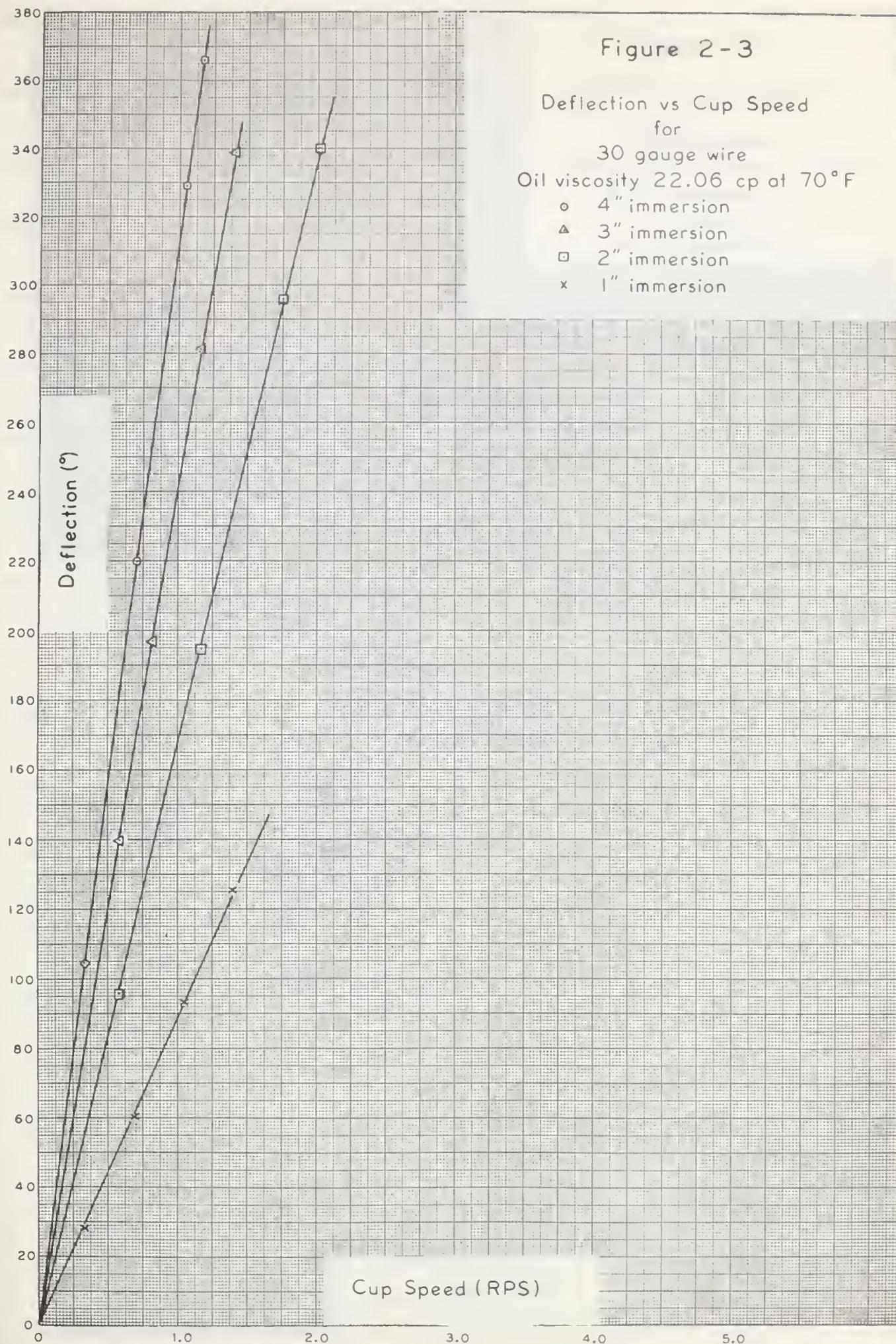
▲ 3" immersion

□ 2" immersion

\* 1" immersion









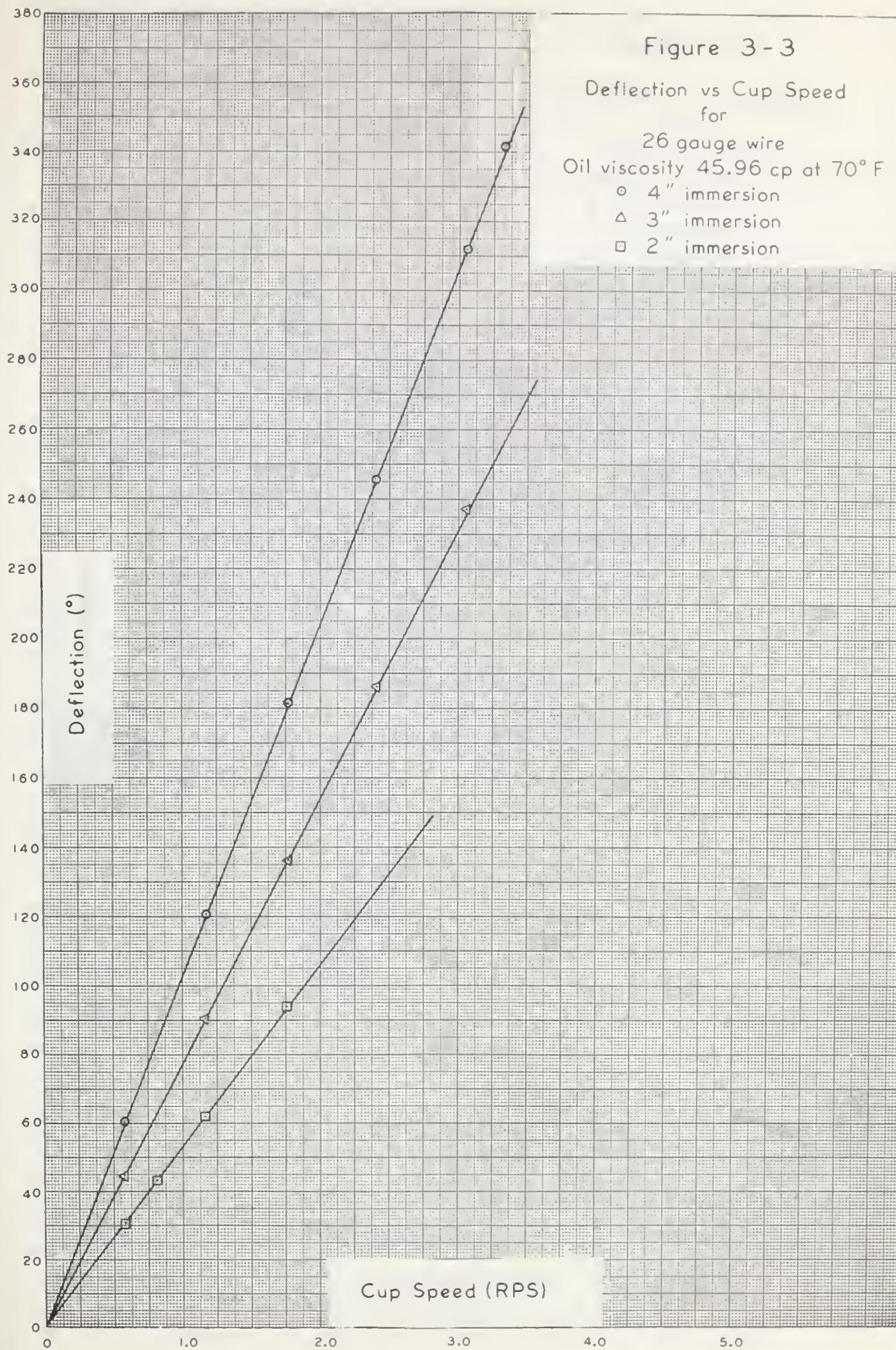
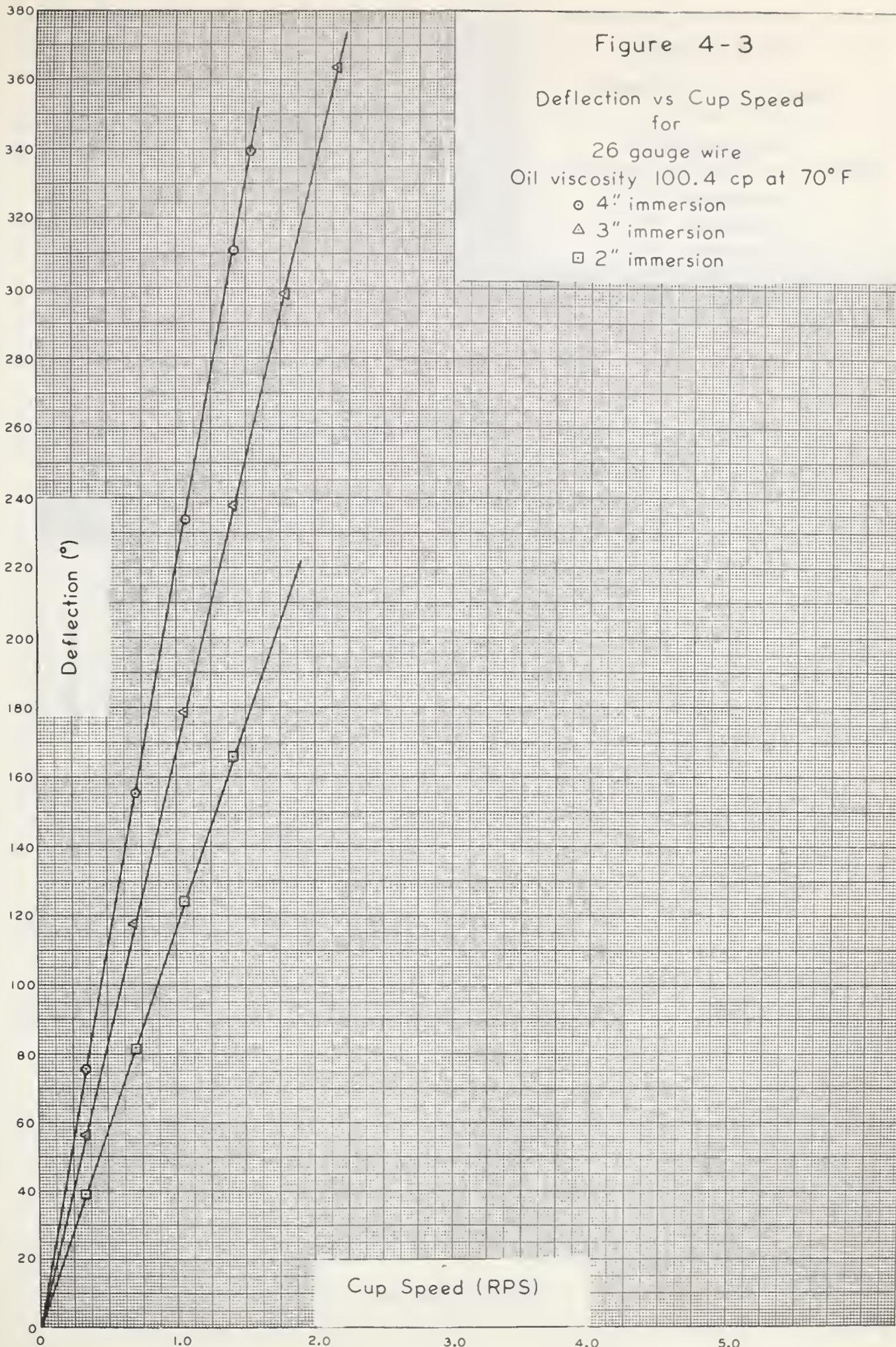


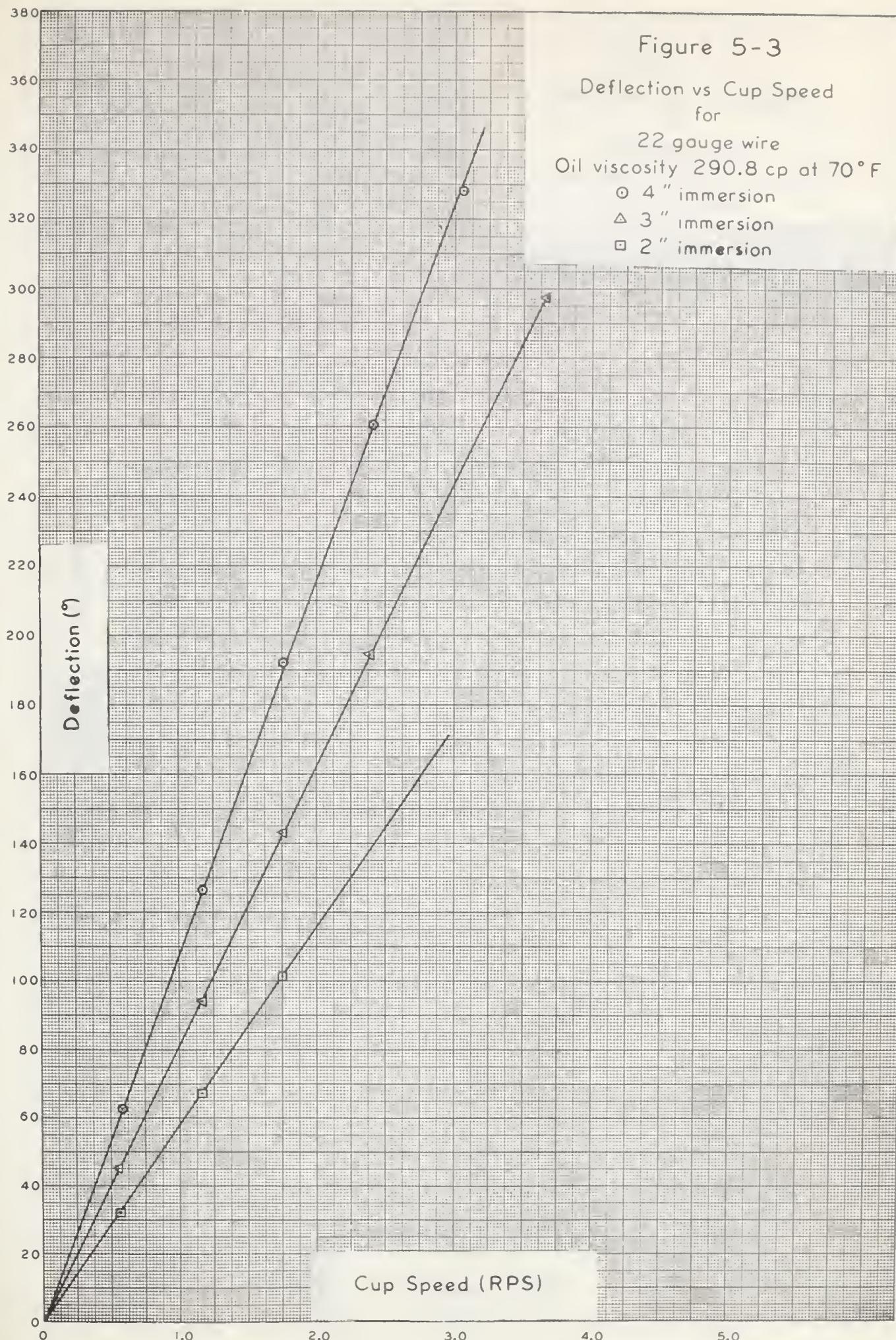
Figure 3-3

Deflection vs Cup Speed  
for  
26 gauge wire  
Oil viscosity 45.96 cp at 70° F  
○ 4" immersion  
△ 3" immersion  
□ 2" immersion

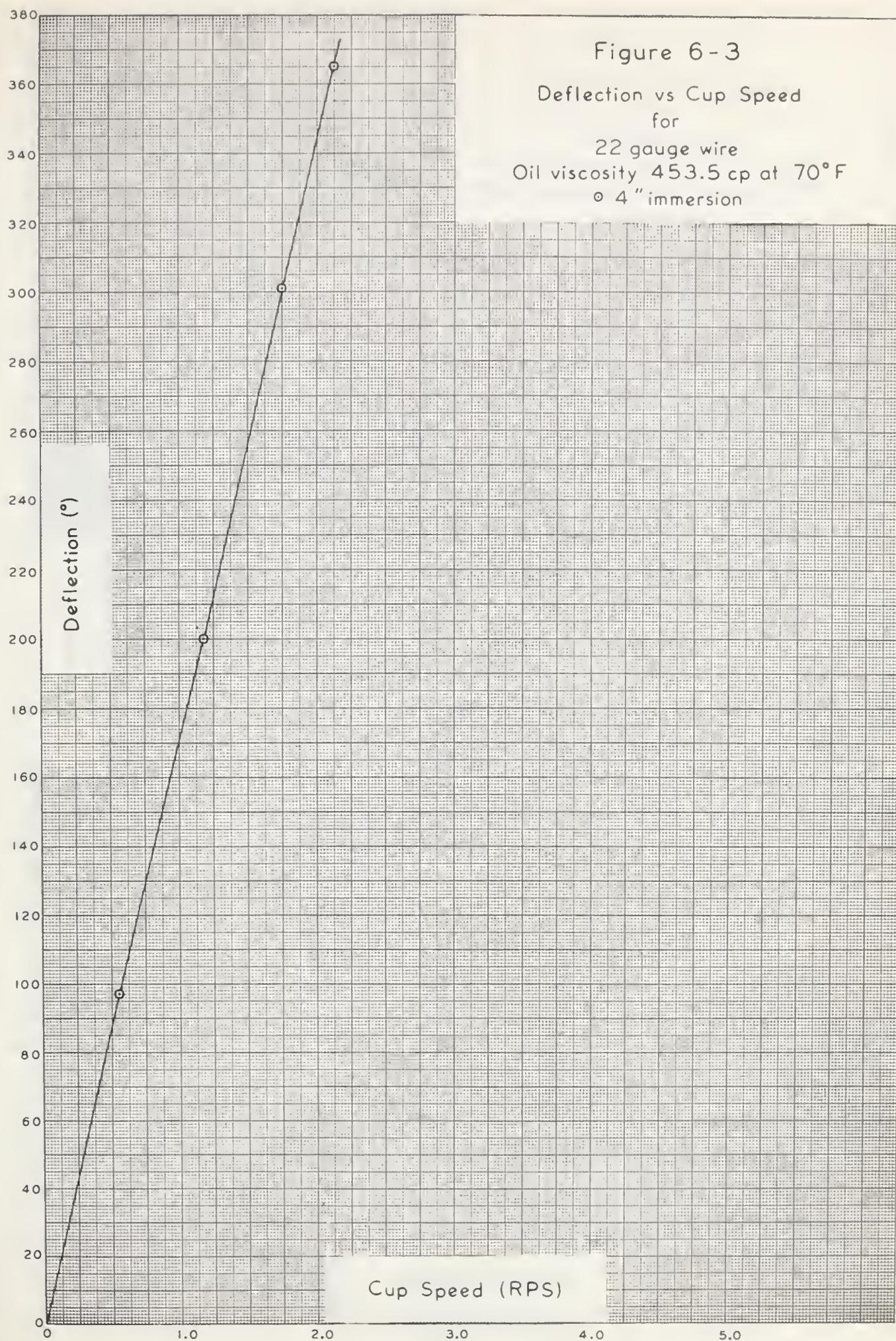




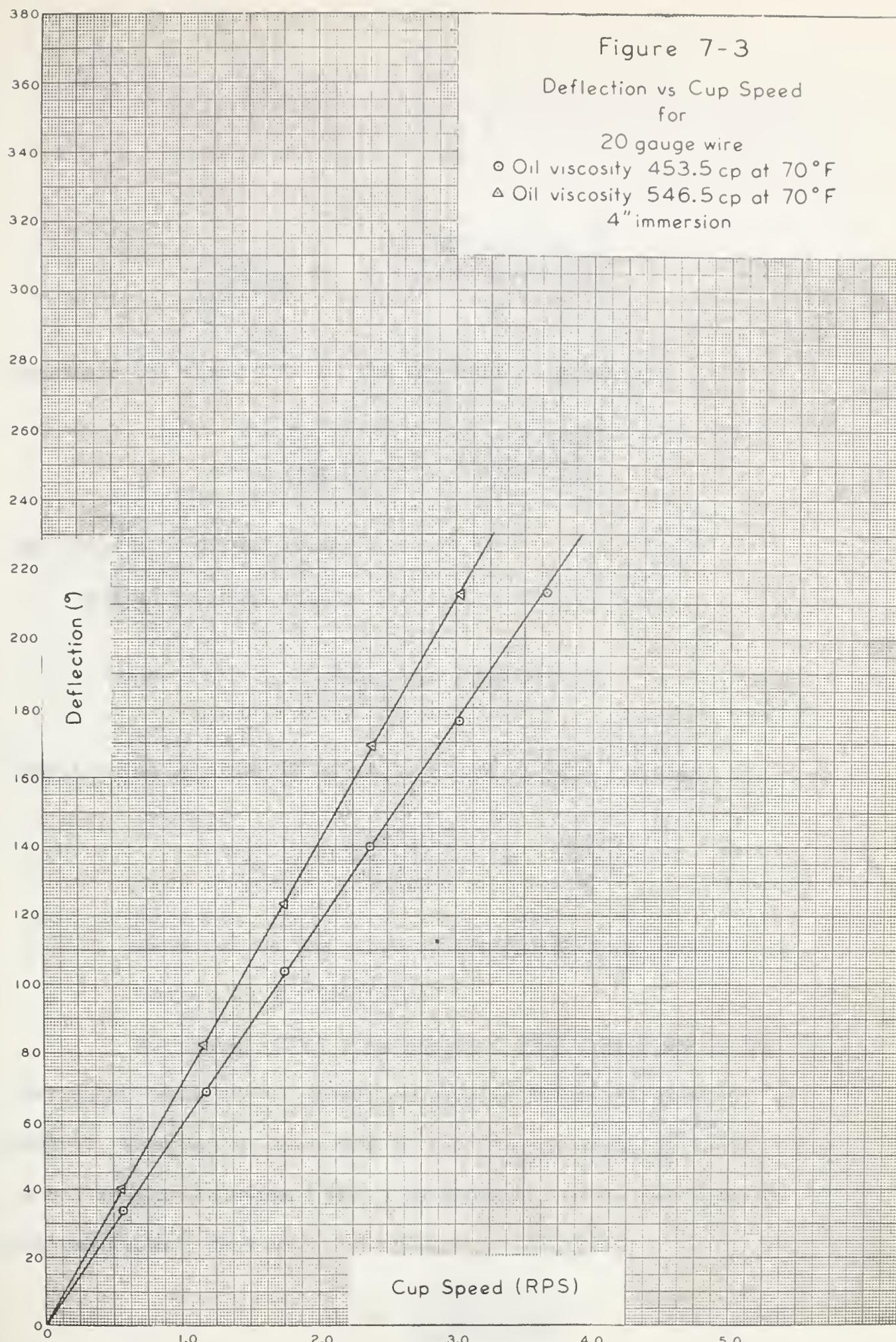














$$-\left(\frac{dv}{dR}\right)_R = \frac{4\pi S (R_1)^2 (R_2)^2}{(R)^2 (R_2^2 - R_1^2)} \quad (76)$$

Therefore the shear rate at the bob wall is given by

$$-\left(\frac{dv}{dR}\right)_W = \frac{4\pi S (R_2)^2}{(R_2^2 - R_1^2)} \quad (33-3)$$

and since  $R_1 = 0.7910$  inches

and  $R_2 = 0.8805$  inches

$$-\left(\frac{dv}{dR}\right)_W = (65.11) S \quad (34-3)$$

Substituting equation (34-3) into equation (32-3) yields

$$a = \frac{\mu(65.11) S}{g_c D} = \frac{\mu(65.11)}{g_c q} \quad (35-3)$$

where "q" is the slope of the appropriate curve on  
Figures (1-3) to (7-3)

The value of "a" from equation (35-3) applies to the  
particular depth of bob immersion used in the measurement of "q".  
However, this may be corrected to the desired depth of 4.225 inches  
by multiplying equation (35-3) by the ratio of actual depth to  
desired depth. That is

$$a = \frac{\mu(65.11) d}{g_c q (4.225)} \quad (36-3)$$



where  $d$  is the depth of immersion used in the calibration.

Consider now the data obtained for the 30 gauge wire with a standard oil of  $11.31 \times 10^{-5}$   $\text{lb}_f \text{ sec}/\text{ft}^2$  viscosity and a depth of bob immersion of 4.225 inches. The slope of the deflection versus rotational speed curve was found to be 78.75 degrees per RPS. Thus from equation (36-3)

$$a = \frac{(11.31 \times 10^{-5})(65.11)(4.225)}{(78.8)(4.225)} = 9.36 \times 10^{-5}$$

All wires were calibrated with two oils of differing viscosity and in some instances various depths of immersion were employed. The values of the constant for each wire are tabulated in Table (2-3) and plotted as a function of wire diameter on Figure (8-3).

In general, satisfactory agreement was attained between the values of "a" arising from the two methods of calibration. The maximum deviation of any data point from the line on Figure (8-3) was approximately 4 percent (28 gauge wire) while the average deviation was 1.3 percent.



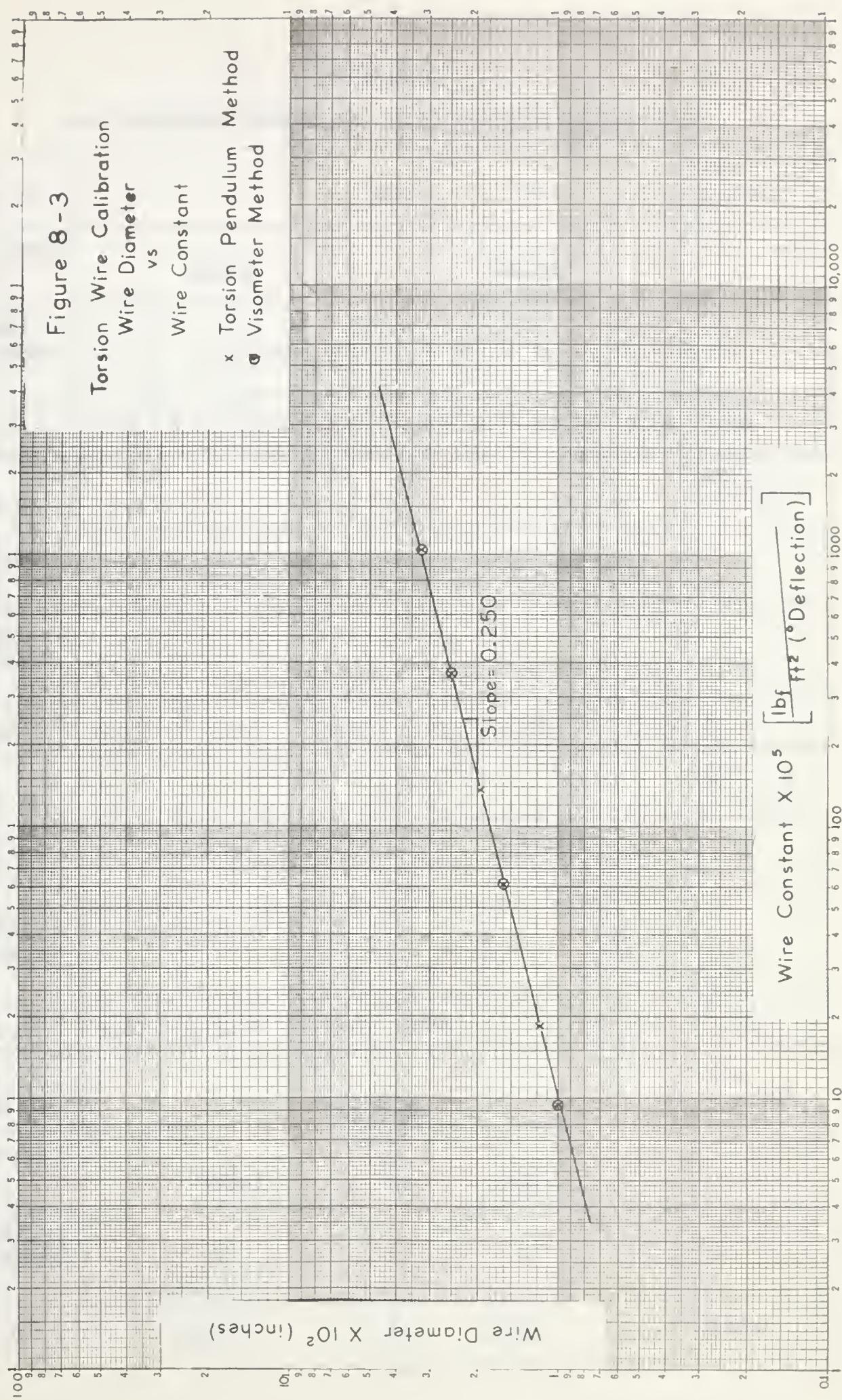




TABLE 2-3

## WIRE CONSTANT DETERMINED BY VISCOMETER CALIBRATION

WIRE GAUGE NO.	30								Ave $a \times 10^5$
OIL VISC (cps)	5.411				22.06				
NOMINAL BOB DEPTH (in)	4	3	2	1	4	3	2	1	
$a \times 10^5$	9.36	9.12	9.30	9.34	9.63	9.54	9.55	9.84	9.46
WIRE GAUGE NO.	26								Ave $a \times 10^4$
OIL VISC (CPS)	45.96				100.4				
NOMINAL BOB DEPTH (in)	4	3	2	4	3	2			
$a \times 10^4$	6.13	6.16	6.21	6.21	6.19	6.17	6.18		
WIRE GAUGE NO.	22								Ave $a \times 10^3$
OIL VISC (CPS)	290.8				453.5				
NOMINAL BOB DEPTH (in)	4	3	2	4	3	2			
$a \times 10^3$	3.67	3.72	3.61	3.60	-	-	3.65		
WIRE GAUGE NO.	20								Ave $a \times 10^3$
OIL VISC (CPS)	453.5				546.5				
NOMINAL BOB DEPTH (in)	4				4				
$a \times 10^3$	10.48				10.51				10.50



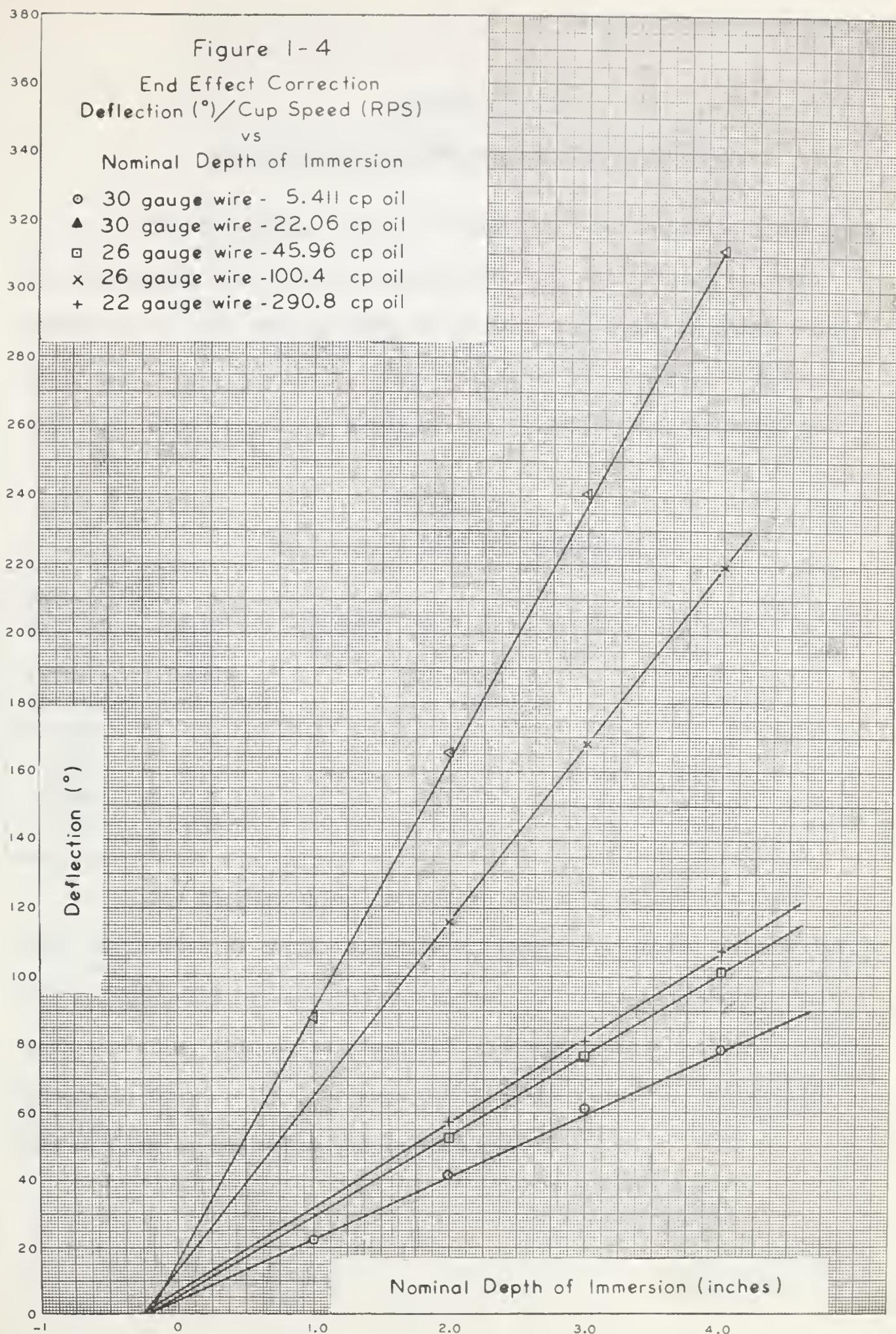
APPENDIX 4END EFFECT CORRECTION

The contribution of the conical bottom of the viscometer bob to the total shearing surface was determined experimentally and expressed in terms of an equivalent length of cylindrical bob. To accomplish this, the ratio of deflection to cup speed, obtained from Figures (1-3) to (5-3) in Appendix 3, was plotted as a function of depth of bob immersion (measured from the base of the cone) on arithmetic coordinates. The resulting linear curves, reproduced in Figures (1-4), were extrapolated toward the left and the negative intercept on the horizontal axis was interpreted as the effective length of the cone. The "nominal" depth of bob immersion was then adjusted to the "true depth" by adding this value to it.

Although the magnitude of the correction varied from 0.200 to 0.250 inches, due to inaccuracies of measurement and extrapolation, the error introduced by using an average value of 0.225 inches was considered to be insignificant at a depth of immersion of 4 inches.

All of the constants "a", tabulated in appendix 3 have been evaluated for a true depth of immersion of 4.225 inches.







APPENDIX 5CALIBRATION OF STOPWATCH AND THERMOCOUPLES

The stopwatch, used for determining the rotational speed of the viscometer cup, was calibrated at three temperatures and over intervals of time ranging from 60 secs. to 240 secs. by comparison with an accurate timepiece. The results of these measurements and the calculated percentage error of the stopwatch are tabulated below.

TABLE 1-5

## CALIBRATION DATA FOR STOPWATCH

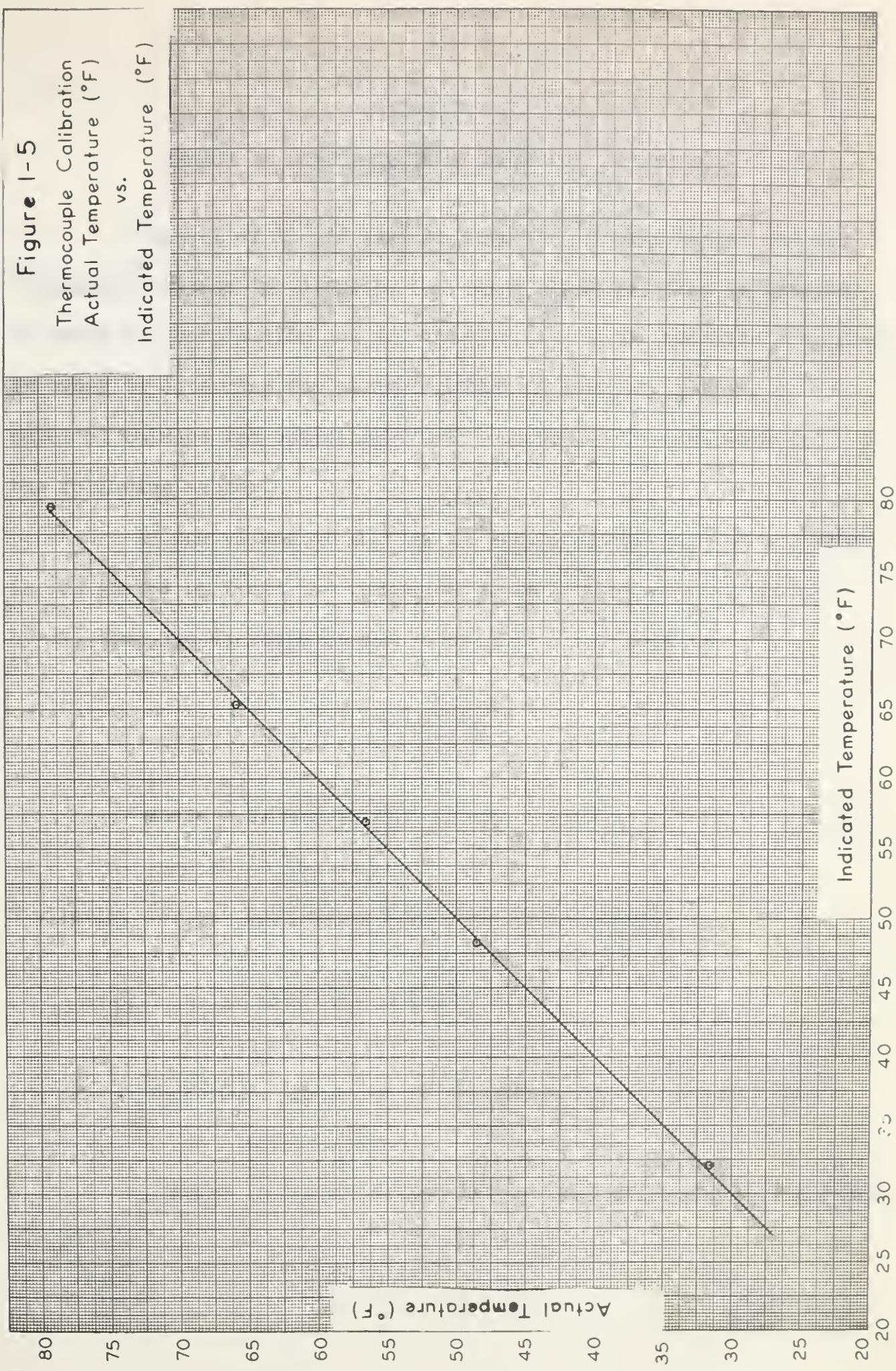
TEMP ( $^{\circ}$ F)	30		45		60	
	ACTUAL TIME INTERVAL (seconds)	INDICATED TIME INTERVAL (seconds)	PERCENT ERROR	INDICATED TIME INTERVAL (seconds)	PERCENT ERROR	INDICATED TIME INTERVAL (seconds)
60	59.5	0.83	59.5	0.83	59.6	0.67
120	119.0	0.83	119.4	0.50	119.4	0.50
180	179.1	0.50	179.3	0.39	179.3	0.39
240	238.9	0.46	238.9	0.46	239.0	0.42

The thermocouples located on the wall of the viscometer bob were calibrated by comparison with an accurate standard thermometer. The relationship between the actual and indicated temperature for each measuring element is presented on Figure (1-5) . The error was generally found to be less than  $0.2^{\circ}$ F, consequently no correction was applied to the thermocouple readings.



**Figure 1-5**

Thermocouple Calibration  
Actual Temperature ( $^{\circ}\text{F}$ )  
vs.  
Indicated Temperature ( $^{\circ}\text{F}$ )





APPENDIX 6CHANGE IN COMPOSITION OF CRUDE OIL IN STORAGE

Removal of liquid samples from the storage vessel and the attendant increase in volume of the vapor phase resulted in changes in crude oil composition due to vaporization of the volatile components. In order to determine the maximum extent of such variations, a material balance was established and reduced to a useful form in the following manner.

If the volume of  $Z$  moles of liquid in the drum at any time is designated by  $V$  and the change in volume due to sample removal by  $dV$ , then the decrease in the total number of moles is

$$dZ = -\frac{\rho dV}{MW} \quad (1-6)$$

where  $\rho$  is the density of the liquid  
and  $MW$  is the molecular weight.

Similarly, for any particular component in the liquid

$$dC = x \left( \frac{\rho}{MW} \right) dV \quad (2-6)$$

where  $C$  is the moles of the particular component under consideration

and  $x$  is the mole fraction of that component in the liquid.



In addition

$$\left( \frac{P}{RT} \right) dV \quad (3-6)$$

moles of liquid will evaporate to occupy the volume provided by removal of the liquid.

Again, the number of moles of the desired component present in the added vapor is

$$dC = y \left( \frac{P}{RT} \right) dV \quad (4-6)$$

where  $y$  is the mole fraction of the component in the vapor in equilibrium with the liquid.

The total change in the number of moles of liquid is then

$$dZ = \left( \frac{\rho}{MW} \right) dV + \left( \frac{P}{RT} \right) dV \quad (5-6)$$

and the total change in the number of moles of any component in the liquid is given by

$$dC = x \left( \frac{\rho}{MW} \right) dV + y \left( \frac{P}{RT} \right) dV \quad (6-6)$$

Now, since the relationship between  $x$  and  $y$  is suitably defined by

$$y = Kx \quad (7-6)$$

where  $K$  is the equilibrium constant, equation (6-6) may be written



$$dC = x \left( \frac{\rho}{MW} \right) dV + x \left( \frac{KP}{RT} \right) dV \quad (8-6)$$

By definition

$$x = \frac{C}{Z} \quad (9-6)$$

therefore

$$dx = \frac{Z dC - C dZ}{Z^2} \quad (10-6)$$

Furthermore

$$Z = \left( \frac{\rho}{MW} \right) V \quad (11-6)$$

and

$$C = x \left( \frac{\rho}{MW} \right) V \quad (12-6)$$

Then, by substituting equation (6-6), (8-6), (11-6) and (12-6) into equation (10-6) it may be shown that

$$\frac{dx}{x} = \left[ \frac{\left( \frac{KP}{RT} \right) - \left( \frac{P}{RT} \right)}{\left( \frac{\rho}{MW} \right)} \right] \frac{dV}{V} \quad (13-6)$$

If now, as a satisfactory approximation for the present purpose, the equilibrium constant is considered to vary inversely with pressure, then only the second term in the numerator of equation (13-6) will be dependent on pressure. Assuming that an arithmetic average pressure is appropriate, equation (13-6) may be integrated to give



$$\log \frac{x_0}{x} = \left[ \frac{\left( \frac{K P}{R T} \right) - \left( \frac{P_{ave}}{R T} \right)}{\left( \frac{\rho}{M W} \right)} \right] \log \frac{V_0}{V} \quad (14-6)$$

Each of the terms appearing in equation (14-6) were evaluated as follows.

### 1) Evaluation of K

Since the initial composition of both the gas and liquid phases was known (Appendix 2), the value of K for each component was readily determined from the relationship

$$y_i = K x_i \quad (7-6)$$

The resulting values of this constant are presented in Table (1-6)

TABLE 1-6

COMPUTED VALUES OF K AND KP FOR EACH VOLATILE COMPONENT

COMPONENT	N <sub>2</sub> *	C <sub>1</sub> *	C <sub>2</sub>	C <sub>3</sub>
K	650	180	21	5.4
KP (psf)	1.46 x 10 <sup>6</sup>	4.05 x 10 <sup>5</sup>	4.74 x 10 <sup>4</sup>	1.22 x 10 <sup>4</sup>
COMPONENT	iC <sub>4</sub>	nC <sub>4</sub>	iC <sub>5</sub>	nC <sub>5</sub>
K	2.6	2.0	0.69	0.52
KP (psf)	5.85 x 10 <sup>3</sup>	4.50 x 10 <sup>3</sup>	1.55 x 10 <sup>3</sup>	1.17 x 10 <sup>3</sup>

\* The small quantities of N<sub>2</sub> and Methane in the liquid phase could not be detected analytically, consequently the K values for these components were taken from the literature (35)(37). The mole fractions of each of these components in the liquid was then computed on the basis of the assumed constants.



Although the K values tabulated above are applicable only at the original pressure conditions (15.6 psia), K is inversely proportional to pressure and the product, KP, in equation (14-6) is approximately constant.

## 2) Evaluation of $V_0$ and V

For purposes of calculation, the volume of oil in the storage vessel was assumed to change from 6.4 cubic feet (42 gals.) to 1.6 cubic feet (10 gals.). However, in reality, the quantity of oil removed during the investigation was considerably less than indicated by these figures.

## 3 Evaluation of Temperature, Density and Molecular Weight

The average temperature of the storage vessel was assumed to be 75°F. Based on the data in Appendix 2, the density under these conditions was 0.835 gm/cc. An approximate molecular weight of 278 was obtained with the aid of a chart in Nelson which relates molecular weight to the density and average boiling point of the crude oil.

Mathematical manipulation of equation (14-6) in terms of the above values resulted in a simplified expression of the form

$$\log x_f = \log x_0 - 3.88 \times 10^{-6} (KP - P_{ave}) \quad (14-6)$$

Then assuming a terminal pressure and thus an average pressure in the storage vessel, the final mole fraction,  $x_f$ , of each component was calculated. In order to test the assumption, the final



$K$  values and subsequently  $x_f$ , the mole fraction of each component in the final gas phase, were determined. The correct terminal pressure (9.5 psia) was considered to be the one at which

$$\sum y_f = 1 \quad (15-6)$$

The results of these calculations and the percent change in concentration of each of the volatile crude oil components are presented in Table (2-6)

TABLE 2-6  
CHANGES IN COMPOSITION OF CRUDE OIL IN STORAGE

COMPONENT	$x_o$	$x_f$	$K_f$	$y_f$	$\Delta x$	PERCENT CHANGE
C <sub>1</sub>	$1.4 \times 10^{-3}$	$3.83 \times 10^{-5}$	296	$0.113 \times 10^{-3}$	$1.4 \times 10^{-3}$	-100
C <sub>2</sub>	$7.75 \times 10^{-3}$	$5.16 \times 10^{-3}$	34.5	0.1780	$2.59 \times 10^{-3}$	33.4
C <sub>3</sub>	$5.36 \times 10^{-2}$	$4.90 \times 10^{-2}$	8.9	0.4350	$4.6 \times 10^{-3}$	8.57
iC <sub>4</sub>	$1.98 \times 10^{-2}$	$1.91 \times 10^{-2}$	4.3	0.0820	$7.0 \times 10^{-4}$	3.54
nC <sub>4</sub>	$7.02 \times 10^{-2}$	$6.87 \times 10^{-2}$	3.3	0.2260	$1.5 \times 10^{-3}$	2.14
iC <sub>5</sub>	$3.09 \times 10^{-2}$	$3.10 \times 10^{-2}$	1.1	0.0341	0	0
nC <sub>5</sub>	$3.60 \times 10^{-2}$	$3.62 \times 10^{-2}$	0.86	<u>0.0311</u>	0	0
$\sum y_f$				0.9975		



APPENDIX 7RHEOLOGICAL DATA

The three sets of tables included in this section contain the measured shear stress decay data (Table (1-7)), the measured shear stress growth data (Table (2-7)) and the measured and computed values of shear stress which are required for correlation of the data in terms of equation (70) (Table (3-7)).

in Table (1-7) the bob deflection, in degrees, and the shear stress (product of bob deflection and the appropriate torsion wire constant), in  $\text{lb}_f/\text{ft}^2$  are presented in terms of time of measurement, in minutes, at each curing temperature,  $T_H$ , testing temperature,  $T_T$ , and cup speed,  $S_H$ . The data on this table are represented graphically on Figures (11) to (25) and Figures (50) to (52). Table (2-7) is constructed in a manner similar to Table (1-7) except that both the cup speed prior to testing,  $S_H$ , as well as the cup speed during the test,  $S_T$ , are included in each case. Graphical representation of these data is provided on Figures (26) to (31). The cup speeds presented in these tables are the average of four or five independent measurements obtained during the course of each test. Table (3-7) contains the pertinent total stresses, the Newtonian stress component and the structural stress components at each curing temperature, testing temperature and shear rate as well as the values of the dimensionless parameter.



$$\frac{T_s - T_{s\infty}}{\frac{T_{s0}^2}{T_{s\infty}} - T_s}$$

defined by equation (70). Figure(45) , which is a logarithmic plot of this parameter as a function of time of shearing, represents the final correlation of the data and a test of the theory.



TABLE 1-7  
SHEAR STRESS DECAY DATA

$T_H$ $75^{\circ}\text{F}$		$T_T$ $90^{\circ}\text{F}$		$S_H$ 0.522 RPS		WIRE GAUGE NO. 30		REF. FIG.
TIME OF TEST (min.)	BOB DEFL. (°)	$\tau \times 10^4$ $\text{lb}_f/\text{ft}^2$	TIME OF TEST (min.)	BOB DEFL. (°)	$\tau \times 10^4$ $\text{lb}_f/\text{ft}^2$	TIME OF TEST (min.)	BOB DEFL. (°)	$\tau \times 10^4$ $\text{lb}_f/\text{ft}^2$
0.25			18	39.5	37.4	37		
0.5	39.7	37.5	19	39.5	37.4	38		
1	39.7	37.5	20	39.5	37.4	39		
2	39.5	37.4	21	39.5	37.4	40		
3	39.5	37.4	22	39.5	37.4	41		
4	39.5	37.4	23	39.5	37.4	42		
5	39.5	37.4	24	39.5	37.4	43		
6	39.5	37.4	25	39.5	37.4	44		
7	39.5	37.4	26	39.5	37.4	45		
8	39.5	37.4	27	39.5	37.4	46		
9	39.5	37.4	28	39.5	37.4	47		
10	39.5	37.4	29	39.5	37.4	48		
11	39.5	37.4	30	39.5	37.4	49		
12	39.5	37.4	31			50		
13	39.5	37.4	32			51		
14	39.5	37.4	33			52		
15	39.5	37.4	34			53		
16	39.5	37.4	35			54		
17	39.5	37.4	36			55		
$T_H$ $75^{\circ}\text{F}$		$T_T$ $90^{\circ}\text{F}$		$S_H$ 0.522 RPS		WIRE GAUGE NO. 30		REF. FIG.
0.25		18	39.7	37.5		37		
0.5	39.7	37.5	19	39.7	37.5	38		
1	39.7	37.5	20	39.7	37.5	39		
2	39.7	37.5	21			40		
3	39.7	37.5	22			41		
4	39.7	37.5	23			42		
5	39.7	37.5	24			43		
6	39.7	37.5	25			44		
7	39.7	37.5	26			45		
8	39.7	37.5	27			46		
9	39.7	37.5	28			47		
10	39.7	37.5	29			48		
11	39.7	37.5	30			49		
12	39.7	37.5	31			50		
13	39.7	37.5	32			51		
14	39.7	37.5	33			52		
15	39.7	37.5	34			53		
16	39.7	37.5	35			54		
17	39.7	37.5	36			55		



TABLE 1-7 (Continued)  
SHEAR STRESS DECAY DATA

$T_H$ 75 F		$T_T$ 90 F		$S_H$ 0.522 RPS		WIRE GAUGE NO. 30		REF. FIG. NO. 11	
TIME OF TEST (min.)	BOB DEFL. (°)	$\tau \times 10^4$ $lb_f/ft^2$	TIME OF TEST (min.)	BOB DEFL. (°)	$\tau \times 10^4$ $lb_f/ft^2$	TIME OF TEST (min.)	BOB DEFL. (°)	$\tau \times 10^4$ $lb_f/ft^2$	
0.25			18	39.0	36.9	37			
0.5	39.0	36.9	19	39.0	36.9	38			
1	39.0	36.9	20	39.0	36.9	39			
2	39.0	36.9	21	39.1	37.0	40			
3	39.0	36.9	22	39.1	37.0	41			
4	39.0	36.9	23	39.1	37.0	42			
5	39.0	36.9	24	39.1	37.0	43			
6	39.0	36.9	25	39.1	37.0	44			
7	39.0	36.9	26			45			
8	39.0	36.9	27			46			
9	39.0	36.9	28			47			
10	39.0	36.9	29			48			
11	39.0	36.9	30			49			
12	39.0	36.9	31			50			
13	39.0	36.9	32			51			
14	39.0	36.9	33			52			
15	39.0	36.9	34			53			
16	39.0	36.9	35			54			
17	39.0	36.9	36			55			
$T_H$ 75° F		$T_T$ 90°F		$S_H$ 0.523 RPS		WIRE GAUGE NO. 30		REF. FIG. NO. 11	
0.25			18	39.8	37.6	37			
0.5	40.3	38.1	19	39.8	37.6	38			
1	40.3	38.1	20	39.8	37.6	39			
2	40.1	37.9	21	39.8	37.6	40			
3	40.1	37.9	22	39.8	37.6	41			
4	40.1	37.9	23	39.8	37.6	42			
5	40.1	37.9	24	39.8	37.6	43			
6	40.0	37.8	25	39.8	37.6	44			
7	40.0	37.8	26	39.8	37.6	45			
8	40.0	37.8	27	39.8	37.6	46			
9	40.0	37.8	28	39.8	37.6	47			
10	39.9	37.7	29	39.8	37.6	48			
11	39.9	37.7	30	39.8	37.6	49			
12	39.9	37.7	31			50			
13	39.9	37.7	32			51			
14	39.9	37.7	33			52			
15	39.9	37.7	34			53			
16	39.8	37.6	35			54			
17	39.8	37.6	36			55			



TABLE 1-7 (Continued)  
SHEAR STRESS DECAY DATA

$T_H$ $75^{\circ}\text{F}$		$T_T$ $90^{\circ}\text{F}$		$S_H$ 0.521 RPS		WIRE GAUGE NO. 28		REF. FIG.	
TIME OF TEST (min.)	BOB DEFL. (°)	$\tau \times 10^4$ $\text{lb}_f/\text{ft}^2$	TIME OF TEST (min.)	BOB DEFL. (°)	$\tau \times 10^4$ $\text{lb}_f/\text{ft}^2$	TIME OF TEST (min.)	BOB DEFL. (°)	$\tau \times 10^4$ $\text{lb}_f/\text{ft}^2$	NO.
0.25			18	19.3	34.4	37			
0.5	19.6	35.0	19	19.3	34.4	38			
1	19.6	35.0	20	19.3	34.4	39			
2	19.5	35.0	21	19.3	34.4	40			
3	19.5	34.8	22	19.3	34.4	41			
4	19.5	34.8	23	19.3	34.4	42			
5	19.4	34.6	24	19.3	34.4	43			
6	19.4	34.6	25	19.3	34.4	44			
7	19.4	34.6	26			45			
8	19.4	34.6	27			46			
9	19.3	34.4	28			47			
10	19.3	34.4	29			48			
11	19.3	34.4	30			49			
12	19.3	34.4	31			50			
13	19.3	34.4	32			51			
14	19.3	34.4	33			52			
15	19.3	34.4	34			53			
16	19.3	34.4	35			54			
17	19.3	34.4	36			55			
$T_H$ $75^{\circ}\text{F}$		$T_T$ $90^{\circ}\text{F}$		$S_H$ 2.473 RPS		WIRE GAUGE NO. 30		REF. FIG.	
0.25		18	191.0	180.6	37				
0.5		19	191.0	180.6	38				
1	191.5	181.1	20	191.0	180.6	39			
2	191.5	181.1	21	191.0	180.6	40			
3	191.5	181.1	22			41			
4	191.3	180.9	23			42			
5	191.2	180.8	24			43			
6	191.1	180.7	25			44			
7	191.1	180.7	26			45			
8	191.1	180.7	27			46			
9	191.0	180.6	28			47			
10	191.0	180.6	29			48			
11	191.0	180.6	30			49			
12	191.0	180.6	31			50			
13	191.0	180.6	32			51			
14	191.0	180.6	33			52			
15	191.0	180.6	34			53			
16	191.0	180.6	35			54			
17	191.0	180.6	36			55			



## SHEAR STRESS DECAY DATA

$T_H$ 75°F		$T_T$ 90°F		$S_H$ 2.469 RPS		WIRE GAUGE NO. 30		REF. FIG. NO. 12	
TIME OF TEST (min.)	BOB DEFL. (°)	$\tau \times 10^4$ $lb_f/ft^2$	TIME OF TEST (min.)	BOB DEFL. (°)	$\tau \times 10^4$ $lb_f/ft^2$	TIME OF TEST (min.)	BOB DEFL. (°)	$\tau \times 10^4$ $lb_f/ft^2$	
0.25			18	191.4	181.0	37	190.9	180.5	
0.5			19	191.4	181.0	38	191.4	181.0	
1	191.7	181.3	20	191.4	181.0	39	191.4	181.0	
2	191.7	181.3	21	191.1	180.7	40	190.9	180.5	
3	191.9	181.5	22	191.1	180.7	41	190.9	180.5	
4	191.7	181.3	23	191.1	180.7	42	189.9	179.6	
5	191.2	180.8	24	191.1	180.7	43	189.9	179.6	
6	190.7	180.3	25	191.1	180.7	44	189.9	179.6	
7	190.4	180.0	26	191.1	180.7	45	189.9	179.6	
8	191.9	181.5	27	191.1	180.7	46	189.9	179.6	
9	191.4	181.0	28			47	189.9	179.6	
10	191.5	181.1	29	190.0	180.5	48	189.2	178.9	
11	192.0	181.6	30	191.1	180.7	49	189.4	179.1	
12	189.6	179.3	31	190.6	180.2	50			
13	191.9	181.5	32	190.6	180.2	51	189.4	179.1	
14	191.5	181.1	33	190.4	180.0	52	189.4	179.1	
15	191.4	181.0	34	190.6	180.2	53	189.4	179.1	
16	191.1	180.7	35	190.8	180.4	54	189.4	179.1	
17	188.9	178.6	36	190.0	180.5	55	190.3	179.9	
$T_H$ 75°F	$T_T$ 90°F			$S_H$ 2.468 RPS		WIRE GAUGE NO. 30		REF. FIG. NO. 12	
0.25				18	194.9	184.3	37		
0.5	193.2	182.7		19	194.9	184.3	38		
1	193.2	182.7		20	194.9	184.3	39		
2	193.2	182.7		21	194.9	184.3	40		
3	193.2	182.7		22	194.9	184.3	41		
4	193.2	182.7		23	195.2	184.6	42		
5	194.2	183.6		24	195.2	184.6	43		
6	194.2	183.6		25			44		
7	194.2	183.6		26			45		
8	194.7	184.1		27			46		
9	194.7	184.1		28			47		
10	194.2	183.6		29			48		
11	194.2	183.6		30			49		
12	194.7	184.1		31			50		
13	194.7	184.1		32			51		
14	194.7	184.1		33			52		
15	194.7	184.1		34			53		
16	194.9	184.3		35			54		
17	194.9	184.3		36			55		



## SHEAR STRESS DECAY DATA

$T_H$ 75°F		$T_T$ 90°F		$S_H$ 2.473 RPS		WIRE GAUGE NO. 30		REF. FIG. NO. 12	
TIME OF TEST (min.)	BOB DEFL. (°)	$\tau \times 10^4$ $lb_f/ft^2$	TIME OF TEST (min.)	BOB DEFL. (°)	$\tau \times 10^4$ $lb_f/ft^2$	TIME OF TEST (min.)	BOB DEFL. (°)	$\tau \times 10^4$ $lb_f/ft^2$	
0.25			18	191.7	181.3	37			
0.5	191.0	180.6	19	191.7	181.3	38			
1	191.0	180.6	20	191.7	181.3	39			
2	191.0	180.6	21	191.7	181.3	40			
3	191.1	180.7	22			41			
4	191.1	180.7	23			42			
5	191.1	180.7	24			43			
6	191.2	180.8	25			44			
7	191.2	180.8	26			45			
8	191.3	180.9	27			46			
9	191.5	181.1	28			47			
10	191.5	181.1	29			48			
11	191.7	181.3	30			49			
12	191.7	181.3	31			50			
13	191.7	181.3	32			51			
14	191.7	181.3	33			52			
15	191.7	181.3	34			53			
16	191.7	181.3	35			54			
17	191.7	181.3	36			55			
$T_H$ 75°F		$T_T$ 90°F		$S_H$ 2.477 RPS		WIRE GAUGE NO. 28		REF. FIG. NO. 12	
0.25		18	97.8	174.5	37				
0.5		19	98.2	175.2	38				
1	97.0	173.0	20	98.0	174.8	39			
2	97.2	173.4	21	98.2	175.2	40			
3	97.8	174.5	22	98.2	175.2	41			
4	97.8	174.5	23	98.2	175.2	42			
5	97.9	174.7	24	98.2	175.2	43			
6	98.0	174.8	25	97.8	174.5	44			
7	98.0	174.8	26	98.0	174.8	45			
8	98.1	175.0	27	98.2	175.2	46			
9	98.0	174.8	28	97.8	174.5	47			
10	98.0	174.8	29	97.8	174.5	48			
11	97.9	174.7	30	98.0	174.8	49			
12	97.8	174.5	31			50			
13	97.8	174.5	32			51			
14	97.8	174.5	33			52			
15	97.8	174.5	34			53			
16	97.8	174.5	35			54			
17	97.8	174.5	36			55			



## SHEAR STRESS DECAY DATA

$T_H$ $75^{\circ}\text{F}$		$T_T$ $90^{\circ}\text{F}$		$S_H$ 4.469 RPS		WIRE GAUGE NO. 28		REF. FIG. NO. 13	
TIME OF TEST (min.)	BOB DEFL. (°)	$\tau \times 10^4$ $\text{lb}_f/\text{ft}^2$	TIME OF TEST (min.)	BOB DEFL. (°)	$\tau \times 10^4$ $\text{lb}_f/\text{ft}^2$	TIME OF TEST (min.)	BOB DEFL. (°)	$\tau \times 10^4$ $\text{lb}_f/\text{ft}^2$	
0.25			18	179.5	320	37			
0.5	179.5	320	19	179.4	320	38			
1	180.0	321	20	179.3	320	39			
2	183.5	327	21	179.3	320	40			
3	184.5	329	22	179.2	320	41			
4	184.2	329	23	179.2	320	42			
5	183.5	327	24	179.2	320	43			
6	183.0	326	25	179.2	320	44			
7	182.7	326	26	179.1	320	45			
8	181.7	324	27	179.1	320	46			
9	181.7	324	28	179.0	319	47			
10	181.5	324	29	179.0	319	48			
11	181.5	324	30	179.0	319	49			
12	181.3	323	31	179.0	319	50			
13	180.8	323	32	179.0	319	51			
14	180.3	322	33	179.0	319	52			
15	180.3	322	34	179.0	319	53			
16	180.2	321	35	180.2	321	54			
17	179.7	321	36			55			
$T_H$ $75^{\circ}\text{F}$		$T_T$ $90^{\circ}\text{F}$		$S_H$ 4.430 RPS		WIRE GAUGE NO. 28		REF. FIG. NO. 13	
0.25			18	181.4	324	37			
0.5			19	181.7	324	38			
1	182.4	325	20	185.4	331	39			
2	181.7	324	21	187.4	334	40			
3	180.2	321	22	188.1	336	41			
4	180.0	321	23	187.2	334	42			
5	180.0	321	24	187.2	334	43			
6	183.0	321	25	187.2	334	44			
7	179.9	321	26	186.8	333	45			
8	179.2	320	27	186.7	333	46			
9	179.2	320	28	175.0	312	47			
10	179.2	320	29	175.2	313	48			
11	179.2	320	30	175.2	313	49			
12	179.4	320	31	175.2	313	50			
13	180.2	321	32	175.2	313	51			
14	180.7	322	33			52			
15	180.7	322	34			53			
16	180.7	322	35			54			
17	181.4	324	36			55			



## SHEAR STRESS DECAY DATA

$T_H$ $75^{\circ}\text{F}$		$T_T$ $90^{\circ}\text{F}$		$S_H$ 4.456 RPS		WIRE GAUGE NO. 28		REF. FIG.
TIME OF TEST (min.)	BOB DEFL. ( )	$\tau \times 10^4$ $\text{lb}_f/\text{ft}^2$	TIME OF TEST (min.)	BOB DEFL. ( )	$\tau \times 10^4$ $\text{lb}_f/\text{ft}^2$	TIME OF TEST (min.)	BOB DEFL. ( )	REF. FIG.
								NO. 13
0.25			18	183.6	328	37		
0.5	179.2	320	19	183.6	328	38		
1	179.2	320	20	183.6	328	39		
2	179.4	320	21	183.6	328	40		
3	180.1	321	22	182.7	326	41		
4	181.4	324	23	182.7	326	42		
5	183.6	328	24	182.9	326	43		
6	184.5	329	25	182.9	326	44		
7	184.2	329	26	182.9	326	45		
8	183.9	328	27	182.9	326	46		
9	183.9	328	28	182.9	326	47		
10	183.9	328	29	183.4	327	48		
11	183.9	328	30	183.4	327	49		
12	183.9	328	31	183.4	327	50		
13	183.9	328	32	183.6	328	51		
14	182.9	326	33	183.6	328	52		
15	183.2	327	34	183.6	328	53		
16	183.4	327	35	183.6	328	54		
17	183.6	328	36	183.6	328	55		
$T_H$ $75^{\circ}\text{F}$		$T_T$ $90^{\circ}\text{F}$		$S_H$ 4.457 RPS		WIRE GAUGE NO. 28		REF. FIG.
								NO. 13
0.25			18	181.7	324	37	182.5	326
0.5	180.7	322	19	182.2	325	38	182.7	326
1	180.7	322	20	182.7	326	39	182.7	326
2	180.2	321	21	181.9	325	40	183.2	327
3	180.2	321	22	181.9	325	41	182.2	325
4	180.2	321	23	182.7	326	42	182.4	325
5	180.2	321	24	183.2	327	43	182.7	326
6	180.2	321	25	182.2	325	44	182.7	326
7	180.5	322	26	182.2	325	45	183.0	326
8	180.6	322	27	182.2	325	46	183.2	327
9	181.2	323	28	182.2	325	47	183.6	328
10	180.6	322	29	182.7	326	48	182.7	326
11	181.0	323	30	182.7	326	49	182.7	326
12	182.2	325	31	183.2	327	50	182.7	326
13	180.7	322	32	182.2	325	51	182.7	326
14	181.2	323	33	181.9	325	52	182.7	326
15	182.2	325	34	182.2	325	53	182.7	326
16			35	182.2	325	54	182.7	326
17	181.7	324	36	182.5	326	55		



## SHEAR STRESS DECAY DATA

$T_H$ $75^{\circ}\text{F}$		$T_T$ $90^{\circ}\text{F}$		$S_H$ 4.468 RPS		WIRE GAUGE NO. 28		REF. FIG.	
TIME OF TEST (min.)	BOB DEFL. ( $^{\circ}$ )	$\tau \times 10^4$ $\text{lb}_f/\text{ft}^2$	TIME OF TEST (min.)	BOB DEFL. ( $^{\circ}$ )	$\tau \times 10^4$ $\text{lb}_f/\text{ft}^2$	TIME OF TEST (min.)	BOB DEFL. ( $^{\circ}$ )	$\tau \times 10^4$ $\text{lb}_f/\text{ft}^2$	
0.25			18	181.5	324	37			
0.5	180.5	322	19	180.5	322	38			
1	179.7	321	20	180.5	322	39			
2	179.2	320	21	180.7	322	40			
3	179.0	319	22	180.7	322	41			
4	179.3	320	23	180.7	322	42			
5	182.0	325	24	180.7	322	43			
6	180.0	321	25	180.7	322	44			
7	180.5	322	26			45			
8	180.2	321	27			46			
9	181.0	323	28			47			
10	180.2	321	29			48			
11	180.2	321	30			49			
12	180.2	321	31			50			
13	180.2	321	32			51			
14	180.5	322	33			52			
15	180.5	322	34			53			
16	180.7	322	35			54			
17	181.0	323	36			55			
$T_H$ $75^{\circ}\text{F}$		$T_T$ $90^{\circ}\text{F}$		$S_H$ 0.506 RPS		WIRE GAUGE NO. 28		REF. FIG.	
0.25		18	36.4	65.0	37				
0.5	37.1	66.2	19	36.4	65.0	38			
1	37.2	66.4	20	36.4	65.0	39			
2	37.0	66.1	21	36.4	65.0	40			
3	36.9	65.8	22	36.4	65.0	41			
4	36.7	65.6	23	36.4	65.0	42			
5	36.8	65.7	24	36.4	65.0	43			
6	36.8	65.7	25	36.4	65.0	44			
7	36.8	65.7	26	36.4	65.0	45			
8	36.8	65.7	27	36.4	65.0	46			
9	36.8	65.7	28	36.4	65.0	47			
10	36.8	65.7	29	36.4	65.0	48			
11	36.8	65.7	30	36.3	64.7	49			
12	36.6	65.3	31			50			
13	36.6	65.3	32			51			
14	36.6	65.3	33			52			
15	36.5	65.2	34			53			
16	36.5	65.2	35			54			
17	36.4	65.0	36			55			



## SHEAR STRESS DECAY DATA

$T_H$ 75 F		$T_T$ 75 F		$S_H$ 0.503 RPS		WIRE GAUGE NO. 18		REF. FIG. NO. 14	
TIME OF TEST (min.)	BOB DEFL. (°)	$\tau \times 10^4$ $lb_f/ft^2$	TIME OF TEST (min.)	BOB DEFL. (°)	$\tau \times 10^4$ $lb_f/ft^2$	TIME OF TEST (min.)	BOB DEFL. (°)	$\tau \times 10^4$ $lb_f/ft^2$	
0.25			18	40.0	71.3	37			
0.5	42.0	75.0	19	40.0	71.3	38			
1	42.0	75.0	20	39.9	71.2	39			
2	41.7	74.4	21	39.9	71.2	40			
3	41.3	73.7	22	39.7	70.9	41			
4	41.2	73.5	23	39.7	70.9	42			
5	40.8	72.8	24	39.6	70.7	43			
6	40.9	73.0	25	39.6	70.7	44			
7	40.8	72.8	26	39.5	70.5	45			
8	40.7	72.7	27	39.5	70.5	46			
9	40.5	72.3	28	39.4	70.4	47			
10	40.5	72.3	29	39.3	70.1	48			
11	40.4	72.1	30	39.3	70.1	49			
12	40.3	71.9	31			50			
13	40.2	71.8	32			51			
14	40.1	71.6	33			52			
15	40.1	71.6	34			53			
16	40.1	71.6	35			54			
17	40.1	71.6	36			55			
$T_H$ 75°F		$T_T$ 75°F		$S_H$ 0.515 RPS		WIRE GAUGE NO. 28		REF. FIG. NO. 14	
0.25				18	41.1	73.3	37	40.7	72.6
0.5	44.4	79.2		19	41.1	73.3	38	40.7	72.6
1	44.1	78.7		20	41.1	73.3	39	40.6	72.4
2	43.7	78.0		21	41.1	73.3	40	40.6	72.4
3	43.2	77.1		22	41.0	73.1	41	40.6	72.4
4	42.9	76.5		23	41.0	73.1	42		
5	42.6	76.0		24	41.0	73.1	43		
6	42.5	75.8		25	41.0	73.1	44		
7	42.3	75.5		26	41.0	73.1	45		
8	42.2	75.3		27	41.0	73.1	46		
9	42.1	75.1		28	41.0	73.1	47		
10	41.9	74.7		29	41.0	73.1	48		
11	41.8	74.6		30	40.9	73.0	49		
12	41.7	74.4		31	40.9	73.0	50		
13	41.7	74.4		32	40.8	72.8	51		
14	41.6	74.2		33	40.8	72.8	52		
15	41.5	74.0		34	40.7	72.6	53		
16	41.4	73.9		35	40.8	72.8	54		
17	41.2	73.5		36	40.7	72.6	55		



## SHEAR STRESS DECAY DATA

$T_H$ 75°F		$T_T$ 75°F		$S_H$ 0.515 RPS		WIRE GAUGE NO. 28		REF. FIG. NO. 14	
TIME OF TEST (min.)	BOB DEFL. (°)	$T \times 10^4$ $\text{lb}_f/\text{ft}^2$	TIME OF TEST (min.)	BOB DEFL. (°)	$T \times 10^4$ $\text{lb}_f/\text{ft}^2$	TIME OF TEST (min.)	BOB DEFL. (°)	$T \times 10^4$ $\text{lb}_f/\text{ft}^2$	
0.25			18	39.7	70.8	37			
0.5	41.7	74.4	19	39.6	70.6	38			
1	41.5	74.0	20	39.5	70.5	39			
2	41.2	73.5	21	39.6	70.6	40			
3	41.0	73.1	22	39.5	70.5	41			
4	40.8	72.8	23	39.5	70.5	42			
5	40.8	72.8	24	39.5	70.5	43			
6	40.5	72.3	25	39.5	70.5	44			
7	40.2	71.7	26	39.3	70.1	45			
8	40.2	71.7	27	39.3	70.1	46			
9	40.1	71.5	28	39.4	70.3	47			
10	40.2	71.7	29	39.2	69.9	48			
11	40.2	71.7	30	39.3	70.1	49			
12	40.2	71.7	31			50			
13	40.1	71.5	32			51			
14	39.8	71.0	33			52			
15	39.8	71.0	34			53			
16	39.8	71.0	35			54			
17	39.6	70.6	36			55			
$T_H$ 75°F		$T_T$ 75°F		$S_H$ 0.504 RPS		WIRE GAUGE NO. 28		REF. FIG. NO. 14	
0.25		18	37.7	67.3	37				
0.5	38.3	68.3	19	37.7	67.3	38			
1	38.4	68.5	20	37.7	67.3	39			
2	38.4	68.5	21	37.7	67.3	40			
3	38.2	68.1	22	37.6	67.1	41			
4	38.1	68.1	23	37.6	67.1	42			
5	38.0	67.8	24	37.6	67.1	43			
6	38.0	67.8	25	37.6	67.1	44			
7	38.0	67.8	26	37.5	66.9	45			
8	37.9	67.6	27	37.5	66.9	46			
9	37.8	67.4	28	37.6	67.1	47			
10	37.8	67.4	29	37.5	66.9	48			
11	37.8	67.4	30	37.5	66.9	49			
12	37.7	67.3	31			50			
13	37.8	67.4	32			51			
14	37.8	67.4	33			52			
15	37.7	67.3	34			53			
16	37.7	67.3	35			54			
17	37.7	67.3	36			55			



## SHEAR STRESS DECAY DATA

$T_H$ $75^{\circ}\text{F}$		$T_T$ $75^{\circ}\text{F}$		$S_H$ 2.490 RPS		WIRE GAUGE NO. 28		REF. FIG. NO. 15	
TIME OF TEST (min.)	BOB DEFL. (°)	$\tau \times 10^3$ $\text{lb}_f/\text{ft}^2$	TIME OF TEST (min.)	BOB DEFL. (°)	$\tau \times 10^3$ $\text{lb}_f/\text{ft}^2$	TIME OF TEST (min.)	BOB DEFL. (°)	$\tau \times 10^3$ $\text{lb}_f/\text{ft}^2$	
0.25			18	156.4	28.0	37			
0.5	169.1	30.2	19	156.4	28.0	38			
1	165.6	29.5	20	156.1	27.9	39			
2	162.6	29.1	21	156.1	27.9	40			
3	161.1	28.7	22	156.0	27.9	41			
4	159.9	28.5	23	155.9	27.9	42			
5	159.0	28.4	24	155.9	27.9	43			
6	158.6	28.3	25	155.7	27.7	44			
7	158.1	28.2	26	155.7	27.7	45			
8	157.9	28.2	27	155.8	27.9	46			
9	157.5	28.1	28	155.8	27.9	47			
10	157.4	28.1	29	155.7	27.7	48			
11	157.3	28.1	30	155.6	27.7	49			
12	157.2	28.1	31			50			
13	156.8	28.0	32			51			
14	156.6	28.0	33			52			
15	156.7	28.0	34			53			
16	156.4	28.0	35			54			
17	156.4	28.0	36			55			
$T_H$ $75^{\circ}\text{F}$		$T_T$ $75^{\circ}\text{F}$		$S_H$ 2.493 RPS		WIRE GAUGE NO. 28		REF. FIG. NO. 15	
0.25		18	156.8	28.0	37	155.5	27.7		
0.5	169.1	30.2	19	156.7	28.0	38	155.5	27.7	
1	165.6	29.5	20	156.7	28.0	39			
2	162.9	29.1	21	156.6	28.0	40			
3	161.1	28.7	22	156.5	28.0	41			
4	160.1	28.6	23	156.4	28.0	42			
5	159.5	28.5	24	156.4	28.0	43			
6	158.9	28.4	25	156.4	28.0	44			
7		26	156.4	28.0	45				
8	158.4	28.3	27	155.9	27.9	46			
9	157.9	28.2	28	155.8	27.9	47			
10	157.7	28.2	29	155.7	27.7	48			
11	157.5	28.1	30	155.7	27.7	49			
12	157.4	28.1	31	155.6	27.7	50			
13	157.3	28.1	32	155.5	27.7	51			
14	157.3	28.1	33	155.5	27.7	52			
15	157.1	28.1	34	155.5	27.7	53			
16	157.0	28.1	35	155.4	27.7	54			
17	156.8	28.0	36	155.5	27.7	55			



## SHEAR STRESS DECAY DATA

$T_H$ $75^{\circ}\text{F}$		$T_T$ $75^{\circ}\text{F}$		$S_H$ 2.497 RPS		WIRE GAUGE NO. 28		REF. FIG. NO. 15	
TIME OF TEST (min.)	BOB DEFL. (°)	$\tau \times 10^3$ $\text{lb}_f/\text{ft}^2$	TIME OF TEST (min.)	BOB DEFL. (°)	$\tau \times 10^3$ $\text{lb}_f/\text{ft}^2$	TIME OF TEST (min.)	BOB DEFL. (°)	$\tau \times 10^3$ $\text{lb}_f/\text{ft}^2$	
0.25			18	157.6	28.1	37	157.0	28.0	
0.5	169.3	30.2	19	157.3	28.1	38	157.0	28.0	
1	166.3	29.7	20	157.4	28.1	39			
2	164.0	29.3	21	157.3	28.1	40			
3	162.3	29.0	22	157.2	28.1	41			
4	161.5	28.8	23	157.2	28.1	42			
5	160.8	28.7	24	157.2	28.1	43			
6	160.2	28.6	25	157.2	28.1	44			
7	159.6	28.5	26	157.1	28.1	45			
8	159.3	28.4	27	157.1	28.1	46			
9	158.9	28.4	28	157.0	28.0	47			
10	158.7	28.3	29	157.0	28.0	48			
11	158.3	28.3	30	157.0	28.0	49			
12	158.3	28.3	31	157.0	28.0	50			
13	158.2	28.2	32	157.0	28.0	51			
14	158.1	28.2	33	156.9	28.0	52			
15	158.0	28.2	34	157.0	28.0	53			
16	157.7	28.2	35	157.0	28.0	54			
17	157.7	28.2	36	157.0	28.0	55			
$T_H$ $75^{\circ}\text{F}$		$T_T$ $75^{\circ}\text{F}$		$S_H$ 2.495 RPS		WIRE GAUGE NO. 28		REF. FIG. NO. 15	
0.25			18	158.8	28.3	37			
0.5	168.1	29.9	19	158.5	28.3	38			
1	166.6	29.7	20	158.3	28.3	39			
2	164.1	29.3	21	158.2	28.2	40			
3	162.4	29.0	22	158.0	28.2	41			
4	161.6	28.8	23	157.9	28.2	42			
5	160.7	28.6	24	157.8	28.2	43			
6	160.3	28.6	25	157.2	28.1	44			
7	160.2	28.6	26	157.2	28.1	45			
8	159.8	28.5	27	157.1	28.1	46			
9	159.6	28.5	28	157.1	28.1	47			
10	159.6	28.5	29	157.0	28.0	48			
11	159.1	28.4	30	157.0	28.0	49			
12	159.2	28.4	31	157.0	28.0	50			
13	158.8	28.3	32	157.1	28.1	51			
14	158.8	28.3	33	157.1	28.1	52			
15	158.8	28.3	34	157.0	28.0	53			
16	158.9	28.4	35	156.9	28.0	54			
17	158.8	28.3	36	156.9	28.0	55			



## SHEAR STRESS DECAY DATA

$T_H$ 75°F		$T_T$ 75°F		$S_H$ 2.500 RPS		WIRE GAUGE NO. 28		REF. FIG. NO. 15	
TIME OF TEST (min.)	BOB DEFL. (°)	$\tau \times 10^3$ $lb_f/ft^2$	TIME OF TEST (min.)	BOB DEFL. (°)	$\tau \times 10^3$ $lb_f/ft^2$	TIME OF TEST (min.)	BOB DEFL. (°)	$\tau \times 10^3$ $lb_f/ft^2$	
0.25			18	156.0	27.9	37			
0.5	165.3	29.5	19	155.9	27.9	38			
1	163.4	29.2	20	155.7	27.7	39			
2	161.2	28.7	21	155.7	27.7	40			
3	160.2	28.6	22	155.6	27.7	41			
4	159.9	28.5	23	155.5	27.7	42			
5	158.4	28.3	24	155.4	27.7	43			
6	157.9	28.2	25	155.4	27.7	44			
7	157.4	28.1	26	155.4	27.7	45			
8	157.0	28.0	27	155.4	27.7	46			
9	156.9	28.0	28	155.4	27.7	47			
10	156.9	28.0	29	155.4	27.7	48			
11	156.6	28.0	30	155.4	27.7	49			
12	156.5	28.0	31	155.4	27.7	50			
13	156.3	27.9	32	155.3	27.7	51			
14	156.1	27.9	33	155.3	27.7	52			
15	156.2	27.9	34	155.3	27.7	53			
16	156.0	27.9	35	155.3	27.7	54			
17	155.9	27.9	36			55			
$T_H$ 75°F		$T_T$ 75°F		$S_H$ 4.470 RPS		WIRE GAUGE NO. 28		REF. FIG. NO. 16	
0.25			18			37	262.3	46.8	
0.5	274.0	48.9	19			38	262.2	46.8	
1	272.0	48.6	20			39	262.1	46.8	
2	269.0	48.0	21			40	261.9	46.8	
3	267.0	47.7	22			41	261.9	46.8	
4	266.8	47.6	23			42	261.7	46.7	
5	266.1	47.5	24			43	261.6	46.7	
6	265.7	47.3	25			44	261.7	46.7	
7	265.1	47.3	26			45	261.6	46.7	
8	264.8	47.2	27			46	261.5	46.7	
9	264.9	47.2	28			47	261.5	46.7	
10	264.7	47.2	29			48			
11	264.7	47.2	30			49			
12	264.6	47.2	31			50			
13	264.5	47.2	32	263.7	47.0	51			
14			33	263.0	46.9	52			
15			34	262.7	46.9	53			
16			35	262.6	46.9	54			
17			36	262.5	46.9	55			



## SHEAR STRESS DECAY DATA

$T_H$ 75°F		$T_T$ 75°F		$S_H$ 4.470 RPS		WIRE GAUGE NO. 28		REF. FIG.
TIME OF TEST (min.)	BOB DEFL. (°)	$T \times 10^3$ $lb_f/ft^2$	TIME OF TEST (min.)	BOB DEFL. (°)	$T \times 10^3$ $lb_f/ft^2$	TIME OF TEST (min.)	BOB DEFL. (°)	$T \times 10^3$ $lb_f/ft^2$
0.25			18			37	273.8	46.7
0.5	278.8	49.8	19			38	273.8	46.7
1	275.8	49.2	20			39	273.8	46.7
2	273.2	48.8	21			40	273.9	46.7
3	272.1	48.6	22			41	273.8	46.7
4	270.8	48.4	23			42	273.8	46.7
5	271.0	48.3	24			43	273.8	46.7
6	270.5	48.2	25			44	273.8	46.7
7	270.8	48.3	26			45	273.8	46.7
8			27			46		
9			28			47		
10			29			48		
11			30			49		
12			31			50		
13			32	274.3	46.8	51		
14			33	274.3	46.8	52		
15			34	274.3	46.8	53		
16			35	274.2	46.8	54		
17			36	273.9	46.7	55		
$T_H$ 75°F		$T_T$ 75°F		$S_H$ 4.470 RPS		WIRE GAUGE NO. 28		REF. FIG.
0.25			18	264.1	47.1	37	264.4	47.2
0.5	276.1	49.3	19	264.1	47.1	38	264.3	47.1
1	272.6	48.7	20	264.2	47.1	39	264.6	47.2
2	269.8	48.1	21	264.2	47.1	40	264.6	47.2
3	267.8	47.8	22	264.2	47.1	41	264.4	47.2
4	267.3	47.7	23	264.1	47.1	42	264.4	47.2
5	265.9	47.7	24	263.9	47.1	43		
6	266.3	47.6	25	263.9	47.1	44		
7	265.9	47.5	26	264.2	47.1	45		
8	265.4	47.3	27	264.4	47.2	46		
9	265.3	47.3	28	264.3	47.1	47		
10	265.0	47.3	29	264.3	47.1	48		
11	264.7	47.2	30	264.2	47.1	49		
12	264.5	47.2	31			50		
13	264.3	47.1	32	264.1	47.1	51		
14	264.3	47.1	33	264.1	47.1	52		
15	264.1	47.1	34	264.3	47.1	53		
16	264.2	47.1	35	264.3	47.1	54		
17	264.0	47.1	36	264.4	47.2	55		



## SHEAR STRESS DECAY DATA

T H 75°F		T T 75°F		S H 4.473 RPS		WIRE GAUGE NO. 28		REF. FIG. NO. 16	
TIME OF TEST (min.)	BOB DEFL. (°)	T x 10 <sup>3</sup> lb <sub>f</sub> /ft <sup>2</sup>	TIME OF TEST (min.)	BOB DEFL. (°)	T x 10 <sup>3</sup> lb <sub>f</sub> /ft <sup>2</sup>	TIME OF TEST (min.)	BOB DEFL. (°)	T x 10 <sup>3</sup> lb <sub>f</sub> /ft <sup>2</sup>	
0.25			18			37	263.6	47.0	
0.5	274.4	49.0	19			38	263.6	47.0	
1	272.2	48.6	20			39	263.6	47.0	
2	269.4	48.1	21			40	263.6	47.0	
3	267.9	47.8	22			41	263.6	47.0	
4	266.9	47.7	23			42	263.6	47.0	
5	266.0	47.5	24			43			
6	265.6	47.5	25			44			
7	265.1	47.3	26			45			
8	264.8	47.2	27	264.6	47.2	46			
9	264.6	47.2	28	264.6	47.2	47			
10	264.2	47.1	29	264.4	47.2	48			
11	264.1	47.1	30	264.3	47.1	49			
12	264.0	47.1	31	263.9	47.1	50			
13	264.0	47.1	32	263.9	47.1	51			
14	263.8	47.1	33	263.7	47.0	52			
15	263.8	47.1	34	263.7	47.0	53			
16	263.8	47.1	35	263.6	47.0	54			
17	264.0	47.1	36	263.5	47.0	55			
T H 75°F		T T 75°F		S H 4.470 RPS		WIRE GAUGE NO. 28	REF. FIG.- NO. 16		
0.25		18	264.0	47.1	37	263.0	46.9		
0.5	276.0	49.2	19	263.9	47.1	38			
1	272.3	48.6	20	263.9	47.1	39			
2	269.4	48.1	21	263.7	47.0	40			
3	268.0	47.8	22	263.7	47.0	41			
4	267.1	47.7	23	263.6	47.0	42			
5	266.5	47.6	24	263.6	47.0	43			
6	266.2	47.6	25	263.6	47.0	44			
7	266.2	47.6	26	263.5	47.0	45			
8	266.2	47.6	27	263.3	47.0	46			
9	266.3	47.6	28	263.2	46.9	47			
10		29	263.0	46.9	48				
11		30	263.2	46.9	49				
12		31	263.1	46.9	50				
13		32	263.2	46.9	51				
14		33	263.1	46.9	52				
15		34	263.0	46.9	53				
16		35	263.0	46.9	54				
17	264.0	47.1	36	263.0	46.9	55			



## SHEAR STRESS DECAY DATA

$T_H$ $75^{\circ}\text{F}$		$T_T$ $60^{\circ}\text{F}$		$S_H$ 0.519 RPS		WIRE GAUGE NO. 26		REF. FIG.	
TIME OF TEST (min.)	BOB DEFL. (°)	$\bar{\tau} \times 10^3$ $\text{lb}_f/\text{ft}^2$	TIME OF TEST (min.)	BOB DEFL. (°)	$\bar{\tau} \times 10^3$ $\text{lb}_f/\text{ft}^2$	TIME OF TEST (min.)	BOB DEFL. (°)	$\bar{\tau} \times 10^3$ $\text{lb}_f/\text{ft}^2$	NO. 17
0.25			18	33.9	20.9	37	32.9	20.3	
0.5	43.6	26.8	19	33.8	20.8	38	32.8	20.2	
1	42.3	26.0	20	33.8	20.8	39	32.8	20.2	
2	39.2	24.1	21	33.6	20.7	40	32.7	20.1	
3	38.1	23.5	22	33.6	20.7	41			
4	37.4	23.0	23	33.5	20.6	42			
5	36.9	22.7	24	33.4	20.6	43			
6	36.3	22.3	25	33.4	20.6	44			
7	35.9	22.1	26	33.3	20.5	45			
8	35.7	22.0	27	33.2	20.4	46			
9	35.4	21.8	28	33.2	20.4	47			
10	35.2	21.7	29	33.1	20.4	48			
11	35.0	21.5	30	33.1	20.4	49			
12	34.8	21.4	31	33.0	20.3	50			
13	34.5	21.2	32	33.0	20.3	51			
14	34.4	21.2	33	33.0	20.3	52			
15	34.3	21.1	34	32.9	20.3	53			
16	34.2	21.1	35	32.9	20.3	54			
17	34.1	21.0	36	32.9	20.3	55			
$T_H$ $75^{\circ}\text{F}$		$T_T$ $60^{\circ}\text{F}$		$S_H$ 0.516 RPS		WIRE GAUGE NO. 26		REF. FIG.	
0.25			18	34.4	21.2	37	33.0	20.3	
0.5	44.7	27.5	19	34.3	21.1	38	33.0	20.3	
1	42.2	26.0	20	34.2	21.1	39	33.0	20.3	
2	40.0	24.6	21	34.1	21.0	40	32.9	20.3	
3	38.6	23.8	22	34.0	20.9	41	32.9	20.3	
4	37.9	23.3	23	33.9	20.8	42	32.8	20.2	
5	37.4	23.0	24	33.8	20.8	43	32.8	20.2	
6	36.8	22.7	25	33.7	20.7	44	32.8	20.2	
7	36.3	22.3	26	33.7	20.7	45	32.8	20.2	
8	36.1	22.2	27	33.6	20.7	46	32.8	20.2	
9	35.8	22.0	28	33.6	20.7	47	32.7	20.1	
10	35.5	21.9	29	33.5	20.6	48	32.7	20.1	
11	35.3	21.7	30	33.5	20.6	49	32.6	20.1	
12	35.1	21.6	31	33.4	20.6	50	32.6	20.1	
13	35.0	21.5	32	33.3	20.5	51			
14	34.8	21.4	33	33.3	20.5	52			
15	34.6	21.3	34	33.2	20.4	53			
16	34.5	21.2	35	33.2	20.4	54			
17	34.4	21.2	36	33.1	20.4	55			



## SHEAR STRESS DECAY DATA

$T_H$ 75°F		$T_T$ 60°F		$S_H$ 0.522		WIRE GAUGE NO. 26		REF. FIG.
TIME OF TEST (min.)	BOB DEFL. (°)	$\tau \times 10^3$ $lb_f/ft^2$	TIME OF TEST (min.)	BOB DEFL. (°)	$\tau \times 10^3$ $lb_f/ft^2$	TIME OF TEST (min.)	BOB DEFL. (°)	$\tau \times 10^3$ $lb_f/ft^2$
0.25			18	33.3	20.5	37	32.1	19.8
0.5	41.9	25.8	19	33.2	20.4	38	32.0	19.7
1	40.8	25.1	20	33.1	20.4	39	32.0	19.7
2	38.4	23.6	21	32.9	20.3	40	32.0	19.7
3	37.4	23.0	22	32.9	20.3	41		
4	36.9	22.7	23	32.9	20.3	42		
5	36.9	22.7	24	32.8	20.2	43		
6	35.5	21.9	25	32.7	20.1	44		
7	35.1	21.6	26	32.6	20.1	45		
8	34.9	21.5	27	32.6	20.1	46		
9	34.7	21.4	28	32.5	20.0	47		
10	34.3	21.1	29	32.4	19.9	48		
11	34.3	21.1	30	32.4	19.9	49		
12	34.1	21.0	31	32.4	19.9	50		
13	33.9	20.9	32	32.3	19.9	51		
14	33.7	20.7	33	32.3	19.9	52		
15	33.6	20.7	34	32.2	19.8	53		
16	33.4	20.6	35	32.2	19.8	54		
17	33.3	20.5	36	32.1	19.8	55		
$T_H$ 75°F	$T_T$ 60°F		$S_H$ 0.524 RPS	WIRE GAUGE NO. 26		REF. FIG.		
0.25			18	33.2	20.4	37	32.1	19.8
0.5	42.4	26.1	19	33.1	20.4	38	32.0	19.7
1	40.2	24.8	20	33.1	20.4	39	32.0	19.7
2	38.1	23.5	21	33.0	20.3	40	32.0	19.7
3	37.3	23.0	22	32.9	20.3	41	31.9	19.6
4	36.6	22.5	23	32.9	20.3	42	31.9	19.6
5	36.1	22.2	24	32.8	20.2	43	31.9	19.6
6	35.6	21.9	25	32.7	20.1	44	31.9	19.6
7	35.3	21.7	26	32.6	20.1	45	32.0	19.7
8	34.9	21.5	27	32.6	20.1	46	32.0	19.7
9	34.6	21.3	28	32.5	20.0	47	32.0	19.7
10	34.4	21.2	29	32.5	20.0	48	31.9	19.6
11	34.3	21.1	30	32.4	19.9	49	31.9	19.6
12	34.1	21.0	31	32.4	19.9	50	31.8	19.6
13	33.9	20.9	32	32.4	19.9	51	31.8	19.6
14	33.7	20.7	33	32.3	19.9	52	31.8	19.6
15	33.5	20.6	34	32.2	19.8	53	31.7	19.5
16	33.4	20.6	35	32.2	19.8	54	31.7	19.5
17	33.3	20.5	36	32.1	19.8	55	31.7	19.5



## SHEAR STRESS DECAY DATA

$T_H$ 75°F		$T_T$ 60°F		$S_H$ 0.525 RPS		WIRE GAUGE NO. 26		REF. FIG.	
TIME OF TEST (min.)	BOB DEFL. (°)	$\tau \times 10^3$ $lb_f/ft^2$	TIME OF TEST (min.)	BOB DEFL. (°)	$\tau \times 10^3$ $lb_f/ft^2$	TIME OF TEST (min.)	BOB DEFL. (°)	$\tau \times 10^3$ $lb_f/ft^2$	NO. 17
0.25			18	33.5	20.6	37	32.4	19.9	
0.5	43.8	27.0	19	33.4	20.6	38	32.4	19.9	
1	41.3	25.4	20	33.4	20.6	39	32.3	19.9	
2	38.9	24.0	21	33.3	20.5	39	32.3	19.9	
3	37.8	23.3	22	33.3	20.5	41	32.3	19.9	
4	37.0	22.8	23	33.2	20.4	42	32.3	19.9	
5	36.4	22.4	24	33.1	20.4	43	32.3	19.9	
6	36.0	22.2	25	33.0	20.3	44	32.2	19.8	
7	35.6	21.9	26	33.0	20.3	45	32.2	19.8	
8	35.3	21.7	27	32.9	20.3	46	32.2	19.8	
9	35.1	21.6	28	32.8	20.2	47	32.2	19.8	
10	34.8	21.4	29	32.8	20.2	48	32.1	19.8	
11	34.6	21.3	30	32.7	20.1	49	32.1	19.8	
12	34.4	21.2	31	32.6	20.1	50	32.1	19.8	
13	34.1	21.0	32	32.6	20.1	51	32.1	19.8	
14	34.0	20.9	33	32.6	20.1	52	32.0	19.7	
15	33.8	20.8	34	32.5	20.0	53	32.0	19.7	
16	33.8	20.8	35	32.5	20.0	54	32.0	19.7	
17	33.6	20.7	36	32.4	19.9	55	32.0	19.7	
$T_H$ 75°F		$T_T$ 60°F		$S_H$ 2.494 RPS		WIRE GAUGE NO. 26		REF. FIG.	
0.25			18	93.4	57.5	37	91.7	56.5	
0.5	110.7	68.2	19	93.2	57.4	38	91.7	56.5	
1	106.7	65.7	20	93.1	57.3	39	91.6	56.4	
2	102.1	63.2	21	92.9	57.2	40	91.6	56.4	
3	100.2	61.7	22	92.8	57.1	41	91.5	56.3	
4	99.1	61.0	23	92.7	57.1	42	91.5	56.3	
5	98.2	60.5	24	92.6	57.0	43	91.4	56.3	
6	97.3	59.9	25	92.4	56.9	44	91.4	56.3	
7	96.7	59.5	26	92.4	56.9	45	91.3	56.2	
8	96.2	59.2	27	92.3	56.8	46	91.3	56.2	
9	95.7	58.9	28	92.2	56.8	47	91.2	56.2	
10	95.2	58.6	29	92.1	56.7	48	91.2	56.2	
11	95.0	58.5	30	92.1	56.7	49	91.2	56.2	
12	94.7	58.3	31	92.0	56.7	50	91.2	56.2	
13	94.5	58.2	32	91.9	56.6	51	91.2	56.2	
14	94.2	58.0	33	91.9	56.6	52	91.1	56.1	
15	94.1	57.9	34	91.9	56.6	53	91.1	56.1	
16	93.9	57.8	35	91.8	56.6	54	91.1	56.1	
17	93.5	57.6	36	91.7	56.5	55	91.1	56.1	



## SHEAR STRESS DECAY DATA

$T_H$ 75°F		$T_T$ 60°F		$S_H$ 2.497 RPS		WIRE GAUGE NO. 26		REF. FIG.
TIME OF TEST (min.)	BOB DEFL. (°)	$T \times 10^3$ $lb_f/ft^2$	TIME OF TEST (min.)	BOB DEFL. (°)	$T \times 10^3$ $lb_f/ft^2$	TIME OF TEST (min.)	BOB DEFL. (°)	$T \times 10^3$ $lb_f/ft^2$
0.25	116.7	71.9	18	95.0	58.5	37	94.2	58.0
0.5	111.7	68.8	19	95.0	58.5	38	94.3	58.1
1	106.9	65.8	20	94.8	58.4	39	94.2	58.0
2	104.4	64.3	21	94.8	58.4	40	94.2	58.0
3	102.7	63.2	22	94.7	58.3	41	94.2	58.0
4	101.2	62.3	23	94.6	58.2	42	94.2	58.0
5	100.0	61.6	24	94.5	58.2	43	94.2	58.0
6	99.7	61.4	25	94.4	58.1	44	94.2	58.0
7	98.2	60.5	26	94.4	58.1	45	94.2	58.0
8	97.7	60.2	27	94.4	58.1	46	94.2	58.0
9	97.3	59.9	28	94.3	58.1	47	94.2	58.0
10	97.0	59.7	29	94.3	58.1	48	94.2	58.0
11	96.7	59.5	30	94.3	58.1	49	94.2	58.0
12	96.2	59.2	31	94.2	58.0	50	94.1	57.9
13	96.0	59.1	32	94.2	58.0	51	94.1	57.9
14	95.7	58.9	33	94.2	58.0	52	94.1	57.9
15	95.5	58.8	34	94.2	58.0	53	94.0	57.9
16	95.2	58.6	35	94.2	58.0	54	94.0	57.9
17	95.1	58.6	36	94.2	58.0	55	93.9	57.8
$T_H$ 75°F	$T_T$ 60°F		$S_H$ 2.500 RPS		WIRE		REF. FIG.	
0.25	113.1	69.6	18	94.2	58.0	37	92.0	56.6
0.5	109.1	67.2	19	94.0	57.9	38	91.9	56.6
1	104.6	64.4	20	93.8	57.8	39	91.8	56.5
2	102.2	62.9	21	93.7	57.7	40	91.7	56.5
3	100.7	62.0	22	93.5	57.6	41	91.8	56.5
4	99.4	61.2	23	93.3	57.4	42	91.6	56.4
5	98.5	60.6	24	93.2	57.4	43	91.6	56.4
6	97.9	60.3	25	93.1	57.3	44	91.6	56.4
7	97.1	59.8	26	92.9	57.2	45	91.6	56.4
8	96.6	59.5	27	92.8	57.1	46	91.6	56.4
9	96.4	59.4	28	92.7	57.1	47	91.6	56.4
10	95.9	59.0	29	92.6	57.0	48	91.6	56.4
11	95.7	58.9	30	92.5	57.0	49	91.5	56.3
12	95.5	58.8	31	92.4	56.9	50	91.5	56.3
13	95.2	58.6	32	92.3	56.8	51	91.5	56.3
14	94.9	58.4	33	92.2	56.8	52	91.5	56.3
15	94.6	58.2	34	92.2	56.8	53	91.4	56.3
16	94.4	58.1	35	92.1	56.7	54	91.4	56.3
17	94.4	58.1	36	92.0	56.6	55	91.4	56.3



## SHEAR STRESS DECAY DATA

$T_H$ $75^{\circ}\text{F}$		$T_T$ $60^{\circ}\text{F}$		$S_H$ 2.500 RPS		WIRE GAUGE NO. 26		REF. FIG.
TIME OF TEST (min.)	BOB DEFL. (°)	$\tau \times 10^3$ $\text{lb}_f/\text{ft}^2$	TIME OF TEST (min.)	BOB DEFL. (°)	$\tau \times 10^3$ $\text{lb}_f/\text{ft}^2$	TIME OF TEST (min.)	BOB DEFL. (°)	$\tau \times 10^3$ $\text{lb}_f/\text{ft}^2$
0.25			18	90.5	55.7	37	89.5	55.1
0.5	106.0	65.3	19	90.4	55.7	38	89.5	55.1
1	102.0	62.8	20	90.2	55.5	39	89.5	55.1
2	98.4	60.6	21	90.3	55.6	40	89.4	55.0
3	96.5	59.4	22	90.2	55.5	41		
4	95.4	58.7	23	90.0	55.4	42		
5	94.5	58.2	24	89.9	55.4	43		
6	93.9	57.8	25	89.9	55.4	44		
7	93.2	57.4	26	89.9	55.4	45		
8	92.9	57.2	27	89.8	55.3	46		
9	92.6	57.0	28	89.7	55.2	47		
10	92.4	56.9	29	89.6	55.2	48		
11	92.1	56.7	30	89.6	55.2	49		
12	91.8	56.5	31	89.6	55.2	50		
13	91.6	56.4	32	89.6	55.2	51		
14	91.3	56.2	33	89.6	55.2	52		
15	91.0	56.0	34	89.6	55.2	53		
16	90.8	55.9	35	89.6	55.2	54		
17	90.6	55.8	36	89.5	55.1	55		
$T_H$ $75^{\circ}\text{F}$		$T_T$ $60^{\circ}\text{F}$		$S_H$ 2.498 RPS		WIRE GAUGE NO. 26		REF. FIG.
0.25			18	89.9	55.4	37	88.1	54.2
0.5	106.5	65.6	19	89.7	55.2	38	88.0	54.2
1	102.5	63.1	20	89.5	55.1	39	88.0	54.2
2	98.7	60.8	21	89.4	55.0	40	88.0	54.2
3	96.5	59.4	22	89.3	55.0	41	88.0	54.2
4	95.3	58.7	23	89.2	54.9	42	87.9	54.1
5	94.3	58.1	24	89.1	54.9	43	87.9	54.1
6	93.6	57.6	25	89.0	54.8	44	87.9	54.1
7	93.0	57.3	26	88.9	54.7	45	87.9	54.1
8	92.5	57.0	27	88.8	54.7	46	87.9	54.1
9	92.0	56.6	28	88.7	54.6	47	87.9	54.1
10	91.6	56.4	29	88.6	54.6	48	87.8	54.1
11	91.3	56.2	30	88.5	54.5	49	87.8	54.1
12	91.0	56.0	31	88.4	54.4	50	87.8	54.1
13	90.7	55.8	32	88.3	54.4	51	87.7	54.0
14	90.5	55.7	33	88.3	54.4	52	87.7	54.0
15	90.3	55.6	34	88.2	54.3	53	87.8	55.1
16	90.1	55.5	35	88.2	54.3	54	87.8	54.1
17	90.1	55.5	36	88.1	54.2	55	87.8	54.1



## SHEAR STRESS DECAY DATA

$T_H$ 75°F		$T_T$ 60°F		$S_H$ 4.470 RPS		WIRE		REF. FIG.	
TIME OF TEST (min.)	BOB DEFL. (°)	$\tau \times 10^3$ $lb_f/ft^2$	TIME OF TEST (min.)	BOB DEFL. (°)	$\tau \times 10^3$ $lb_f/ft^2$	TIME OF TEST (min.)	BOB DEFL. (°)	$\tau \times 10^3$ $lb_f/ft^2$	NO. 19
0.25	176.0	108.4	18	150.5	92.7	37	149.3	91.9	
0.5	169.5	104.4	19	150.3	92.5	38	149.3	91.9	
1	163.5	100.7	20	150.1	92.4	39	149.3	91.9	
2	160.0	98.5	21	150.1	92.4	40	149.3	91.9	
3	158.0	97.3	22	150.0	92.4	41	149.3	91.9	
4	156.6	96.4	23	149.9	92.3	42	149.2	91.9	
5	155.4	95.7	24	149.8	92.2	43	149.2	91.9	
6	154.5	95.1	25	149.7	92.2	44	149.1	91.8	
7	153.9	94.8	26	149.7	92.2	45	149.0	91.7	
8	153.4	94.4	27	149.7	92.2	46	149.0	91.7	
9	152.8	94.1	28	149.6	92.1	47	149.0	91.7	
10	152.4	93.8	29	149.6	92.1	48	149.0	91.7	
11	152.2	93.7	30	149.7	92.2	49	149.0	91.7	
12	151.8	93.5	31	149.7	92.2	50	149.0	91.7	
13	151.5	93.3	32	149.6	92.1	51			
14	151.2	93.1	33	149.5	92.0	52			
15	151.1	93.0	34	149.4	92.0	53			
16	151.0	93.0	35	149.4	92.0	54			
17	150.8	92.8	36	149.4	92.0	55			
$T_H$ 75°F		$T_T$ 60°F		$S_H$ 4.468 RPS		WIRE		REF. FIG.	
0.25			18	144.3	88.8	37	144.4	88.9	
0.5	169.0	104.1	19	144.3	88.8	38	144.4	88.9	
1	163.5	101.7	20	144.4	88.9	39	144.5	89.0	
2	158.0	97.3	21	144.5	89.0	40	144.4	88.9	
3	155.1	95.5	22	144.7	89.1	41	144.4	88.9	
4	153.2	94.3	23	144.7	89.1	42	144.4	88.9	
5	151.7	93.4	24	144.9	89.2	43	144.3	88.8	
6	150.4	92.6	25	145.1	89.3	44	144.2	88.8	
7	149.5	92.0	26	145.2	89.4	45	144.1	88.7	
8	148.9	91.7	27	145.3	89.5	46	144.1	88.7	
9	148.2	91.2	28	145.2	89.4	47	144.1	88.7	
10	147.7	90.9	29	144.8	89.2	48	144.1	88.7	
11	147.0	90.5	30	144.9	89.2	49	144.5	89.0	
12	146.6	90.3	31	144.9	89.2	50	144.7	89.1	
13	146.1	90.0	32	144.6	89.0	51	144.9	89.2	
14	145.6	89.6	33	144.6	89.0	52	144.5	89.0	
15	145.3	89.5	34	144.5	89.0	53	144.5	89.0	
16	144.8	89.2	35	144.7	89.1	54	144.5	89.0	
17	144.3	88.8	36	144.4	88.9	55	144.5	89.0	



## SHEAR STRESS DECAY DATA

$T_H$ $75^{\circ}\text{F}$		$T_T$ $60^{\circ}\text{F}$		$S_H$ 4.468 RPS		WIRE GAUGE NO. 26		REF. FIG.
TIME OF TEST (min.)	BOB DEFL. (°)	$\tau \times 10^3$ $\text{lb}_f/\text{ft}^2$	TIME OF TEST (min.)	BOB DEFL. (°)	$\tau \times 10^3$ $\text{lb}_f/\text{ft}^2$	TIME OF TEST (min.)	BOB DEFL. (°)	$\tau \times 10^3$ $\text{lb}_f/\text{ft}^2$
0.25			18	148.5	91.4	37	146.8	90.4
0.5	175.9	108.3	19	148.5	91.4	38	146.8	90.4
1	162.9	100.3	20	148.5	91.4	39	146.9	90.4
2	160.9	99.1	21	148.6	91.5	40	146.8	90.4
3	158.3	97.5	22	148.6	91.5	41	146.9	90.4
4	156.2	96.2	23	148.6	91.5	42	147.0	90.5
5	154.4	95.1	24	148.3	91.3	43	147.1	90.6
6	153.1	94.3	25	147.7	90.9	44	147.1	90.6
7	152.2	93.7	26	147.4	90.8	45	147.0	90.5
8	151.5	93.3	27	147.4	90.8	46	147.0	90.5
9	151.0	93.0	28	147.3	90.7	47	147.1	90.6
10	150.4	92.6	29	147.0	90.5	48	147.1	90.6
11	150.0	92.4	30	145.7	90.3	49	147.2	90.6
12	149.6	92.1	31	146.6	90.3	50	147.2	90.6
13	149.5	92.0	32	146.6	90.3	51	147.2	90.6
14	149.3	91.9	33	146.6	90.3	52	147.2	90.6
15	149.0	91.7	34	146.6	90.3	53	147.2	90.6
16	148.7	91.6	35	146.8	90.4	54	147.3	90.7
17	148.6	91.5	36	146.7	90.3	55	147.3	90.7
$T_H$ $75^{\circ}\text{F}$		$T_T$ $60^{\circ}\text{F}$		$S_H$ 4.496 RPS		WIRE GAUGE NO. 26		REF. FIG.
0.25			18	145.4	89.5	37	145.0	89.3
0.5	166.4	102.5	19	145.4	89.5	38	145.0	89.3
1	162.9	100.3	20	145.4	89.5	39	145.1	89.3
2	157.4	96.9	21	145.3	89.5	40	145.2	89.4
3	154.4	95.1	22	145.3	89.5	41	145.2	89.4
4	152.4	93.8	23	145.2	89.4	42	145.3	89.5
5	150.9	92.9	24	145.2	89.4	43	145.3	89.5
6	149.8	92.2	25	145.2	89.4	44	145.2	89.4
7	148.9	91.7	26	145.1	89.3	45	145.2	89.4
8	148.4	91.4	27	145.1	89.3	46	145.2	89.4
9	147.9	91.1	28	145.1	89.3	47	145.2	89.4
10	147.4	90.8	29	145.1	89.3	48	145.2	89.4
11	146.9	90.4	30	145.1	89.3	49	145.2	89.4
12	146.6	90.3	31	145.0	89.3	50	145.2	89.4
13	146.3	90.1	32	145.0	89.3	51	145.2	89.4
14	146.2	90.0	33	145.0	89.3	52	145.2	89.4
15	145.9	89.8	34	145.0	89.3	53	145.2	89.4
16	145.7	89.7	35	144.9	89.2	54	145.2	89.4
17	145.5	89.6	36	144.9	89.2	55	145.2	89.4



## SHEAR STRESS DECAY DATA

$T_H$ 75°F		$T_T$ 60°F		$S_H$ 4.486 RPS	WIRE		REF. FIG.	
TIME OF TEST (min.)	BOB DEFL. (°)	$\tau \times 10^3$ $lb_f/ft^2$	TIME OF TEST (min.)	BOB DEFL. (°)	$\tau \times 10^3$ $lb_f/ft^2$	TIME OF TEST (min.)	BOB DEFL. (°)	$\tau \times 10^3$ $lb_f/ft^2$
0.25			18	152.8	94.1	37	152.1	93.6
0.5	177.1	109.0	19	152.7	94.0	38	152.1	93.6
1	171.1	105.3	20	152.6	94.0	39	152.1	93.6
2	165.1	101.7	21	152.6	94.0	40	152.1	93.6
3	161.8	99.6	22	152.6	94.0	41		
4	159.6	98.3	23	152.5	93.9	42		
5	158.1	97.3	24	152.4	93.8	43		
6	156.9	96.6	25	152.3	93.8	44		
7	156.2	96.2	26	152.3	93.8	45		
8	155.4	95.7	27	152.3	93.8	46		
9	155.0	95.4	28	152.3	93.8	47		
10	154.8	95.3	29	152.3	93.8	48		
11	154.3	95.0	30	152.3	93.8	49		
12	154.0	94.8	31	152.2	93.7	50		
13	153.8	94.7	32	152.2	93.7	51		
14	153.4	94.4	33	152.1	93.6	52		
15	153.3	94.4	34	152.2	93.7	53		
16	153.2	94.3	35	152.2	93.7	54		
17	152.9	94.1	36	152.2	93.7	55		
$T_H$ 75°F		$T_T$ 44.5°F		$S_H$ 0.520 RPS	WIRE		REF. FIG.	
					GAUGE NO. 26		NO:	20
0.25			18	91.4	56.3	37	85.4	52.6
0.5	157.2	96.8	19	90.9	56.0	38	85.2	52.5
1	139.7	86.0	20	90.6	55.8	39	85.0	52.3
2	123.9	76.3	21	90.0	55.4	40	84.8	52.2
3	115.9	71.4	22	89.7	55.2	41	84.7	52.1
4	110.5	68.0	23	89.3	55.0	42	84.6	52.1
5	107.4	66.1	24	89.0	54.8	43	84.5	52.0
6	104.4	64.3	25	88.7	54.6	44	84.3	51.9
7	102.3	63.0	26	88.4	54.4	45	84.1	51.8
8	100.3	61.8	27	88.1	54.2	46	83.9	51.7
9	98.6	60.7	28	87.7	54.0	47	83.8	51.6
10	97.0	59.7	29	87.5	53.9	48	83.7	51.5
11	95.9	59.0	30	87.2	53.7	49	83.5	51.4
12	95.0	58.5	31	86.9	53.5	50	83.4	51.3
13	94.2	58.0	32	86.7	53.4	51	83.3	51.3
14	93.7	57.7	33	86.5	53.3	52	83.2	51.2
15	93.1	57.3	34	86.2	53.1	53	83.1	51.2
16	92.5	57.0	35	85.8	52.8	54	83.0	51.1
17	92.1	56.7	36	85.6	52.7	55	82.9	51.0



## SHEAR STRESS DECAY DATA

$T_H$ 75°F		$T_T$ 44.5°F		$S_H$ 0.526 RPS		WIRE GAUGE NO. 26		REF. FIG.
TIME OF TEST (min.)	BOB DEFL. (°)	$\tau \times 10^3$ $lb_f/ft^2$	TIME OF TEST (min.)	BOB DEFL. (°)	$\tau \times 10^3$ $lb_f/ft^2$	TIME OF TEST (min.)	BOB DEFL. (°)	$\tau \times 10^3$ $lb_f/ft^2$
0.25	179.0	110.2	18	88.9	54.7	37	82.5	50.8
0.5	159.0	97.9	19	88.2	54.3	38	82.2	50.6
1	138.0	85.0	20	87.9	54.1	39	82.0	50.5
2	122.5	75.4	21	87.2	53.7	40	81.8	50.4
3	114.5	70.5	22	86.6	53.3	41	81.6	50.2
4	109.2	67.2	23	86.4	53.2	42	81.5	50.2
5	105.4	64.9	24	86.0	53.0	43	81.4	50.1
6	103.7	63.8	25	85.5	52.6	44	81.3	50.1
7	102.6	63.2	26	85.0	52.3	45	81.0	49.9
8	102.0	62.8	27	84.8	52.2	46	81.0	49.9
9	96.5	59.4	28	84.5	52.0	47	80.8	49.7
10	95.6	58.9	29	84.3	51.9	48	80.6	49.6
11	94.5	58.2	30	84.0	51.7	49	80.4	49.5
12	93.5	57.6	31	83.8	51.6	50	80.2	49.4
13	92.2	56.8	32	83.6	51.5	51	80.2	49.4
14	91.4	56.3	33	83.4	51.3	52	80.1	49.3
15	90.6	55.8	34	83.2	51.2	53	80.0	49.3
16	90.2	55.5	35	83.0	51.1	54	79.9	49.2
17	89.6	55.2	36	82.7	50.9	55	79.8	49.1
$T_H$ 75°F		$T_T$ 44.5°F		$S_H$ 0.526 RPS		WIRE GAUGE NO. 26		REF. FIG.
0.25	171.4	105.5	18	88.3	54.4	37	82.6	50.9
0.5	154.4	95.1	19	87.9	54.1	38	82.4	50.7
1	134.4	82.8	20	87.6	53.9	39	82.2	50.6
2	119.4	73.5	21	86.9	53.5	40	82.0	50.5
3	111.6	68.7	22	86.6	53.3	41	82.0	50.5
4	106.9	65.8	23	86.3	53.1	42	81.8	50.4
5	103.4	63.7	24	85.9	52.9	43	81.6	50.2
6	100.9	62.1	25	85.4	52.6	44	81.5	50.2
7	98.7	60.8	26	85.3	52.5	45	81.3	50.1
8	97.2	59.8	27	85.0	52.3	46	81.2	50.0
9	95.8	59.0	28	84.7	52.1	47	81.1	49.9
10	94.5	58.2	29	84.4	52.0	48	80.9	49.8
11	93.5	57.6	30	84.2	51.8	49	80.8	49.7
12	92.3	56.8	31	84.0	51.7	50	80.8	49.7
13	91.4	56.3	32	83.4	51.3	51	80.4	49.5
14	91.0	56.0	33	83.4	51.3	52	80.5	49.6
15	89.9	55.4	34	83.4	51.3	53	80.4	49.5
16	89.6	55.2	35	83.2	51.2	54	80.4	49.5
17	88.9	54.7	36	82.8	51.0	55	80.3	49.4



## SHEAR STRESS DECAY DATA

$T_H$ 75°F		$T_T$ 44.5°F		$S_H$ 0.527 RPS		WIRE GAUGE NO. 26		REF. FIG. NO. 20	
TIME OF TEST (min.)	BOB DEFL. (°)	$\tau \times 10^3$ $lb_f/ft^2$	TIME OF TEST (min.)	BOB DEFL. (°)	$\tau \times 10^3$ $lb_f/ft^2$	TIME OF TEST (min.)	BOB DEFL. (°)	$\tau \times 10^3$ $lb_f/ft^2$	
0.25	183.5	113.0	18	92.3	56.8	37	85.9	52.9	
0.5	161.6	99.5	19	91.7	56.5	38	85.1	52.4	
1	141.7	87.2	20	91.0	56.0	39	85.2	52.2	
2	127.2	78.3	21	90.6	55.8	40	85.1	52.4	
3	118.7	73.1	22	90.2	55.5	41	84.7	52.1	
4	113.3	69.8	23	89.7	55.2	42	84.7	52.1	
5	109.3	67.3	24	89.3	55.0	43	84.5	52.0	
6	106.5	65.6	25	89.0	54.8	44	84.5	52.0	
7	103.8	63.9	26	88.6	54.6	45	84.4	52.0	
8	102.3	63.0	27	88.2	54.3	46	84.1	51.8	
9	100.3	61.8	28	87.5	53.9	47	83.7	51.5	
10	98.9	60.9	29	87.8	54.1	48	83.5	51.4	
11	97.6	60.1	30	87.5	53.9	49	83.5	51.4	
12	96.4	59.4	31	87.2	53.7	50	83.3	51.3	
13	95.4	58.7	32	87.0	53.6	51	83.3	51.3	
14	95.2	58.6	32	86.7	53.4	52	83.2	51.2	
15	94.3	58.1	34	86.5	53.3	53	83.1	51.2	
16	93.4	57.5	35	86.1	53.0	54	83.0	51.1	
17	92.8	57.1	36	86.0	53.0	55	82.8	51.0	
$T_H$ 75°F	$T_T$ 44.5°F		$S_H$ 0.526 RPS		WIRE GAUGE NO. 24		REF. FIG. NO. 20		
0.25	81.6	111.9	18	40.1	55.0	37	37.4	51.3	
0.5	72.6	99.5	19	39.9	54.7	38	37.3	51.1	
1	62.9	86.2	20	39.6	54.3	39	37.2	51.0	
2	55.3	75.8	21	39.5	54.2	40	37.1	50.9	
3	51.6	70.7	22	39.4	54.0	41	36.9	50.6	
4	49.2	67.5	23	39.1	53.6	42	36.8	50.5	
5	47.5	65.1	24	38.9	53.3	43	36.7	50.3	
6	45.9	62.9	25	38.7	53.1	44	36.7	50.3	
7	45.2	62.0	26	38.6	52.9	45	36.7	50.3	
8	44.4	60.9	27	38.5	52.8	46	36.6	50.2	
9	43.6	59.8	28	38.3	52.5	47	36.6	50.2	
10	43.0	59.0	29	38.1	52.2	48	36.5	50.0	
11	42.6	58.4	30	38.0	52.1	49	36.4	49.9	
12	42.1	57.7	31	37.8	51.8	50	36.3	49.8	
13	41.6	57.0	32	37.7	51.7	51	36.2	49.6	
14	41.3	56.6	33	37.6	51.5	52	36.2	49.6	
15	40.9	56.1	34	37.6	51.5	53	36.2	49.6	
16	40.6	55.7	35	37.5	51.4	54	36.1	49.5	
17	40.4	55.4	36	37.4	51.3	55	36.1	49.5	



## SHEAR STRESS DECAY DATA

$T_H$ 75°F		$T_T$ 44.5°F		$S_H$ 2.492 RPS		WIRE GAUGE NO. 26		REF. FIG.
TIME OF TEST (min.)	BOB DEFL. (°)	$T \times 10^3$ $\text{lb}_f/\text{ft}^2$	TIME OF TEST (min.)	BOB DEFL. (°)	$T \times 10^3$ $\text{lb}_f/\text{ft}^2$	TIME OF TEST (min.)	BOB DEFL. (°)	$T \times 10^3$ $\text{lb}_f/\text{ft}^2$
0.25	314.9	193.9	18	191.6	118.0	37	187.9	115.7
0.5	279.9	172.3	19	-	-	38	187.7	115.6
1	251.9	155.1	20	195.2	120.2	39	187.5	115.4
2	229.9	141.5	21	194.1	119.5	40	187.3	115.3
3	219.9	135.4	22	192.9	118.8	41	187.1	115.2
4	213.4	131.4	23	191.9	118.2	42	186.9	115.1
5	207.4	127.7	24	191.2	117.7	43	186.8	115.0
6	205.1	126.3	25	190.5	117.3	44	186.9	115.1
7	202.4	124.6	26	190.1	117.0	45	187.0	115.1
8	199.9	123.1	27	189.5	116.7	46	187.1	115.2
9	197.9	121.8	28	189.2	116.5	47	187.1	115.2
10	196.4	120.9	29	189.0	116.4	48	187.0	115.1
11	194.9	120.0	30	188.8	116.2	49	187.1	115.2
12	193.7	119.3	31	188.6	116.1	50	187.0	115.1
13	192.9	118.8	32	188.4	116.0	51	187.0	115.1
14	192.0	118.2	33	188.3	115.9	52	187.0	115.1
15	191.5	117.9	34	188.2	115.9	53	187.0	115.1
16	191.2	117.7	35	188.1	115.8	54	187.1	115.2
17	192.0	118.2	36	188.0	115.8	55	187.1	115.2
$T_H$ 75°F		$T_T$ 44.5°F		$S_H$ 2.498 RPS		WIRE GAUGE NO. 26		REF. FIG.
0.25	-	-	18	188.0	115.8	37	187.8	115.6
0.5	268.0	165.0	19	187.4	115.4	38	187.5	115.4
1	243.6	150.0	20	187.1	115.2	39	187.1	115.2
2	224.0	137.9	21	186.7	115.0	40	187.0	115.1
3	214.0	131.8	22	186.2	114.6	41	186.7	115.0
4	208.0	128.1	23	185.8	114.4	42	186.5	114.8
5	203.8	125.5	24	185.5	114.2	43	186.2	114.6
6	200.4	123.4	25	185.2	114.0	44	185.9	114.5
7	198.4	122.2	26	185.0	113.9	45	185.9	114.5
8	196.5	121.0	27	184.8	113.8	46	185.6	114.3
9	195.1	120.1	28	184.5	113.6	47	185.4	114.2
10	193.5	119.1	29	-	-	48	185.0	113.9
11	192.4	118.5	30	190.3	117.2	49	184.9	113.8
12	191.6	118.0	31	193.7	119.3	50	184.6	113.7
13	190.7	117.4	32	192.1	118.3	51	184.5	113.6
14	190.0	117.0	33	190.7	117.4	52	184.3	113.5
15	189.1	116.4	34	189.5	116.7	53	184.0	113.3
16	188.9	116.3	35	188.9	116.3	54	183.6	113.0
17	188.5	116.1	36	188.4	116.0	55	183.4	112.9



## SHEAR STRESS DECAY DATA

$T_H$ 75°F		$T_T$ 44.5°F		$S_H$ 2.491 RPS		WIRE GAUGE NO. 26		REF. FIG.
TIME OF TEST (min.)	BOB DEFL. (°)	$\tau \times 10^3$ $\text{lb}_f/\text{ft}^2$	TIME OF TEST (min.)	BOB DEFL. (°)	$\tau \times 10^3$ $\text{lb}_f/\text{ft}^2$	TIME OF TEST (min.)	BOB DEFL. (°)	$\tau \times 10^3$ $\text{lb}_f/\text{ft}^2$
0.25	278.8	171.7	18	187.2	115.3	37	178.6	110.5
0.5	263.8	162.4	19	186.2	114.6	38	178.3	109.8
1	243.8	150.1	20	185.4	114.2	39	177.9	109.5
2	224.6	138.3	21	184.8	113.8	40	177.8	109.5
3	215.2	132.6	22	184.0	113.3	41	177.6	109.3
4	209.6	129.1	23	183.8	113.2	42	177.5	109.3
5	205.8	126.7	24	182.9	112.6	43	177.3	109.2
6	201.3	123.9	25	182.6	112.4	44	177.0	109.0
7	198.4	122.2	26	182.0	112.1	45	176.8	108.9
8	196.8	121.2	27	181.6	111.8	46	176.7	108.8
9	195.0	120.1	28	181.2	111.6	47	176.4	108.6
10	193.2	119.0	29	180.9	111.4	48	176.2	108.5
11	191.8	118.1	30	180.6	111.2	49	176.1	108.4
12	190.4	117.2	31	180.3	111.0	50	175.9	108.3
13	189.0	116.4	32	180.0	110.8	51	175.7	108.2
14	188.3	115.9	33	179.7	110.6	52	175.5	108.1
15			34	179.3	110.4	53	175.2	107.9
16	189.6	116.7	35	179.0	110.2	54	175.1	107.8
17	188.1	115.8	36	178.8	110.1	55	175.0	107.7
$T_H$ 75°F		$T_T$ 44.5°F		$S_H$ 2.501 RPS		WIRE GAUGE NO. 26		REF. FIG.
0.25	293.0	180.4	18	185.7	114.3	37	181.0	111.4
0.5	260.0	160.1	19	185.1	114.0	38	180.8	111.3
1	238.0	146.5	20	184.7	113.7	39	180.6	111.2
2	219.3	135.0	21	184.3	113.5	40	180.6	111.2
3	209.5	129.0	22	184.1	113.4	41	180.5	111.1
4	205.7	126.6	23	183.7	113.1	42	180.4	111.1
5	201.5	124.1	24	183.5	113.0	43	180.3	111.0
6	199.5	122.8	25	183.8	113.2	44	180.2	110.9
7	196.2	120.8	26	183.6	113.0	45	180.1	110.9
8	194.5	119.8	27	183.3	112.9	46	180.0	110.8
9	192.8	118.8	28	183.0	112.7	47	179.9	110.8
10	191.2	117.7	29	182.5	112.4	48	179.8	110.7
11	189.2	116.5	30	182.0	112.1	49	179.7	110.6
12	188.3	115.9	31	181.9	112.0	50	179.6	110.6
13	188.0	115.8	32	181.8	111.9	51	179.5	110.5
14	187.8	115.6	33	181.6	111.8	52	179.5	110.5
15	187.1	115.2	34	181.3	111.6	53	179.5	110.5
16	186.7	115.0	35	181.2	111.6	54	179.4	110.5
17	186.2	114.6	36	181.1	111.5	55	179.4	110.5



## SHEAR STRESS DECAY DATA

$T_H$ 75°F		$T_T$ 44.5°F		$S_H$ 2.501 RPS		WIRE GAUGE NO. 24		REF. FIG. NO. 21	
TIME OF TEST (min.)	BOB DEFL. (°)	$\tau \times 10^3$ $\text{lb}_f/\text{ft}^2$	TIME OF TEST (min.)	BOB DEFL. (°)	$\tau \times 10^3$ $\text{lb}_f/\text{ft}^2$	TIME OF TEST (min.)	BOB DEFL. (°)	$\tau \times 10^3$ $\text{lb}_f/\text{ft}^2$	
0.25	132.1	181.1	18	84.1	115.3	37	81.1	111.2	
0.5	122.6	168.1	19	83.8	114.9	38	81.0	111.1	
1	111.1	152.3	20	83.6	114.6	39	80.9	110.9	
2	102.3	140.3	21	83.5	114.5	40	80.8	110.8	
3	97.5	133.7	22	83.4	114.3	41	80.7	110.6	
4	94.7	129.8	23	83.1	113.9	42	80.6	110.5	
5	92.6	127.0	24	82.8	113.5	43	80.5	110.4	
6	91.1	124.9	25	82.6	113.2	44	80.4	110.2	
7	89.7	123.0	26	82.4	113.0	45	80.4	110.2	
8	88.6	121.5	27	82.2	112.7	46	80.4	110.2	
9	88.0	120.6	28	82.1	112.6	47	80.3	110.1	
10	87.3	119.7	29	82.0	112.4	48	80.3	110.1	
11	86.6	118.7	30	81.9	112.3	49	80.3	110.1	
12	86.2	118.2	31	81.8	112.2	50	80.2	110.0	
13	85.7	117.5	32	81.6	111.9	51	80.1	109.8	
14	85.3	116.9	33	81.5	111.7	52	80.1	109.8	
15	85.0	116.5	34	81.4	111.6	53	80.0	109.7	
16	84.7	116.1	35	81.3	111.5	54	80.0	109.7	
17	84.3	115.6	36	81.2	111.3	55	80.0	109.7	
$T_H$ 75°F		$T_T$ 44.5°F		$S_H$ 4.490 RPS		WIRE GAUGE NO. 24		REF. FIG. NO. 22	
0.25	162.4	222.7	18	112.6	154.4	37	109.9	150.7	
0.5	152.4	208.9	19	112.4	154.1	38	109.9	150.7	
1	141.9	194.5	20	112.2	153.8	39	109.8	150.5	
2	132.4	181.5	21	111.9	153.4	40	109.7	150.4	
3	127.0	174.1	22	111.7	153.1	41	109.5	150.1	
4	123.7	169.6	23	111.4	152.7	42	109.4	150.0	
5	121.9	167.1	24	111.3	152.6	43	109.2	149.7	
6	120.1	164.7	25	111.1	152.3	44	109.2	149.7	
7	119.1	163.3	26	110.8	151.9	45	109.2	149.7	
8	118.2	162.1	27	110.7	151.8	46	109.1	149.6	
9	117.2	160.7	28	110.6	151.6	47	109.0	149.4	
10	116.6	159.9	29	110.4	151.4	48	109.0	149.4	
11	115.8	158.8	30	110.2	151.1	49	109.0	149.4	
12	115.1	157.8	31	110.1	150.9	50	109.0	149.4	
13	114.7	157.3	32	110.1	150.9	51	108.9	149.3	
14	114.3	156.7	33	110.1	150.9	52	108.9	149.3	
15	113.8	156.0	34	110.0	150.8	53	108.8	149.2	
16	113.4	155.5	35	110.0	150.8	54	108.8	149.2	
17	112.9	154.8	36	110.0	150.8	55	108.8	149.2	



## SHEAR STRESS DECAY DATA

$T_H$ $75^{\circ}\text{F}$		$T_T$ $44.5^{\circ}\text{F}$		$S_H$ 4.480		WIRE GAUGE NO. 24		REF. FIG. NO. 22	
TIME OF TEST (min.)	BOB DEFL. (°)	$T \times 10^3$ $\text{lb}_f/\text{ft}^2$	TIME OF TEST (min.)	BOB DEFL. (°)	$T \times 10^3$ $\text{lb}_f/\text{ft}^2$	TIME OF TEST (min.)	BOB DEFL. (°)	$T \times 10^3$ $\text{lb}_f/\text{ft}^2$	
0.25	155.3	212.9	18	113.6	155.7	37	110.9	152.0	
0.5			19	113.4	155.5	38	110.7	151.8	
1	138.4	189.7	20	113.2	155.2	39	110.6	151.6	
2	132.4	181.5	21	113.1	155.1	40	110.6	151.6	
3	128.0	175.5	22	112.9	154.8	41	110.6	151.6	
4	124.8	171.1	23	112.6	154.4	42	110.5	151.5	
5	122.5	167.9	24	112.4	154.1	43	110.5	151.5	
6	120.7	165.5	25	112.3	154.0	44	110.4	151.4	
7	119.5	163.8	26	112.1	153.7	45	110.4	151.4	
8	118.4	162.3	27	112.0	153.6	46	110.4	151.4	
9	117.6	161.2	28	111.9	153.4	47	110.3	151.2	
10	116.8	160.1	29	111.7	153.1	48	110.3	151.2	
11	116.2	159.3	30	111.6	153.0	49	110.2	151.1	
12	115.6	158.5	31	111.5	152.9	50	110.2	151.1	
13	115.0	157.7	32	111.4	152.7	51	110.2	151.1	
14	114.5	157.0	33	111.3	152.6	52	110.2	151.1	
15	114.4	156.8	34	111.2	152.5	53	110.1	150.9	
16	114.1	156.4	35	111.1	152.3	54	110.1	150.9	
17	113.9	156.2	36	111.0	152.2	55	110.1	150.9	
$T_H$ $75^{\circ}\text{F}$		$T_T$ $44.5^{\circ}\text{F}$		$S_H$ 4.483 RPS		WIRE GAUGE NO. 24		REF. FIG. NO. 22	
0.25	176.0	241.3	18	117.7	161.4	37	114.8	157.4	
0.5	161.0	220.7	19	117.2	160.7	38	114.7	157.3	
1	148.5	203.6	20	117.0	160.4	39	114.6	157.1	
2	138.0	189.2	21	116.9	160.3	40	114.5	157.0	
3	132.6	181.8	22	116.7	160.0	41	114.4	156.8	
4	128.7	176.4	23	116.5	159.7	42	114.3	156.7	
5	127.0	174.1	24	116.4	159.6	43	114.2	156.6	
6	125.0	171.4	25	116.2	159.3	44	114.0	156.3	
7	124.6	170.8	26	116.0	159.0	45	113.9	156.2	
8	123.7	169.6	27	115.9	158.9	46	113.8	156.0	
9	122.9	168.5	28	115.8	158.8	47	113.7	155.9	
10	121.9	167.1	29	115.7	158.6	48	113.6	155.7	
11	121.1	166.0	30	115.6	158.5	49	113.5	155.6	
12	120.4	165.1	31	115.5	158.4	50	113.4	155.5	
13	119.7	164.1	32	115.4	158.2	51	113.3	155.3	
14	119.2	163.4	33	115.3	158.1	52	113.2	155.2	
15	118.8	162.9	34	115.2	157.9	53	113.1	155.1	
16	118.4	162.3	35	115.0	157.7	54	113.0	154.9	
17	118.0	161.8	36	114.9	157.5	55	112.9	154.8	



## SHEAR STRESS DECAY DATA

$T_H$ $75^{\circ}\text{F}$		$T_T$ $44.5^{\circ}\text{F}$		$S_H$ 4.480 RPS		WIRE GAUGE NO. 24		REF. FIG.
TIME OF TEST (min.)	BOB DEFL. (°)	$T \times 10^3$ $\text{lb}_f/\text{ft}^2$	TIME OF TEST (min.)	BOB DEFL. (°)	$T \times 10^3$ $\text{lb}_f/\text{ft}^2$	TIME OF TEST (min.)	BOB DEFL. (°)	$T \times 10^3$ $\text{lb}_f/\text{ft}^2$
0.25	169.5	232.4	18	116.3	159.4	37	113.2	155.2
0.5	153.5	210.4	19	116.0	159.0	38	113.1	155.1
1	143.7	197.0	20	115.7	158.6	39	113.0	154.9
2	134.0	183.7	21	115.5	158.4	40	112.8	154.6
3	129.5	177.5	22	115.3	158.1	41	112.6	154.4
4	126.6	173.6	23	115.1	157.8	42	112.5	154.2
5	124.4	170.6	24	114.9	157.5	43	112.5	154.2
6	122.7	168.2	25	114.8	157.4	44	112.4	154.1
7	121.7	166.9	26	114.6	157.1	45	112.2	153.8
8	121.0	165.9	27	114.5	157.0	46	112.2	153.8
9	120.1	164.7	28	114.4	156.8	47	112.2	153.8
10	119.4	163.7	29	114.3	156.7	48	112.1	153.7
11	118.9	163.0	30	114.2	156.6	49	111.9	153.4
12	118.4	162.3	31	114.0	156.3	50	111.8	153.3
13	117.9	161.6	32	113.9	156.2	51	111.6	153.0
14	117.5	161.6	33	113.8	156.0	52	111.4	152.7
15	117.1	160.5	34	113.6	155.7	53	111.1	152.3
16	116.9	160.3	35	113.5	155.6	54	111.0	152.2
17	116.6	159.9	36	113.4	155.5	55	111.0	152.2
$T_H$ $75^{\circ}\text{F}$	$T_T$ $44.5^{\circ}\text{F}$		$S_H$ 4.481 RPS	WIRE GAUGE NO. 24		REF. FIG.		
0.25	168.7	231.3	18	113.5	155.6	37	109.3	149.9
0.5	156.7	214.8	19	113.0	154.9	38	109.2	149.7
1	145.2	199.1	20	112.7	154.5	39	109.1	149.6
2	134.7	184.7	21	112.4	154.1	40	109.0	149.4
3	129.3	177.3	22	112.2	153.8	41	108.9	149.3
4	126.0	172.7	23	111.8	153.3	42	108.8	149.2
5	123.7	169.6	24	111.7	153.1	43	108.7	149.0
6	122.0	167.3	25	111.5	152.9	44	108.6	148.9
7	120.5	165.2	26	111.2	152.5	45	108.5	148.8
8	119.2	163.4	27	111.0	152.2	46	108.4	148.6
9	118.3	162.2	28	110.8	151.9	47	108.3	148.5
10	117.3	160.8	29	110.6	151.6	48	108.2	148.3
11	116.7	160.0	30	110.5	151.5	49	108.1	148.2
12	116.0	159.0	31	110.2	151.1	50	108.0	148.1
13	115.5	158.4	32	110.0	150.8	51	107.9	147.9
14	114.7	157.3	33	109.8	150.5	52	107.8	147.8
15	114.6	157.1	34	109.7	150.4	53	107.7	147.7
16	114.3	156.7	35	109.6	150.3	54	107.7	147.7
17	113.9	156.2	36	109.4	150.0	55	107.6	147.5



## SHEAR STRESS DECAY DATA

$T_H$ $75^{\circ}\text{F}$		$T_T$ $30^{\circ}\text{F}$		$S_H$ Q. 536 RPS		WIRE GAUGE NO. 24		REF. FIG. NO. 23	
TIME OF TEST (min.)	BOB DEFL. (°)	$T \times 10^3$ $\text{lb}_f/\text{ft}^2$	TIME OF TEST (min.)	BOB DEFL. (°)	$T \times 10^3$ $\text{lb}_f/\text{ft}^2$	TIME OF TEST (min.)	BOB DEFL. (°)	$T \times 10^3$ $\text{lb}_f/\text{ft}^2$	
0.25	196.1	268.9	18	85.5	117.2	37	77.8	106.7	
0.5	169.2	232.0	19	85.2	116.8	38	77.5	106.3	
1	146.3	200.6	20	84.5	115.8	39	77.2	105.8	
2	129.3	177.3	21	84.0	115.2	40	77.0	105.6	
3	119.1	163.3	22	83.5	114.5	41	76.8	105.3	
4	111.9	153.4	23	82.9	113.7	42	76.9	105.4	
5	106.4	145.9	24	82.3	112.8	43	76.4	105.2	
6	102.8	140.9	25	81.9	112.3	44	76.4	104.7	
7	99.6	136.6	26	81.5	111.7	45	76.2	104.5	
8	97.1	133.1	27	81.0	111.1	46	76.0	104.2	
9	95.6	131.1	28	80.6	110.5	47	75.8	103.9	
10	95.1	130.4	29	80.3	110.1	48	75.6	103.6	
11	93.2	127.8	30	79.9	109.5	49	75.4	103.4	
12	91.6	125.6	31	79.6	109.1	50	75.2	103.1	
13	90.0	123.4	32	79.3	108.7	51	75.1	103.0	
14	89.0	122.0	33	78.9	108.2	52	74.9	102.7	
15	87.6	120.1	34	78.6	107.8	53	74.7	102.4	
16	87.0	119.3	35	78.4	107.5	54	74.5	102.1	
17	86.3	118.3	36	78.1	107.1	55	74.4	102.0	
$T_H$ $75^{\circ}\text{F}$		$T_T$ $30^{\circ}\text{F}$		$S_H$ 0.539 RPS		WIRE GAUGE NO. 24		REF. FIG. NO. 23	
0.25	195.9	268.6	18	90.0	123.4	37	81.5	101.7	
0.5	162.9	223.3	19	89.4	122.6	38	81.2	101.3	
1	141.9	194.5	20	88.6	121.5	39	80.9	100.9	
2	127.9	175.4	21	87.7	120.2	40	80.6	100.5	
3	122.9	168.5	22	87.3	119.7	41	80.2	100.0	
4	119.9	164.4	23	86.6	118.7	42	80.0	109.7	
5	117.5		24	86.1	118.0	43	79.8	109.4	
6	115.9	158.9	25	85.7	117.5	44	79.6	109.1	
7	111.9	153.4	26	85.3	116.9	45	79.4	108.9	
8	107.9	147.9	27	84.8	116.3	46	79.2	108.6	
9	103.9	142.4	28	84.4	115.7	47	79.0	108.3	
10	100.7	138.1	29	83.9	115.0	48	78.8	108.0	
11	98.5	135.0	30	83.6	114.6	49	78.6	107.8	
12	96.9	132.8	31	83.2	114.1	50	78.4	107.5	
13	95.1	130.4	32	82.9	113.7	51	78.2	107.2	
14	93.9	128.7	33	82.6	113.2	52	78.0	106.9	
15	92.8	127.2	34	82.2	112.7	53	77.8	106.7	
16	91.7	125.7	35	81.9	112.3	54	77.6	106.4	
17	90.9	124.6	36	81.7	112.0	55	77.5	106.3	



## SHEAR STRESS DECAY DATA

$T_H$ 75°F		$T_T$ 30°F		$S_H$ 0.540 RPS		WIRE GAUGE NO. 24		REF. FIG. NO. 23	
TIME OF TEST (min.)	BOB DEFL. (°)	$T \times 10^3$ $\text{lb}_f/\text{ft}^2$	TIME OF TEST (min.)	BOB DEFL. (°)	$T \times 10^3$ $\text{lb}_f/\text{ft}^2$	TIME OF TEST (min.)	BOB DEFL. (°)	$T \times 10^3$ $\text{lb}_f/\text{ft}^2$	
0.25	190.2	260.8	18	84.6	116.0	37	76.7	105.2	
0.5	162.2	222.4	19	84.0	115.2	38	76.5	104.9	
1	141.2	193.6	20	83.2	114.1	39	76.3	104.6	
2	126.2	193.6	21	82.7	113.4	40	76.0	104.2	
3	119.4	163.7	22	82.2	112.7	41	75.8	103.9	
4	115.2	157.9	23	81.7	112.0	42	75.7	103.8	
5	109.6	150.3	24	81.2	111.3	43	75.4	103.4	
6	103.7	142.2	25	80.8	110.8	44	75.1	103.0	
7	100.0	137.1	26	80.3	110.1	45	74.9	102.7	
8	97.2	133.3	27	79.9	109.5	46	74.7	102.4	
9	94.8	130.0	28	79.6	109.1	47	74.5	102.1	
10	92.8	127.2	29	79.2	108.6	48	74.3	101.9	
11	91.4	125.3	30	78.9	108.2	49	74.2	101.7	
12	90.0	123.4	31	78.6	107.8	50	74.0	101.5	
13	89.8	123.1	32	78.2	107.2	51	73.8	101.2	
14	87.9	120.5	33	77.9	106.8	52	73.7	101.1	
15	87.0	119.3	34	77.7	106.5	53	73.5	100.8	
16	86.0	117.9	35	77.4	106.1	54	73.3	100.5	
17	85.7	117.5	36	77.0	105.6	55	73.2	100.3	
$T_H$ 75°F		$T_T$ 30°F		$S_H$ 0.539 RPS		WIRE GAUGE NO. 22		REF. FIG. NO. 23	
0.25	76.7	279.6	18	33.5	122.1	37	30.6	111.6	
0.5	64.7	235.9	19	33.3	121.4	38	30.5	111.2	
1	56.7	206.7	20	33.1	120.7	39	30.5	111.2	
2	50.2	183.0	21	32.9	120.0	40	30.4	110.8	
3	46.2	168.4	22	32.7	119.2	41	30.3	110.5	
4	44.4	161.9	23	32.5	118.5	42	30.2	110.1	
5	42.4	154.6	24	32.3	117.8	43	30.2	110.1	
6	40.8	148.8	25	32.2	117.4	44	30.1	109.7	
7	39.3	143.3	26	32.0	116.7	45	30.0	109.4	
8	38.3	139.6	27	31.8	115.9	46	29.9	109.0	
9	37.4	136.4	28	31.7	115.6	47	29.8	108.7	
10	36.8	134.2	29	31.5	114.8	48	29.8	108.7	
11	36.3	132.3	30	31.4	114.5	49	29.7	108.3	
12	35.7	130.2	31	31.3	114.1	50	29.6	107.9	
13	35.3	128.7	32	31.2	113.8	51	29.6	107.9	
14	34.9	127.2	33	31.0	113.0	52	29.6	107.9	
15	34.5	125.8	34	30.9	112.7	53	29.5	107.6	
16	34.0	124.0	35	30.8	112.3	54	29.5	107.6	
17	33.8	123.2	36	30.7	111.9	55	29.5	107.6	



## SHEAR STRESS DECAY DATA

$T_H$ 75°F		$T_T$ 30°F		$S_H$ 0.537 RPS		WIRE GAUGE NO. 22		REF. FIG. NO. 23	
TIME OF TEST (min.)	BOB DEFL. (°)	$T \times 10^3$ $lb_f/ft^2$	TIME OF TEST (min.)	BOB DEFL. (°)	$T \times 10^3$ $lb_f/ft^2$	TIME OF TEST (min.)	BOB DEFL. (°)	$T \times 10^3$ $lb_f/ft^2$	
0.25	70.1	255.6	18	33.6	122.5	37	30.5	111.2	
0.5	59.6	217.3	19	33.3	121.4	38	30.4	110.8	
1	52.1	190.0	20	33.0	120.3	39	30.3	110.5	
2	46.4	169.2	21	32.7	119.2	40	30.2	110.1	
3	43.6	159.0	22	32.6	118.9	41	30.1	109.7	
4	42.6	155.3	23	32.5	118.5	42	30.1	109.7	
5	42.2	153.9	23	32.3	117.8	43	30.0	109.4	
6	41.6	151.7	25	32.1	117.0	44	30.0	109.4	
7	40.1	146.2	26	31.9	116.3	45	29.9	109.0	
8	38.8	141.5	27	31.7	115.6	46	29.8	108.7	
9	38.2	139.3	28	31.6	115.2	47	29.8	108.7	
10	37.2	135.6	29	31.5	114.8	48	29.7	108.3	
11	36.6	133.4	30	31.3	114.1	49	29.6	107.9	
12	35.9	130.9	31	31.2	113.8	50	29.6	107.9	
13	35.3	128.7	32	31.1	113.4	51	29.5	107.6	
14	34.8	126.9	33	31.0	113.0	52	29.4	107.2	
15	34.5	125.8	34	30.8	112.3	53	29.4	107.2	
16	34.2	124.7	35	30.7	111.9	54	29.3	106.8	
17	33.8	123.2	36	30.6	111.6	55	29.2	106.5	
$T_H$ 75°F		$T_T$ 30°F		$S_H$ 2.501 RPS		WIRE GAUGE NO. 22		REF. FIG. NO. 24	
0.25	104.8	382.1	18	58.7	214.0	37	56.0	204.2	
0.5	94.8	345.6	19	58.4	212.9	38	55.9	203.8	
1	85.8	312.8	20	58.3	212.6	39	55.9	203.8	
2	75.4	274.9	21	58.0	211.5	40	55.8	203.4	
3	70.1	255.6	22	57.9	211.0	41	55.8	203.4	
4	67.3	245.4	23	57.7	210.4	42	55.7	203.1	
5	65.4	238.4	24	57.5	209.6	43	55.6	202.7	
6	64.3	234.4	25	57.3	208.9	44	55.5	202.4	
7	63.3	230.8	26	57.2	208.6	45	55.4	202.0	
8	62.4	227.5	27	57.1	208.2	46	55.4	201.6	
9	61.4	225.3	28	56.9	207.5	47	55.3	201.6	
10	61.3	223.5	29	56.8	207.1	48	55.2	201.3	
11	60.8	221.7	30	56.7	206.7	49	55.1	200.9	
12	60.4	220.2	31	56.7	206.7	50	55.0	200.5	
13	60.0	218.8	32	56.6	206.4	51	55.0	200.5	
14	59.7	217.7	33	56.4	205.6	52	54.9	200.2	
15	59.4	216.6	34	56.3	205.3	53	54.9	200.2	
16	59.2	215.8	35	56.2	204.9	54	54.8	199.8	
17	58.9	214.7	36	56.1	204.5	55	54.7	199.4	



## SHEAR STRESS DECAY DATA

$T_H$ 75°F		$T_T$ 30°F		$S_H$ 2.496 RPS		WIRE GAUGE NO. 22		REF. FIG. NO. 24	
TIME OF TEST (min.)	BOB DEFL. (°)	$T \times 10^3$ $\text{lb}_f/\text{ft}^2$	TIME OF TEST (min.)	BOB DEFL. (°)	$T \times 10^3$ $\text{lb}_f/\text{ft}^2$	TIME OF TEST (min.)	BOB DEFL. (°)	$T \times 10^3$ $\text{lb}_f/\text{ft}^2$	
0.25	101.5	370.1	18	59.0	215.1	37	56.6	206.4	
0.5	92.5	337.3	19	58.8	214.4	38	56.6	206.4	
1	85.5	311.7	20	58.6	213.7	39	56.5	206.0	
2	77.5	282.6	21	58.4	212.9	40	56.4	205.6	
3	71.5	260.7	22	58.2	212.2	41	56.3	205.3	
4	68.0	247.9	23	58.0	211.5	42	56.2	204.9	
5	66.0	240.1	24	57.9	211.1	43	56.2	204.9	
6	64.7	235.9	25	57.8	210.7	44	56.1	204.5	
7	63.8	232.6	26	57.6	210.0	45	56.0	204.2	
8	62.8	229.0	27	57.5	209.6	46	56.0	204.2	
9	62.2	226.8	28	57.4	209.3	47	56.0	204.2	
10	61.6	224.6	29	57.3	208.9	48	55.9	203.8	
11	61.2	223.1	30	57.2	208.6	49	55.8	203.4	
12	60.7	221.3	31	57.1	208.2	50	55.8	203.4	
13	60.5	220.6	32	57.0	207.8	51	55.8	203.4	
14	60.1	219.1	33	56.9	207.5	52	55.7	203.1	
15	59.9	218.3	34	56.9	207.5	53	55.7	203.1	
16	59.6	217.3	35	56.8	207.1	54	55.7	203.1	
17	59.3	216.2	36	56.7	206.7	55	55.7	203.1	
$T_H$ 75°F		$T_T$ 30°F		$S_H$ 2.500 RPS		WIRE GAUGE NO. 22		REF. FIG. NO. 24	
0.25	106.8	389.4	18	59.8	218.0	37	57.1	208.2	
0.5	96.8	352.9	19	59.6	217.3	38	57.1	208.2	
1	85.0	309.9	20	59.3	216.2	39	57.0	207.8	
2	75.5	275.3	21	59.2	215.8	40	56.9	207.5	
3	71.3	260.0	22	59.0	215.1	41	56.8	207.1	
4	68.9	251.2	23	58.8	214.3	42	56.7	206.7	
5	67.0	244.3	24	58.7	214.0	43	56.7	206.7	
6	66.1	241.0	25	58.5	213.3	44	56.6	206.4	
7	64.8	236.3	26	58.4	212.9	45	56.5	206.0	
8	64.1	233.7	27	58.2	212.2	46	56.4	205.6	
9	63.4	213.2	28	58.1	211.8	47	56.4	205.6	
10	62.7	228.6	29	58.0	211.5	48	56.4	205.6	
11	62.2	226.8	30	57.8	210.7	49	56.3	205.3	
12	61.7	225.0	31	57.7	210.4	50	56.3	205.3	
13	61.4	223.4	32	57.6	210.0	51	56.2	204.9	
14	61.0	222.4	33	57.5	209.6	52	56.1	204.5	
15	60.7	221.3	34	57.4	209.3	53	56.0	204.2	
16	60.4	220.2	35	57.3	208.9	54	56.0	204.2	
17	60.1	219.0	35	57.2	208.6	55	56.0	204.2	



## SHEAR STRESS DECAY DATA

$T_H$ 75°F		$T_T$ 30°F		$S_H$ 2.503 RPS		WIRE GAUGE NO. 22		REF. FIG. NO. 24	
TIME OF TEST (min.)	BOB DEFL. (°)	$\tau \times 10^3$ $lb_f/ft^2$	TIME OF TEST (min.)	BOB DEFL. (°)	$\tau \times 10^3$ $lb_f/ft^2$	TIME OF TEST (min.)	BOB DEFL. (°)	$\tau \times 10^3$ $lb_f/ft^2$	
0.25	99.9	364.2	18	58.8	214.4	37	56.0	204.2	
0.5	88.2	321.6	19	58.5	213.3	38	55.9	203.8	
1	80.1	292.0	20	58.4	212.9	39	55.8	203.4	
2	72.7	265.1	21	58.2	212.2	40	55.7	203.1	
3	69.1	251.9	22	58.0	211.5	41	55.6	202.7	
4	66.9	243.9	23	57.8	210.7	42	55.5	202.4	
5	65.6	239.2	24	57.6	210.0	43	55.4	202.0	
6	64.4	234.8	25	57.4	209.3	44	55.3	201.6	
7	63.6	231.9	26	57.3	208.9	45	55.2	201.3	
8	62.8	229.0	27	57.1	208.2	46	55.1	200.9	
9	62.1	226.4	28	57.1	208.2	47	55.0	200.5	
10	61.6	224.6	29	57.0	207.8	48	54.9	200.2	
11	61.6	222.8	30	56.8	207.1	49	54.8	199.8	
12	60.7	221.3	31	56.7	206.7	50	54.7	199.4	
13	60.3	219.9	32	56.5	206.0	51	54.6	199.1	
14	60.1	219.1	33	56.4	205.6	52	54.5	198.7	
15	59.7	217.7	34	56.3	205.3	53	54.4	198.3	
16	59.3	216.2	35	56.2	204.9	54	54.4	198.3	
17	59.1	215.5	36	56.1	204.5	55	54.4	198.3	
$T_H$ 75°F		$T_T$ 30°F		$S_H$ 2.500 RPS		WIRE GAUGE NO. 22		REF. FIG. NO. 24	
0.25	106.1	386.8	18	61.9	225.7	37	58.8	214.4	
0.5	94.6	312.1	19	61.7	225.0	38	58.7	214.0	
1	85.6	312.1	20	61.5	224.2	39	58.6	213.7	
2	77.1	281.1	21	61.2	223.1	40	58.5	213.3	
3	73.4	267.6	22	60.9	222.0	41	58.4	212.9	
4	70.9	258.5	23	60.7	221.3	42	58.3	212.6	
5	69.2	252.3	24	60.6	220.9	43	58.2	212.2	
6	67.9	247.6	25	60.5	220.5	44	58.1	211.8	
7	66.7	243.1	26	60.3	219.9	45	58.1	211.8	
8	65.9	240.3	27	60.1	219.1	46	58.0	211.5	
9	65.3	238.1	28	60.0	218.8	47	57.9	211.1	
10	64.8	236.3	29	59.9	218.4	48	57.8	210.7	
11	64.2	234.1	30	59.7	217.7	49	57.7	210.4	
12	63.8	232.6	31	59.6	217.3	50	57.6	210.0	
13	63.4	231.2	32	59.4	216.6	51	57.5	209.6	
14	63.1	230.1	33	59.2	215.8	52	57.4	209.3	
15	62.7	228.6	34	59.1	215.5	53	57.3	208.9	
16	62.4	227.5	35	59.0	215.1	54	57.3	208.9	
17	62.1	226.4	36	58.9	214.7	55	57.2	208.6	



## SHEAR STRESS DECAY DATA

$T_H$ 75°F		$T_T$ 30°F		$S_H$ 4.505 RPS		WIRE GAUGE NO. 22		REF. FIG.
TIME OF TEST (min.)	BOB DEFL. (°)	$\tau \times 10^3$ $lb_f/ft^2$	TIME OF TEST (min.)	BOB DEFL. (°)	$\tau \times 10^3$ $lb_f/ft^2$	TIME OF TEST (min.)	BOB DEFL. (°)	$\tau \times 10^3$ $lb_f/ft^2$
0.25	142.9	521	18	84.3	307	37	80.4	293
0.5	124.9	455	19	84.1	307	38	80.3	293
1	112.1	409	20	83.7	305	39	80.2	292
2	102.9	375	21	83.4	304	40	80.1	292
3	98.4	359	22	83.1	303	41	79.9	291
4	95.2	347	23	82.8	302	42	79.8	291
5	93.4	341	24	82.6	301	43	79.7	291
6	92.9	339	25	82.4	300	44	79.6	290
7	90.6	330	26	82.2	300	45	79.4	289
8	89.7	327	27	82.1	299	46	79.3	289
9	88.8	324	28	82.0	299	47	79.2	289
10	88.1	321	29	81.8	298	48	79.0	288
11	87.5	319	30	81.7	298	49	78.9	288
12	86.8	316	31	81.5	297	50	78.8	287
13	86.3	315	32	81.3	296	51	78.7	287
14	85.8	313	33	81.1	296	52	78.6	287
15	85.4	311	34	80.9	295	53	78.5	286
16	85.0	310	35	80.8	295	54	78.4	286
17	84.6	308	36	80.6	294	55	78.3	285
$T_H$ 75°F		$T_T$ 30°F		$S_H$ 4.503 RPS		WIRE GAUGE NO. 22		REF. FIG.
0.25	133.2	486	18	83.8	306	37	79.9	291
0.5	120.7	440	19	83.5	304	38	79.8	291
1	109.7	400	20	83.2	303	39	79.7	291
2	101.9	372	21	83.0	303	40	79.5	290
3	98.1	358	22	82.8	302	41	79.4	289
4	94.2	343	23	82.5	301	42	78.3	285
5	92.2	336	24	82.3	300	43	78.2	285
6	91.0	332	25	82.0	299	44	78.0	284
7	89.8	327	26	81.9	299	45	78.0	284
8	88.7	323	27	81.7	298	46	77.9	284
9	87.8	320	28	81.5	297	47	77.8	284
10	87.2	318	29	81.2	296	48	77.6	283
11	85.6	316	30	81.1	296	49	77.5	283
12	86.1	314	31	89.9	295	50	77.4	282
13	85.6	312	32	80.7	294	51	77.3	282
14	85.2	311	33	80.5	294	52	77.2	281
15	84.8	309	34	80.3	293	53	77.1	281
16	84.3	307	35	80.2	292	54	77.0	281
17	84.1	307	36	80.0	292	55	77.0	281



## SHEAR STRESS DECAY DATA

$T_H$ 75°F		$T_T$ 30°F		$S_H$ 4.505 RPS		WIRE GAUGE NO. 22		REF. FIG. NO. 25	
TIME OF TEST (min.)	BOB DEFL. (°)	$T \times 10^3$ $lb_f/ft^2$	TIME OF TEST (min.)	BOB DEFL. (°)	$T \times 10^3$ $lb_f/ft^2$	TIME OF TEST (min.)	BOB DEFL. (°)	$T \times 10^3$ $lb_f/ft^2$	
0.25	140.7	513	18	83.2	303	37	79.0	288	
0.5	125.7	458	19	82.8	302	38	78.9	288	
1	113.2	413	20	82.5	301	39	78.8	287	
2	102.8	375	21	82.2	300	40	78.7	287	
3	97.8	357	22	81.9	299	41	78.6	287	
4	94.9	346	23	81.7	298	42	78.5	286	
5	92.8	338	24	81.4	297	43	78.3	285	
6	91.3	333	25	81.2	296	44	78.2	285	
7	89.8	327	26	81.0	295	45	78.1	285	
8	88.8	324	27	80.8	295	46	78.0	284	
9	87.8	320	28	80.6	294	47	77.8	284	
10	87.1	318	29	80.4	293	48	77.7	283	
11	86.4	315	30	80.2	292	49	77.6	283	
12	85.7	312	31	80.0	292	50	77.5	283	
13	85.4	311	32	79.8	291	51	77.4	282	
14	84.8	309	33	79.6	290	52	77.3	282	
15	84.3	307	34	79.4	289	53	77.2	281	
16	83.9	306	35	79.2	289	54	77.1	281	
17	83.5	304	36	79.1	288	55	77.0	281	
$T_H$ 75°F		$T_T$ 30°F		$S_H$ 4.510 RPS		WIRE GAUGE NO. 22		REF. FIG. NO. 25	
0.25	138.7	506	18	82.8	302	37	78.3	285	
0.5	123.7	451	19	82.5	301	38	78.2	285	
1	112.0	408	20	82.2	300	39	78.0	284	
2	103.7	378	21	81.8	298	40	77.8	284	
3	98.0	357	22	81.5	297	41	77.7	283	
4	94.8	346	23	81.2	296	42	77.6	283	
5	92.8	338	24	80.9	295	43	77.4	282	
6	91.4	333	25	80.6	294	44	77.3	282	
7	89.8	327	26	80.3	293	45	77.2	281	
8	88.8	324	27	80.1	292	46	77.1	281	
9	87.8	320	28	79.9	291	47	76.9	280	
10	86.9	317	29	79.6	290	48	76.8	280	
11	86.2	314	30	79.4	289	49	76.7	280	
12	85.5	312	31	79.2	289	50	76.6	279	
13	85.0	310	32	79.0	288	51	76.5	279	
14	84.5	308	33	78.8	287	52	76.4	279	
15	84.0	306	34	78.6	287	53	76.3	278	
16	83.6	305	35	78.5	286	54	76.2	278	
17	83.2	303	36	78.4	286	55	76.1	277	



## SHEAR STRESS DECAY DATA

$T_H$ 75°F		$T_T$ 30°F		$S_H$ 4.526 RPS		WIRE GAUGE NO. 22		REF. FIG.
TIME OF TEST (min.)	BOB DEFL. (°)	$\tau \times 10^3$ $lb_f/ft^2$	TIME OF TEST (min.)	BOB DEFL. (°)	$\tau \times 10^3$ $lb_f/ft^2$	TIME OF TEST (min.)	BOB DEFL. (°)	$\tau \times 10^3$ $lb_f/ft^2$
0.25	142.7	520	18	85.6	312	37	81.8	298
0.5	128.7	469	19	85.3	311	38	81.6	298
1	115.2	420	20	85.0	310	39	81.4	297
2	104.7	382	21	84.7	309	40	81.2	296
3	100.3	366	22	84.5	308	41	81.1	296
4	97.2	354	23	84.3	307	42	81.0	295
5	95.0	346	24	84.0	306	43	80.9	295
6	93.4	340	25	83.8	306	44	80.8	295
7	90.8	331	26	83.6	305	45	80.7	294
8	90.1	329	27	83.4	304	46	80.6	294
9	89.5	326	28	83.2	303	47	80.4	293
10	88.7	323	29	83.0	303	48	80.3	293
11	88.2	322	30	82.8	302	49	80.2	292
12	87.9	320	31	82.6	301	50	80.1	292
13	87.7	320	32	82.3	300	51	80.0	292
14	87.2	318	33	82.3	300	52	79.9	291
15	86.7	316	34	82.2	300	53	79.8	291
16	86.4	315	35	82.1	299	54	79.7	291
17	86.0	314	36	82.0	299	55	79.6	290
$T_H$ 15°F		$T_T$ 60°F		$S_H$ 0.524 RPS		WIRE GAUGE NO. 28		REF. FIG.
0.25			18	91.4	16.3	37	87.1	15.5
0.5	127.9	22.8	19	91.0	16.2	38	87.0	15.5
1	118.1	21.1	20	90.6	16.2	39	86.8	15.5
2	109.4	19.5	21	90.3	16.1	40	86.7	15.5
3	104.9	18.7	22	90.0	16.1	41	86.7	15.5
4	102.6	18.3	23	89.8	16.0	42	86.6	15.5
5	100.7	18.0	24	89.5	16.0	43	86.5	15.4
6	99.4	17.7	25	89.1	15.9	44	86.3	15.4
7	98.2	17.5	26	88.8	15.8	45	86.2	15.4
8	97.2	17.3	27	88.6	15.8	46	86.1	15.4
9	96.6	17.2	28	88.8	15.8	47	86.0	15.3
10	95.7	17.1	29	88.6	15.8	48	85.9	15.3
11	95.1	17.0	30	88.3	15.8	49	85.8	15.3
12	94.4	16.8	31	88.0	15.7	50	85.6	15.3
13	93.8	16.7	32	87.8	15.7	51	85.5	15.3
14	92.7	16.5	33	87.6	15.6	52	85.4	15.2
15	92.4	16.5	34	87.4	15.6	53	85.1	15.2
16	91.9	16.4	35	87.3	15.6	54	85.0	15.2
17	91.7	16.4	36	87.2	15.6	55	84.9	15.2



## SHEAR STRESS DECAY DATA

$T_H$ 15°F		$T_T$ 60°F		$S_H$ 0.524 RPS		WIRE GAUGE NO. 28		REF. FIG. NO. 50	
TIME OF TEST (min.)	BOB DEFL. (°)	$\tau \times 10^3$ $lb_f/ft^2$	TIME OF TEST (min.)	BOB DEFL. (°)	$\tau \times 10^3$ $lb_f/ft^2$	TIME OF TEST (min.)	BOB DEFL. (°)	$\tau \times 10^3$ $lb_f/ft^2$	
0.25			18	92.4	16.5	37	-87.1	15.5	
0.5	129.4	23.1	19	92.0	16.4	38	87.0	15.5	
1	120.6	21.5	20	91.6	16.3	39	86.9	15.5	
2	111.6	19.9	21	91.2	16.3	40	86.7	15.5	
3	107.6	19.2	22	90.9	16.2	41	86.5	15.4	
4	104.6	18.7	23	90.6	16.2	42	86.4	15.4	
5	102.4	18.3	24	90.3	16.1	43	86.2	15.4	
6	100.4	17.9	25	89.9	16.0	44	86.1	15.4	
7	99.4	17.7	26	89.7	16.0	45	86.0	15.3	
8	98.4	17.6	27	89.4	16.0	46	85.8	15.3	
9	97.5	17.4	28	89.1	15.9	47	85.7	15.3	
10	96.6	17.2	29	88.8	15.8	48	85.5	15.3	
11	95.8	17.1	30	88.6	15.8	49	85.4	15.2	
12	95.1	17.0	31	88.3	15.8	50	85.8	15.3	
13	94.6	16.9	32	88.1	15.7	51	86.1	15.4	
14	94.1	16.8	33	87.8	15.7	52	85.7	15.3	
15	93.7	16.7	34	87.6	15.6	53	85.8	15.3	
16	93.1	16.6	35	87.4	15.6	54	85.5	15.3	
17	92.8	16.6	36	87.2	15.6	55	85.4	15.2	
$T_H$ 15°F		$T_T$ 60°F		$S_H$ 0.525 RPS		WIRE GAUGE NO. 28		REF. FIG. NO. 50	
0.25			18	91.0	16.2	37	86.4	15.4	
0.5	125.8	22.4	19	90.5	16.2	38	86.2	15.4	
1	116.0	20.7	20	90.2	16.1	39	86.0	15.3	
2	107.8	19.2	21	90.0	16.1	40	85.8	15.3	
3	104.3	18.6	22	89.8	16.0	41	85.6	15.3	
4	101.5	18.1	23	89.6	16.0	42	85.4	15.2	
5	99.4	17.7	24	89.3	15.9	43	85.3	15.2	
6	98.3	17.5	25	89.0	15.9	44	85.2	15.2	
7	97.5	17.4	26	88.6	15.8	45	85.0	15.2	
8	96.8	17.3	27	88.3	15.8	46	84.8	15.1	
9	96.1	17.1	28	88.1	15.7	47	84.7	15.1	
10	95.4	17.0	29	87.8	15.7	48	84.6	15.1	
11	94.8	16.9	30	87.6	15.6	49	84.5	15.1	
12	94.3	16.8	31	87.4	15.6	50	84.4	15.1	
13	93.7	16.7	32	87.2	15.6	51	84.4	15.1	
14	93.0	16.6	33	87.0	15.5	52	84.4	15.1	
15	92.4	16.5	34	86.8	15.5	53	84.3	15.0	
16	92.0	16.4	35	86.6	15.5	54	84.3	15.0	
17	91.5	16.3	36	86.5	15.4	55	84.2	15.0	



## SHEAR STRESS DECAY DATA

$T_H$ $15^{\circ}\text{F}$		$T_T$ $60^{\circ}\text{F}$		$S_H$ 0.527 RPS		WIRE GAUGE NO. 26		REF. FIG. NO. 50	
TIME OF TEST (min.)	BOB DEFL. (°)	$\tau \times 10^3$ $\text{lb}_f/\text{ft}^2$	TIME OF TEST (min.)	BOB DEFL. (°)	$\tau \times 10^3$ $\text{lb}_f/\text{ft}^2$	TIME OF TEST (min.)	BOB DEFL. (°)	$\tau \times 10^3$ $\text{lb}_f/\text{ft}^2$	
0.25			18	26.2	16.1	37	25.0	15.4	
0.5	35.4	21.8	19	26.1	16.1	38	25.0	15.4	
1	32.8	20.2	20	26.0	16.0	39	24.9	15.3	
2	30.9	19.0	21	25.9	16.0	40	24.9	15.3	
3	29.7	18.3	22	25.9	16.0	41	24.8	15.3	
4	28.9	17.8	23	25.8	15.9	42	24.8	15.3	
5	28.5	17.6	24	25.8	15.9	43	24.7	15.2	
6	28.2	17.4	25	25.7	15.8	44	24.7	15.2	
7	27.8	17.1	26	25.7	15.8	45	24.7	15.2	
8	27.5	16.9	27	25.6	15.8	46	24.6	15.2	
9	27.8	17.1	28	25.5	15.7	47	24.6	15.2	
10	27.6	17.0	29	25.5	15.7	48	24.6	15.2	
11	27.3	16.8	30	25.4	15.6	49	24.5	15.1	
12	27.1	16.7	31	25.4	15.6	50	24.6	15.2	
13	26.9	16.6	32	25.3	15.6	51	24.6	15.2	
14	26.7	16.4	33	25.3	15.6	52	24.5	15.1	
15	26.5	16.3	34	25.2	15.5	53	24.5	15.1	
16	26.4	16.3	35	25.1	15.5	54	24.5	15.1	
17	26.3	16.2	36	25.0	15.4	55	24.5	15.1	
$T_H$ $15^{\circ}\text{F}$		$T_T$ $60^{\circ}\text{F}$		$S_H$ 0.511 RPS		WIRE GAUGE NO. 26		REF. FIG. NO. 50	
0.25			18	25.8	15.9	37	24.5	15.1	
0.5	36.0	22.2	19	25.7	15.8	38	24.5	15.1	
1	33.3	20.5	20	25.6	15.8	39	24.4	15.0	
2	30.9	19.0	21	25.5	15.7	40	24.4	15.0	
3	29.9	18.4	22	25.4	15.6	41	24.3	15.0	
4	29.1	17.9	23	25.4	15.6	42	24.3	15.0	
5	28.5	17.6	24	25.3	15.6	43	24.2	14.9	
6	28.2	17.4	25	25.2	15.5	44	24.2	14.9	
7	27.9	17.2	26	25.1	15.5	45	24.2	14.9	
8	27.6	17.0	27	25.1	15.5	46	24.2	14.9	
9	27.3	16.8	28	25.0	15.4	47	24.1	14.8	
10	27.0	16.6	29	25.0	15.4	48	24.1	14.8	
11	26.8	16.5	30	24.9	15.3	49	24.0	14.8	
12	26.6	16.4	31	24.8	15.3	50	24.0	14.8	
13	26.4	16.3	32	24.8	15.3	51	23.9	14.7	
14	26.2	16.1	33	24.7	15.2	52	23.9	14.7	
15	26.1	16.1	34	24.7	15.2	53	23.9	14.7	
16	26.0	16.0	35	24.6	15.1	54	23.9	14.7	
17	25.9	16.0	36	24.6	15.1	55	23.8	14.7	



## SHEAR STRESS DECAY DATA

$T_H$ 15°F		$T_T$ 60°F		$S_H$		WIRE		REF. FIG.	
				2.530 RPS		GAUGE NO. 26		NO. 51	
TIME OF TEST (min.)	BOB DEFL. (°)	$\tau \times 10^3$ $\text{lb}_f/\text{ft}^2$	TIME OF TEST (min.)	BOB DEFL. (°)	$\tau \times 10^3$ $\text{lb}_f/\text{ft}^2$	TIME OF TEST (min.)	BOB DEFL. (°)	$\tau \times 10^3$ $\text{lb}_f/\text{ft}^2$	
0.25			18	82.1	50.5	37	79.2	48.8	
0.5	99.9	61.5	19	81.9	50.4	38	79.1	48.7	
1	96.0	59.1	20	81.7	50.3	39	79.0	48.6	
2	92.2	56.8	21	81.5	50.2	40	78.9	48.6	
3	89.9	55.4	22	81.3	50.1	41	78.8	48.5	
4	88.6	54.6	23	81.1	49.9	42	78.8	48.5	
5	87.6	53.9	24	80.9	49.8	43	78.7	48.5	
6	86.7	53.4	25	80.7	49.7	44	78.7	48.5	
7	86.0	53.0	26	80.5	49.6	45	78.6	48.4	
8	85.4	52.6	27	80.4	49.5	46	78.5	48.3	
9	84.9	52.3	28	80.2	49.4	47	78.5	48.3	
10	84.4	52.0	29	80.1	49.3	48	78.4	48.3	
11	84.0	51.7	30	79.9	49.2	49	78.4	48.3	
12	83.7	51.5	31	79.8	49.1	50	78.3	48.2	
13	83.4	51.3	32	79.7	49.1	51	78.2	48.1	
14	83.0	51.1	33	79.6	49.0	52	78.1	48.1	
15	82.7	50.9	34	79.5	48.9	53	78.0	48.0	
16	82.5	50.8	35	79.4	48.9	54	78.0	48.0	
17	82.3	50.7	36	79.3	48.8	55	77.9	48.0	
$T_H$ 15°F		$T_T$ 60°F		$S_H$		WIRE		REF. FIG.	
				2.521 RPS		GAUGE NO. 26		NO. 51	
0.25			18	79.1	48.7	37	77.0	47.4	
0.5	95.0	58.5	19	78.9	48.6	38	76.8	47.3	
1	91.2	56.2	20	78.7	48.5	39	76.7	47.2	
2	89.2	54.9	21	78.5	48.3	40	76.6	47.2	
3	85.9	52.9	22	78.3	48.2	41	76.6	47.1	
4	84.7	52.1	23	78.2	48.1	42	76.5	47.1	
5	83.7	51.5	24	78.0	48.0	43	76.4	47.0	
6	82.9	51.0	25	77.9	48.0	44	76.4	47.0	
7	82.4	50.7	26	77.8	47.9	45	76.4	47.0	
8	81.9	50.4	27	77.7	47.8	46	76.3	47.0	
9	81.4	50.1	28	77.6	47.8	47	76.2	46.9	
10	81.0	49.9	29	77.6	47.8	48	76.2	46.9	
11	80.7	49.7	30	77.5	47.7	49	76.1	46.9	
12	80.5	49.6	31	77.5	47.7	50	76.1	46.9	
13	80.3	49.4	32	77.4	47.7	51	76.0	46.8	
14	80.1	49.3	33	77.3	47.6	52	76.0	46.8	
15	79.8	49.1	34	77.3	47.6	53	75.9	46.7	
16	79.5	48.9	35	77.2	47.5	54	75.9	46.7	
17	79.3	48.8	36	77.1	47.5	55	75.8	46.7	



## SHEAR STRESS DECAY DATA

$T_H$ 15°F		$T_T$ 60°F		$S_H$ 2.531 RPS		WIRE GAUGE NO. 26		REF. FIG. NO. 51	
TIME OF TEST (min.)	BOB DEFL. (°)	$T \times 10^3$ $\text{lb}_f/\text{ft}^2$	TIME OF TEST (min.)	BOB DEFL. (°)	$T \times 10^3$ $\text{lb}_f/\text{ft}^2$	TIME OF TEST (min.)	BOB DEFL. (°)	$T \times 10^3$ $\text{lb}_f/\text{ft}^2$	
0.25			18	81.4	50.1	37	78.5	48.3	
0.5	99.7	61.4	19	812	50.0	38	78.4	48.3	
1	95.8	59.0	20	81.0	49.9	39	78.3	48.2	
2	92.1	56.7	21	80.8	49.7	40	78.2	48.1	
3	89.9	55.4	22	80.6	49.6	41	78.1	48.1	
4	88.5	54.5	23	80.4	49.5	42	78.0	48.0	
5	87.4	53.8	24	80.2	49.4	43	77.9	48.0	
6	86.5	53.3	25	80.0	49.3	44	77.8	47.9	
7	85.9	52.9	26	79.9	49.2	45	77.7	47.8	
8	85.2	52.5	27	79.7	49.1	46	77.6	47.8	
9	84.6	52.1	28	79.6	49.0	47	77.5	47.7	
10	84.0	51.7	29	75.5	48.9	48	77.4	47.7	
11	83.6	51.5	30	79.4	48.9	49	77.3	47.6	
12	83.2	51.2	31	79.3	48.8	50	77.2	47.5	
13	82.9	51.0	32	79.2	48.8	51	77.2	47.5	
14	82.5	50.8	33	79.0	48.6	52	77.1	47.5	
15	82.2	50.6	34	78.9	48.6	53	77.0	47.4	
16	81.9	50.4	35	78.8	48.5	54	76.9	47.3	
17	81.6	50.2	36	78.7	48.5	55	76.8	47.3	
$T_H$ 15°F		$T_T$ 60°F		$S_H$ 2.502 RPS		WIRE GAUGE NO. 26		REF. FIG. NO. 51	
0.25			18	80.1	49.3	37	77.1	47.5	
0.5	98.1	60.4	19	79.8	49.1	38	77.0	47.4	
1	93.9	57.8	20	79.6	49.0	39	76.9	47.3	
2	90.1	55.5	21	79.4	48.9	40	76.8	47.3	
3	87.9	54.1	22	79.2	48.8	41	76.7	47.2	
4	86.7	53.4	23	79.0	48.6	42	76.5	47.1	
5	85.6	52.7	24	78.9	48.6	43	76.4	47.0	
6	84.4	52.0	25	78.7	48.5	44	76.3	47.0	
7	84.0	51.7	26	78.5	48.3	45	76.2	46.9	
8	83.4	51.3	27	78.4	48.3	46	76.1	46.9	
9	82.9	51.0	28	78.2	48.1	47	76.0	46.8	
10	82.4	50.7	29	78.1	48.1	48	76.0	46.8	
11	82.0	50.5	30	78.0	48.0	49	75.9	46.7	
12	81.6	50.2	31	77.8	47.9	50	75.8	46.7	
13	81.2	50.0	32	77.7	47.8	51	75.8	46.7	
14	80.9	49.8	33	77.6	47.8	52	75.7	46.6	
15	80.7	49.7	34	77.5	47.7	53	75.7	46.6	
16	80.5	49.6	35	77.4	47.7	54	75.6	46.5	
17	80.3	49.4	36	77.2	47.5	55	75.6	46.5	



## SHEAR STRESS DECAY DATA

$T_H$ 15°F		$T_T$ 60°F		$S_H$ 2.520 RPS		WIRE GAUGE NO. 26		REF. FIG.
TIME OF TEST (min.)	BOB DEFL. (°)	$\tau \times 10^3$ $\text{lb}_f/\text{ft}^2$	TIME OF TEST (min.)	BOB DEFL. (°)	$\tau \times 10^3$ $\text{lb}_f/\text{ft}^2$	TIME OF TEST (min.)	BOB DEFL. (°)	$\tau \times 10^3$ $\text{lb}_f/\text{ft}^2$
0.25			18	79.3	48.8	37	77.0	47.4
0.5	95.9	59.0	19	79.2	48.8	38	76.9	47.3
1	91.3	59.0	20	79.0	48.6	39	76.8	47.3
2	88.0	54.2	21	78.8	48.5	40	76.7	47.2
3	86.2	53.1	22	78.7	48.5	41	76.6	47.2
4	85.0	52.3	23	78.6	48.4	42	76.5	47.1
5	84.1	51.8	24	78.4	48.3	43	76.4	47.0
6	83.4	51.3	25	78.3	48.2	44	76.4	47.0
7	82.8	51.0	26	78.2	48.1	45	76.3	47.0
8	82.2	50.6	27	78.1	48.1	46	76.3	47.0
9	81.9	50.4	28	77.9	48.0	47	76.2	46.9
10	81.4	50.1	29	77.8	47.9	48	76.2	46.9
11	81.1	49.9	30	77.7	47.9	49	76.1	46.9
12	80.8	49.7	31	77.6	47.8	50	76.1	46.9
13	80.5	49.6	32	77.5	47.7	51	76.0	46.8
14	80.2	49.4	33	77.4	47.7	52	76.0	46.8
15	79.9	49.2	34	77.3	47.6	53	75.9	46.7
16	79.7	49.1	35	77.2	47.5	54	75.9	46.7
17	79.5	48.9	36	77.1	47.5	55	75.9	46.7
$T_H$ 15°F		$T_T$ 60°F		$S_H$ 4.418 RPS		WIRE GAUGE NO. 26		REF. FIG.
0.25			18	126.6	77.9	37	121.6	74.9
0.5	150.5	92.7	19	126.0	77.6	38	121.4	74.7
1	146.0	89.9	20	125.6	77.3	39	121.3	74.7
2	141.0	86.8	21	125.4	77.2	40	121.2	74.6
3	138.8	85.5	22	125.0	77.0	41	121.0	74.5
4	136.7	84.2	23	124.7	76.8	42	120.9	74.4
5	135.1	83.2	24	124.3	76.5	43	120.7	74.3
6	133.9	82.4	25	124.1	76.4	44	120.6	74.3
7	132.7	81.7	26	123.8	76.2	45	120.5	74.2
8	131.7	81.1	27	123.5	76.0	46	120.3	74.1
9	130.8	80.5	28	123.4	76.0	47	120.1	73.9
10	130.4	80.3	29	123.2	75.9	48	120.0	73.9
11	130.0	80.0	30	123.0	75.7	49	119.9	73.8
12	129.6	79.8	31	122.8	75.6	50	119.8	73.8
13	129.0	79.4	32	122.6	75.5	51	119.7	73.7
14	128.5	79.1	33	122.4	75.4	52	119.6	73.6
15	128.0	78.8	34	122.2	75.2	53	119.4	73.5
16	127.6	78.6	35	122.0	75.1	54	119.3	73.5
17	127.1	78.3	36	121.8	75.0	55	119.2	73.4



## SHEAR STRESS DECAY DATA

$T_H$ 15°F		$T_T$ 60°F		$S_H$ 4.438 RPS		WIRE GAUGE NO. 26		REF. FIG. NO. 52	
TIME OF TEST (min.)	BOB DEFL. (°)	$\tau \times 10^3$ $lb_f/ft^2$	TIME OF TEST (min.)	BOB DEFL. (°)	$\tau \times 10^3$ $lb_f/ft^2$	TIME OF TEST (min.)	BOB DEFL. (°)	$\tau \times 10^3$ $lb_f/ft^2$	
0.25			18	128.0	78.8	37	123.4	76.0	
0.5	152.9	94.1	19	127.7	78.6	38	123.2	75.9	
1	147.9	91.1	20	127.3	78.4	39	123.1	75.8	
2	143.1	88.1	21	127.0	78.2	40	123.0	75.7	
3	140.4	86.4	22	126.7	78.0	41	122.8	75.6	
4	138.4	85.2	23	126.4	77.8	42	122.6	75.5	
5	136.6	84.1	24	126.0	77.6	43	122.5	75.4	
6	135.3	83.3	25	125.7	77.4	44	122.3	75.3	
7	134.2	82.6	26	125.4	77.2	45	122.1	75.2	
8	133.5	82.2	27	125.1	77.0	46	122.0	75.1	
9	132.6	81.6	28	124.9	76.9	47	121.9	75.1	
10	131.8	81.1	29	124.7	76.8	48	121.8	75.0	
11	131.1	80.7	30	124.6	76.7	49	121.7	74.9	
12	130.5	80.3	31	124.4	76.6	50	121.6	74.9	
13	130.1	80.1	32	124.2	76.5	51	121.4	74.7	
14	129.5	79.7	33	124.0	76.3	52	121.3	74.7	
15	129.1	79.5	34	123.9	76.3	53	121.2	74.6	
16	128.6	79.2	35	123.7	76.2	54	121.1	74.6	
17	128.4	79.1	36	123.5	76.0	55	121.1	74.6	
$T_H$ 15°F		$T_T$ 60°F		$S_H$ 4.441 RPS		WIRE GAUGE NO. 26		REF. FIG. NO. 52	
0.25			18	128.2	78.9	37	125.6	77.3	
0.5	150.4	92.6	19	128.0	78.8	38	125.6	77.3	
1	146.4	90.1	20	127.7	78.6	39	125.5	77.3	
2	141.6	87.2	21	127.5	78.5	40	125.5	77.3	
3	138.9	85.5	22	127.3	78.4	41	125.4	77.2	
4	137.0	84.4	23	127.1	78.3	42	125.4	77.2	
5	135.4	83.4	24	126.9	78.1	43	125.3	77.1	
6	134.4	82.8	25	126.7	78.0	44	125.3	77.1	
7	133.4	82.1	26	126.6	77.9	45	125.2	77.1	
8	132.5	81.6	27	126.5	77.9	46	125.2	77.1	
9	131.7	81.1	28	126.4	77.8	47	125.2	77.1	
10	131.1	80.7	29	126.3	77.8	48	125.1	77.0	
11	130.6	80.4	30	126.2	77.7	49	125.1	77.0	
12	130.1	80.1	31	126.1	77.6	50	125.0	77.0	
13	129.7	79.9	32	126.0	77.6	51	125.0	77.0	
14	129.4	79.7	33	125.9	77.5	52	125.0	77.0	
15	129.1	79.5	34	125.8	77.5	53	125.0	77.0	
16	128.8	79.3	35	125.7	77.4	54	125.0	77.0	
17	128.4	79.1	36	125.7	77.4	55	124.9	76.9	



## SHEAR STRESS DECAY DATA

$T_H$ 15°F		$T_T$ 60°F		$S_H$ 4.427 RPS		WIRE GAUGE NO. 26		REF. FIG.
TIME OF TEST (min.)	BOB DEFL. (°)	$T \times 10^3$ $lb_f/ft^2$	TIME OF TEST (min.)	BOB DEFL. (°)	$T \times 10^3$ $lb_f/ft^2$	TIME OF TEST (min.)	BOB DEFL. (°)	$T \times 10^3$ $lb_f/ft^2$
0.25			18	130.6	80.4	37	127.0	78.2
0.5	156.6	96.4	19	130.3	80.2	38	126.8	78.1
1	150.9	92.9	20	129.9	80.0	39	126.7	78.0
2	145.6	89.6	21	129.6	79.8	40	126.6	77.9
3	142.6	87.8	22	129.4	79.7	41	126.5	77.9
4	140.6	86.6	23	129.1	79.5	42	126.3	77.8
5	138.9	85.5	24	128.9	79.4	43	126.2	77.7
6	137.5	84.7	25	128.7	79.2	44	126.1	77.6
7	136.4	84.0	26	128.5	79.1	45	126.0	77.6
8	135.6	83.5	27	128.3	79.0	46	125.9	77.5
9	134.8	83.0	28	128.1	78.9	47	125.8	77.5
10	134.2	82.6	29	127.9	78.7	48	125.7	77.4
11	133.4	82.1	30	127.7	78.6	49	125.6	77.3
12	132.9	81.8	31	127.6	78.6	50	125.5	77.3
13	132.5	81.6	32	127.5	78.5	51	125.4	77.2
14	132.2	81.4	33	127.4	78.4	52	125.3	77.1
15	131.6	81.0	34	127.3	78.4	53	125.2	77.1
16	131.2	80.8	35	127.2	78.3	54	125.1	77.0
17	130.9	80.6	36	127.1	78.3	55	125.0	77.0
$T_H$ 15°F		$T_T$ 60°F		$S_H$ 4.427 RPS		WIRE GAUGE NO. 26		REF. FIG.
0.25			18	129.8	79.9	37	125.6	77.3
0.5	155.0	95.4	19	129.4	79.7	38	125.5	77.3
1	149.5	92.0	20	129.1	79.5	39	125.3	77.1
2	144.2	88.9	21	128.8	79.3	40	125.2	77.1
3	141.2	86.9	22	128.5	79.1	41	125.1	77.0
4	139.4	85.8	23	128.2	78.9	42	125.0	77.0
5	137.7	84.8	24	127.9	78.7	43	124.8	76.8
6	136.5	84.0	25	127.7	78.6	44	124.6	76.7
7	135.4	83.4	26	127.5	78.5	45	124.5	76.7
8	134.6	82.9	27	127.3	78.4	46	124.4	76.6
9	133.9	82.4	28	127.2	78.3	47	124.3	76.5
10	133.2	82.0	29	127.0	78.2	48	124.0	76.3
11	132.7	81.7	30	126.8	78.1	49	123.9	76.3
12	132.1	81.3	31	126.6	77.9	50	123.7	76.2
13	131.7	81.1	32	126.4	77.8	51	123.6	76.1
14	131.2	80.8	33	126.2	77.7	52	123.5	76.0
15	130.8	80.5	34	126.0	77.6	53	123.4	76.0
16	130.5	80.3	35	125.8	77.5	54	123.3	75.9
17	130.2	80.2	36	125.7	77.4	55	123.3	75.9



## SHEAR STRESS (GROWTH) DATA

$T_H$ $75^{\circ}\text{F}$		$T_T$ $60^{\circ}\text{F}$		$S_H$ 0.519 RPS		$S_T$ 0.515 RPS		WIRE GAUGE NO. 26		REF. FIG. NO. 17
TIME OF TEST (min.)	BOB DEFL. (°)	$\tau \times 10^3$ $\text{lb}_f/\text{ft}^2$	TIME OF TEST (min.)	BOB DEFL. (°)	$\tau \times 10^3$ $\text{lb}_f/\text{ft}^2$	TIME OF TEST (min.)	BOB DEFL. (°)	$\tau \times 10^3$ $\text{lb}_f/\text{ft}^2$		
0.25			18	56.0	19.8	37	55.7			
0.5			19	56.0	19.8	38	55.7	19.6		
1	56.5	20.1	20	56.0	19.8	39	55.6	19.5		
2	56.5	20.1	21	56.0	19.8	40	55.6	19.5		
3	56.5	20.1	22	56.0	19.8	41	55.6	19.5		
4	56.4	20.0	23	56.0	19.8	42	55.6	19.5		
5	56.4	20.0	24	55.9	19.7	43	55.6	19.5		
6	56.4	20.0	25	55.9	19.7	44	55.6	19.5		
7	56.3	19.9	26	55.8	19.6	45	55.6	19.5		
8	56.3	19.9	27	55.8	19.6	46	55.6	19.5		
9	56.3	19.9	28	55.8	19.6	47	55.6	19.5		
10	56.2	19.9	29	55.8	19.6	48	55.6	19.5		
11	56.2	19.9	30	55.8	19.6	49	55.6	19.5		
12	56.2	19.9	31	55.8	19.6	50	55.5	19.5		
13	56.2	19.9	32	55.8	19.6	51	55.5	19.5		
14	56.1	19.8	33	55.8	19.6	52	55.5	19.5		
15	56.1	19.8	34	55.8	19.6	53	55.5	19.5		
16	56.1	19.8	35	55.8	19.6	54	55.5	19.5		
17	56.0	19.8	36	55.7	19.6	55	55.5	19.5		
$T_H$ $75^{\circ}\text{F}$	$T_T$ $60^{\circ}\text{F}$	$S_H$ 2.494 RPS		$S_T$ 0.506 RPS		WIRE GAUGE NO. 26		REF. FIG. NO. 26		
0.25			18	21.6	13.3	37	22.0	13.6		
0.5	21.0	12.9	19	21.7	13.4	38	22.1	13.6		
1	21.1	13.0	20	21.7	13.4	39	22.1	13.6		
2	21.2	13.1	21	21.7	13.4	40	22.1	13.6		
3	21.2	13.1	22	21.7	13.4	41	22.1	13.6		
4	21.2	13.1	23	21.7	13.4	42	22.1	13.6		
5	21.2	13.1	24	21.7	13.4	43	22.1	13.6		
6	21.3	13.1	25	21.8	13.4	44	22.1	13.6		
7	21.3	13.1	26	21.8	13.4	45	22.2	13.7		
8	21.3	13.1	27	29.9	13.5	46	22.2	13.7		
9	21.3	13.1	28	21.9	13.5	47	22.2	13.7		
10	21.3	13.1	29	21.9	13.5	48	22.2	13.7		
11	21.4	13.2	30	21.9	13.5	49	22.2	13.7		
12	21.4	13.2	31	21.9	13.5	50	22.2	13.7		
13	21.5	13.2	32	21.9	13.5	51	22.2	13.7		
14	21.5	13.2	33	21.9	13.5	52	22.2	13.7		
15	21.5	13.2	34	22.0	13.6	53	22.3	13.7		
16	21.5	13.2	35	22.0	13.6	54	22.3	13.7		
17	21.6	13.3	36	22.0	13.6	55	22.3	13.7		



TABLE 2-7 (continued)  
SHEAR STRESS (GROWTH) DATA

$T_H$ $75^{\circ}\text{F}$	$T_T$ $60^{\circ}\text{F}$	$S_H$ 2.500 RPS	$S_T$ 2.485 RPS	WIRE		REF. FIG.	
TIME OF TEST (min.)	BOB DEFL. (°)	$\tau \times 10^3$ $\text{lb}_f/\text{ft}^2$	TIME OF TEST (min.)	BOB DEFL. (°)	$\tau \times 10^3$ $\text{lb}_f/\text{ft}^2$	GAUGE NO. 26	NO. 18
						BOB DEFL. (°)	$\tau \times 10^3$ $\text{lb}_f/\text{ft}^2$
0.25			18	90.9	56.0	37	90.2 55.5
0.5			19	90.8	55.9	38	90.2 55.5
1	91.4	56.3	20	90.8	55.9	39	90.1 55.5
2	91.3	56.2	21	90.8	55.9	40	90.0 55.4
3	91.3	56.2	22	90.8	55.9	41	89.9 55.4
4	91.3	56.2	23	90.8	55.9	42	89.8 55.3
5	91.3	56.2	24	90.7	55.8	43	89.8 55.3
6	91.2	56.2	25	90.7	55.8	44	
7	91.2	56.2	26	90.7	55.8	45	
8	91.2	56.2	27	90.7	55.8	46	
9	91.2	56.2	28	90.6	55.8	47	
10	91.2	56.2	29	90.6	55.8	48	
11	91.1	56.1	30	90.6	55.8	49	
12	91.1	56.1	31	90.5	55.8	50	
13	91.1	56.1	32	90.5	55.7	51	
14	91.1	56.1	33	90.4	55.7	52	
15	91.0	56.0	34	90.3	55.6	53	
16	91.0	56.0	35	90.3	55.6	54	
17	91.0	56.0	36	90.3	55.6	55	
$T_H$ $75^{\circ}\text{F}$	$T_T$ $60^{\circ}\text{F}$	$S_H$ 4.470 RPS	$S_T$ 0.510 RPS	WIRE		REF. FIG.	
				GAUGE NO. 26		NO. 26	
0.25	19.0	11.7	18	20.0	12.3	37	20.4 12.6
0.5	19.0	11.7	19	20.0	12.3	38	20.5 12.6
1	19.1	11.8	20	20.0	12.3	39	20.5 12.6
2	19.2	11.8	21	20.0	12.3	40	20.5 12.6
3	19.2	11.8	22	20.1	12.4	41	
4	19.3	11.9	23	20.1	12.4	42	
5	19.4	11.9	24	20.1	12.4	43	
6	19.5	12.0	25	20.2	12.4	44	
7	19.6	12.1	26	20.2	12.4	45	
8	19.7	12.1	27	20.2	12.4	46	
9	19.7	12.1	28	20.2	12.4	47	
10	19.7	12.1	29	20.3	12.5	48	
11	19.8	12.2	30	20.3	12.5	49	
12	19.8	12.2	31	20.3	12.5	50	
13	19.8	12.2	32	20.3	12.5	51	
14	19.8	12.2	33	20.3	12.5	52	
15	19.8	12.2	34	20.4	12.6	53	
16	19.9	12.3	35	20.4	12.6	54	
17	20.0	12.3	36	20.4	12.6	55	



## SHEAR STRESS GROWTH DATA

$T_H$ $75^{\circ}\text{F}$	$T_T$ $60^{\circ}\text{F}$		$S_H$ 4.468 RPS		$S_T$ 2.497 RPS		WIRE GAUGE NO. 26		REF. FIG. NO. 27
TIME OF TEST (min.)	BOB DEFL. (°)	$\tau \times 10^3$ $\text{lb}_f/\text{ft}^2$	TIME OF TEST (min.)	BOB DEFL. (°)	$\tau \times 10^3$ $\text{lb}_f/\text{ft}^2$	TIME OF TEST (min.)	BOB DEFL. (°)	$\tau \times 10^3$ $\text{lb}_f/\text{ft}^2$	
0.25			18	85.6	52.7	37	87.2	53.7	
0.5	84.2	51.8	19	85.7	52.8	38	87.4	53.8	
1	84.4	52.0	20	85.7	52.8	39	87.5	53.9	
2	84.5	52.0	21	85.8	52.8	40	87.5	53.9	
3	84.6	52.1	22	85.9	52.9	41	87.5	53.9	
4	84.6	52.1	23	86.0	53.0	42	87.6	53.9	
5	84.7	52.1	24	86.1	53.0	43	87.7	54.0	
6	84.8	52.2	25	86.2	53.1	44	87.8	54.1	
7	84.8	52.2	26	86.4	53.2	45	87.9	54.1	
8	84.8	52.2	27	86.5	53.3	46	87.9	54.1	
9	84.9	52.3	28	86.6	53.3	47	88.0	54.2	
10	85.0	52.3	29	86.6	53.3	48	88.0	54.2	
11	85.1	52.4	30	86.7	53.4	49	88.1	54.2	
12	85.1	52.4	31	86.8	53.4	50	88.1	54.2	
13	85.2	52.4	32	86.9	53.5	51	88.1	54.2	
14	85.3	52.5	33	86.9	53.5	52	88.1	54.2	
15	85.4	52.6	34	87.0	53.6	53	88.1	54.2	
16	85.4	52.6	35	87.1	53.6	54	88.2	54.3	
17	85.5	52.6	36	87.1	53.6	55	88.2	54.3	
$T_H$ $75^{\circ}\text{F}$	$T_T$ $60^{\circ}\text{F}$		$S_H$ 4.486 RPS	$S_T$ 4.475 RPS	WIRE GAUGE NO. 26		REF. FIG. NO. 19		
0.25			18	152.2	93.7	37			
0.5			19	152.2	93.7	38			
1	152.1	93.6	20	152.2	93.7	39			
2	152.0	93.6	21			40			
3	152.0	93.6	22			41			
4	151.9	93.5	23			42			
5	152.0	93.6	24			43			
6	152.0	93.6	25			44			
7	152.0	93.6	26			45			
8	152.0	93.6	27			46			
9	152.1	93.6	28			47			
10	152.1	93.6	29			48			
11	152.2	93.7	39			49			
12	152.3	93.7	31			50			
13	152.2	93.7	32			51			
14	152.2	93.7	33			52			
15	152.2	93.7	34			53			
16	152.2	93.7	35			54			
17	152.2	93.7	36			55			



## SHEAR STRESS (GROWTH) DATA

$T_H$ 75°F	$T_T$ 44.5°F	$S_H$ 0.520 RPS	$S_T$ 0.517 RPS	WIRE		REF. FIG.	
TIME OF TEST (min.)	BOB DEFL. (°)	$\tau \times 10^3$ $lb_f/ft^2$	TIME OF TEST (min.)	BOB DEFL. (°)	$\tau \times 10^3$ $lb_f/ft^2$	GAUGE NO. 26	NO. 20
0.25			18	81.1	49.9	37	79.8 49.1
0.5	82.8	51.0	19	81.0	49.9	38	79.8 49.1
1	82.7	50.9	20	80.9	49.8	39	79.8 49.1
2	82.5	50.8	21	80.8	49.7	40	79.7 49.1
3	82.4	50.7	22	80.7	49.7	41	79.7 49.1
4	82.3	50.7	23	80.6	49.6	42	79.7 49.1
5	82.2	50.6	24	80.5	49.6	43	79.6 49.0
6	82.2	50.6	25	80.5	49.6	44	79.6 49.0
7	82.1	50.5	26	80.5	49.6	45	79.5 48.9
8	81.9	50.4	27	80.4	49.5	46	79.5 48.9
9	81.8	50.4	28	80.4	49.5	47	
10	81.8	50.4	29	80.3	49.4	48	
11	81.7	50.3	30	80.2	49.4	49	
12	81.6	50.2	31	80.2	49.4	50	
13	81.6	50.2	32	80.2	49.4	51	
14	81.5	50.2	33	80.1	49.3	52	
15	81.4	50.1	34	80.0	49.3	53	
16	81.3	50.1	35	79.9	49.2	54	
17	81.2	50.0	36	79.9	49.2	55	
$T_H$ 75°F	$T_T$ 44.5°F	$S_H$ 2.492 RPS	$S_T$ 0.520 RPS	WIRE		REF. FIG.	
TIME OF TEST (min.)	BOB DEFL. (°)	$\tau \times 10^3$ $lb_f/ft^2$	TIME OF TEST (min.)	BOB DEFL. (°)	$\tau \times 10^3$ $lb_f/ft^2$	GAUGE NO. 26	NO. 28
0.25			18	57.3	35.3	37	58.1 35.8
0.5	48.4	29.8	19	57.3	35.3	38	58.2 35.8
1	49.7	30.6	20	57.4	35.3	39	58.2 35.8
2	51.8	31.9	21	57.5	35.4	40	58.2 35.8
3	52.9	32.6	22	57.6	35.5	41	58.2 35.8
4	54.0	33.2	23	57.6	35.5	42	58.3 35.9
5	54.7	33.7	24	57.6	35.5	43	58.3 35.9
6	55.1	33.9	25	57.7	35.5	44	58.3 35.9
7	55.6	34.2	26	57.7	35.5	45	58.3 35.9
8	56.0	34.5	27	57.7	35.5	46	58.3 35.9
9	56.2	34.6	28	57.7	35.5	47	58.4 36.0
10	56.4	34.7	29	57.8	35.6	48	58.4 36.0
11	56.7	34.9	30	57.8	35.6	49	58.4 36.0
12	56.8	35.0	31	57.8	35.6	50	58.4 36.0
13	56.9	35.0	32	57.9	35.6	51	
14	57.0	35.1	33	57.9	35.6	52	
15	57.1	35.2	34	58.0	35.7	53	
16	57.2	35.2	35	58.0	35.7	54	
17	57.2	35.2	36	58.1	35.8	55	



## SHEAR STRESS (GROWTH) DATA

$T_H$ $75^{\circ}$ F	$T_T$ $44.5^{\circ}$ F	$S_H$ 2.491 RPS	$S_T$ 2.490 RPS	WIRE		REF. FIG.	
TIME OF TEST (min.)	BOB DEFL. ( $^{\circ}$ )	$\tau \times 10^3$ $lb_f/ft^2$	TIME OF TEST (min.)	BOB DEFL. ( $^{\circ}$ )	$\tau \times 10^3$ $lb_f/ft^2$	GAUGE NO. 26	NO. 21
0.25			18	172.3	106.1	37	170.1 104.7
0.5	174.9	107.7	19	172.2	106.0	38	170.0 104.7
1	174.7	107.6	20	172.1	106.0	39	169.8 104.5
2	174.6	107.5	21	171.9	105.8	40	169.8 104.5
3	174.3	107.3	22	171.8	105.8	41	169.6 104.4
4	174.2	107.3	23	171.6	105.7	42	169.6 104.4
5	174.1	107.2	24	171.4	105.5	43	169.6 104.4
6	173.9	107.1	25	171.4	105.5	44	169.5 104.4
7	173.8	107.0	26	171.3	105.5	45	169.5 104.4
8	173.7	106.9	27	171.2	105.4	46	
9	173.6	106.9	28	171.1	105.3	47	
10	173.5	106.8	29	171.0	105.3	48	
11	173.3	106.7	30	170.8	105.2	49	
12	173.1	106.6	31	170.7	105.1	50	
13	172.9	106.5	32	170.6	105.0	51	
14	172.7	106.3	33	170.5	105.0	52	
15	172.6	106.3	34	170.5	105.0	53	
16	172.5	106.2	35	170.5	105.0	54	
17	172.4	106.1	36	170.4	104.9	55	
$T_H$ $75^{\circ}$ F	$T_T$ $44.5^{\circ}$ F	$S_H$ 4.490 RPS	$S_T$ 0.534 RPS	WIRE		REF. FIG.	
				GAUGE NO. 24		NO. 28	
0.25	20.6	28.2	18	23.7	32.5	37	
0.5	20.7	28.4	19	23.7	32.5	38	
1	21.2	29.1	20	23.7	32.5	39	
2	22.0	30.2	21	23.7	32.5	40	
3	22.5	30.8	22	23.7	32.5	41	
4	22.9	31.4	23	23.7	32.5	42	
5	23.1	31.7	24	23.7	32.5	43	
6	23.4	32.1	25	23.7	32.5	44	
7	23.6	32.4	26	23.7	32.5	45	
8	23.6	32.4	27	23.5	32.2	46	
9	23.6	32.4	28	23.5	32.2	47	
10	23.6	32.4	29	23.5	32.2	48	
11	23.7	32.5	30	23.5	32.2	49	
12	23.7	32.5	31			50	
13	23.7	32.5	32			51	
14	23.7	32.5	33			52	
15	23.7	32.5	34			53	
16	23.7	32.5	35			54	
17	23.7	32.5	36			55	



## SHEAR STRESS (GROWTH) DATA

$T_H$ 75° F		$T_T$ 44.5° F		$S_H$ 4.483 RPS		$S_T$ 2.492 RPS		WIRE		REF. FIG.
TIME OF TEST (min.)	BOB DEFL. (°)	$T \times 10^3$ $lb_f/ft^2$	TIME OF TEST (min.)	BOB DEFL. (°)	$T \times 10^3$ $lb_f/ft^2$	TIME OF TEST (min.)	BOB DEFL. (°)	$T \times 10^3$ $lb_f/ft^2$	GAUGE NO. 24	NO. 29
0.25	65.8	90.2	18	68.8	94.3	37				
0.5	66.1	90.6	19	68.9	94.5	38				
1	66.7	91.4	20	68.9	94.5	39				
2	67.2	92.1	21	69.0	94.6	40				
3	67.6	92.7	22	69.0	94.6	41				
4	67.8	93.0	23	69.0	94.6	42				
5	67.9	93.1	24	69.0	94.6	43				
6	68.1	93.4	25	69.0	94.6	44				
7	68.3	93.6	26	69.0	94.6	45				
8	68.3	93.6	27	69.1	94.7	46				
9	68.4	93.8	28	69.1	94.7	47				
10	68.5	93.9	29	69.1	94.7	48				
11	68.5	93.9	30	69.1	94.7	49				
12	68.5	93.9	31	69.1	94.7	50				
13	68.6	94.1	32	69.1	94.7	51				
14	68.6	94.1	33	69.1	94.7	52				
15	68.6	94.1	34	69.1	94.7	53				
16	68.7	94.2	35	69.1	94.7	54				
17	68.8	94.3	36	69.1	94.7	55				
$T_H$ 75° F	$T_T$ 44.5° F	$S_H$ 4.481 RPS		$S_T$ 4.488 RPS		WIRE		REF. FIG.		
0.25		18	106.7	146.3	37	106.0	145.3			
0.5		19	106.7	146.3	38	106.0	145.3			
1	107.5	147.4	20	106.7	146.3	39	106.0	145.3		
2	107.5	147.5	21	106.6	146.1	40	105.9	145.2		
3	107.4	147.2	22	106.6	146.1	41	105.8	145.1		
4	107.3	147.1	23	106.6	146.1	42	105.7	144.9		
5	107.2	147.0	24	106.6	146.1	43	105.7	144.9		
6	107.1	146.8	25	106.5	146.0	44	105.7	144.9		
7	107.0	146.7	26	106.5	146.0	45	105.7	144.9		
8	106.9	146.6	27	106.4	145.9	46	105.7	144.9		
9	106.9	145.6	28	106.4	145.9	47				
10	106.9	146.6	29	106.4	145.9	48				
11	106.9	146.6	30	106.4	145.9	49				
12	106.9	146.6	31	106.3	145.7	50				
13	106.8	146.4	32	106.2	145.6	51				
14	106.8	146.4	33	106.1	145.5	52				
15	106.8	146.4	34	106.1	145.5	53				
16	106.8	146.4	35	106.1	145.5	54				
17	106.8	146.4	36	106.0	145.3	55				



## SHEAR STRESS (GROWTH) DATA

$T_H$ 75° F	$T_T$ 30° F	$S_H$ 0.536 RPS	$S_T$ 0.533 RPS	WIRE GAUGE NO. 24		REF. FIG.			
TIME OF TEST (min.)	BOB DEFL. (°)	$T \times 10^3$ $lb_f/ft^2$	TIME OF TEST (min.)	BOB DEFL. (°)	$T \times 10^3$ $lb_f/ft^2$	TIME OF TEST (min.)	BOB DEFL. (°)	$T \times 10^3$ $lb_f/ft^2$	NO. 23
0.25			18	71.5	98.0	37	69.6	95.4	
0.5	73.9	101.3	19	71.3	97.8	38	69.5	95.3	
1	73.8	101.2	20	71.2	97.6	39	69.4	95.1	
2	73.6	100.9	21	71.1	97.5	40	69.3	95.0	
3	73.4	100.6	22	70.9	97.2	41	69.2	94.9	
4	73.3	100.5	23	70.8	97.1	42	69.1	94.7	
5	73.1	100.2	24	70.7	96.9	43	69.0	94.6	
6	73.0	100.1	25	70.6	96.8	44	68.9	94.5	
7	72.8	99.8	26	70.5	96.7	45	68.8	94.3	
8	72.7	99.7	27	70.5	96.7	46	68.8	94.3	
9	72.6	99.5	28	70.4	96.5	47	68.7	94.2	
10	72.4	99.3	29	70.3	96.4	48	68.6	94.1	
11	72.3	99.1	30	70.2	96.2	49	68.6	94.1	
12	72.1	98.8	31	70.1	96.1	50	68.5	93.9	
13	72.0	98.7	32	70.0	96.0	51	68.4	93.8	
14	71.9	98.6	33	70.0	96.0	52	68.4	93.8	
15	71.8	98.4	34	69.9	95.8	53	68.4	93.8	
16	71.7	98.3	35	69.8	95.7	54	68.3	93.6	
17	71.6	98.2	36	69.7	95.6	55	68.3	93.6	
$T_H$ 75° F	$T_T$ 30° F	$S_H$ 2.501 RPS	$S_T$ 0.525 RPS	WIRE GAUGE NO. 22		REF. FIG.			
0.25	18.4	67.1	18	20.9	76.2	37	20.4	74.4	
0.5	18.8	68.5	19	20.9	76.2	38	20.3	74.0	
1	20.0	72.9	20	20.9	76.2	39	20.3	74.0	
2	20.9	76.2	21	20.8	75.8	40	20.3	74.0	
3	21.2	77.3	22	20.8	75.8	41	20.3	74.0	
4	21.4	78.0	23	20.8	75.8	42	20.3	74.0	
5	21.4	78.0	24	20.8	75.8	43	20.3	74.0	
6	21.4	78.0	25	20.7	75.5	44	20.3	74.0	
7	21.4	78.0	26	20.7	75.5	45	20.3	74.0	
8	21.4	78.0	27	20.6	75.1	46	20.3	74.0	
9	21.3	77.7	28	20.6	75.1	47			
10	21.3	77.7	29	20.6	75.1	48			
11	21.3	77.7	30	20.5	74.7	49			
12	21.2	77.3	31	20.5	74.7	50			
13	21.1	77.3	32	20.5	74.7	51			
14	21.1	77.3	33	20.5	74.7	52			
15	21.1	77.3	34	20.5	74.7	53			
16	21.0	76.6	35	20.4	74.4	54			
17	21.0	76.6	36	20.4	74.4	55			



## SHEAR STRESS (GROWTH) DATA

$T_H$ $75^{\circ}\text{F}$	$T_T$ $30^{\circ}\text{F}$	$S_H$ 2.500 RPS	$S_T$ 2.499 RPS	WIRE		REF. FIG.	
TIME OF TEST (min.)	BOB DEFL. ( $^{\circ}$ )	$\tau \times 10^3$ $\text{lb}_f/\text{ft}^2$	TIME OF TEST (min.)	BOB DEFL. ( $^{\circ}$ )	$\tau \times 10^3$ $\text{lb}_f/\text{ft}^2$	GAUGE NO. 22	NO. 24
0.25			18	55.3	202	37	54.7 199
0.5	55.9	204	19	55.3	202	38	54.7 199
1	55.8	203	20	55.2	201	39	54.7 199
2	55.8	203	21	55.2	201	40	54.7 199
3	55.8	203	22	55.2	201	41	54.6 199
4	55.7	203	23	55.1	201	42	54.6 199
5	55.7	203	24	55.0	201	43	54.6 199
6	55.7	203	25	55.0	201	44	54.6 199
7	55.6	203	26	55.0	201	45	54.5 199
8	55.6	203	27	54.9	200	46	54.5 199
9	55.6	203	28	54.9	200	47	54.5 199
10	55.5	202	29	54.9	200	48	54.5 199
11	55.5	202	30	54.9	200	49	54.4 198
12	55.5	202	31	54.8	200	50	54.4 198
13	55.4	202	32	54.8	200	51	54.4 198
14	55.4	202	33	54.8	200	52	54.3 198
15	55.3	202	34	54.8	200	53	54.3 198
16	55.3	202	35	54.8	200	54	54.3 198
17	55.3	202	36	54.7	199	55	54.3 198
$T_H$ $75^{\circ}\text{F}$	$T_T$ $30^{\circ}\text{F}$	$S_H$ 4.505 RPS	$S_T$ 0.532 RPS	WIRE		REF. FIG.	
TIME OF TEST (min.)	BOB DEFL. ( $^{\circ}$ )	$\tau \times 10^3$ $\text{lb}_f/\text{ft}^2$	TIME OF TEST (min.)	BOB DEFL. ( $^{\circ}$ )	$\tau \times 10^3$ $\text{lb}_f/\text{ft}^2$	GAUGE NO. 22	NO. 30
0.25	18.6	67.8	18	23.9	87.1	37	22.7 82.8
0.5	21.8	79.5	19	23.8	86.8	38	22.7 82.8
1	24.2	88.2	20	23.7	86.4	39	22.7 82.8
2	24.7	90.1	21	23.6	86.0	40	22.6 82.4
3	25.0	91.2	22	23.6	86.0	41	22.6 82.4
4	25.2	91.9	23	23.6	86.0	42	22.6 82.4
5	25.2	91.9	24	23.5	85.7	43	22.6 82.4
6	25.2	91.9	25	23.4	85.3	44	22.5 82.0
7	25.1	91.5	26	23.4	85.3	45	22.5 82.0
8	25.0	91.2	27	23.3	85.0	46	22.4 81.7
9	24.9	90.8	28	23.2	84.6	47	22.4 81.7
10	24.7	90.1	29	23.1	84.2	48	22.3 81.3
11	24.6	89.7	30	23.1	84.2	49	22.3 81.3
12	24.5	89.3	31	23.1	84.2	50	22.2 80.9
13	24.4	89.0	32	23.1	84.2	51	22.2 80.9
14	24.3	88.6	33	23.0	83.9	52	22.2 80.9
15	24.2	88.2	34	22.9	83.5	53	22.2 80.9
16	24.1	87.9	35	22.9	83.5	54	22.1 80.6
17	24.0	87.5	36	22.8	83.1	55	22.1 80.6



## SHEAR STRESS (GROWTH) DATA

$T_H$ $75^{\circ}\text{F}$	$T_T$ $30^{\circ}\text{F}$	$S_H$ 4.505 RPS	$S_T$ 2.506 RPS	WIRE GAUGE NO. 22		REF. FIG.		
TIME OF TEST (min.)	BOB DEFL. ( $^{\circ}$ )	$\tau \times 10^3$ $\text{lb}_f/\text{ft}^2$	TIME OF TEST (min.)	BOB DEFL. ( $^{\circ}$ )	$\tau \times 10^3$ $\text{lb}_f/\text{ft}^2$	TIME OF TEST (min.)	BOB DEFL. ( $^{\circ}$ )	$\tau \times 10^3$ $\text{lb}_f/\text{ft}^2$
0.25	48.0	175.0	18	49.9	181.9	37		
0.5	48.8	177.9	19	49.9	181.9	38		
1	49.5	180.5	20	49.9	181.9	39		
2	50.0	182.3	21	49.9	181.9	40		
3	50.2	183.0	22	49.9	181.9	41		
4	50.3	183.4	23	49.9	181.9	42		
5	50.3	183.4	24	49.4	181.9	43		
6	50.3	183.4	25	49.9	181.9	44		
7	50.2	183.0	26	49.9	181.9	45		
8	50.2	183.0	27	49.9	181.9	46		
9	50.2	183.0	28	49.9	181.9	47		
10	50.1	182.7	29	49.9	181.9	48		
11	50.1	182.7	30	49.9	181.9	49		
12	50.0	182.3	31	49.9	181.9	50		
13	50.0	182.3	32	49.9	181.9	51		
14	50.0	182.3	33	49.9	181.9	52		
15	49.9	181.9	34	49.9	181.9	53		
16	49.9	181.9	35	49.9	181.9	54		
17	49.9	181.9	36	49.9	181.9	55		
$T_H$ $75^{\circ}\text{F}$	$T_T$ $30^{\circ}\text{F}$	$S_H$ 4.526 RPS	$S_T$ 4.522 RPS	WIRE GAUGE NO. 22		REF. FIG.		
TIME OF TEST (min.)	BOB DEFL. ( $^{\circ}$ )	$\tau \times 10^3$ $\text{lb}_f/\text{ft}^2$	TIME OF TEST (min.)	BOB DEFL. ( $^{\circ}$ )	$\tau \times 10^3$ $\text{lb}_f/\text{ft}^2$	TIME OF TEST (min.)	BOB DEFL. ( $^{\circ}$ )	$\tau \times 10^3$ $\text{lb}_f/\text{ft}^2$
0.25			18	77.6	283	37	75.9	277
0.5	79.3	289	19	77.5	283	38	75.9	277
1	79.2	289	20	77.5	282	39	75.8	276
2	79.1	288	21	77.4	282	40	75.8	276
3	78.9	288	22	77.3	282	41	75.7	276
4	78.8	287	23	77.2	281	42	75.7	276
5	78.7	287	24	77.1	281	43	75.6	276
6	78.7	287	25	77.1	281	44	75.6	276
7	78.6	287	26	77.0	281	45	75.5	275
8	78.5	286	27	75.9	280	46	75.5	275
9	78.4	286	28	75.8	280	47	75.4	275
10	78.3	285	29	76.7	280	48	75.3	275
11	78.2	285	30	76.6	279	49	75.2	274
12	78.1	285	31	76.5	279	50	75.2	274
13	78.0	284	32	76.4	279	51	75.1	274
14	77.9	284	33	76.3	278	52	75.1	274
15	77.8	284	34	76.2	278	53	75.0	273
16	77.7	283	35	76.1	277	54	74.9	273
17	77.6	283	36	76.0	277	55	74.9	273



TABLE 3-7  
COMPUTED RHEOLOGICAL DATA

$T_H$ (°F)	75	$T_T$ (°F)	75	$\frac{dv}{dR}$ (sec <sup>-1</sup> )	165
$\tau_\mu \times 10^3$ (lb./ft. <sup>2</sup> )	24.5	$\tau_o \times 10^3$ (lb./ft. <sup>2</sup> )	31.0	$\tau_\infty \times 10^3$ (lb./ft. <sup>2</sup> )	26.6
$\tau_{so} \times 10^3$ (lb./ft. <sup>2</sup> )	6.5	$\tau_{s\infty} \times 10^3$ (lb./ft. <sup>2</sup> )	2.1	$\frac{\tau_{so}^2}{\tau_{s\infty}}$	20.1
TIME OF TEST (min.)	$\tau \times 10^3$ (lb./ft. <sup>2</sup> )	$\tau_s \times 10^3$ (lb./ft. <sup>2</sup> )	$\tau_s - \tau_{s\infty}$ $\times 10^3$	$\frac{\tau_{so}^2}{\tau_{s\infty}} - \tau_s$	$\frac{\tau_s - \tau_{s\infty}}{\tau_{so}^2/\tau_{s\infty} - \tau_s}$
0.1					
0.25	30.3	5.8	3.7	14.3	0.259
0.5	29.9	5.4	3.3	14.7	0.224
1	29.5	5.0	2.9	15.1	0.192
2	29.1	4.6	2.6	15.5	0.168
5	28.6	4.1	2.1	16.0	0.131
10	28.2	3.7	1.7	16.4	0.104
20	28.0	3.5	1.5	16.6	0.0904
30	27.9	3.4	1.4	16.7	0.0838
$T_H$ (°F)	75	$T_T$ (°F)	75	$\frac{dv}{dR}$ (sec <sup>-1</sup> )	296
$\tau_\mu \times 10^3$ (lb./ft. <sup>2</sup> )	43.5	$\tau_o \times 10^3$ (lb./ft. <sup>2</sup> )	50.0	$\tau_\infty$ (lb./ft. <sup>2</sup> )	45.5
$\tau_{so} \times 10^3$ (lb./ft. <sup>2</sup> )	6.5	$\tau_{s\infty} \times 10^3$ (lb./ft. <sup>2</sup> )	2.0	$\frac{\tau_{so}^2}{\tau_{s\infty}}$	21.1
TIME OF TEST (min.)	$\tau \times 10^3$ (lb./ft. <sup>2</sup> )	$\tau_s \times 10^3$ (lb./ft. <sup>2</sup> )	$\tau_s - \tau_{s\infty}$ $\times 10^3$	$\frac{\tau_{so}^2}{\tau_{s\infty}} - \tau_s$	$\frac{\tau_s - \tau_{s\infty}}{\tau_{so}^2/\tau_{s\infty} - \tau_s}$
0.1					
0.25	49.4	5.9	3.9	15.2	0.256
0.5	49.1	5.6	3.6	15.5	0.232
1	48.6	5.1	3.1	16.0	0.194
2	48.1	4.6	2.6	16.5	0.158
5	47.6	4.1	2.1	17.0	0.124
10	47.25	3.75	1.75	17.35	0.101
20	47.05	3.55	1.55	17.55	0.883
30	47.0	3.5	1.5	17.6	0.852



TABLE 3-7 (continued)  
 COMPUTED RHEOLOGICAL DATA

$T_H$ (°F)	75	$T_T$ (°F)	60	$\frac{dv}{dR}$ (sec <sup>-1</sup> )	37.0
$\tau_\mu \times 10^3$ (lb./ft. <sup>2</sup> )	7.8	$\tau_o \times 10^3$ (lb./ft. <sup>2</sup> )	33.0	$\tau_\infty \times 10^3$ (lb./ft. <sup>2</sup> )	16.5
$\tau_{so} \times 10^3$ (lb./ft. <sup>2</sup> )	25.2	$\tau_{s\infty} \times 10^3$ (lb./ft. <sup>2</sup> )	8.7	$\frac{\tau_{so}^2}{\tau_{s\infty}}$	77.4
TIME OF TEST (min.)	$\tau_x \times 10^3$ (lb./ft. <sup>2</sup> )	$\tau_s \times 10^3$ (lb./ft. <sup>2</sup> )	$\tau_s - \tau_{s\infty}$ $\times 10^3$	$\frac{\tau_{so}^2}{\tau_{s\infty}} - \tau_s$	$\frac{\tau_s - \tau_{s\infty}}{\tau_{so}^2/\tau_{s\infty} - \tau_s}$
0.1	29.9	22.1	13.4	55.3	0.242
0.25	28.1	20.3	11.6	57.1	0.203
0.5	26.6	18.8	10.1	58.6	0.172
1	25.3	17.5	8.8	59.9	0.147
2	23.8	16.0	7.3	61.4	0.119
5	22.3	14.5	5.8	62.9	0.0922
10	21.5	13.7	5.0	63.7	0.0785
20	20.65	12.85	4.15	64.55	0.0642
30	20.25	12.45	3.75	64.95	0.0577
60	19.75	11.95	3.25	65.45	0.0497
$T_H$ (°F)	75	$T_T$ (°F)	60	$\frac{dv}{dR}$ (sec <sup>-1</sup> )	170
$\tau_\mu \times 10^3$ (lb./ft. <sup>2</sup> )	35.5	$\tau_o \times 10^3$ (lb./ft. <sup>2</sup> )	80.0	$\tau_\infty \times 10^3$ (lb./ft. <sup>2</sup> )	50
$\tau_{so} \times 10^3$ (lb./ft. <sup>2</sup> )	44.5	$\tau_{s\infty} \times 10^3$ (lb./ft. <sup>2</sup> )	14.5	$\frac{\tau_{so}^2}{\tau_{s\infty}}$	136.6
TIME OF TEST (min.)	$\tau_x \times 10^3$ (lb./ft. <sup>2</sup> )	$\tau_s \times 10^3$ (lb./ft. <sup>2</sup> )	$\tau_s - \tau_{s\infty}$ $\times 10^3$	$\frac{\tau_{so}^2}{\tau_{s\infty}} - \tau_s$	$\frac{\tau_s - \tau_{s\infty}}{\tau_{so}^2/\tau_{s\infty} - \tau_s}$
0.1	74.5	39.0	24.5	97.6	0.251
0.25	71.2	35.7	21.2	100.9	0.210
0.5	68.0	32.5	18.0	104.1	0.173
1	65.5	30.0	15.5	106.6	0.145
2	63.0	27.5	13.0	109.1	0.119
5	60.3	24.8	10.3	111.8	0.0921
10	58.5	23.0	8.5	113.6	0.0748
20	57.0	21.5	7.0	115.1	0.0608
30	56.3	20.8	6.3	115.8	0.0544
60	55.7	20.2	4.7	116.4	0.0490



## COMPUTED RHEOLOGICAL DATA

$T_H$ (°F)	75	$T_T$ (°F)	60	$\frac{dv}{dR}$ (sec <sup>-1</sup> )	300
$\tau_\mu \times 10^3$ (lb./ft. <sup>2</sup> )	63.0	$\tau_o \times 10^3$ (lb./ft. <sup>2</sup> )	122.0	$\tau_\infty \times 10^3$ (lb./ft. <sup>2</sup> )	81.0
$\tau_{so} \times 10^3$ (lb./ft. <sup>2</sup> )	59.0	$\tau_{s\infty} \times 10^3$ (lb./ft. <sup>2</sup> )	18.0	$\frac{\tau_{so}^2}{\tau_{s\infty}}$	193.4
TIME OF TEST (min.)	$\tau \times 10^3$ (lb./ft. <sup>2</sup> )	$\tau_s \times 10^3$ (lb./ft. <sup>2</sup> )	$\tau_s - \tau_{s\infty}$ $\times 10^3$	$\frac{\tau_{so}^2}{\tau_{s\infty}} - \tau_s$	$\frac{\tau_s - \tau_{s\infty}}{\tau_{so}^2 / \tau_{s\infty} - \tau_s}$
0.1	115.0	52.0	34.0	141.4	0.240
0.25	110.0	47.0	29.0	146.4	0.198
0.5	106.0	43.0	25.0	150.4	0.166
1	102.5	39.5	21.5	153.9	0.136
2	99.0	36.0	18.0	157.4	0.114
5	95.2	32.2	14.2	161.2	0.0881
10	93.0	30.0	12.0	163.5	0.0734
20	91.5	28.5	10.5	164.9	0.0637
30	91.0	28.0	10.0	165.4	0.0604
60	89.9	26.9	8.9	166.5	0.0535
$T_H$ (°F)	75	$T_T$ (°F)	44.5	$\frac{dv}{dR}$ (sec <sup>-1</sup> )	38.0
$\tau_\mu \times 10^3$ (lb./ft. <sup>2</sup> )	12.4	$\tau_o \times 10^3$ (lb./ft. <sup>2</sup> )	132.0	$\tau_\infty \times 10^3$ (lb./ft. <sup>2</sup> )	35.0
$\tau_{so} \times 10^3$ (lb./ft. <sup>2</sup> )	119.6	$\tau_{s\infty} \times 10^3$ (lb./ft. <sup>2</sup> )	22.6	$\frac{\tau_{so}^2}{\tau_{s\infty}}$	632.9
TIME OF TEST (min.)	$\tau \times 10^3$ (lb./ft. <sup>2</sup> )	$\tau_s \times 10^3$ (lb./ft. <sup>2</sup> )	$\tau_s - \tau_{s\infty}$ $\times 10^3$	$\frac{\tau_{so}^2}{\tau_{s\infty}} - \tau_s$	$\frac{\tau_s - \tau_{s\infty}}{\tau_{so}^2 / \tau_{s\infty} - \tau_s}$
0.1	122.0	109.6	87.0	523.3	0.166
0.25	105.0	92.6	70.0	540.3	0.130
0.5	94.0	81.6	59.0	551.3	0.107
1	83.0	70.6	48.0	562.3	0.0853
2	74.0	61.6	39.0	571.3	0.0683
5	64.0	51.6	29.0	581.3	0.0499
10	58.6	46.2	23.6	586.7	0.0402
20	54.8	42.4	29.8	590.5	0.0335
30	52.5	40.1	17.5	592.8	0.0295
60	59.6	37.2	14.6	595.7	0.0245



## COMPUTED RHEOLOGICAL DATA

$T_H$ (°F)	75	$T_T$ (°F)	44.5	$\frac{dv}{dR}$ (sec <sup>-1</sup> )	180
$\tau_\mu \times 10^3$ (lb./ft. <sup>2</sup> )	58.5	$\tau_o \times 10^3$ (lb./ft. <sup>2</sup> )	211.0	$\tau_\infty \times 10^3$ (lb./ft. <sup>2</sup> )	90.0
$\tau_{so} \times 10^3$ (lb./ft. <sup>2</sup> )	152.5	$\tau_{s\infty} \times 10^3$ (lb./ft. <sup>2</sup> )	31.5	$\frac{\tau_{so}^2}{\tau_{s\infty}}$	738.3
TIME OF TEST (min.)	$\tau \times 10^3$ (lb./ft. <sup>2</sup> )	$\tau_s \times 10^3$ (lb./ft. <sup>2</sup> )	$\tau_s - \tau_{s\infty}$ $\times 10^3$	$\frac{\tau_{so}^2}{\tau_{s\infty}} - \tau_s$	$\frac{\tau_s - \tau_{s\infty}}{\tau_{so}^2/\tau_{s\infty} - \tau_s}$
0.1	198.0	139.5	108.0	498.8	0.180
0.25	174.0	115.5	84.0	622.8	0.135
0.5	160.0	101.5	70.0	636.8	0.110
1	148.0	89.5	58.0	648.8	0.0894
2	137.0	78.5	47.0	659.8	0.0712
5	125.0	66.5	35.0	671.8	0.0521
10	119.0	60.5	29.0	677.8	0.0428
20	114.0	55.5	24.0	682.8	0.0351
30	112.0	52.5	22.0	684.8	0.034
60	109.0	50.5	19.0	687.8	0.0276
$T_H$ (°F)	75	$T_T$ (°F)	44.5	$\frac{dv}{dR}$ (sec <sup>-1</sup> )	318
$\tau_\mu \times 10^3$ (lb./ft. <sup>2</sup> )	102.0	$\tau_o \times 10^3$ (lb./ft. <sup>2</sup> )	264.0	$\tau_\infty \times 10^3$ (lb./ft. <sup>2</sup> )	131.0
$\tau_{so} \times 10^3$ (lb./ft. <sup>2</sup> )	162.0	$\tau_{s\infty} \times 10^3$ (lb./ft. <sup>2</sup> )	29.0	$\frac{\tau_{so}^2}{\tau_{s\infty}}$	905.0
TIME OF TEST (min.)	$\tau \times 10^3$ (lb./ft. <sup>2</sup> )	$\tau_s \times 10^3$ (lb./ft. <sup>2</sup> )	$\tau_s - \tau_{s\infty}$ $\times 10^3$	$\frac{\tau_{so}^2}{\tau_{s\infty}} - \tau_s$	$\frac{\tau_s - \tau_{s\infty}}{\tau_{so}^2/\tau_{s\infty} - \tau_s}$
0.1	247.0	145.0	116.0	760.0	0.152
0.25	225.0	123.0	94.0	782.0	0.120
0.5	208.0	106.0	77.0	799.0	0.064
1	194.0	92.0	63.0	813.0	0.775
2	183.0	81.0	52.0	824.0	0.0631
5	169.0	67.0	38.0	838.0	0.0453
10	163.0	61.0	32.0	844.0	0.0379
20	157.0	55.0	26.0	850.0	0.0306
30	154.0	52.0	23.0	853.0	0.0270
60	150.5	48.5	19.5	856.5	0.0228



## COMPUTED RHEOLOGICAL DATA

$T_H$ (°F)	75	$T_H$ (°F)	30	$\frac{dv}{dR}$ (sec <sup>-1</sup> )	39.5
$\tau_\mu \times 10^3$ (lb./ft. <sup>2</sup> )	21.0	$\tau_0 \times 10^3$ <del>(lb./ft.<sup>2</sup>)</del>	356.0	$\tau_\infty \times 10^3$ (lb./ft. <sup>2</sup> )	70.0
$\tau_{so} \times 10^3$ (lb./ft. <sup>3</sup> )	335.0	$\tau_{s\infty} \times 10^3$ (lb./ft. <sup>2</sup> )	49.0	$\frac{\tau_{so}^2}{\tau_{s\infty}} \times 10^3$	2290
TIME OF TEST (min.)	$\tau \times 10^3$ (lb./ft. <sup>2</sup> )	$\tau_s \times 10^3$ (lb./ft. <sup>2</sup> )	$\tau_s - \tau_{s\infty}$ $\times 10^3$	$\frac{\tau_{so}^2}{\tau_{s\infty}} - \tau_s$	$\frac{\tau_s - \tau_{s\infty}}{\tau_{so}^2/\tau_{s\infty} - \tau_s}$
0.1	308	287	238	2003	0.119
0.25	254	233	184	2057	0.0895
0.5	220	199	150	2091	0.0717
1	189	168	119	2122	0.0561
2	168	147	98	2143	0.0457
5	145	124	75	2166	0.0346
10	128	107	58	2183	0.0266
20	116	95	46	2195	0.0210
30	111	90	41	2200	0.0186
60	103	82	33	2208	0.0149
$T_H$ (°F)	75	$T_T$ (°F)	30	$\frac{dv}{dR}$ (sec <sup>-1</sup> )	178
$\tau_\mu \times 10^3$ (lb./ft. <sup>2</sup> )	94	$\tau_0 \times 10^3$ (lb./ft. <sup>2</sup> )	497	$\tau_\infty \times 10^3$ (lb./ft. <sup>2</sup> )	160
$\tau_{so} \times 10^3$ (lb./ft. <sup>2</sup> )	403	$\tau_{s\infty} \times 10^3$ (lb./ft. <sup>2</sup> )	66.0	$\frac{\tau_{so}^2}{\tau_{s\infty}} \times 10^3$	2461
TIME OF TEST (min.)	$\tau \times 10^3$ (lb./ft. <sup>2</sup> )	$\tau_s \times 10^3$ (lb./ft. <sup>2</sup> )	$\tau_s - \tau_{s\infty}$ $\times 10^3$	$\frac{\tau_{so}^2}{\tau_{s\infty}} - \tau_s$	$\frac{\tau_s - \tau_{s\infty}}{\tau_{so}^2/\tau_{s\infty} - \tau_s}$
0.1	430	336	270	2125	0.127
0.25	375	281	215	2180	0.0986
0.5	335	241	175	2220	0.0788
1	300	206	140	2255	0.0629
2	274	180	114	2281	0.0500
5	242	148	82	2313	0.0355
10	225	131	65	2330	0.0279
20	215	121	55	2340	0.0235
30	208	114	48	2347	0.0205
60	200	106	40	2355	0.0170



## COMPUTED RHEOLOGICAL DATA

$T_H$ (°F)	75	$T_T$ (°F)	30	$\frac{dv}{dR}$ (sec <sup>-1</sup> )	310
$\tau_\mu \times 10^3$ (lb./ft. <sup>2</sup> )	163	$\tau_0 \times 10^3$ (lb./ft. <sup>2</sup> )	642	$\tau_\infty \times 10^3$ (lb./ft. <sup>2</sup> )	235
$\tau_{so} \times 10^3$ (lb./ft. <sup>2</sup> )	479	$\tau_{s\infty} \times 10^3$ (lb./ft. <sup>2</sup> )	72.0	$\frac{\tau_{so}^2}{\tau_{s\infty}} \times 10^3$	3187
TIME OF TEST (min.)	$\tau \times 10^3$ (lb./ft. <sup>2</sup> )	$\tau_s \times 10^3$ (lb./ft. <sup>2</sup> )	$\tau_s - \tau_{s\infty}$ $\times 10^3$	$\frac{\tau_{so}^2}{\tau_{s\infty}} - \tau_s$	$\frac{\tau_s - \tau_{s\infty}}{\tau_{so}^2 / \tau_{s\infty} - \tau_s}$
0.1	570	407	335	2780	0.121
0.25	498	335	263	2852	0.0922
0.5	450	287	215	2900	0.0741
1	403	240	168	2947	0.0570
2	370	207	135	2980	0.0453
5	338	175	103	3012	0.0342
10	318	155	83	3032	0.0274
20	302	139	67	3048	0.0220
30	295	132	60	3055	0.0196
60	282	119	47	3068	0.0153



APPENDIX 8ESTIMATION OF INITIAL SHEAR STRESS,  $\tau_{so}$ .

The initial shear stress, or the shear stress obtaining at zero time at any rotational speed, was determined through the application of two independent graphical extrapolation techniques. In the first method, the incremental change in shear stress, occurring during equal (15 second) intervals of time, was plotted as a function of the time interval number on logarithmic coordinates. Thus the period between 15 seconds and 30 seconds represented the second time interval, the period between 30 seconds and 45 seconds represented the third interval and so forth. Extrapolation of the resulting straight line toward the left provided the change in shear stress during the first interval and therefore the stress at time zero. This procedure may be demonstrated most clearly with the aid of an example.

Consider the data obtained at a rotational speed of 4.48 RPS and a test temperature of 60°F. The shear stress, time of measurement, change in shear stress and time interval number are indicated on Table (1-8) and presented graphically on Figure (1-8) and Figure (2-8).

Extrapolation of the straight line, formed by the data points on Figure (2-8) to the intersection with the vertical line corresponding to the first time interval number, indicates a change in shear stress of  $10.0 \times 10^{-3} \text{ lb}_f/\text{ft}^2$ . This value, when added



**Figure 1-8**

Shear Stress vs Time  
Test Temperature 60°F  
Cup Speed = 4.48 RPS

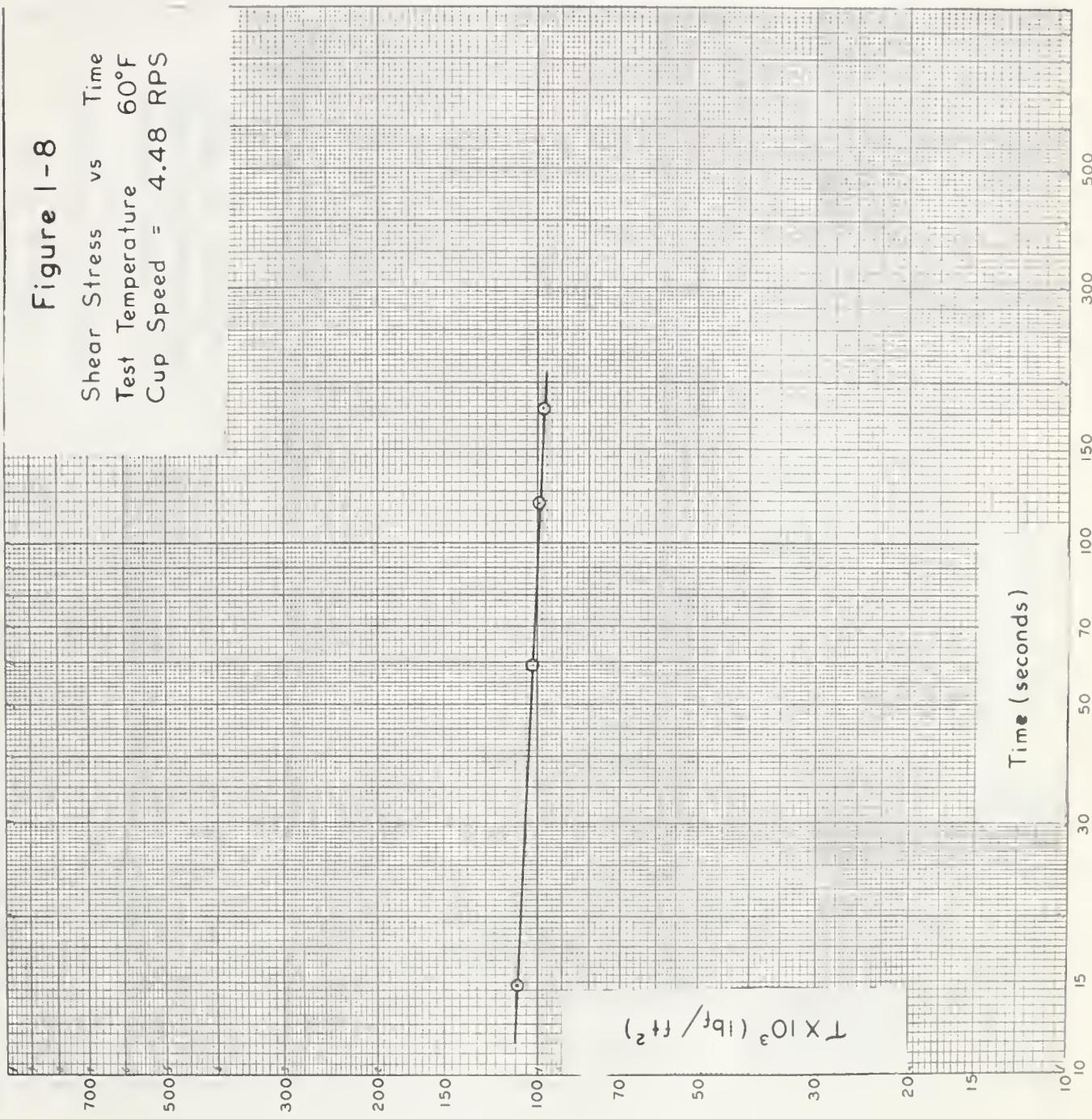
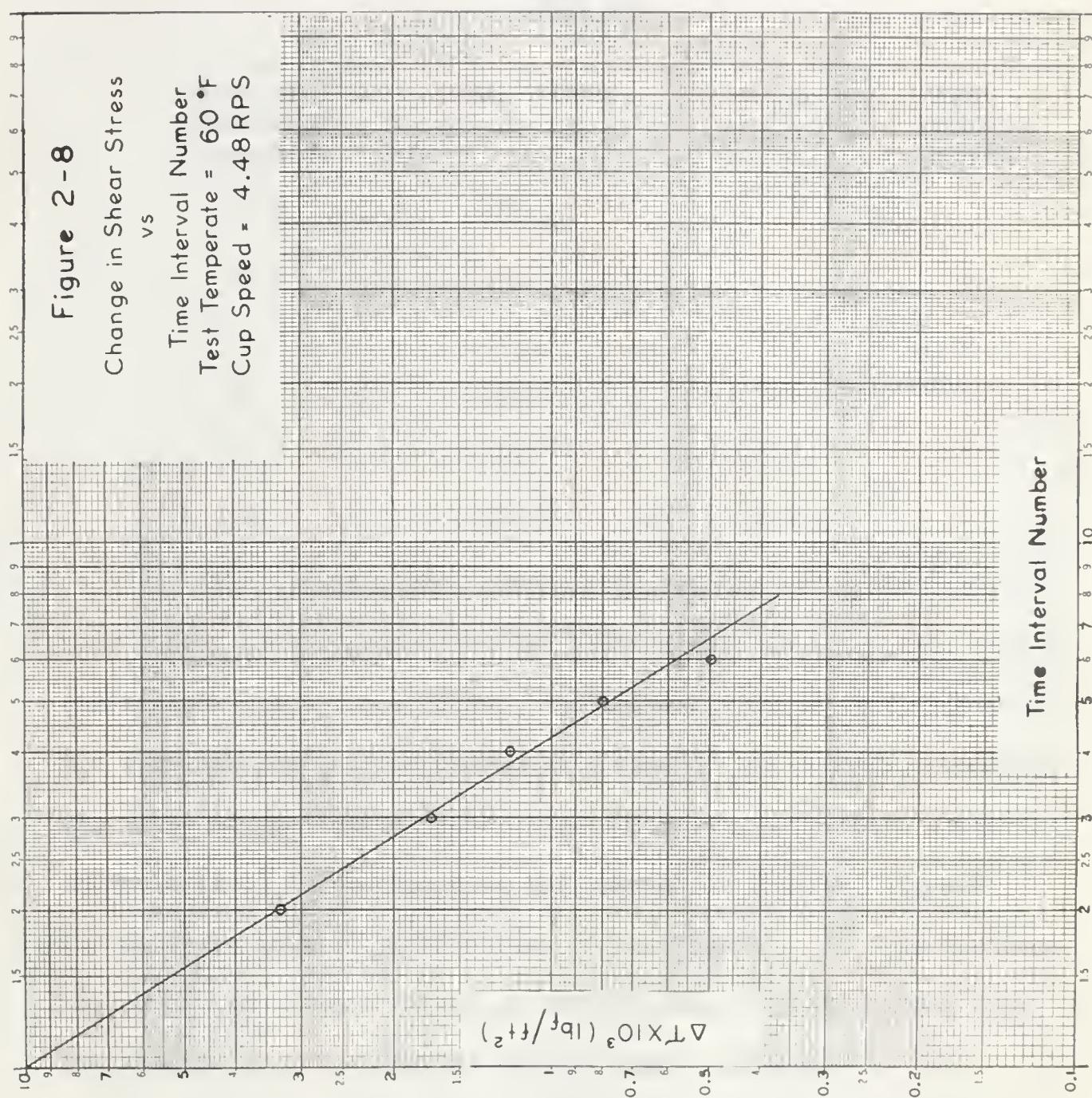




Figure 2-8





to the shear stress obtaining at 15 seconds, yields an initial shear stress of  $118 \text{ lb}_f/\text{ft}^2$ .

TABLE 1-8

TIME OF MEASUREMENT (seconds)	SHEAR STRESS $\tau_s \times 10^3 (\text{lb}_f/\text{ft}^2)$	$\Delta\tau_s \times 10^3$ ( $\text{lb}_f/\text{ft}^2$ )	TIME INTERVAL NUMBER
15	108.3	.	
30	105.0	3.3	2
45	103.3	1.7	3
60	102.1	1.2	4
75	101.3	0.8	5
90	100.8	0.5	6

The second method merely required the extrapolation of a near linear plot representing the shear stress as a function of time (in seconds) plus ten seconds. The intersection of this line with the vertical line corresponding to a time of ten seconds, provided the value of the initial shear stress directly. The data appearing in Table (1-8) is presented in this manner on Figure (3-8) and indicates an initial yield stress of  $121 \text{ lb}_f/\text{ft}^2$ . In this instance, the deviation between values of initial shear stress arising from the two methods of extrapolation is less than 3 percent.

Average values of initial shear stress, obtained in an identical manner with the data at other temperatures and rotational speeds, are presented in Table 2-8.



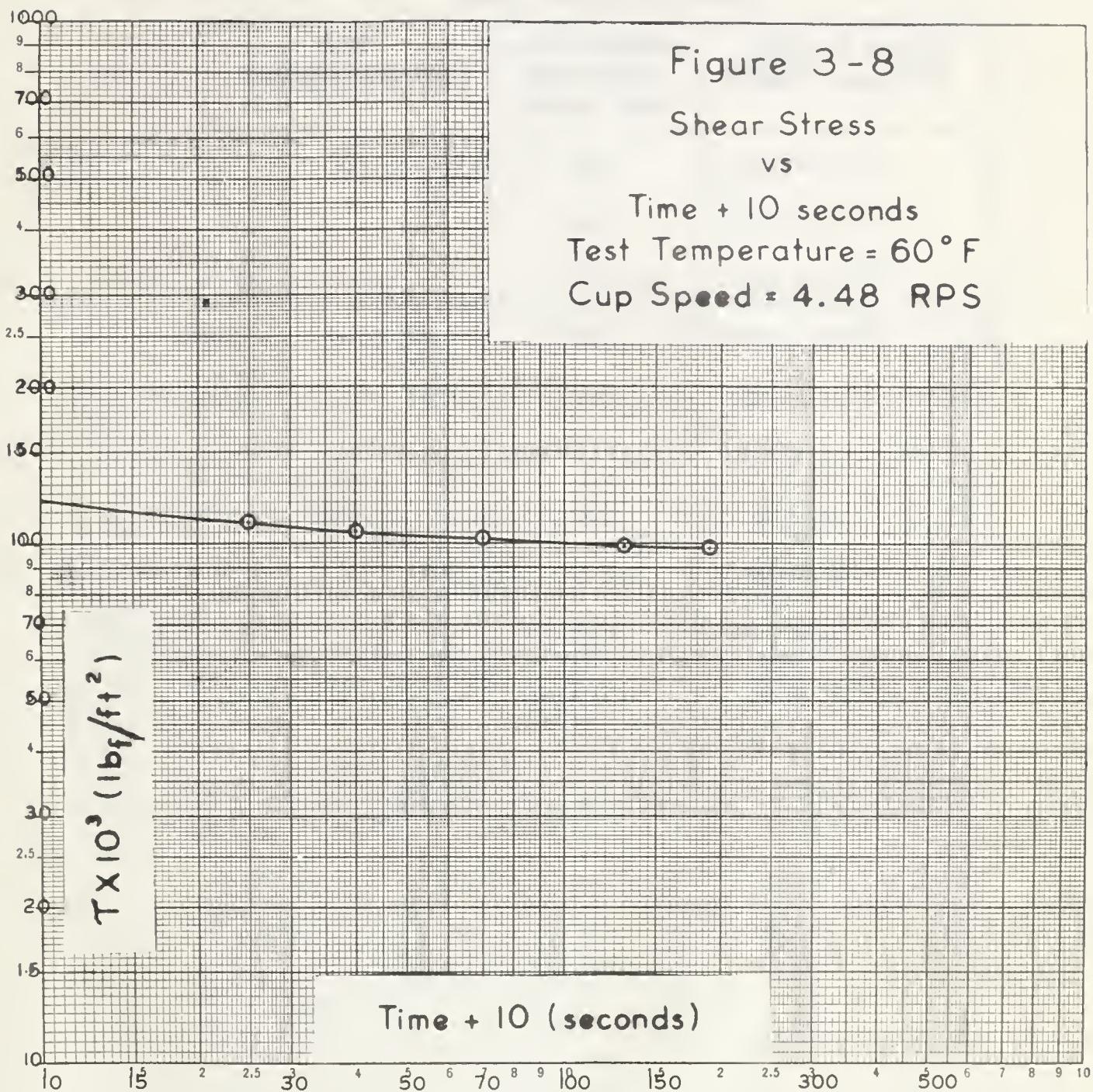




TABLE 2-8

INITIAL SHEAR STRESS AT VARIOUS TEMPERATURES  
AND ROTATIONAL SPEEDS

TEST TEMPERATURE ( $^{\circ}$ F)	APPROXIMATE ROTATIONAL SPEED (RPS)	INITIAL SHEAR STRESS ( $lb_f/ft^2$ )
30	2.5	$380 \times 10^{-3}$
	4.5	$510 \times 10^{-3}$
	4.5	$660 \times 10^{-3}$
44.5	0.5	$142 \times 10^{-3}$
	2.5	$217 \times 10^{-3}$
	4.5	$272 \times 10^{-3}$
60	0.5	$34 \times 10^{-3}$
	2.5	$80 \times 10^{-3}$
	4.5	$120 \times 10^{-3}$
75	2.5	$31 \times 10^{-3}$
	4.5	$50 \times 10^{-3}$



APPENDIX 9STABILITY OF FLOW PATTERN IN THE VISCOMETER

The various stability criteria proposed by Couette, Taylor and Serrin may all be written in the form

$$\frac{2\pi N \rho}{\mu} < M \quad (1-9)$$

in which the constant  $M$ , which is a function of the radii of the viscometer bob and cup, is assigned different values by each of the authors. Since, in the course of the present study, rheological data was obtained with and without the aid of an auxiliary sleeve in the viscometer, two geometries were involved and hence two values of  $M$  were necessary for definition of each of the criterion. The appropriate values are summarized in Table (1-9).

TABLE 1-9VALUES OF M FOR EACH OF THE STABILITY CRITERION

AUTHOR	COUETTE	TAYLOR	SERRIN
WITHOUT SLEEVE	4,160	7,700	217
WITH SLEEVE	12,600	23,200	690

The viscometer data tested for stability was that obtained at 90°F and 75°F at rotational speeds of 2.5 and 4.5 RPS (without the auxiliary sleeve) and that obtained at 75°F and a rotational speed of 8.4 RPS (with the auxiliary sleeve). The density and viscosity



of the fluid under each of the conditions specified above and the magnitude of the term on the left hand side of equation (1-9) are presented in Table (2-9). For convenience, the information in Table (1-9) is also included in this tabulation.

TABLE 2-9  
COMPARISON OF STABILITY CRITERION

TEMP. °F	90		75 (WITHOUT) (SLEEVE)		75 (WITH) (SLEEVE)
DENSITY (gm/cc)	0.830		0.835		0.835
ROTATIONAL SPEED (RPS)	2.5	4.5	2.5	4.5	8.4
VISCOSITY (POISES)	0.0535	0.0535	0.0814	0.0751	0.0704
$\frac{2\pi N \rho}{\mu}$	244*	439*	162	315*	626
COUETTE	4,160		4,160		12,600
TAYLOR	7,700		7,700		23,200
SERRIN	217		217		690

The stability of the basic laminar flow pattern of those samples whose stability "coefficients" are designated by an asterisk in Table (2-9) is placed in some doubt when viewed in terms of the stability criterion proposed by Serrin. The conclusions, based on careful consideration of this problem, have been discussed in the text.













**B29796**